



STANFORD RESEARCH INSTITUTE  
Menlo Park, California 94025 · U.S.A.

*Final Report*

*August 1973*

## ATMOSPHERIC PHOTOCHEMICAL SMOG MEASUREMENTS OVER SAN FRANCISCO BAY

*By:* L. A. CAVANAGH and J. H. SMITH

*Prepared for:*

COORDINATING RESEARCH COUNCIL  
30 ROCKEFELLER PLAZA  
NEW YORK, N.Y. 10020

ENVIRONMENTAL PROTECTION AGENCY  
DIVISION OF METEOROLOGY  
RESEARCH TRIANGLE PARK, NORTH CAROLINA 27711  
CRC APRAC CONTRACT CAPA-12-72 and EPA CONTRACT 68-02-1009

AIR RESOURCES BOARD  
1025 P STREET  
SACRAMENTO, CALIFORNIA 95814  
CONTRACT 2-021

SRI Projects 2092 and 2098

*Approved by:*

R. T. H. COLLIS, *Director*  
*Atmospheric Sciences Laboratory*

R. L. LEADABRAND, *Executive Director*  
*Electronics and Radio Sciences Division*

LIBRARY  
AIR RESOURCES BOARD  
P. O. BOX 2815  
SACRAMENTO, CA 95812



## ABSTRACT

In a research program to measure composition and concentration of smog constituents in a moving air parcel, SRI outfitted a houseboat for use as a mobile laboratory and used a helicopter as an airborne laboratory. From these laboratories a research team made measurements over San Francisco Bay in the autumn of 1972.

Four sampling days were analyzed extensively, and the observed measurements were correlated. A data tape containing all of the air quality measurements is available. The data from the four selected days were analyzed to determine the correlation of the ratio  $\frac{[\text{NO}][\text{O}_3]}{[\text{NO}_2]}$  to solar intensity and NO concentrations. The correlation to solar intensity was low (correlation coefficient = -0.09), and the correlation to NO concentrations was high (correlation coefficient = 0.87). The concentrations of NO over the Bay appear to be inhomogeneously distributed. The NO concentration varied by factors as high as 6 (from 6 to 40 pphm) over distances of 5 kilometers or less.

Operational techniques and the appropriate logistics were developed to effectively coordinate the surface and airborne mobile laboratories. The study substantiated that a mobile laboratory can follow marked air parcels if meteorological conditions are favorable. Virtually no photochemical activity was present during the experimental program. However, the measurement data obtained could provide useful data for simulation modeling at concentration levels equivalent to air quality standards.



## CONTENTS

ABSTRACT . . . . .	iii
LIST OF ILLUSTRATIONS . . . . .	vii
LIST OF TABLES . . . . .	xi
GLOSSARY . . . . .	xiii
ACKNOWLEDGMENTS . . . . .	xv
I INTRODUCTION . . . . .	1
II SUMMARY . . . . .	5
III THE 1972 SMOG SEASON . . . . .	9
A. September 1972 . . . . .	10
B. October 1972 . . . . .	12
C. November 1972 . . . . .	13
D. Effects of Unusual Conditions . . . . .	13
IV MEASUREMENT TECHNIQUES . . . . .	15
A. General Operational Techniques . . . . .	15
B. Mobile Laboratory--Houseboat . . . . .	17
C. Airborne Laboratory--Helicopter . . . . .	23
D. Operation of the Mobile Laboratories . . . . .	24
V PRESENTATION AND INTERPRETATION OF THE DATA . . . . .	33
A. Overview of the Sampling Days . . . . .	33
B. Selected Sampling Days . . . . .	39
1. 21 September 1972 . . . . .	39
2. 25 October 1972 . . . . .	48
3. 26 October 1972 . . . . .	63
4. 2 November 1972 . . . . .	69
VI PRELIMINARY ANALYTICAL RESULTS BASED ON COMBINED DATA FROM SELECTED SAMPLING DAYS . . . . .	83
A. Usefulness of the Data . . . . .	83

B. Mass Balance. . . . .	91
C. The $[\text{NO}][\text{O}_3]/[\text{NO}_2]$ Ratio. . . . .	93
D. Observed Pollutant Inhomogeneity over San Francisco Bay .	105
VII CONCLUSIONS AND RECOMMENDATIONS . . . . .	109
A. Applicability of Methods and Data for Model Verification. . . . .	109
B. Recommendations for Further Research. . . . .	112
APPENDICES	
A THE CLIMATOLOGY OF THE SAN FRANCISCO BAY AREA . . . . .	A-1
B AIR QUALITY INSTRUMENTATION AND CALIBRATION . . . . .	B-1
C AIR QUALITY AND METEOROLOGICAL DATA FOR SELECTED SAMPLING DAYS . . . . .	C-1
D DESCRIPTION OF EDITED DATA TAPE . . . . .	D-1
E CHRONOLOGICAL SUPPORTING DATA FOR SELECTED SAMPLE DAYS. . . . .	E-1
F AIHL REPORT NO. 148 BY THE AIR RESOURCES BOARD. . . . .	F-1
REFERENCES . . . . .	R-1

## ILLUSTRATIONS

1	Overall Area of San Francisco Bay with Sampling Area Inset. . . . .	11
2	Prevalent Surface Wind Flow Pattern for October . . . . .	16
3	Air Pollution Levels, Surface Wind Flow, and Houseboat Course, 21 September 1972 . . . . .	40
4	Rawinsonde Temperature and Dew Point Observations, 21 September 1972 . . . . .	42
5	Pollutant Concentrations Observed During Tetron Run, 21 September 1972, 1037 to 1226 PST. . . . .	43
6	Aerosol Particle Counter Data for Various Average Times, 21 September 1972 . . . . .	44
7	Air Pollutant Levels, Surface Wind Flow, and Houseboat Course, 25 October 1972 . . . . .	49
8	Rawinsonde Temperature and Dew Point Observations, 25 October 1972 . . . . .	53
9	Sampling Paths of Mobile Laboratories on 25 October 1972 . . . . .	54
10	Pollutant Concentrations Observed During Tetron Run, 25 October 1972, 1138 to 1218 PST. . . . .	55
11	Pollutant Measurements During Traverses of the Bay, 25 October 1972. . . . .	56
12	Aerosol Particle Counter Data for Various Average Times, 25 October 1972, 1143 to 1226 PST. . . . .	58
13	Air Pollution Levels, Surface Wind Flow, and Houseboat Course, 26 October 1972. . . . .	64
14	Rawinsonde Temperature and Dew Point Observations, 26 October 1972. . . . .	66
15	Pollutant Concentrations Observed During Tetron Run, 26 October 1972, 0907 to 0947 PST . . . . .	67

ILLUSTRATIONS (Continued)

16	Air Pollutant Levels, Surface Wind Flow, and Houseboat Course, 2 November 1972. . . . .	70
17	Rawinsonde Temperature and Dew Point Observations, 2 November 1972. . . . .	75
18	Pollutant Concentrations Observed During Traverse of the Bay, West to East, 2 November 1972, 0843 to 0957 PST. . .	76
19	Pollutant Concentrations Observed During Tetroon Run, 2 November 1972, 1141 to 1316 PST. . . . .	77
20	Pollutant Concentrations Observed in Vicinity of San Mateo Bridge During Tetroon Run, 2 November 1972, 1253 to 1327 PST. . . . .	80
21	Representative Smog Chamber Run in SRI Chamber, Automobile Exhaust (7.5 ppm C) and NO (75 pphm) . . . . .	84
22	Ratios of Pollutants to CO Concentrations Observed During Tetroon Runs (5-Minute Averages) . . . . .	86
23	$[\text{NO}][\text{O}_3]/[\text{NO}_2]$ Ratios Versus Solar Intensity for Tetroon Runs (5-Minute Averages). . . . .	96
24	$[\text{NO}][\text{O}_3]/[\text{NO}_2]$ Ratios Versus Solar Intensity, Combined Data from Figure 23 . . . . .	98
25	$[\text{NO}][\text{O}_3]/[\text{NO}_2]$ Ratios Versus NO Concentration for Tetroon Runs (5-Minute Averages). . . . .	99
26	$[\text{NO}][\text{O}_3]/[\text{NO}_2]$ Ratio Versus NO Concentration, Combined Data from Figure 25 (5-Minute Averages) . . . . .	101
27	Combined Data from Figures 25 and 26 with Data for NO Concentrations Greater Than 15 pphm Omitted (5-Minute Averages). . . . .	103

ILLUSTRATIONS (Continued)

A-1	The San Francisco Bay Area . . . . .	A-4
A-2	Prevalent Surface Wind Flow Pattern for October. . . . .	A-7
A-3	July Average Maximum Temperatures. . . . .	A-9
A-4	October Average Maximum Temperature. . . . .	A-10
A-5	Percentage of Observations of Fog or Stratus at 1030 PST During Summer . . . . .	A-13
A-6	Normal Annual Total Precipitation. . . . .	A-15
A-7	Average Oxidant Concentration on Comparable Warm Days for each BAAPCD Station . . . . .	A-17
B-1	Schematic for Gas Sample Lines and Instrumentation . . . . .	B-5
B-2	Particulate Sample Line and Inlet System . . . . .	B-6
B-3	High Resolution Gas Chromatogram of Hydrocarbon Distribution on 25 October 1972. . . . .	B-24
C-1	Overall Area of San Francisco Bay Showing Sampling Area Inset. . . . .	C-4
C-2	Air Pollution Levels, Surface Wind Flow, and Houseboat Course, 6 October 1972. . . . .	C-5
C-3	Rawinsonde Temperature and Dew Point Observations, 6 October 1972. . . . .	C-11
C-4	Air Pollution Levels, Surface Wind Flow, and Houseboat Course, 7 October 1972. . . . .	C-12
C-5	Rawinsonde Temperature and Dew Point Observations, 7 October 1972. . . . .	C-15
C-6	Air Pollution Levels, Surface Wind Flow, and Houseboat Coarse, 19 October 1972 . . . . .	C-16
C-7	Rawinsonde Temperatures and Dew Point Observations, 19 October 1972 . . . . .	C-17
C-8	Air Pollution Levels, Surface Wind Flow, and Houseboat Course, 6 November 1972 . . . . .	C-18

ILLUSTRATIONS (Concluded)

C-9	Rawinsonde Temperature and Dew Point Observations, 6 November 1972 . . . . .	C-21
C-10	Sampling Paths of Mobile Laboratories on 19 October 1972 . . . . .	C-22
C-11	Sampling Paths of Mobile Laboratories on 31 October 1972 . . . . .	C-23
C-12	Sampling Paths of Mobile Laboratories on 6 November 1972 . . . . .	C-24
D-1	Grid Coordinate Overlay Map of the Bay Area . . . . .	D-7

TABLES

1	Project Instrumentation . . . . .	20
2	Helicopter Instrumentation . . . . .	23
3	Summary of Sampling Days . . . . .	34
4	Data for 25 October 1972, 1137 to 1258 PST . . . . .	61
5	Chemical Analyses of Particulate Matter Collected on Glass Fiber Filters, 25 October 1972 . . . . .	63
6	Chemical Analyses of Particulate Matter Collected on Glass Fiber Filters, 2 November 1972 . . . . .	81
7	Pollutant Formation or Loss Rates . . . . .	89
8	Linear Least-Squares Fit to Values of K . . . . .	102
9	Values of $[\text{NO}][\text{O}_3]/[\text{NO}_2]$ from Other Work . . . . .	105
A-1	Percentage Frequency of Light Variable Surface Winds in the San Francisco Bay Area . . . . .	A-6
A-2	Frequency and Average Inversion Base Heights by Months for Oakland . . . . .	A-12
B-1	Project Instrumentation . . . . .	B-4
B-2	Particulate Instrumentation Sampling Rates . . . . .	B-8
B-3	Calibration Data for Houseboat NO/NO <sub>x</sub> Analyzer . . . . .	B-12
B-4	Relative Retention Times of C <sub>1</sub> -C <sub>3</sub> Hydrocarbons on Phenylisocyanate on Porasil C . . . . .	B-21
B-5	Elution Order of Auto Exhaust Constituents . . . . .	B-25
B-6	APC Calibration Data . . . . .	B-30
B-7	APC Calibration Data . . . . .	B-31
B-8	Lundgren Impactor Samples . . . . .	B-35
C-1	Helicopter Measurements for 19 October 1972 . . . . .	C-25
C-2	Helicopter Measurements for 30 October 1972 . . . . .	C-26

TABLES (Concluded)

C-3	Helicopter Measurements for 6 November 1972. . . . .	C-27
C-4	Chemical Analyses of Particulate Matter Collected on Glass Fiber Filters . . . . .	C-29
C-5	Gas Chromatograph Data--Cryogenic Trap Samples . . . . .	C-30
D-1	Units Used in Data Summary . . . . .	D-4
D-2	Engineering Unit Magnetic Tape Record Format . . . . .	D-5
E-1	Houseboat Data for 21 September 1972, 0912 to 1000 PST . . . . .	E-4
E-2	Temperature and Relative Humidity for Bay Area . . . . .	E-5
E-3	Houseboat Data for 25 October 1972, 0546 to 0636 PST . . . . .	E-6
E-4	Data for 25 October 1972, 0801 to 0825 PST . . . . .	E-8
E-5	Helicopter Data for 25 October 1972, Vertical Profile. . . . .	E-8
E-6	Houseboat Data for 25 October 1972, 1135 to 1215 PST . . . . .	E-10
E-7	Data for 25 October 1972, 1137 to 1148 PST . . . . .	E-11
E-8	Data for 25 October 1972, 1210 to 1258 PST . . . . .	E-12
E-9	Helicopter Measurements for 25 October 1972. . . . .	E-13
E-10	Houseboat Data for 25 October 1972, 1220 to 1255 PST . . . . .	E-15
E-11	Cryogenic Trap Data 25 October 1972, 0845 PST. . . . .	E-17
E-12	Houseboat Data for 26 October 1972, 0656 to 0704 PST . . . . .	E-19
E-13	Pollutant Concentrations During High Speed Run Around Treasure Island . . . . .	E-20
E-14	Cryogenic Trap Data, 26 October 1972, 0929 PST . . . . .	E-22
E-15	Houseboat Data for 2 November 1972, 0846 to 1244 PST . . . . .	E-24
E-16	Ethane, Ethylene and Acetylene Concentrations, 2 November 1972. . . . .	E-26
E-17	Cryogenic Trap Data, 2 November 1972 . . . . .	E-27

## GLOSSARY

APC	aerosol particle counter
ARB	California Air Resources Board
BAAPCD	Bay Area Air Pollution Control District
BB	San Francisco Bay Bridge
CN	condensation nuclei
CRC	Coordinating Research Council
DDi	distilled deionized
EPA	Environmental Protection Agency
ESCA	Electron Scattering Cross-Section Analysis
FID	flame ionization detector
GC	gas chromatograph
GC-MS	gas chromatograph-mass spectrometer
HC	total hydrocarbon, excluding methane
HP	Hunter's Point
NDIR	nondispersive infrared
NO <sub>x</sub>	the sum of NO and NO <sub>2</sub> concentrations
OP	Oyster Point
PAN	peroxyacyl nitrate
ppb	parts per billion
pphm	parts per hundred million
ppm	parts per million
ppm C	parts per million carbon, as hexane
PVC	polyvinyl chloride
SF	San Francisco
SLH	San Leandro Harbor
THC	total hydrocarbon



## ACKNOWLEDGMENTS

The authors of this report gratefully acknowledge the significant contributions of many people, including the other members of the houseboat crew: Mr. Louis Salas, Mr. Albert H. Smith, and Ms. Joyce Kealoha. Mr. Irwin Sauer was the instrument operator on board the helicopter. The analysis phase could not have been completed without the assistance of Mr. F. L. Ludwig. Laboratory support was ably provided by Mr. August Pijma.



## I INTRODUCTION

Photochemical smog results from photochemical reactions in the atmosphere that occur when nitrogen oxides and hydrocarbons are present. The reaction products include ozone, peroxyacyl nitrates (PAN), aldehydes, and a variety of secondary reaction products. To date, knowledge of the photochemical smog reaction process is largely based on controlled experiments in laboratory test chambers (smog chambers) and on statistical correlation analyses using atmospheric data on photochemical smog. In the latter case, most of the data have come from observations in the Los Angeles Basin.

As yet not satisfactorily resolved in the smog-forming process is the question of the importance of specific types of hydrocarbons, i.e., the olefins and other highly reactive types as compared to the less reactive aromatics. Another question is the significance of the ratio of nitrogen oxides to hydrocarbons in the photochemical mixture. Chamber experiments are now being used to judge the significance of hydrocarbon reactivity and hydrocarbon to  $\text{NO}_x$  ratios in order to postulate smog formation mechanisms. Ultimately, such studies could serve as a basis for revised air pollution control regulations and air quality standards on photochemical smog constituents such as  $\text{NO}_2$ , hydrocarbons, and oxidant or ozone. Chamber studies cannot simulate all the variabilities of the real atmosphere, and thus increased efforts have been made to carry out detailed aerometric analyses in Los Angeles. The basic goal is a realistic simulation model of photochemical smog.

The interpretation of aerometric measurements from Los Angeles, however, presents major problems. One of the more important is the great complexity of the area sources and their emissions. For example, any

sampling station in Los Angeles will be surrounded by sources of both hydrocarbons and  $\text{NO}_x$  at distances varying from the street just outside the door to the freeway 20 miles away. As a result, each sample will contain a wide mixture of emissions that have had various histories, times for reaction, and exposures to atmospheric influences. Although partial evaluations of the Los Angeles aerometric data have been published, the analyses leave unanswered many questions about the real photochemical smog system because of the difficulties in interpretation.

Knowledge of photochemical processes gained through laboratory and aerometric studies is frequently applied to the development or improvement of photochemical simulation models. Progress in improved simulation models is limited to a great extent by the lack of suitable aerometric data to evaluate these models. Photochemical models that are recognized to provide a realistic simulation of photochemical processes include those developed by Eschenroeder,<sup>1</sup> Seinfeld,<sup>2</sup> and Wayne.<sup>3</sup> The model developed by McCracken is currently used for prediction of carbon monoxide concentrations.<sup>4</sup> However, the McCracken model will be extended to include reactive pollutants and applied to the San Francisco Bay Area. Aerometric data, primarily from the Los Angeles Basin, have been used to evaluate the above photochemical models.

A research program was undertaken by SRI employing a concept unique to aerometric surveys, where both surface and airborne measurements were made in a marked, moving air parcel. The measurements were made over San Francisco Bay where changes in composition and concentration of pollutants occur without significant addition of fresh reactants. The primary objective of the program was to obtain aerometric data in a different locality, and to relate the changes in composition and concentration in an aging air mass to time and meteorological factors. The acquired data are presented in a format

suitable for evaluation of recognized photochemical models.

A secondary objective was to evaluate the methodology and techniques required to study smog constituents in a marked, moving air parcel. In addition to the study of gaseous pollutants funded by the Coordinating Research Council and the Environmental Protection Agency, a complementary research program funded by the California Air Resources Board was undertaken concurrently to demonstrate the feasibility of studying the aerosol constituents of photochemical smog from a mobile laboratory on the Bay. The data from these two research projects were to be coordinated and shared. Therefore, this final report incorporates data from both projects and is submitted to all organizations supporting this research.



## II SUMMARY

The primary objective of the research program undertaken by SRI was to measure the changes in composition and concentration of pollutants in a marked, moving air parcel. The photochemical reactions that occur in a single air mass were studied in a Lagrangian mode by a unique measurement approach. A houseboat was outfitted as a mobile air quality laboratory to measure smog constituents over San Francisco Bay. A helicopter was outfitted with instrumentation and used as an airborne laboratory to measure pollutant gradients, both horizontal and vertical. The air parcel to be measured was marked by a free-floating constant level balloon (a tetron). The changes that occurred in the pollutant concentrations were related to time and meteorological factors.

The measurement phase of the research program was undertaken during the autumn of 1972. Unfortunately, the normal meteorological conditions conducive to smog formation did not develop. The autumn of 1972 was the "cleanest" year during the 10-year period that measurements have been made by the Bay Area Air Pollution Control District. Although, photochemical activity was uniformly low throughout the measurement period, pollutant concentration data were obtained on 15 days; of these, four sampling days have been analyzed in detail. These analyses address meteorological factors, pollutant concentrations, pollutant concentration gradients, particulate compositions, and particulate size distributions where appropriate. The four days selected for analysis were 21 September, 25 October, 26 October, and 2 November of 1972. On September 21, measurements were made following an air parcel from downwind of San Francisco for 2 hours down the axis of the Bay. Moderate photochemical activity

was observed during this sampling day. On October 25, an air parcel was tracked for 45 minutes near San Mateo Bridge; limited photochemical activity was observed. On October 26, an air parcel was tracked from San Francisco to Berkeley; little or no photochemical activity was observed. On 2 November, an air parcel was tracked for 2 hours from mid San Francisco Bay to a point south of the San Mateo Bridge; moderate photochemical activity was observed.

The conclusions reached on the basis of the experimental data indicate that the approach used is a viable technique for the study of photochemical smog processes. The methods and techniques that were developed for operating a houseboat mobile laboratory in conjunction with an airborne mobile laboratory were successful. The data obtained during the experimental program will be useful for modeling photochemical processes when pollutant concentrations approach the ambient air quality standards. The data will be of limited usefulness to verify models under conditions of moderate to heavy photochemical activity. The  $[\text{NO}][\text{O}_3]/[\text{NO}_2]^*$  ratio is discussed in detail on the basis of observed measurements of solar intensity and NO concentrations. On the basis of limited data analysis, a good correlation of the ratio with NO (correlation coefficient = 0.87) concentrations and a poor correlation with solar intensity was obtained (correlation coefficient = -0.09). Removal of data when the NO concentration was greater than 15 pphm (indicative of the injection of freshly polluted air to the air mass) did not improve the correlation with solar intensity.

The observed concentrations of NO over the Bay appear to be inhomogeneously distributed. The NO concentrations varied by factors

---

\* Square brackets are used to indicate the concentration of a gas.

of as high as 6 (from 6 to 40 pphm) over distances of 5 kilometers or less. These inhomogeneities in NO concentrations were not accompanied by corresponding significant increases in the concentration of NO<sub>2</sub>, CO, or Aiken nuclei. The concentration of ozone, though present at low concentrations, does not decrease markedly in the areas where high concentration of NO are observed. Careful examination of the data, the mode of operation of the houseboat, and instrument functionality indicate that the observed measurements are valid. The cause or origin of these NO inhomogeneities cannot be identified on the basis of available meteorological data.

A data tape containing all the air quality measurements obtained by the houseboat mobile laboratory and a description of the tape format are provided as part of this final report.



### III THE 1972 SMOG SEASON

This research program was undertaken in anticipation of "normal" meteorological conditions in the San Francisco Bay Area. Usually, during the smog season the occurrence of low wind-speed conditions results in several intervals in which pronounced photochemical activity is observed. In 1971, a CRC-EPA funded study was undertaken to determine the feasibility of investigating the formation of photochemical smog in the San Francisco Bay Area. Although 1971 was considered the cleanest year of a decade by the San Francisco Bay Area Air Pollution Control District (BAAPCD), oxidant measurements made during 1971 by SRI, and analysis of BAAPCD oxidant measurements from 1967, indicated that a comprehensive research program undertaken during a normal year could produce valuable data about formation and scavenging of photochemical pollutants. It was emphasized in the report of the feasibility study that a comprehensive research program should be undertaken over a period of two years to ensure that the mobile laboratories could be operational over a sufficient number of sampling days in which appreciable photochemical activity was present. However, it was anticipated that even if 1972 was as clean as 1971, the objectives of the research program could be accomplished in a single smog season.

During the interval from May through October 1971, there were 13 days when peak oxidant concentrations exceeded 10 pphm on the same day at each of four South Bay BAAPCD stations: Redwood City, San Leandro, Fremont, and San Jose. Of these 13 days in 1971, 12 occurred in the months of September and October. In contrast, during September and October of 1972, oxidant values never exceeded 10 pphm at the four South Bay Stations during any one day.

The BAAPCD prepares monthly summaries of weather and pollution conditions within the district. Figure 1 shows the locations of BAAPCD stations around the South Bay Area where the houseboat experiments were conducted. The BAAPCD summaries document the highly unusual character of the weather and pollutant conditions prevailing during the fall season of 1972.<sup>5,6,7</sup>

A. September 1972

According to the BAAPCD:

Sunny but cool weather characterized September, with percentage of sunshine at San Francisco 10 percent above normal. Mean wind speeds were very close to monthly normals, and the ventilation index was slightly below. Mean maximum temperatures were almost 3<sup>o</sup>F below normal, and precipitation was above normal.

The State standards<sup>\*</sup> for carbon monoxide, sulfur dioxide, and nitrogen dioxide were not exceeded during the month. On the 21st, however, the highest hourly value of 0.23 ppm for nitrogen dioxide at San Jose did approach the standard.

The State 0.10 ppm hourly standard for oxidant was exceeded on 13 days, the lowest number for September in our 10 years of continuous record. Moreover, the greatest single high hourly value was 0.14 ppm at Vallejo on the 21st.

In the southern part of the Bay, where the experiments were conducted, Fremont and San Leandro showed the highest oxidant concentration (0.13 ppm) for the month. Fremont also had the highest number of days with oxidant levels equal to, or greater than, 0.10 ppm. Although

---

\*The California State standards are: Oxidants - 0.1 ppm for 1 hour; carbon monoxide 40 ppm for 1 hour or 10 ppm for 12 hours; nitrogen dioxide - 0.25 ppm for 1 hour; sulfur dioxide - 0.5 ppm for 1 hour or 0.04 ppm for 24 hours; suspended particulate - 100  $\mu\text{gm m}^{-3}$  annual geometric mean.

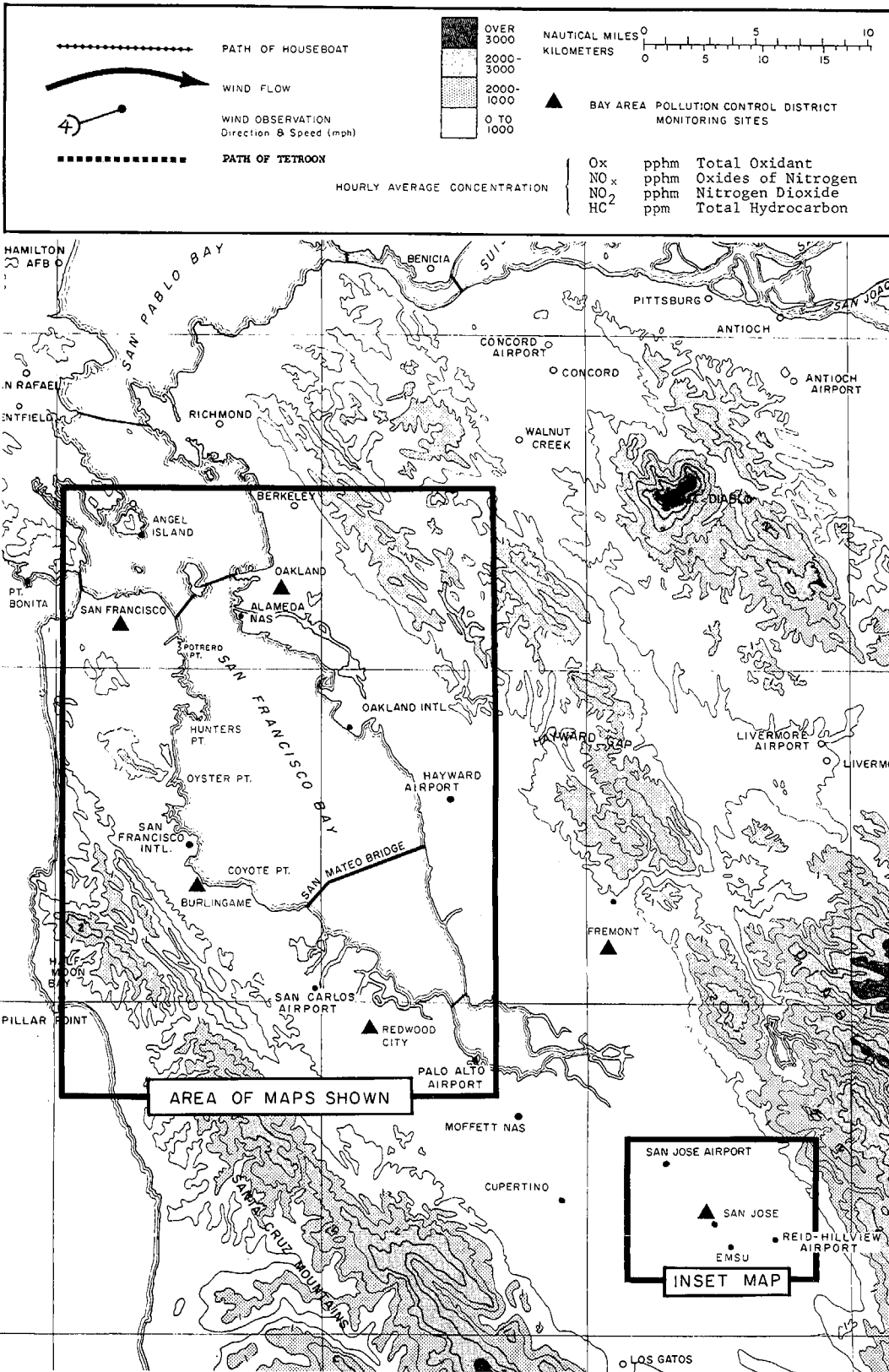


FIGURE 1 OVERALL AREA OF SAN FRANCISCO BAY WITH SAMPLING AREA INSET

there were 13 days in September when one or more stations of the total complement of BAAPCD stations recorded oxidant levels at or above 0.10 ppm, there were only seven days when one or more of the eight stations surrounding the southern part of the Bay had such concentrations. On September 12, Fremont and Redwood City each had high hourly readings of 0.10 ppm. On September 20 and 21, San Leandro reached 0.10 ppm on both days and Fremont reached 0.13 and 0.12 for those two days, respectively. On September 29, Fremont reached 0.11 ppm, San Leandro 0.13, and Oakland 0.12. No other days during the month had more than one station reach the 0.1-ppm oxidant level.

B. October 1972

The BAAPCD<sup>6</sup> describes the month of October as follows:

October of 1972 was the third wettest since the start of record at San Francisco in 1849, with precipitation more than 400 percent above normal. All-time October records were set for maximum hourly rainfall and for consecutive rainy days. Hours of sunshine were 20 percent below normal and mean maximum temperatures almost 3° F below normal. Wind speeds and ventilation were somewhat above their means. The stagnation periods which climatologically characterize October did not occur this year.

As a consequence of the protracted rains and good ventilation, this was the cleanest October since the start of continuous monitoring. State standards for carbon monoxide, sulfur dioxide, and nitrogen dioxide were not exceeded during the month.

There were only four days over the State 0.10 ppm oxidant standard this October compared with 23 in 1964, the worst season. Moreover, there were no days over the 0.15 ppm eye irritation level, and there were no 0.10 ppm days at 13 of our 20 oxidant monitoring stations. Most of the excesses occurred on October 5th, 6th, and 7th. With southerly air-flow in this period the highest values were in the North District. Maximum high hour values were 0.13 at Napa on the 6th, and 0.12 at Santa Rosa on the 5th.

Around the southern part of the Bay, the 0.1-ppm oxidant standard was reached on only three days and at only three stations: San Leandro, Fremont, and Redwood City. These three stations reached 0.11 ppm on October 5, and the latter two reached 0.1 ppm on October 7. Fremont had a high reading of 0.1 on October 23.

C. November 1972

The last day of field observations was November 17. The last week of the month was relatively clear and sunny. However, according to the BAAPCD<sup>7</sup>, the month as a whole was characterized by:

...cold, wet, cloudy, windy conditions...The 6.40 inches of rainfall at San Francisco established the second highest monthly value in over a century of record, and the all-time 24-hour rainfall record was set on November 13-14. The average maximum temperature, almost 4° F below normal, was the all-time lowest November value of record. However, the final week of the month did bring a period of sunshine and high stability. The continuing rains and good ventilation resulted in generally clean air during the month.

No station in the district exceeded the oxidant standard in November before the end of the experimental period. Among the South Bay stations, the highest value reached was 0.07 ppm at Fremont on November 2.

D. Effects of Unusual Conditions

Appendix A describes the climatology of the San Francisco Bay Area and the expected weather conditions. The above summaries of 1972 autumn weather and pollutant conditions refer frequently to unusual occurrences. The emphasis in the preceding discussion was on pollutant concentrations and meteorological conditions conducive to high values of these concentrations, because high pollutant concentrations were one of the two major conditions deemed desirable for the planned experiments.

The other condition desired was the frequent occurrence of air trajectories passing over San Francisco, followed by long fetches over the open waters of the Bay. With the highly unusual atmospheric conditions discussed above, it is not surprising that the second type of hoped-for conditions also failed to materialize very often. Large-scale air motions from the northwest are typical of the San Francisco Bay Area in the autumn; these produce the desired trajectories. Such winds occurred infrequently in 1972. During the autumn of 1972, breezes often blew outward from the Bay all around its perimeter. During these intervals of onshore winds, the Bay appeared to be in an area of clear air relative to the surrounding landmass. Measurements on the houseboat indicated pollutant concentration levels similar to background levels in clean atmospheres.

East or west winds were also more commonly encountered than winds from the northwest. The northwest wind direction permits longer tracking of tetroons during sampling runs because the axis of the Bay lies northwest to southeast. Other wind directions, similar to those common during the 1972 smog season, severely restrict the tracking time or preclude the use of San Francisco as an emission source.

## IV MEASUREMENT TECHNIQUES

### A. General Operational Techniques

San Francisco Bay was selected as an area to study and define active photochemical processes because of the unique topography and consistent wind flow patterns that are typically present during meteorological conditions conducive to smog formation. The typical prevalent wind flow pattern that occurred during a four-year period was reported by Smalley<sup>8</sup> and a more recent wind study was reported by Meteorology Research Inc.<sup>9</sup> During the autumn, the prevalent wind flow pattern is one where marine air passes over San Francisco and then divides with a flow to the northeast and one to the southwest down the axis of the Bay. The prevalent wind flow pattern as reported by Smalley for the month of October is shown in Figure 2.<sup>8</sup> The clean marine air accumulates a burden of pollutants typical of a large urban source during passage over San Francisco and then flows down the axis of the Bay. There are no additional significant pollutant sources where fresh reactants are added to the atmospheric burden for distances of approximately 32 kilometers or more. Thus, under meteorological conditions conducive to smog formation, San Francisco Bay provides a location to study photochemical smog processes where addition of fresh reactants does not complicate data interpretation. Since the measurements are made in the real atmosphere rather than in laboratory test chambers, this type of study provides a link or a bridge between laboratory measurements and conventional aerometric surveys. The San Francisco Bay, under appropriate meteorological conditions, provides essentially a wall-less smog chamber in which transformation processes of smog constituents can be studied and

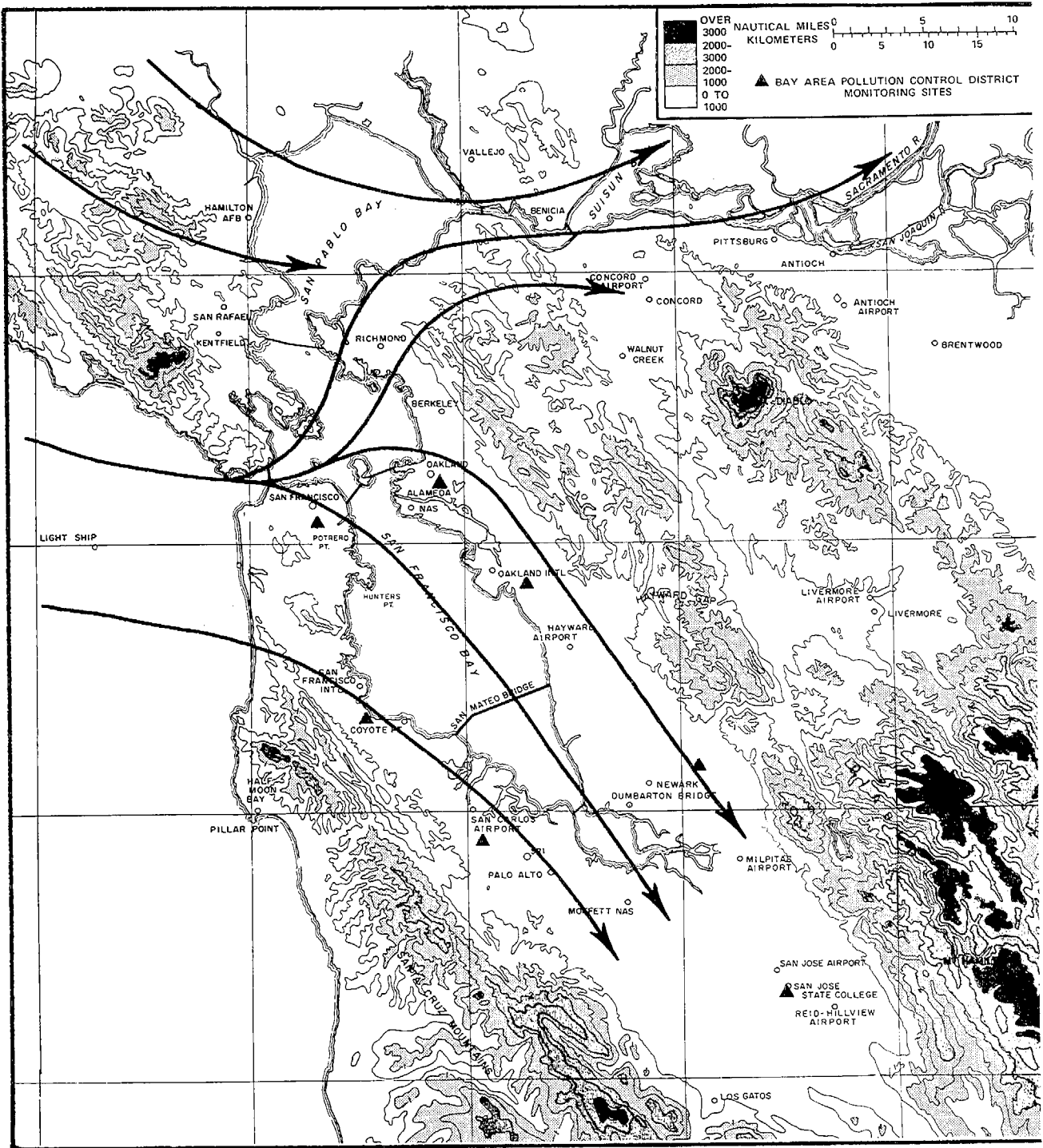


FIGURE 2 PREVALENT SURFACE WIND FLOW PATTERN FOR OCTOBER (Mean wind speed at San Francisco - 9 mph; Oakland - 6 mph)<sup>8</sup>

defined with less ambiguity than with either test chamber studies or previous aerometric studies.

This research project studied smog constituents using a Lagrangian approach where the changes of smog constituents due to aging and atmospheric influences were measured within a moving air parcel. A tetroon, a constant level balloon, was launched to mark a single parcel of air. The houseboat, was maintained in a position directly beneath the tetroon during its free flight over San Francisco Bay. Measurements were made of composition and concentration of atmospheric pollutants within the air parcel during movement down the Bay. In addition to the houseboat laboratory, an instrumented helicopter was used to obtain pollutant concentration gradients both vertically and horizontally with respect to the marked air parcel. Sampling runs where tetroons were followed were begun immediately downwind of a significant pollutant source. Background measurements of pollutant concentration and composition immediately downwind of the source were made prior to launch of the tetroon.

#### B. Mobile Laboratory--Houseboat

The houseboat used in this study was rented on a monthly basis and outfitted as a mobile laboratory. The boat was 12.5 meters in length with a 3.7 meter beam and a planing hull. The size and hull design provided a stable platform for the instrumentation. The craft was powered by twin 225-horsepower Chrysler inboard-outboard marine engines. The maximum cruising speed of the fully instrumented houseboat was about 24 km/hr. With the outdrives in normal position, the draft was 90 centimeters. The shallow draft permitted operation of the houseboat in shallow areas of the Bay. The boat was equipped with duplicate controls in the forward cabin and on the flying bridge. A VHF marine radio provided ship-to-ship-to-shore communication. A portable VHF transceiver operating on the aircraft intercom frequency (124.95 MHz)

was used for communication between the houseboat and the helicopter. The mobile laboratory was also equipped with a depth finder and inflatable life raft to ensure safety during operation.

It was vital to this research program to locate the position of the houseboat on the Bay at frequent intervals. Azimuthal sightings, made with a hand-held bearing compass, were used to obtain a position fix of the houseboat relative to known landmarks. By trial and error, a location was found forward of the flying bridge at which minimal deviation errors were introduced into azimuthal measurements taken by the hand-held bearing compass. This location was marked and used as a sighting location for all navigational fixes. However, even at this deck position, the steel hull and engines introduced a significant deviation to azimuthal readings made approximately 60 degrees to either side of the center line of the stern of the houseboat. To overcome this problem, at the beginning or end of each sampling run, the boat could be maneuvered so that fixes of any appropriate landmark could be made over the forward end. Even with these precautions, deviations introduced by the mass of the craft were larger than the errors associated with reading azimuthal angle on the hand-held bearing compass. Finally, a navigation compass was installed on the flying bridge, which compensated for the deviations introduced by the steel hull. A chart table complete with drafting machine was installed in the forward cabin of the houseboat so that the craft's position could be plotted on a chart during each sampling run.

During trial runs on the Bay, 24 landmarks located on and around the perimeter of the Bay were selected to serve as reference points for navigational fixes. These landmarks were coded as a three-digit alphanumeric designation so that navigational fixes could be entered onto the onboard data tape.

## 1. Air Quality Instrumentation

The air quality instrumentation installed aboard the houseboat, including instrumentation for aerosol measurements funded by the California Air Resources Board (ARB), is listed in Table 1. Appendix B gives details of the air quality instrumentation, calibration procedures, and analysis techniques. In addition to the air quality instruments, up to 10 compressed gas cylinders were mounted within or below the main cabin of the houseboat. An extremely stable source of 115 V, 60 Hz was required to power the data tape recorder and the computer. The 6-kVA motor generator aboard the houseboat did not provide adequate voltage of frequency stability for this application. Therefore, deep-cycle, lead-acid storage batteries in conjunction with an inverter were installed to power the tape recorder and computer. The batteries provided power for a period in excess of 8 hours and were recharged overnight by a battery charger.

The location of instrumentation and associated equipment in the interior of the houseboat was governed by two primary factors: (1) the houseboat could not be permanently modified, and (2) a reasonable distribution of weight had to be maintained so as not to jeopardize performance or safety.

Before fabrication of the sample inlet system, it was necessary to ensure that the location and height planned for the system would provide samples not contaminated with engine exhaust. A test run was therefore made in the houseboat using a hand-operated condensation nuclei (CN) counter while following a tethered balloon to establish an exhaust-free location and height. The sampling inlet to the CN counter was a length of 0.25-inch Teflon tubing supported on a telescoping pole that could be extended to 9 meters above the

Table 1

## PROJECT INSTRUMENTATION

<u>Measurement</u>	<u>Measurement Principle</u>	<u>Supplier and Model</u>
<u>Funded by Coordinating Research Council</u>		
Ozone	Chemiluminescent	Bendix Model 8002
NO and NO <sub>x</sub>	Chemiluminescent	Bendix Model 8101 B
Total hydrocarbon	Flame ionization detector	Beckman Model 400 A
Carbon monoxide	Mercury displacement	Bacharach Model US400L
Carbon monoxide	Nondispersive infrared	Beckman Model 315AL
Turbidity	Integrating nephelometer	Meteorological Research Model 1550
Temperature	Thermistor (dry)	
Relative humidity	Thermistor (wet)	
Solar intensity	Thermopile	Honeywell
Hydrocarbon distribution	Gas chromatography	Hewlett Packard Model 5750*
<u>Funded by the California Air Resources Board</u>		
Total sulfur	Flame photometric	Meloy Model SA120
Condensation nuclei	Continuous reading	Environment/One, Model Rich-100
Particle size distribution	90° Light scattering	SRI
Total particulate	Hi-vol filter	
Particulate distribution	Lundgren impactor	Environmental Research

\*Two columns: C<sub>1</sub> to C<sub>3</sub> on 1/8 in. × 3 meters packed column on phenyl-isocyanate on Porasil C; C<sub>3</sub> to C<sub>10</sub> on 0.02 in. × 300 ft capillary column coated with squalane. Grab samples were collected cryogenically.

upper deck. It was found that the proposed sampling point 4 meters above the deck of the flying bridge next to the wheel was acceptable. Separate sample inlet lines were used for gaseous and particulate pollutants. All gas samples were collected through 0.25-inch diameter FEP Teflon tubing. Teflon fittings were used up through the O<sub>3</sub> and NO<sub>x</sub> sample take-off points. Beyond these inlets, stainless steel fittings and Teflon tubing were used. The particulate sampling line was 6.5 cm polyvinyl chloride pipe. The details of these sampling lines may be found in Appendix B.

## 2. Data Acquisition System

The automated digital data recording system developed during CRC/EPA Contract CAPA 3-68(1-69) was installed on the mobile laboratory to facilitate collection and processing of data acquired on the Bay study. This system accepts analog voltage inputs, digitizes them, and records the data on magnetic tape. Data are acquired at three rates--every 15 seconds, 30 seconds, and 4.7 minutes--to accommodate the various data rates of the onboard instrumentation. Pollutant measurements of O<sub>3</sub>, total hydrocarbon (THC), atmospheric turbidity (integrating nephelometer), CO, total sulfur, and CN are acquired at a 15-second rate and are stored in computer memory. Pollutant measurements of NO, NO<sub>2</sub>, total nitrogen oxides (NO<sub>x</sub>), dry and wet bulb temperatures, and solar intensity are acquired at a 30-second rate and stored in computer memory. The aerosol particle counter is interrogated every 4.7 minutes. At 5-minute intervals, the collected raw data stored in computer memory are recorded on magnetic tape. The computer, in addition, converts the raw data to engineering units, computes 5-minute averages, and prints a summary of the measurements by means of an onboard teletype. The computer's internal clock provides the time sequence required to

operate the program.

Computer software was developed to permit the time of each navigational fix, plus up to five observed azimuths of known landmarks, to be entered by teletype into the onboard computer. Thus, the navigational information could be recorded on magnetic tape concurrently with the air quality data. The computer will accept 24 landmarks coded as a three-digit alphanumeric designation. Inappropriately encoded entries and azimuths greater than 360 degrees are rejected by the computer.

### 3. Tetroons

The tetroons, purchased from Raven Industries, Sioux Falls, South Dakota, had a volume of 240 liters and were fabricated of 2-mil-thick orange Mylar. The inflated tetroons were too bulky to pass through doors or windows of the houseboat cabin. Therefore, canvas cover was fabricated to encircle the roof overhang forward of the main deck pilot house to provide a sheltered area for inflation and weigh-off of the tetroon. The houseboat was driven with the wind, at the speed of the wind, during weigh-off. This procedure provided the least turbulence within the tetroon shelter for weigh-off. The tetroons were overpressurized to ensure that the volume of the tetroon would not increase at operating altitude. A payload of aluminum pellets and steel BB shot was added until zero buoyancy was achieved. The free lift required to achieve flight at a particular altitude is given by:  $l = V(\rho_o - \rho_a)$ , where

$V$  - volume in  $\text{cm}^3$

$\rho_o$  = sea level air density in  $\text{g/cm}^3$

$\rho_a$  = air density at the selected altitude in  $\text{g/cm}^3$

$l$  = free lift in g.

The tetroon payload was then adjusted to allow the tetroon to float at an altitude of 60 to 120 meters.

The tetroons were difficult to weigh to a reproducible positive buoyancy under field conditions. Although the operational technique described previously provided the least turbulence within the tetroom shelter, much more reproducible tetroom flight altitudes could have been attained through the use of a turbulence-free shelter. However, permanent modifications to the houseboat would have been required to significantly improve the facility for tetroom flight preparation.

C. Airborne Laboratory--Helicopter

The helicopter instrument package (Table 2) was designed initially for installation and operation in a Bell 47J-2A helicopter. Although total assembly, including operator, was within the rated load capacity of the 47J-2A, the performance of the aircraft was inadequate to ensure safe operation.

Table 2

HELICOPTER INSTRUMENTATION

<u>Measurement</u>	<u>Measurement Principle</u>	<u>Supplier and Model</u>
Total oxidant	Electrochemical	MAST 724A
NO - NO <sub>x</sub>	Chemiluminescent	Bendix Model 8101B
Carbon monoxide	Mercury displacement	Bacharach US400L
Temperature	Thermistor	SRI

Therefore, the instrument package was redesigned and assembled for use in the higher performance Bell Jet Ranger. The package was inspected and certified by the Federal Aviation Administration. The Bell Jet Ranger and the 47J-2A were available for use on short notice. The performance of the Jet Ranger was adequate in all aspects of the flight requirements. However, the cost per flying hour of the Jet

Ranger was \$240 per hour as opposed to \$145 per hour for the Bell 47J-A2.

The sampling inlet system of the airborne laboratory utilized 0.25-inch Teflon tubing and fittings. The inlet was attached to the outside of the helicopter cabin, passed through the window, and was connected to a glass and Teflon manifold. The manifold was vented to the cabin to relieve the ram pressure built up in the system by the forward velocity of the helicopter.

The Jet Ranger had 100 A at 24 V from the alternator, of which 80 percent was available to power sampling instruments (the 47J-2A had only 50 A total power). A 1-kW Topaz inverter provided 110-V power at 60 Hz for the sampling instruments. The airborne measurement data were recorded with a four-channel inkless strip chart recorder.

#### D. Operation of the Mobile Laboratories

The operating crew of the houseboat consisted of four people on sampling days without helicopter airborne measurements. The crew functions for the houseboat were as follows:

- Guidance of the houseboat and direction of experiments
- Instrumentation monitoring and operation of data acquisition system
- Operation of onboard gas chromatograph
- Navigation.

When the helicopter was operating, one additional houseboat crew member was required in addition to the operator aboard the helicopter. This additional observer recorded the location of the helicopter with respect to time and the houseboat.

The operating personnel of the houseboat and helicopter were continuously on standby during the smog season and available to

operate the mobile laboratory on short notice. The manning and operation of the houseboat had priority over all normal assignments and commitments of the project team members. Although backup team members were designated, they were seldom required to substitute for the operating boat crew.

The houseboat was berthed at the Port of Redwood City during outfitting of the craft as a mobile laboratory. This location, about 13 kilometers from SRI, provided convenient access for SRI personnel and equipment during the installation phase. During the operational phase of the research project, the houseboat was berthed at Oyster Point Marina, South San Francisco. The selection of Oyster Point Marina for a permanent berth during the operational phase was based on several criteria. First, the over-water travel time was 45 minutes or less to either San Francisco or the East Bay. Second, the facilities at Oyster Point were well suited for operating a research craft. There was ease of access to the houseboat for heavy equipment, ample parking, and water and power to each berth. Third, the vehicle travel time from SRI was 45 minutes or less.

The helicopter used for this research program was based at Oakland International Airport. The instrument package was installed and removed after each flight.

The BAAPCD routinely forecasts smog potential on a short-term basis; however, these forecasts are developed to predict the occurrence of moderate to heavy pollution. During a smog season like 1972, with atypical meteorological patterns, the basis for developing accurate forecasts was inadequate. Therefore, accurate forecasts could not be developed by either the BAAPCD or SRI.

The BAAPCD was contacted on a daily basis to ascertain the peak concentrations of total oxidant,  $\text{NO}_2$ , and CO recorded at monitoring

stations in Redwood City and San Jose. This daily contact was initiated on 21 August 1972, and a log was maintained throughout the smog season. The pollutant concentrations and the hour when peak concentrations occurred were obtained by 1630 on the same day the measurements were made. This information permitted evaluation of the trends of photochemical activity in sufficient time to plan operation of the mobile houseboat laboratory for the following day. In addition, both long-and short-term weather forecasts were obtained from the U.S. Weather Bureau on a frequent basis. On days when the meteorological conditions were predicted to be appropriate for photochemical smog formation, Mr. Sandberg of the BAAPCD was consulted to obtain a supplementary forecast evaluation for smog potential.

The temperatures and wind direction at various altitudes were obtained from the Upper Air Group at the Oakland Airport. The Oakland Airport meteorological soundings provided information about the depth of the mixing layer, upper air wind directions and speeds, and stability of the inversion when it was present.

To conserve resources, the houseboat was frequently activated without simultaneous activation of the helicopter. Several factors influenced this operational approach. First, the helicopter was expensive to operate(\$240 per hour plus the expense of the instrumentation operator). Second, the lead time to activate the helicopter was longer than that required to activate the houseboat. Third, on some occasions the helicopter was not available for operation on a specific day because of maintenance requirements or because a pilot was not available at the time. During the latter portion of the smog season, visual observations of the Bay area were made at sunrise (from the home of one of the crew members) to supplement the smog potential forecasts. On the basis of these visual observations, the houseboat crew was frequently contacted by telephone, and the houseboat was activated.

It would be underway and operational within 2 hours after the decision to activate.

When the houseboat reached a position beyond the entrance to Oyster Point Harbor, it was stopped, and a small weighted, helium-filled balloon was released to determine wind direction and speed. On the basis of the observed wind direction and predicted meteorological conditions, a tentative tetron launching site was selected. During transit to the selected tetron launching site, marker balloons were released periodically. Although precautions were taken to maintain a heading into the wind while releasing these marker balloons, there was a possibility of inadvertent exhaust contamination during the short interval when the houseboat was nearly motionless.

Once the final location for launching the tetron had been selected, the tetron was weighed off using the procedures described in Section B.1.C. Exhaust gas contamination resulted prior to each tetron run during this interval. Therefore, the pumps for the particulate filter samples were shut off so that the integrity of these collections would not be compromised. The remainder of the air quality instruments were left in an operating mode because the sample line residence time was short. The houseboat was maneuvered into the wind to provide a contamination-free atmospheric sample for both the gaseous and particulate samplers prior to tetron launch. The houseboat was steered at a course 60 degrees to 90 degrees away from the direction that the tetron would travel at the moment of launch to obviate exhaust gas contamination. Then the houseboat was maneuvered in a circular path back to the trajectory of the tetron at a speed greater than the wind until a position was reached directly beneath the tetron. The houseboat was then slowed to reduce the surface speed to equal the flight speed of the tetron.

While the houseboat maintained a speed equal to that of the tetroon, staying beneath the tetroon, the wind speed was measured by an anemometer at the bow end of the flying bridge. The measured forward wind speed was about 1 m/sec during tracking. Thus, the wind shear was about  $-0.01$  m/sec/m. The surface to tetroon wind speed differential seemed to be reasonably consistent, providing the tetroon speed exceeded about 2 m/sec. Due to this surface boundary layer wind shear, the houseboat continuously moved faster than the air at the surface and encountered both air mixing down from above and new air at the surface, when moving directly under a tetroon-marked air parcel.

At the times when obvious exhaust gas contamination occurred, simultaneous increases were observed in the concentration of NO, CO, and CN. Frequently during intervals when tetroons were tracked by the houseboat, marked changes occurred in NO concentrations within short intervals of time. No corresponding increase in CN or CO occurred to suggest exhaust contamination. In other instances, changes occurred in CN without corresponding changes in CO and NO concentration. Similar observations were made during traverses of the Bay at high speeds where exhaust contamination from the houseboat could not contribute. Underwater exhaust gas exit ports, as used on the houseboat, are not likely to provide any scrubbing mechanism that would preferentially remove CN or CO without significantly reducing NO concentrations. These observed changes in NO concentrations and CN are thus probably real and indicate the inhomogeneity of pollutant distribution over the Bay.

Although the approach to tracking tetroons under a variety of wind speeds had been planned in advance, much innovation was required in the field to select the most satisfactory approach for a particular tetroon release. Several tetroon runs were made during intervals when the wind patterns offshore had not stabilized. During these sample

runs, the course of the tetroon varied greatly in direction and speed during the flight interval. If the speed of the tetroon did not exceed about 2 m/sec, one of the engines of the houseboat would be turned off during the run to minimize the volume of exhaust gases emitted. At very slow tetroon speeds, contamination by exhaust gases could not be eliminated without incorporating additional precautions in the tracking procedure. During these intervals of very slow speed tracking, a helium-filled balloon was tethered to the flying bridge of the houseboat to float a few feet above the sample intake. The tethered balloon was used as an indicator to ensure that the houseboat always maintained a forward speed relative to the wind. The tetroon was tracked by maneuvering a series of figure-eight patterns perpendicular to the path of the tetroon with the cross-over point of the figure eight below, but slightly behind the floating tetroon. The turns at the ends of the figure eights were made by turning upwind in each instance. The figure-eight pattern extended some 100 to 150 meters to each side of the tetroon flight path.

The decision to activate the helicopter mobile laboratory was made on the basis of either predicted meteorological conditions or the pollutant measurements observed in the morning from the houseboat. The helicopter instrument package was located at Butler Aviation Company at San Francisco Airport, who also provided access to line power for instrument warm-up. The airborne instruments were turned on to warm up for 1 to 2 hours prior to installation in the helicopter. The airborne instruments were usually activated by a member of the houseboat crew prior to activation of the houseboat mobile laboratory. The airborne instrument package was stored on a pallet jack along with two 12-volt batteries. After the helicopter had landed at Butler Aviation from its Oakland base, the airborne instruments were

disconnected from line power and transferred to battery power. The instrument package was then moved manually to the helicopter. The instrument package was elevated to the floor of the helicopter, moved into place, and secured. The instrument package was then transferred from the batteries to the helicopter power supply. At the conclusion of each flight the operation was reversed, with the instrument package stored unpowered until the next flight.

The helicopter mobile laboratory provided three types of pollutant concentration and temperature gradient measurements to supplement those measurements made by the houseboat laboratory:

- Vertical Profiles--The measurement of the vertical gradients of pollutant concentrations and temperature gradients was accomplished by performing a slow, vertical ascent spiral over or near a known landmark. The vertical profiles began near the surface (30 meters altitude or less) with an ascent rate of about 30 meters per minute to an altitude of 150 meters. During the interval from 30 to 150 meters, the ascent was usually performed stepwise in 30 meter increments. Above 150 meters and below 300 meters, the helicopter ascended at the rate of about 60 meters per minute. Above 300 meters, the helicopter ascent rate was accelerated because only the temperature profiles are of major interest at altitudes in excess of 300 meters.
- Horizontal Traverses--The measurement of horizontal pollutant concentration gradients was accomplished by traverses upwind of the tetron launch site and parallel to the tetron flight path. Zigzag flight patterns were also made to obtain measurements of the spatial distribution of pollutants over the Bay. The flight paths of the helicopter during specific sampling days are shown in Appendix C.
- Airborne Tracking of the Tetron--Both horizontal and vertical pollutant concentration gradients were measured in the vicinity of the tetron during flight. The helicopter flew in a circular pattern around the tetron, maintaining the same altitude as the tetron, as it ascended to operating altitude. During each circle of the tetron, the instrument operator in the helicopter noted on the recorder chart the location where the helicopter compass indicated north. The

helicopter maintained a constant air speed of 30 or 40 mph. The helicopter observer of the houseboat crew noted in a log the exact time, synchronized with the houseboat computer clock, when the helicopter crossed the line of sight from the houseboat to a known landmark. The radius of the helicopter circles based on a constant speed and the time required for completion of a circle, varied from 200 meters to 500 meters with an average radius of 300 to 400 meters.

The usual operating procedure consisted of tracking the tetroon from launch to the estimated midpoint of the tetroon flight. Horizontal traverses were made during the midportion of the tetroon flight to determine pollutant concentration gradients. The helicopter returned to the tetroon for the remainder of the sampling run. Vertical profiles were usually undertaken prior to, or immediately following, a tetroon flight.



## V PRESENTATION AND INTERPRETATION OF THE DATA

### A. Overview of the Sampling Days

This section contains maps displaying streamlines, houseboat sample paths, tetron paths, pollutant concentrations reported by the BAAPCD, and pertinent wind speed and direction data of four selected sampling days. In Appendix C are maps of the remaining sample days that showed significant pollution. These maps graphically illustrate the hourly meteorological conditions encountered on sampling days during intervals preceding and succeeding tetron runs or other intervals of interest. Rawinsonde observations for the sample days are also included in this section and in Appendix C. The measurement data obtained by the houseboat mobile laboratory during all sampling days have been consolidated, edited, and recorded on a single reel of magnetic tape. This data tape is included as part of this final report. The contents of the data tape and the format are described in Appendix D.

Following is a brief summary of representative sample days, including tetron tracking intervals and the course of the houseboat. A capsule summary of all sampling days is given in Table 3.

- September 21<sup>\*</sup> --A tetron was released at 1030 on the north side of the Bay Bridge between San Francisco and Treasure Island. The tetron drifted slowly toward San Francisco, drifted south within 300 meters of the shore, and then drifted back over the Bay at 1056. The houseboat passed under the Bay Bridge at 1050. At 1100 the houseboat was again beneath the tetron and tracking resumed (1100 to

---

\* All times are Pacific Standard Time (PST).

Table 3

## SUMMARY OF SAMPLING DAYS

Date (1972)	Time (hr:min)		Follow Tetron	Heli- copter	Houseboat Course
	Start	Stop			
9/21	0835	1030	N	N	* OP to SF* to point just north of BB.*
	1030	1235	Y	N	Tetron went over SF, then south over west side of Bay.
9/30	0630	0850	N	N	OP to SF. Drifted south of BB. Checked operation of instruments.
	0850	0930	N	N	Returned to OP.
10/6	0620	0742	N	N	OP to HP,* then to OA.*
	0742	0835	Y	N	Tetron moved north along east side of Bay. Lost near Alameda.
10/7	0920	1056	N	N	Alameda to BB near SF.
	1056	1140	Y	N	Tetron moved south west side of Bay. Over land near HP.
	1230	1300	Y	N	Same path as 1208-1240.
	1300	1446	N	N	Returned to OP, refueled, and headed for center of Bay.
	1446	1526	Y	N	Tetron headed south to SMB. Lost over shallow water.
	1526	1545	N	N	Passed under SMB.* Tetron in sight but far away over shallow water.
	0615	0832	N	N	OP to HP, then southeast to Alameda.
10/19	0833	0905	Y	Y	Tetron, moved north on east side of Bay. Lost over Alameda.
	0908	1035	N	Y	Headed for center of Bay. Helicopter instruments inoperative.
	1035	1124	Y	N	Tetron moved from center of Bay to OA.
	0622	0828	N	N	OP slowly to SF near Ferry Building, just north of BB.
10/24	0828	0930	N	N	Returned to OP. Refueled. Summary from 0950 to 1056 not available.
	1041	1120	Y	Y	Tetron moved from OP east northeast to OA.
	1120	1220	N	N	Returned to OP.
	0955	1152	N	N	OP to HP, then to middle of the Bay.
	1153	1216	N	N	Tetron released but port engine clutch failed. Forced return to OP.

Table 3 (Continued)

Date (1972)	Time (hr:min)		Follow Tetron	Heli- copter	Houseboat Course
	Start	Stop			
10/25	0545	0700	N	N	OP to San Leandro.
	0700	0753	N	N	Held position near San Leandro.
	0754	0855	Y	Y	Tetron moved east to OP.
	0855	1000	N	N	Returned to San Leandro, refueled.
	1045	1134	N	N	San Leandro to 1 mi north of center of SMB.
	1135	1220	Y	Y	Tetron moved west to Coyote Point. Helicopter followed for extra 0.5 hr.
10/26	1221	1406	N	N	Returned to OP.
	0600	0707	N	N	OP slowly to north of BB near SF.
	0708	0905	N	N	Monitored pollutants in vicinity of SF.
	0906	0948	Y	Y	Tetron moved from SF to Berkeley.
	0950	1140	N	Y	Refueled at Berkeley. Wind off SF too strong. Returned to OP.
	10/31	1040	1351	N	N
1352		1407	Y	Y	Tetron moved from shore north of HP to Alameda.
1408		1500	N	N	Returned to HP. Wind strong. Returned to OP.
11/2		0830	1120	N	N
	1123	1317	Y	Y	Tetron moved from center of Bay south over SMB center span.
	1326	1400	N	Y	Returned to OP to refuel.
	1438	1633	N	N	OP to HP to Alameda to SF. Engine ignition trouble repaired.
	1635	1657	Y	N	Tetron moved west from SF to Alameda.
	1658	1738	N	N	Alameda to HP. Wind strong, returned to OP.
11/6	1038	1201	N	N	From OP headed east, then southeast to 2 mi. north of SMB.
	1218	1253	Y	Y	Tetron headed south over SMB.
	1254	1405	N	Y	Returned to OP.

Table 3 (Concluded)

Date (1972)	Time (hr:min)		Follow Tetron	Heli- copter	Houseboat Course
	Start	Stop			
11/17	1030	1115	N	N	OP to San Leandro Harbor for refueling.
	1227	1308	N	N	San Leandro to point midway between HP and OA.
	1317	1347	Y	N	Twin tetron release. Lost over OA. Returned to OP.

Note: Incomplete data were also collected on 07, 11, and 13 September.

N = No.

Y = Yes.

n.a. = not available.

\* OP = Oyster Point; SF = San Francisco; BB = Oakland-S.F. Bay Bridge; SMB = Hayward-San Mateo Bridge; HP = Hunter's Point; OA = Oakland Airport.

1235). The tetron was tracked during a flight trajectory down the middle of the Bay at an average speed of about 9.0 km/hr until the tetron descended to the houseboat at 1235. The meteorological conditions for 21 September closely approached the "ideal" conditions for marking and monitoring a single air parcel. The pollution levels on this day were the highest observed during the course of the project.

- October 6--A tetron was released near Oakland Airport and was tracked for 1 hour (0742 to 0835). The onshore breezes developed a northerly component after 1000. Two tetroons were released downwind of San Francisco (1056 to 1140, and 1230 to 1300). The northerly wind component did not become established and onshore breezes were reestablished. Another tetron released south of Hunters Point was tracked to shallow water off Coyote Point (1446 to 1526). Although the north wind appeared established at tetron launch, wind speed deteriorated to stagnation conditions, followed by onshore breezes. Low pollutant levels and variable winds characterized this sample day.
- October 7--Onshore breezes again dominated the early morning hours. A tetron was released with an anticipated fetch toward San Francisco (0833 to 0905), but the sample run terminated because of onshore breezes. A tetron released near the Bay center was tracked for about 45 minutes (1035 to 1124). A sudden front entered the area accompanied by high winds, which ended the sample day. October 7 was characterized by low pollutant levels and unusual meteorological conditions.
- October 19--Background measurements were made off San Francisco (0825 to 0843). A tetron released near Oyster Point was tracked to Oakland Airport (1041 to 1120). The helicopter was operational during the tetron run. The Bayshore Freeway and South San Francisco provided the upward pollution sources. This day was characterized by west winds and low pollution levels.
- October 24--A tetron run was attempted south of Treasure Island but failed due to the high wind velocity. The high chloride-to-sulfur ratio in the collected particulate is evidence that clean marine air was sampled in the absence of contributions to photochemical smog.

- October 25--The houseboat laboratory mapped pollutant concentrations from Oyster Point to Oakland Airport (0545 to 0627). A tetron run was made from Oakland Airport to Oyster Point (0754 to 0855). The helicopter was operational during this run. The houseboat again mapped pollutant concentrations from Oyster Point to Oakland (0915 to 0957). The three traverses were over nearly identical paths. A tetron was released north of the San Mateo Bridge (1135 to 1220). The helicopter was operational during this tetron run. The houseboat then proceeded north to map pollutant concentrations (1215 to 1400). This day was characterized by an established east wind in the morning, deteriorating to onshore breezes in the afternoon. Pollution was light, but evidence of photochemistry was observed.
  
- October 26--Background pollutant concentration measurements were made immediately downwind of San Francisco (0716 to 0905). A tetron was released and tracked from San Francisco to Berkeley (0906 to 0948). The helicopter was operational but little data are available due to instrument malfunction. This day was characterized by variable pollutant concentration but little evidence of photochemistry.
  
- October 31--A tetron launched off Hunters Point was tracked to Alameda (1252 to 1407). The helicopter was operational during this tetron run. This day was characterized by low pollution levels with relatively high wind speeds.
  
- November 2--The houseboat mapped pollutant concentrations during the morning, when the winds were variable, from Oyster Point to San Leandro Harbor (0830 to 0954). A tetron was released and tracked from mid-Bay to south of San Mateo Bridge (1123 to 1317). The houseboat refueled and moved to Alameda (1438 to 1520). A tetron released near San Francisco traveled to the Alameda Naval Air Station (1635 to 1657). Although the pollution levels were relatively high, the tetron flight was of such limited duration that photochemistry was not observed. November 2 was characterized by light to moderate pollution with meteorological conditions approaching those suitable for measurement.

- November 6--The houseboat departed Oyster Point at 1025 with nearly calm winds. A tetron was released north of San Mateo Bridge (1218 to 1253). The helicopter was operational during this tetron flight and continued tracking the tetron after the houseboat terminated tracking. Pollutant concentrations were low with minimal photochemical activity on this day.
- November 17--The houseboat mapped pollutant concentration from Oyster Point to San Leandro Harbor (1030 to 1115). Two tetroons released simultaneously at mid-Bay between Hunters Point and Oakland Airport (1317 to 1347) floated at about the same altitude and within 60 meters of each other for the first 10 minutes. They were separated by 90 to 120 meters at the termination of the run at 1347. The wind speed during this run was about 2 m/sec. This day was characterized by variable winds and low pollution.

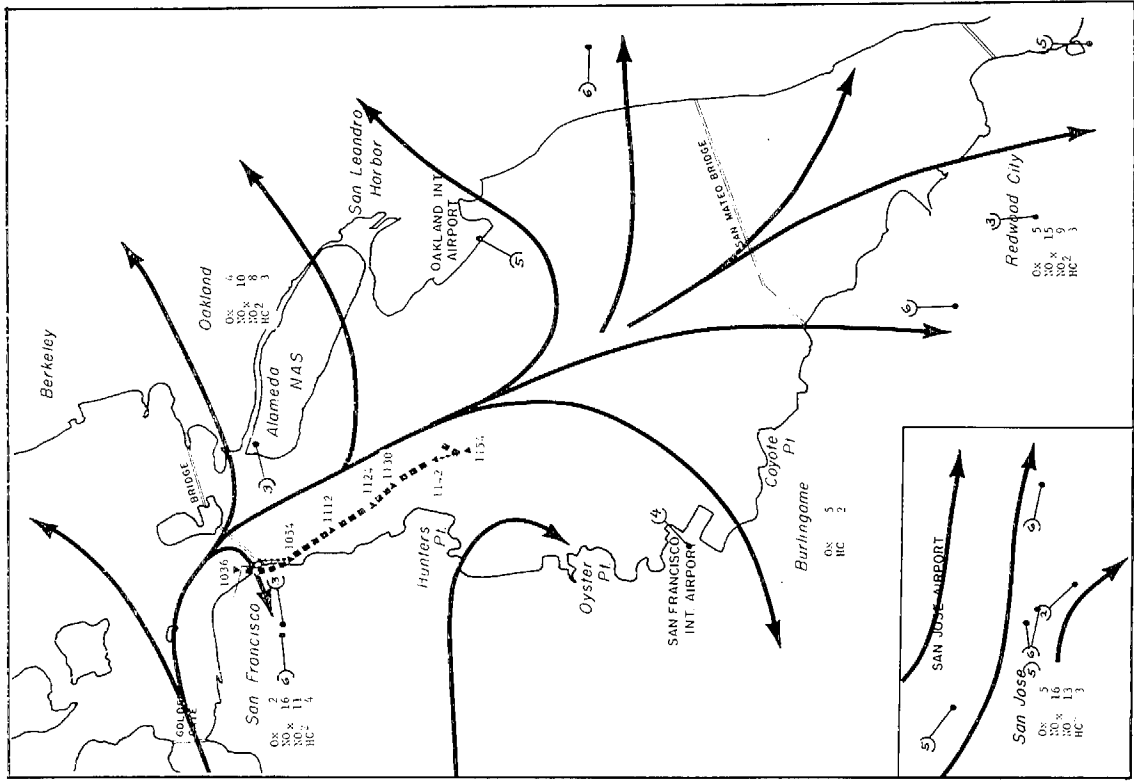
#### B. Selected Sampling Days

Four days were selected for detailed analysis. The following sections give a summary analysis for each day, including graphical presentations of meteorological conditions, houseboat and tetron paths, and pollutant concentrations. For convenience of the reader, only a summary is presented in the body of the report. Additional supporting information for users of these data will be found in Appendix E.

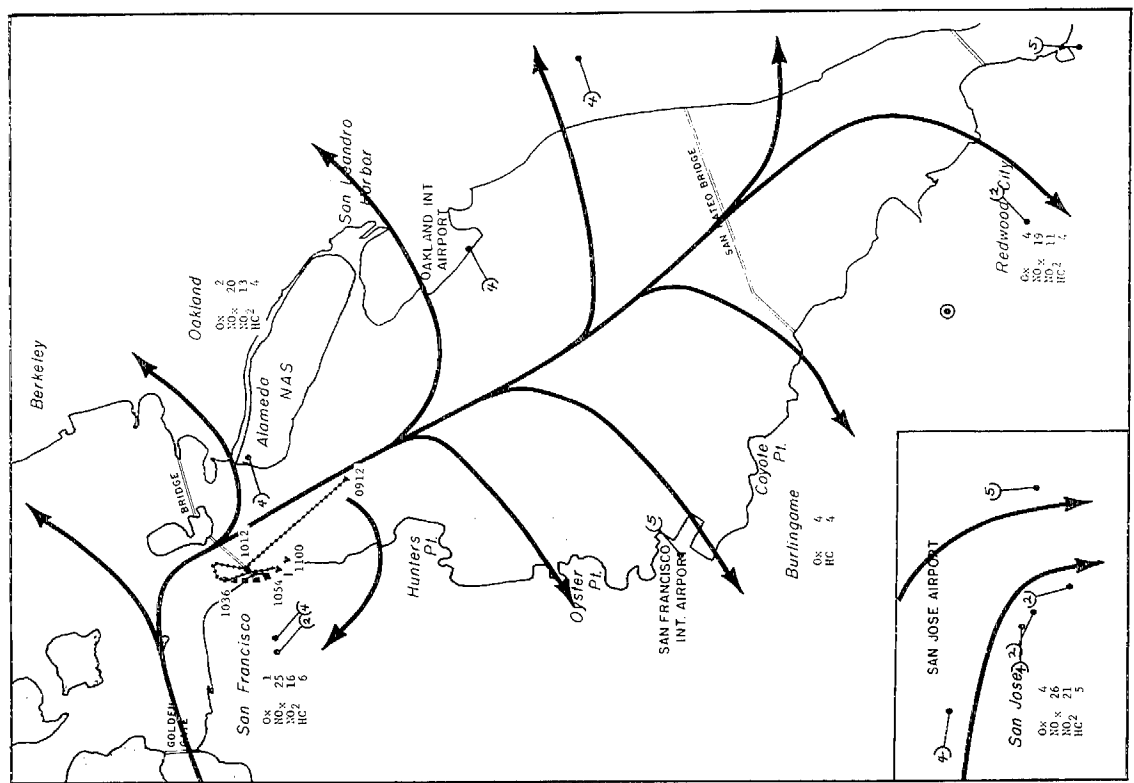
##### 1. 21 September 1972

This day was selected because the tetron run occurred under almost ideal conditions. The tetron launched downwind of San Francisco was tracked for over 2 hours down the axis of the Bay. The pollution levels were the highest observed during the operational period of the mobile laboratories.

Figures 3 through 6 are maps illustrating wind flow patterns, houseboat sampling paths, tetron trajectories, rawinsonde observations,

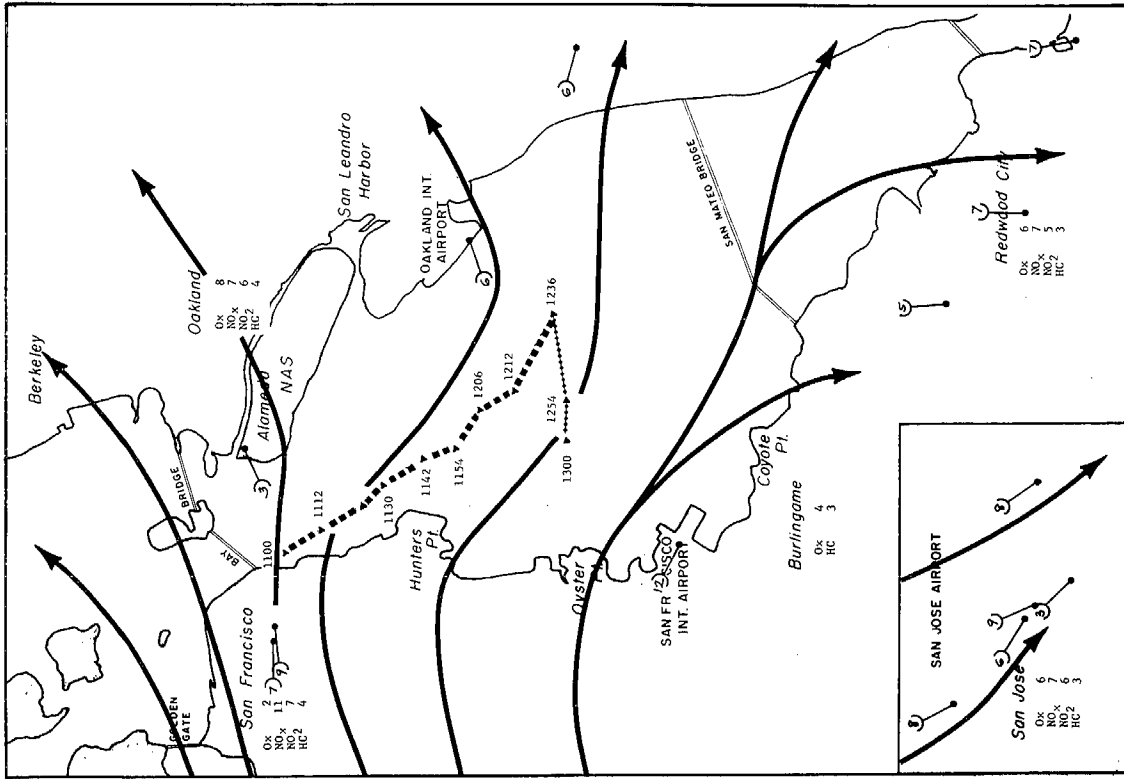


(a) 1000 PST

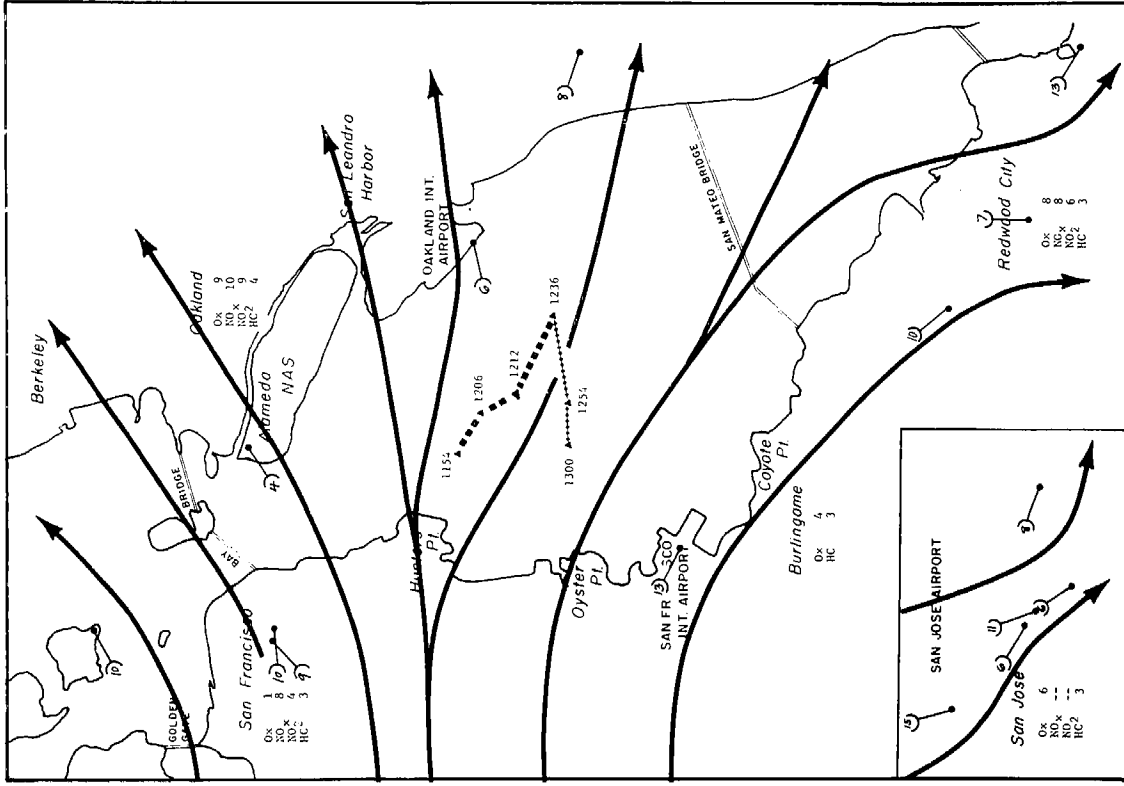


(b) 1100 PST

FIGURE 3 AIR POLLUTION LEVELS, SURFACE WIND FLOW, AND HOUSEBOAT COURSE, 21 SEPTEMBER 1972



(c) 1200 PST



(d) 1300 PST

FIGURE 3 AIR POLLUTION LEVELS, SURFACE WIND FLOW, AND HOUSEBOAT COURSE, 21 SEPTEMBER 1972 (Concluded)

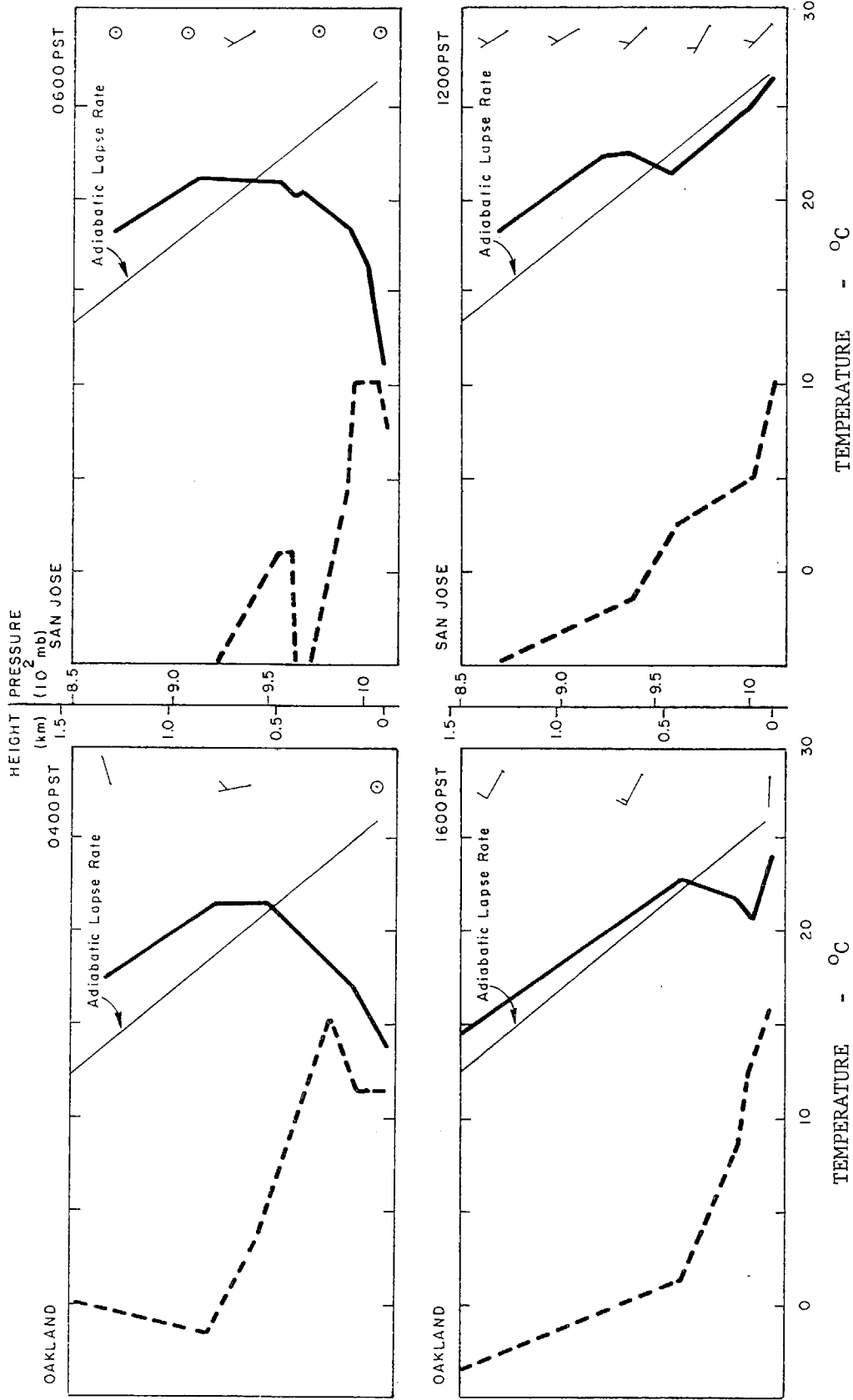


FIGURE 4 RAWINSONDE TEMPERATURE AND DEW POINT OBSERVATIONS, 21 SEPTEMBER 1972

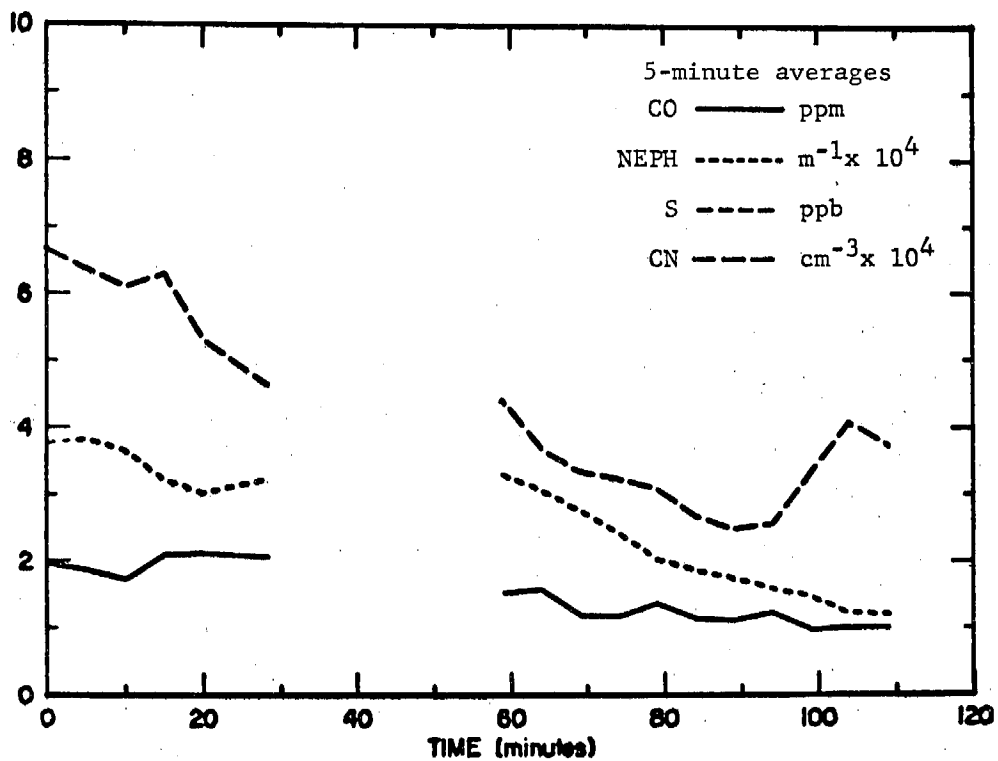
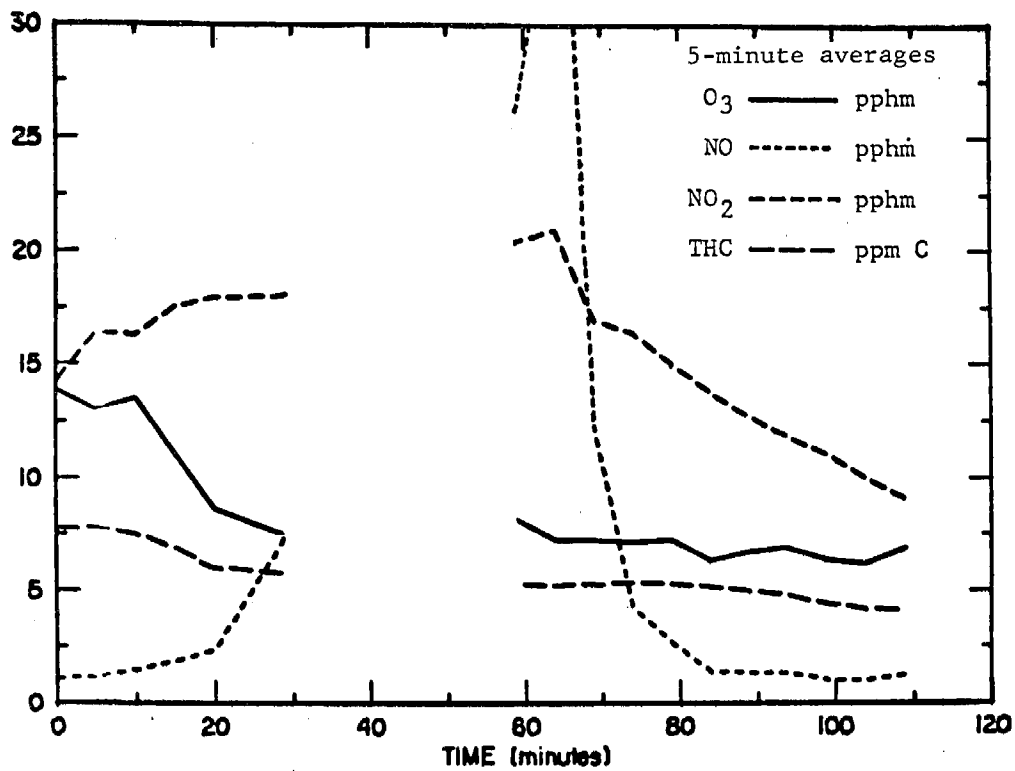


FIGURE 5 POLLUTANT CONCENTRATIONS OBSERVED DURING TETROON RUN, 21 SEPTEMBER 1972, 1037 to 1226 PST

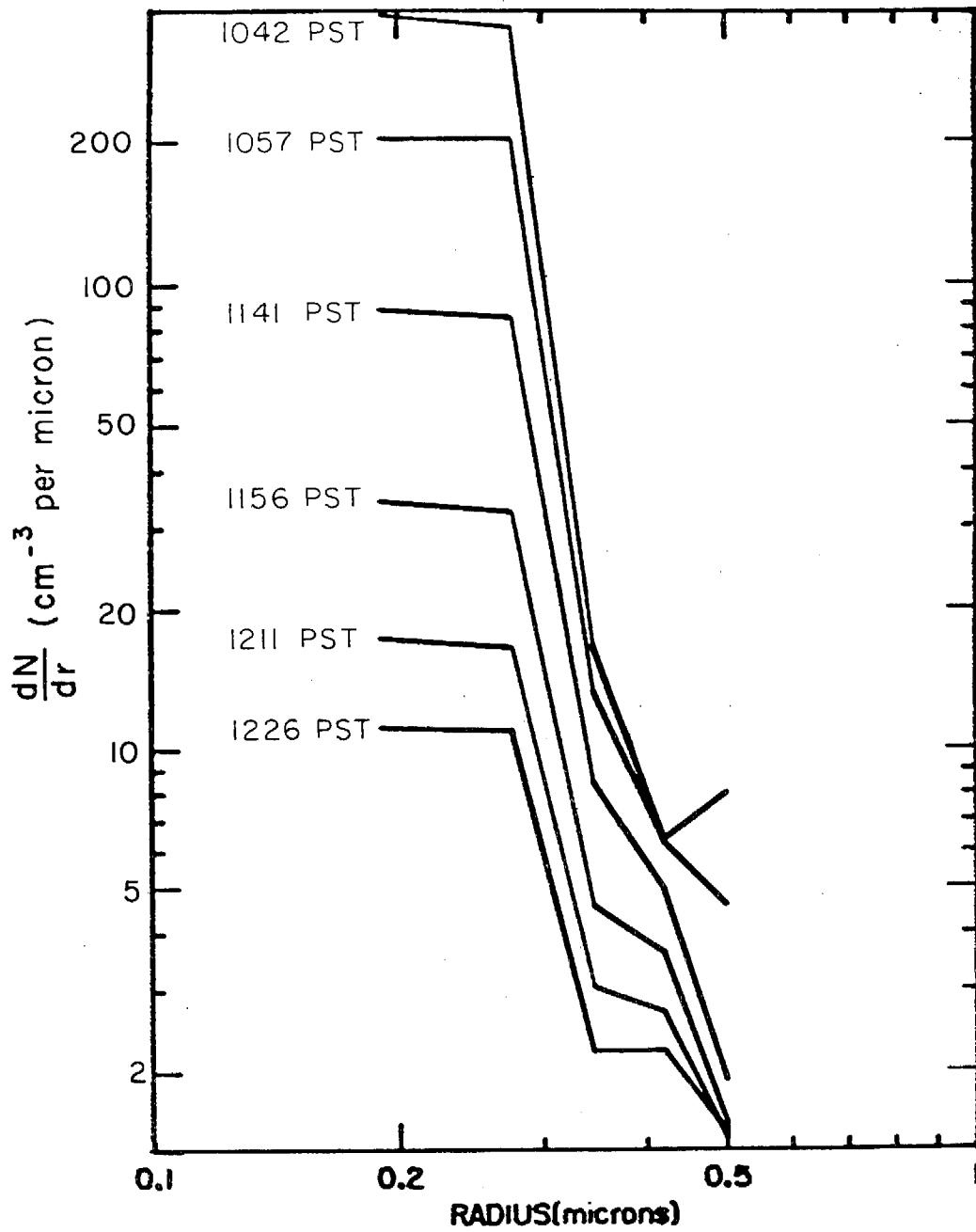


FIGURE 6 AEROSOL PARTICLE COUNTER DATA FOR VARIOUS AVERAGE TIMES, 21 SEPTEMBER 1972

pollutant concentrations, and aerosol particle data. The morning soundings for Oakland and San Jose showed a strong surface-based inversion extending to 0.5 kilometers thick isothermal layer causing very stable conditions. The noon San Jose soundings and the afternoon Oakland sounding showed that the inversion persisted throughout the day.

Meteorological observations showed calm or light winds around San Francisco during the early morning hours. From about 0900 to 1100, southeasterly air flow was observed in San Francisco; the winds in the South Bay were predominantly onshore so that wind direction was dependent on shoreline orientation. Between 1200 and 1300, a strong westerly sea breeze developed and rapidly blew the polluted air out of the Bay Area.

Samples collected near Hunter's Point from 0915 to 1000 indicated that the air mass was well aged and that substantial pollution levels were present ( $\text{NO} \sim 5$  pphm,  $\text{NO}_2 \sim 15$  pphm,  $\text{O}_3 \sim 4$  pphm). Therefore, the houseboat was moved to a location about 1 mile north of the Bay Bridge and 1 mile east of San Francisco and a tetron was released (1030). The concentration of NO averaged 6 pphm,  $\text{NO}_2$  averaged 15 pphm, and  $\text{O}_3$  averaged 5 pphm. The ratio of NO to  $\text{NO}_2$  was low, a characteristic of well-aged smog. The  $\text{O}_3$  concentration was also relatively high. The tetron drifted slowly toward San Francisco and passed over the shoreline at 1037.

The tetron was over the land between 1037 and 1056. During this interval it rose several hundred feet but was never more than 200 meters from the shoreline. Because the computer failed between 1105 and 1130, no data are available for this interval. However, the 5-minute average at 1102 (30 minutes elapsed time) is the pollutant concentration measured immediately after the houseboat resumed track-

ing of the tetroon. The NO and NO<sub>2</sub> concentrations increased and the O<sub>3</sub> concentration decreased while the air mass was over San Francisco.

The tetroon was tracked until it descended to the houseboat at 1235. If the tetroon had not descended, it probably could have been tracked for 1 to 2 more hours. During this interval, both photochemical activity and dilutional effects were observed.

There was a data acquisition system failure between 1105 and 1130, probably due to the decrease in the voltage output of the batteries used to power the computer. When the computer was started again, the concentration of NO was observed to be very high. As can be seen from the houseboat course (Figure 3), the houseboat was just below the Pacific Gas and Electric (PG&E) power plant stacks at Hunters Point and Potrero Point and may have passed through their plumes. To examine this possibility in greater detail, a simple model was used to evaluate the importance of two large, point sources of oxides of nitrogen in the southeastern part of the city of San Francisco. These two power plants, about 3.1 kilometers apart, emit a total of about 15 tons per day of NO<sub>x</sub>.<sup>10</sup> The stacks at these plants are about 75 meters or less in height. To calculate concentrations, an equation was used to describe concentrations under conditions where diffusion proceeds fairly rapidly below an elevated inversion that prevents transfer of material to greater heights.<sup>11</sup>

The potential contribution of the power plants to the observed NO concentrations at 1040 on 21 September was estimated using wind speed and direction based on the observed trajectory of the tetroon. The path of the houseboat was generally along the periphery of the areas where the NO concentrations from the power plants were predicted to be a few parts per billion or less. At the center of these plumes, calculations indicated that NO concentrations could reach several tens of parts per billion. These calculated concentrations are based on hourly average concentrations.

The atmospheres below about 3000 meters was moderately unstable during the morning of 21 September, based on Turner's stability algorithm.<sup>12</sup> This unstable layer was capped by an inversion, hence, providing the necessary elements for "fumigation," and relatively large, short-term fluctuations of concentration. The period of high NO concentrations observed between 1134 and 1146 may have been caused by NO from the Potrero power plant. The plume from this plant may have penetrated the inversion layer at an earlier time and drifted over the area to the southeast with little lateral or vertical spreading; then as the lower parts of the inversion layer disintegrated, the relatively high concentrations may have been mixed to the surface by the motions in the moderately unstable air below. The increases in NO concentration are unaccompanied by comparable increases in the concentration of CO or CN, thereby indicating non-automotive pollution. Furthermore, the morning sounding at Oakland showed near calm winds within the inversion layer, a condition likely to cause the accumulation of relatively large pollutant concentrations within the layer. Admittedly, the above explanation cannot be fully documented, however, it appears to offer a reasonable explanation for the observations.

The aerosol particle counter (APC) data are summarized in Figure 6. Each point is  $dN/dr$ , which is the average number of particles per cubic centimeter per micron, measured during a 15-minute interval versus the particle size range for the channel. The lines connect counts for the same time period, as indicated by the average time adjacent to each line. The observation that there were equal number of particles in the 0.2-micron and 0.3-micron ranges was unexpected. Based on previous observations by SRI and other laboratories, the 0.2-micron particle count should be much larger than the 0.3-micron count. The dilutional effects can account for only about one-half of the dramatic decrease in the number of particles during the tetroon run. The remainder is probably due to evaporation of water from the particles.

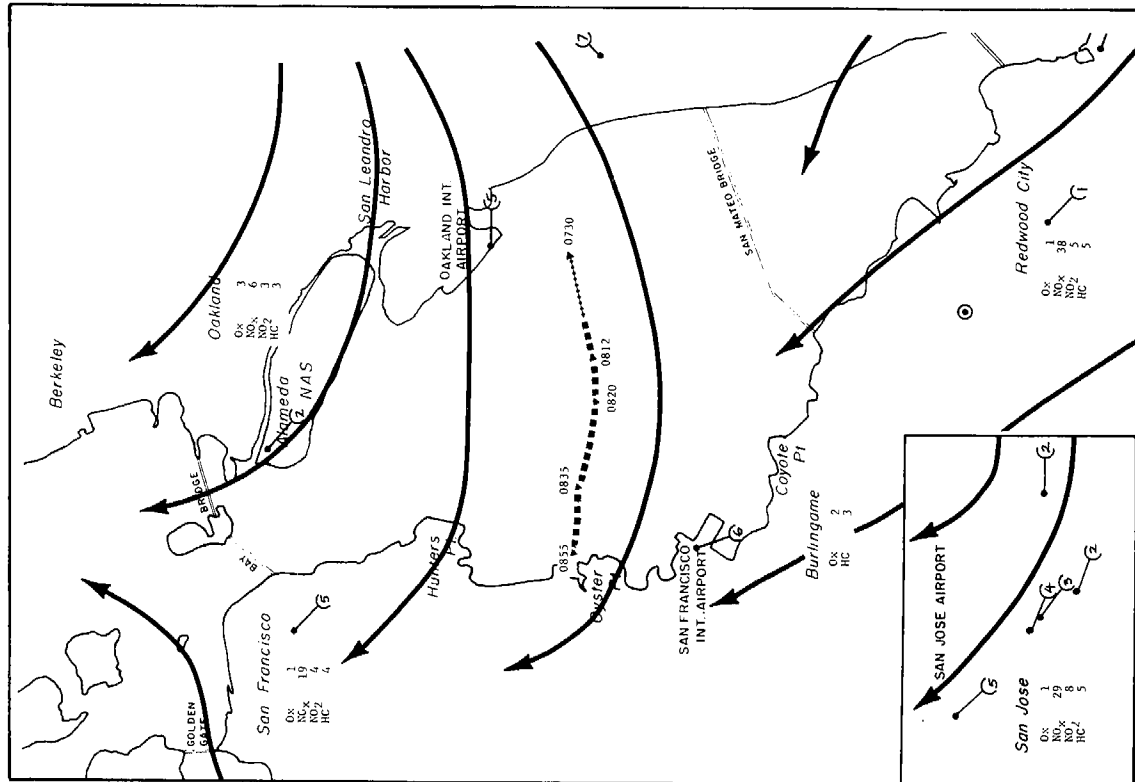
This day was the first test of the houseboat mobile laboratory. Difficulties with the temperature sensor and the steady voltage decrease of the computer power supply resulted in the loss of valuable data. The highest smog levels for the entire sampling program were observed that day. It was also a day of ideal meteorological conditions; the air flow was southeasterly down the axis of the Bay at about 5 mph. If the tetroon had not descended to the surface because of a leak, the run would have been at least 4 hours instead of 2 hours. The high NO concentrations observed near Hunters Point were observed again on other days. On this particular day, the concentrations can be ascribed with near certainty to a portion of the Potrero PG&E power plant plume. On later days, the explanation is not as definitive. The experiment was highly successful in that it demonstrated that under meteorological conditions conducive to smog formation, valid pollutant concentration data can be obtained and the wind speeds and direction are such that long intervals of tetroon tracking are likely.

## 2. 25 October 1972

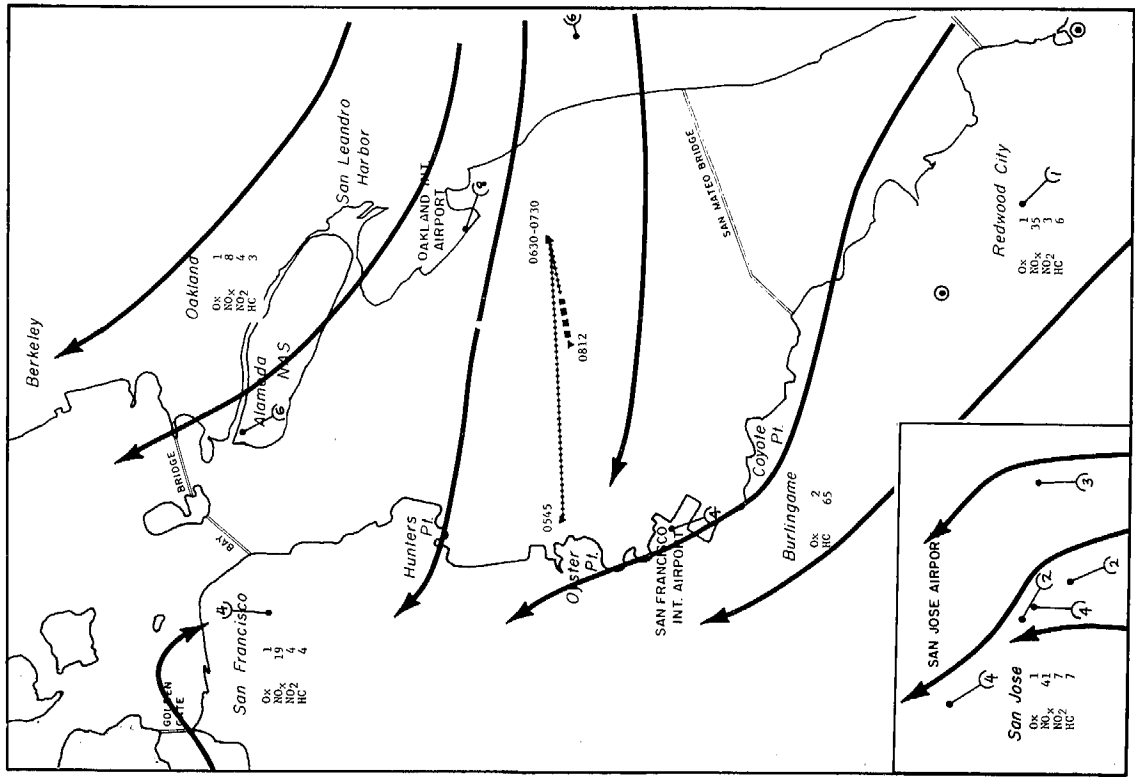
This sampling day was selected because a tetroon run was made in conjunction with airborne measurements of concentration gradients during an interval of photochemical activity. In addition, pollutant concentration mapping of the South Bay showed interesting evidence of pollutant inhomogeneities over the Bay.

Figures 7 through 12 are maps illustrating wind flow patterns, houseboat sampling paths, tetroon trajectories, rawinsonde observations, helicopter flight paths, pollutant concentrations, and aerosol particle data.

In the early morning, offshore breezes dominated the area. An easterly wind was established before 0800 and continued until about 1000. The onshore breeze was reestablished after 1000 and dominated the remainder of the day.

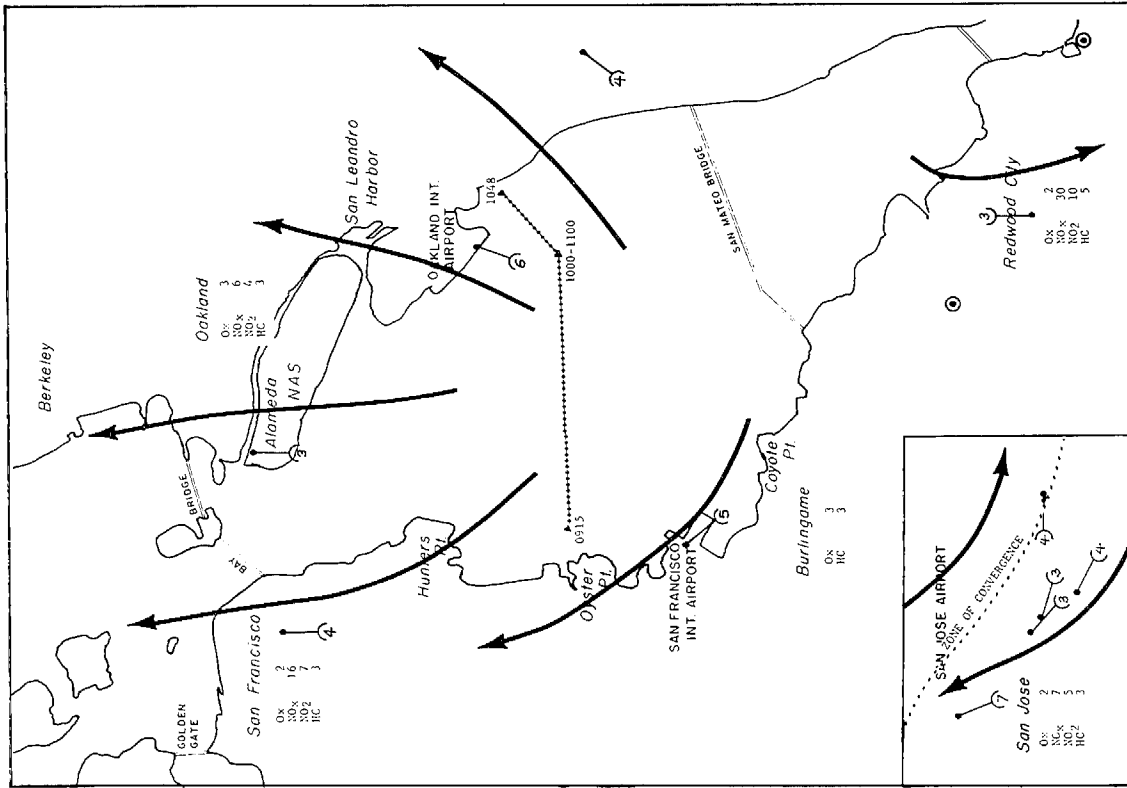


(a) 0700 PST

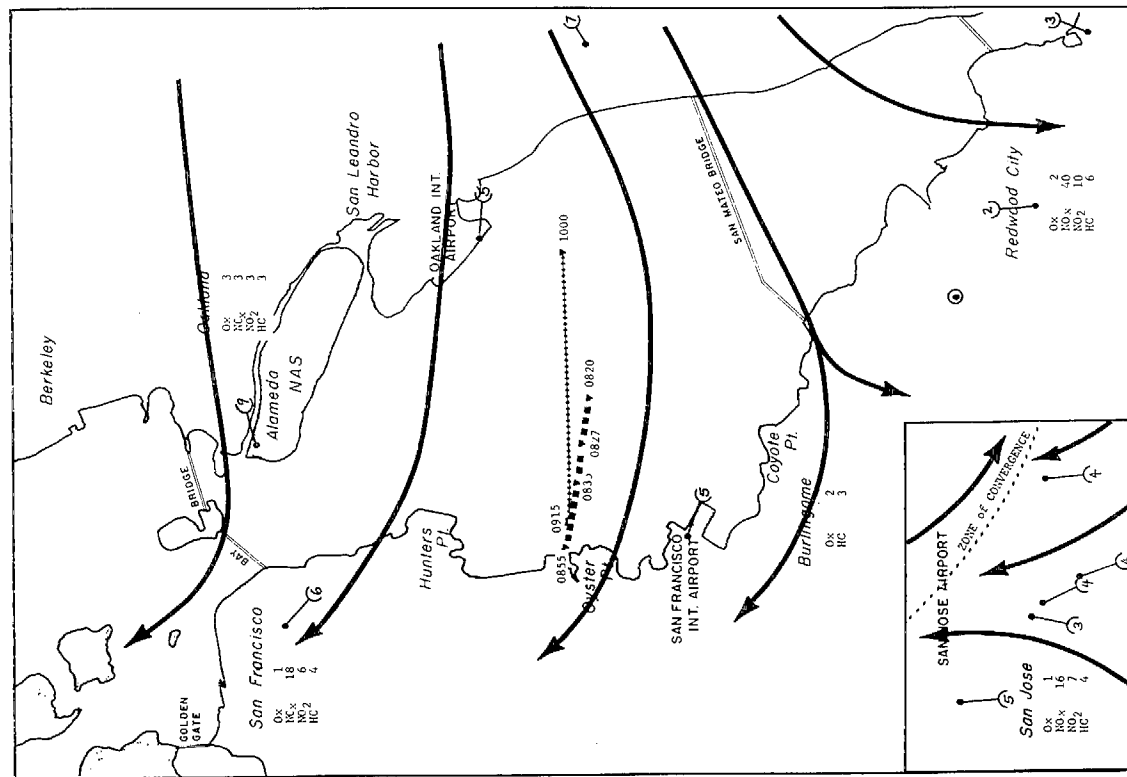


(b) 0800 PST

FIGURE 7 AIR POLLUTION LEVELS, SURFACE WIND FLOW, AND HOUSEBOAT COURSE, 25 OCTOBER 1972

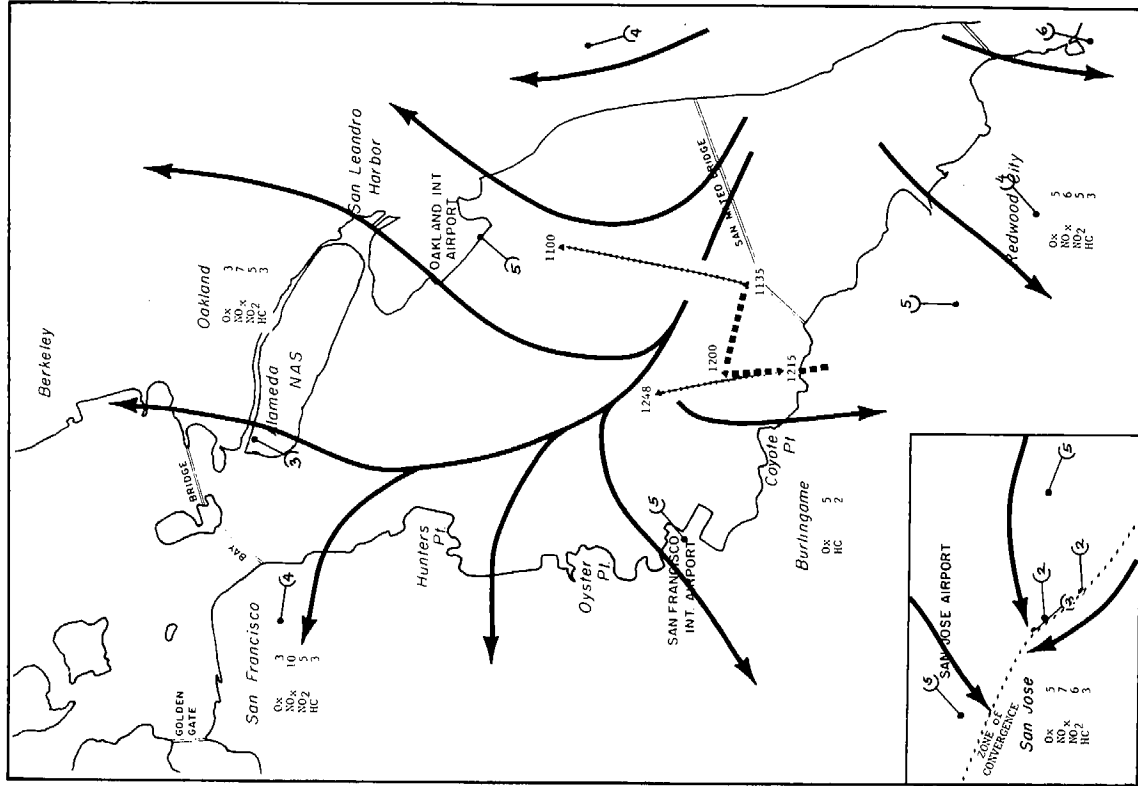


(c) 0900 PST

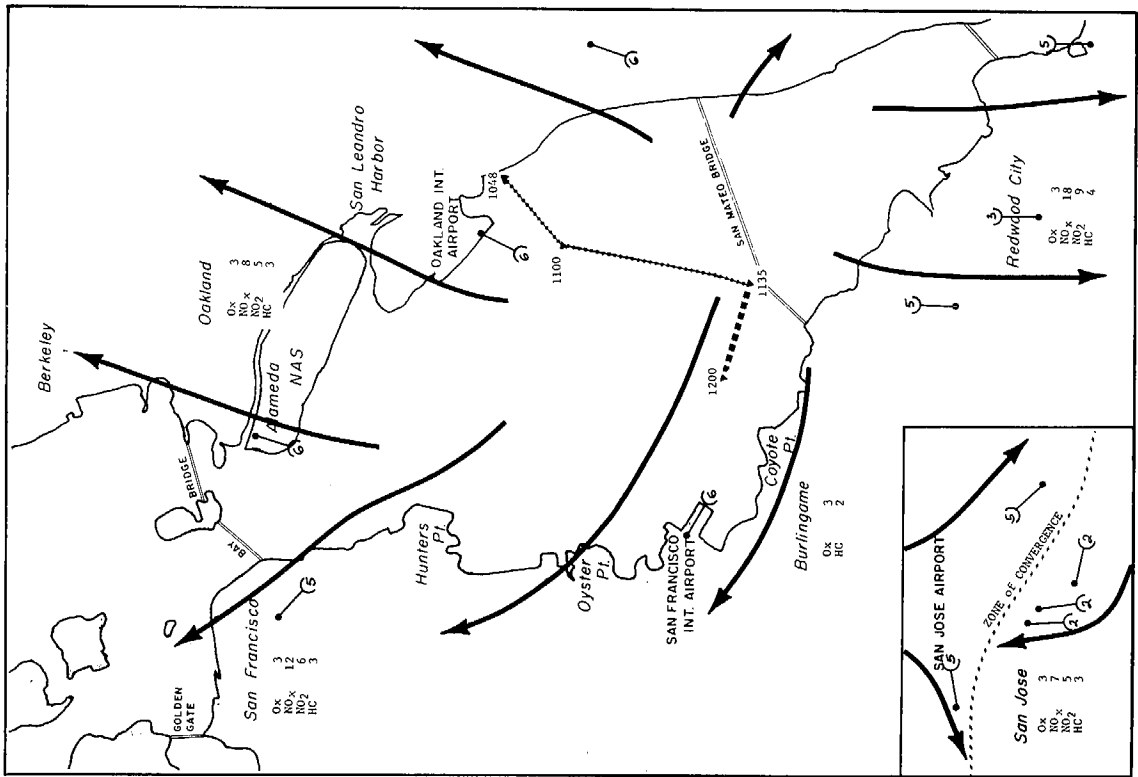


(d) 1000 PST

FIGURE 7 AIR POLLUTION LEVELS, SURFACE WIND FLOW, AND HOUSEBOAT COURSE, 25 OCTOBER 1972 (Continued)

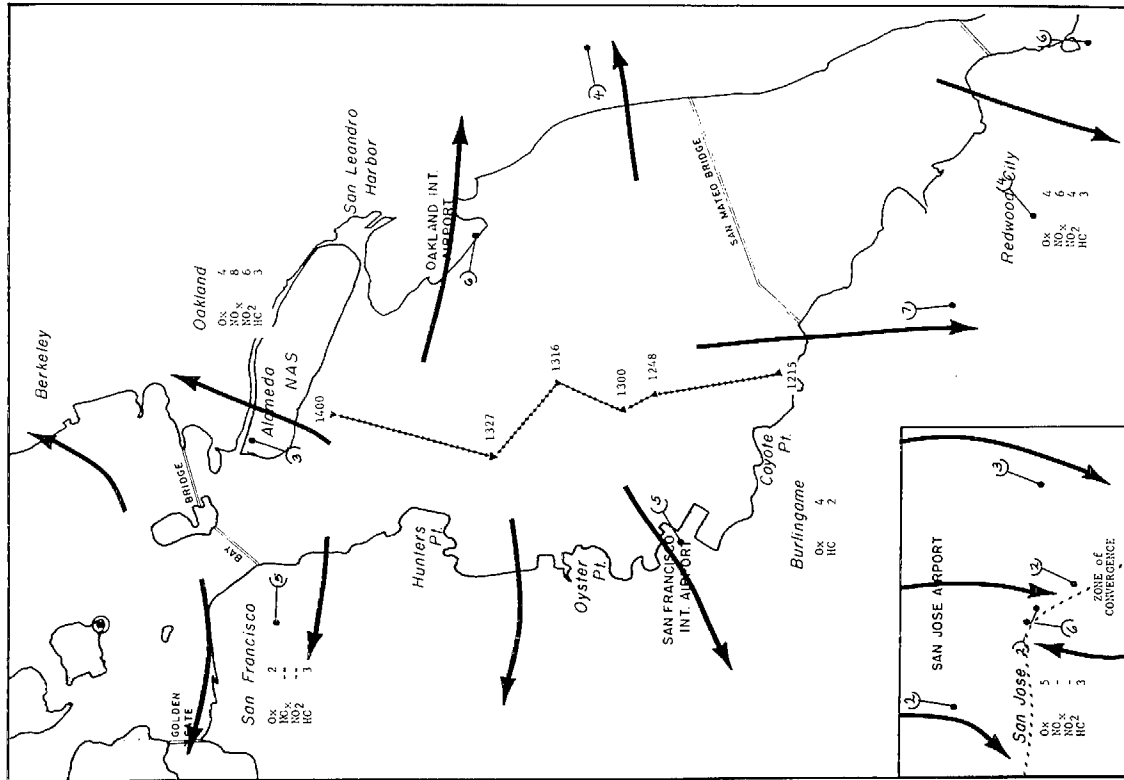


(f) 1200 PST



(e) 1100 PST

FIGURE 7 AIR POLLUTION LEVELS, SURFACE WIND FLOW, AND HOUSEBOAT COURSE, 25 OCTOBER 1972 (Continued)



(g) 1300 PST

FIGURE 7 AIR POLLUTION LEVELS, SURFACE WIND FLOW, AND HOUSEBOAT COURSE, 25 OCTOBER 1972 (Concluded)

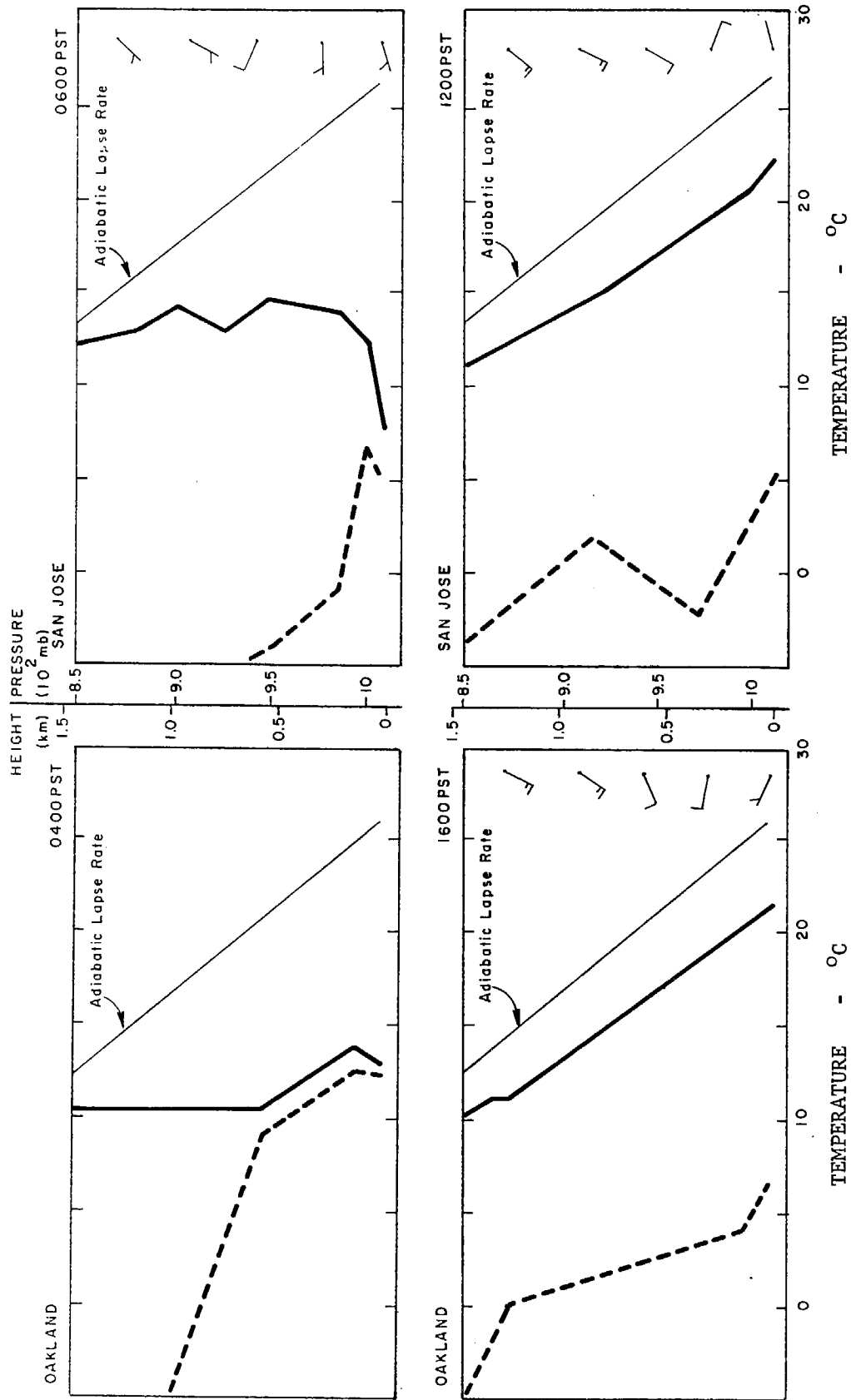


FIGURE 8 RAWINSONDE TEMPERATURE AND DEW POINT OBSERVATIONS, 25 OCTOBER 1972  
 (Temperature ———, Dew Point - - - - )

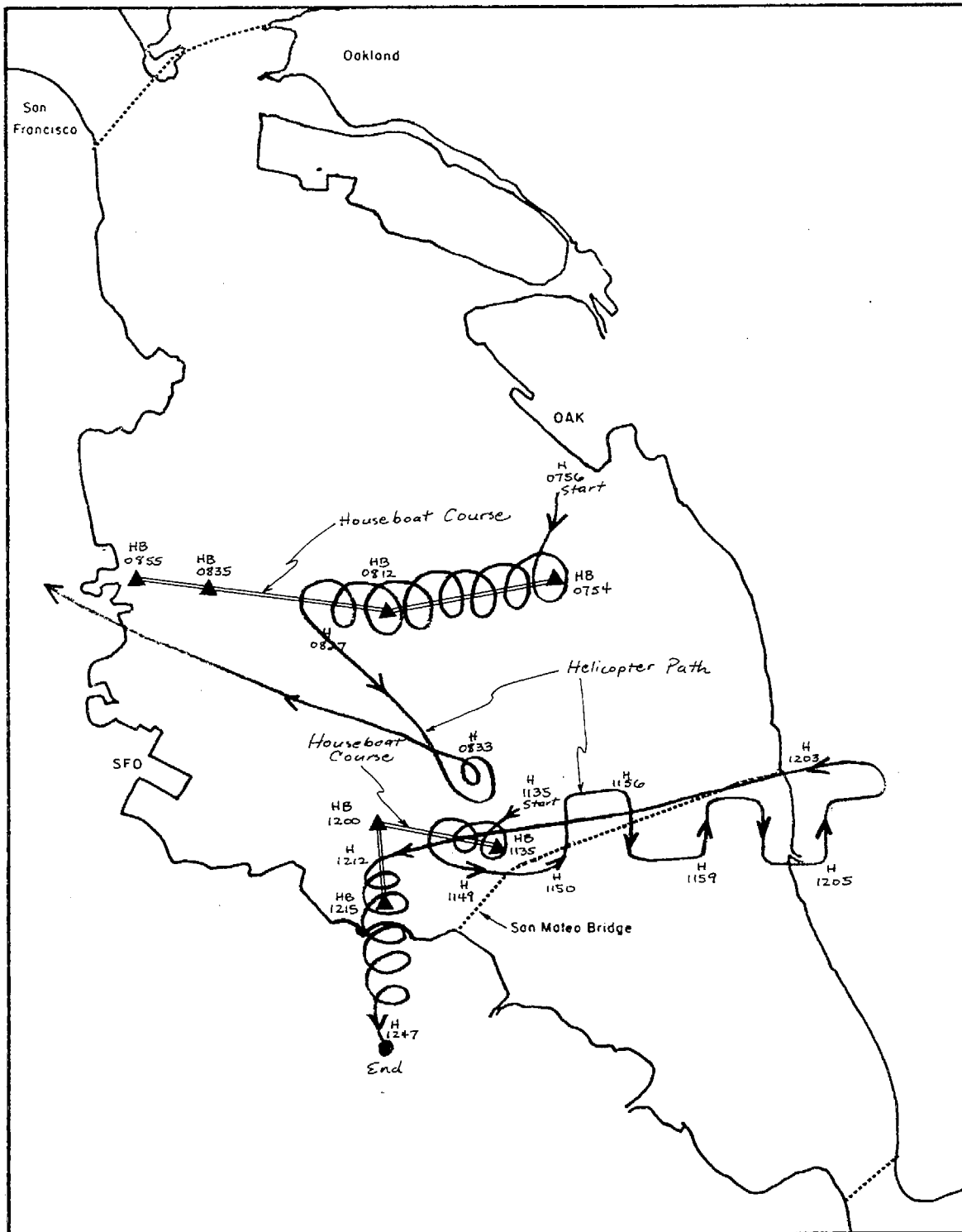


FIGURE 9 SAMPLING PATHS OF MOBILE LABORATORIES ON 25 OCTOBER 1972  
(HB - houseboat, H - helicopter)

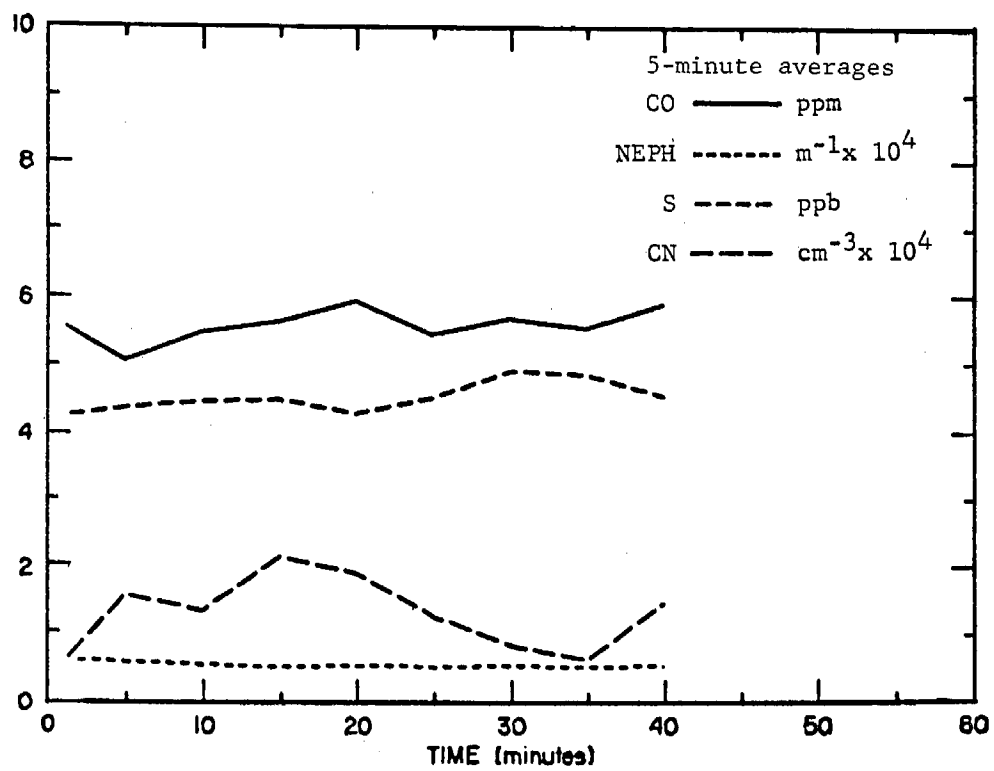
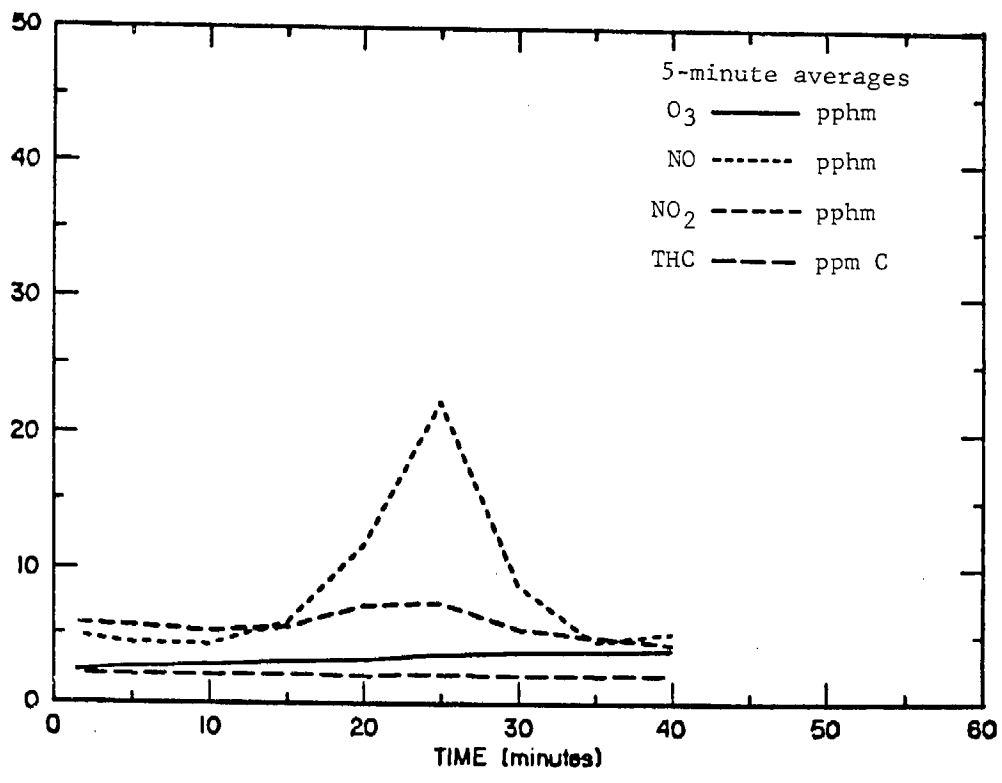
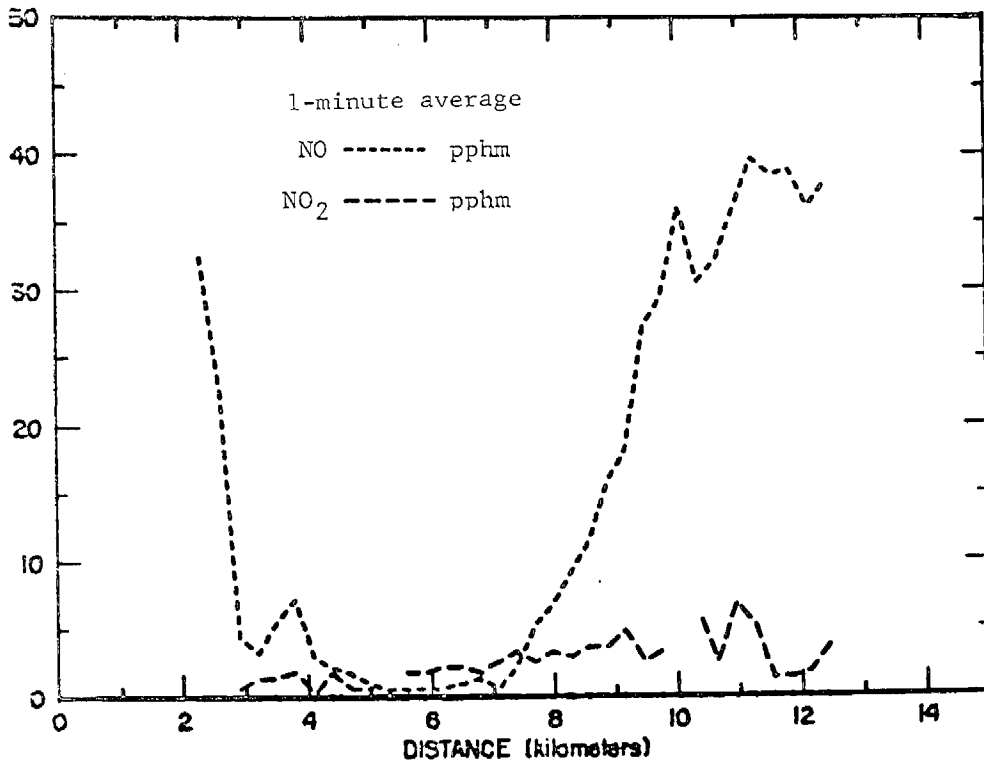
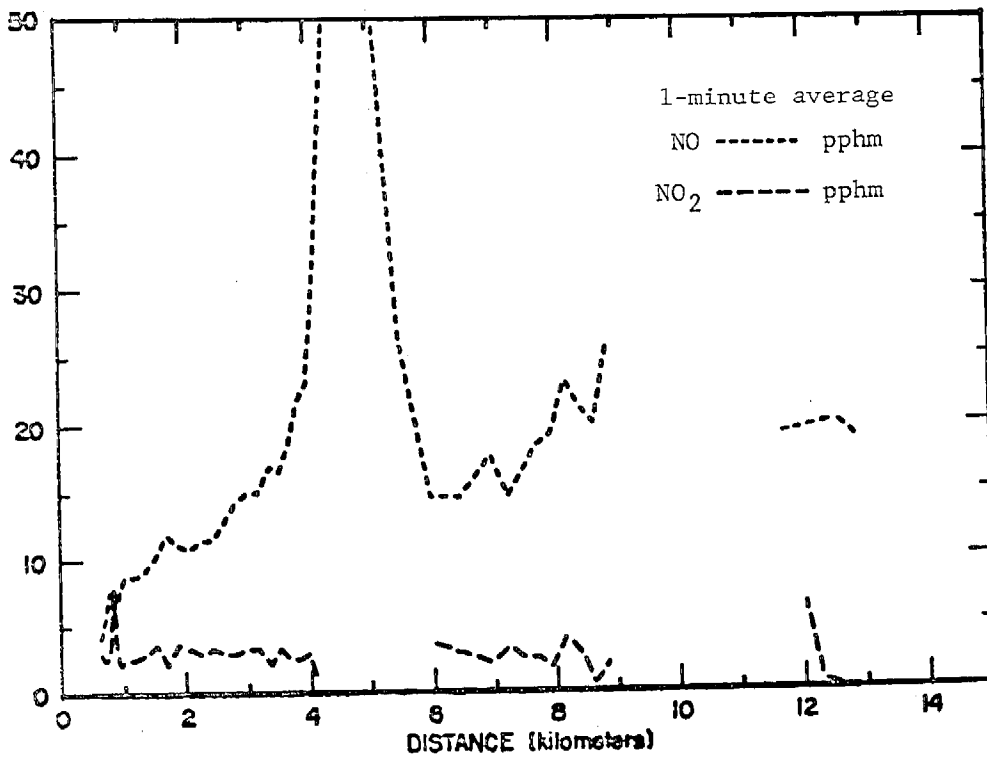


FIGURE 10 POLLUTANT CONCENTRATIONS OBSERVED DURING TETROON RUN, 25 OCTOBER 1972, 1138 to 1218 PST

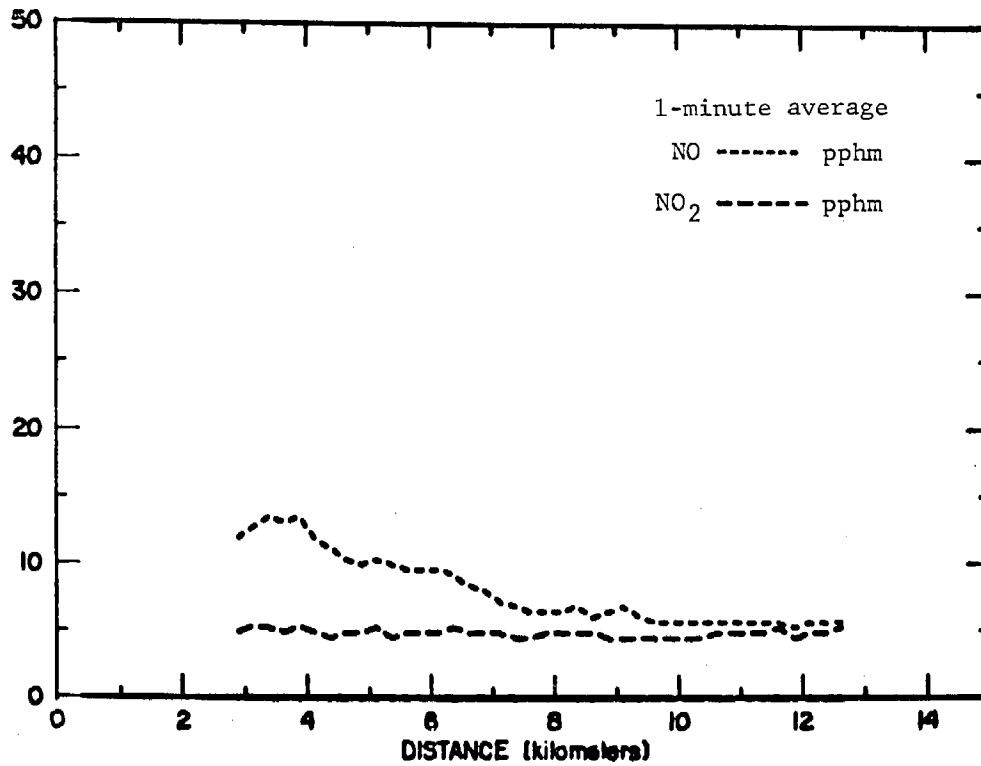


(a) WEST TO EAST, 0551 to 0625 PST



(b) EAST TO WEST, TRACKING TETROON, 0758 to 0855 PST

FIGURE 11 POLLUTANT MEASUREMENTS DURING TRAVERSES OF THE BAY,  
 25 OCTOBER 1972



(c) WEST TO EAST, 0916 to 0955 PST

FIGURE 11 POLLUTANT MEASUREMENTS DURING TRAVERSES OF THE BAY,  
 25 OCTOBER 1972 (Concluded)

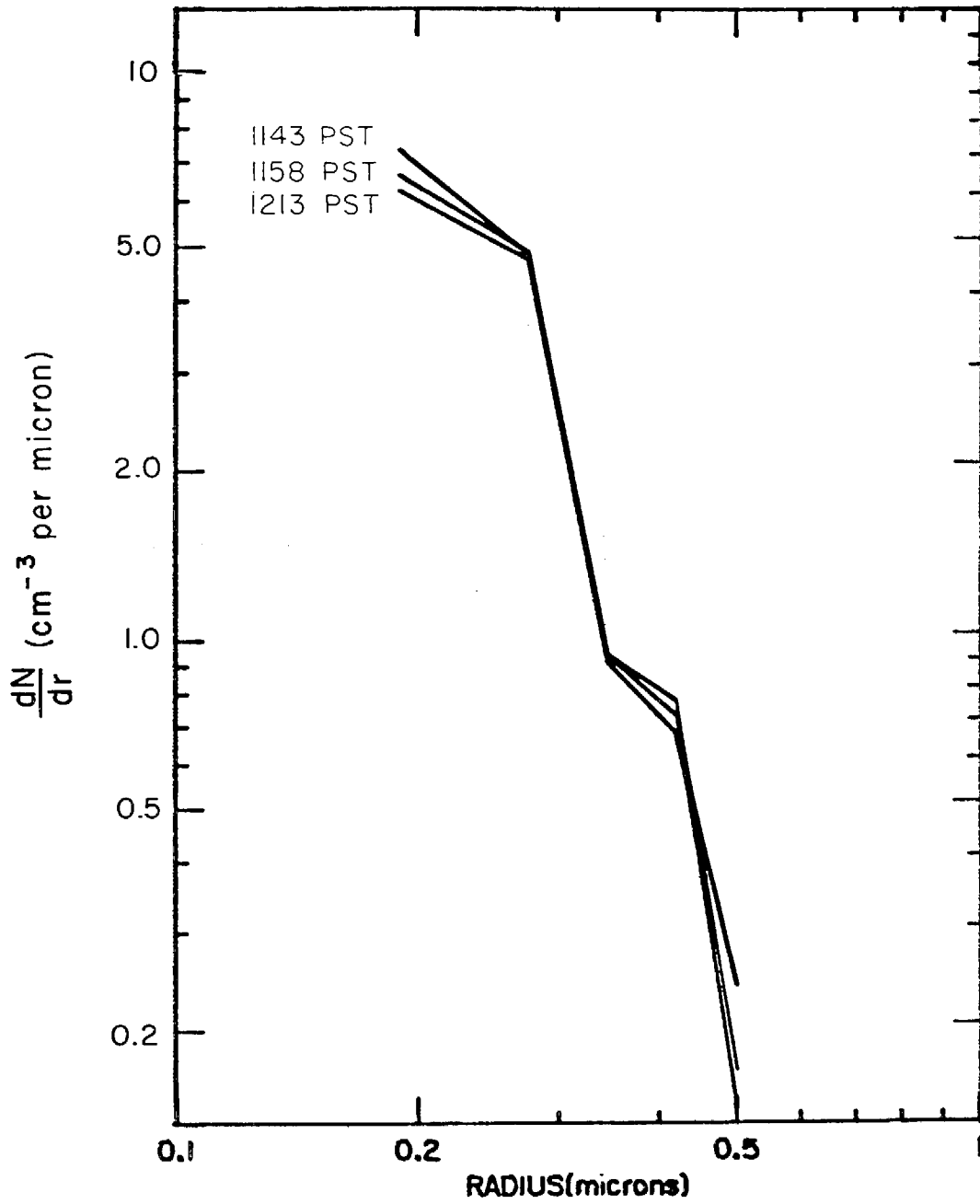


FIGURE 12 AEROSOL PARTICLE COUNTER DATA FOR VARIOUS AVERAGE TIMES,  
25 OCTOBER 1972, 1143 to 1226 PST

The rawinsonde data, shown in Figure 8, indicate that a shallow inversion (90 meters) was observed at Oakland Airport at 0400. The helicopter soundings measured from 0831 to 0849 indicate that the atmosphere was relatively stable at the lower altitudes and that the soundings more nearly resembled those obtained at San Jose from the 0600 rawinsonde than those from Oakland.

Two tetroon runs were made on 25 October, the first 0756 to 0857, and the second 1135 to 1220. The first run was not analyzed since complete air quality data were not available due to instrument malfunctions. The path of the second tetroon run is shown in Figure 7. The tetroon, released near the San Mateo Bridge, drifted west until a period of stagnation occurred at 1156 that lasted until 1208. When the tetroon began moving again, the wind direction had shifted, causing the tetroon to move southward as shown in Figure 7(f). During the period of stagnation, the tetroon continued to move at slow speeds with erratic direction of flight. Contamination by the exhaust gases of the houseboat was unavoidable during this interval.

The plots of pollutant concentrations versus time are shown in Figure 10 for  $O_3$ , NO,  $NO_2$ , and THC. The  $O_3$  plot indicates a concentration increase during the sampling run, though it must be emphasized that the observed  $O_3$  concentration was not substantially above background levels. The  $O_3$  concentration increased from 2.4 pphm to 4.0 pphm during the 45-minute interval of the tetroon run. The increase in  $O_3$  during this sample run indicates that photochemistry had taken place. The THC concentration decreased during this interval from 2.2 ppm C to 2.0 ppm C. This reduction in THC, though not large, is greater than experimental error.

A plot of total S, nephelometer, CN, and CO is shown in Figure 10. The concentration of CO remains relatively constant throughout the tetroon run, indicating that the marked air parcel was undergoing dilution with adjacent air parcels containing similar concentrations of CO as the marked parcel rather than unpolluted air. The total sulfur concentration increased during the tetroon run from 8.5 ppb to 9.7 ppb. This could be attributed to presence of shallow water with decomposition of organics on the mud floor of the Bay.

The CN count varied considerably on a short term basis throughout the tetroon run. A corresponding increase in NO that would substantiate exhaust gas contamination was not observed until stagnation. The NO to NO<sub>2</sub> ratio indicates the presence of well-aged smog even though the sample run was started downwind of the San Mateo Bridge. The source of pollutants is probably auto exhaust from the East Bay or the South Bay. The emissions from automobiles on the San Mateo Bridge did not significantly alter the pollutant mixture. During the tetroon run, pollutant measurements were made by the helicopter to determine concentration gradients. Table 4 is a comparison of houseboat measurements with the helicopter measurements. The concentration gradient measurements made by the helicopter from 1148 to 1210 are not included in Table 4. The helicopter continued to track the tetroon after houseboat tracking was terminated.

The helicopter measurements correlate reasonably well with the concentrations observed on the houseboat (except for NO<sub>x</sub> concentrations at 1142 and 1148). Vertical and horizontal pollutant concentration gradients were small. The measurements from the helicopter indicate that the pollutant concentrations decreased until near background levels were reached after the houseboat terminated the run.

Table 4

DATA FOR 25 OCTOBER 1972, 1137 TO 1258 PST  
(1-Minute Averages)

Houseboat					Helicopter					
Time	NO (pphm)	NO <sub>x</sub> (pphm)	O <sub>3</sub> (pphm)	Temp (°C)	Time	Alt (ft)	NO (pphm)	NO <sub>x</sub> (pphm)	O <sub>x</sub> (pphm)	Temp (°C)
1137	5.6	11.9	2.3		1137	200	4.8	9.6	1.8	24.2
1140	5.3	11.9	2.3		1140	300	5.0	10.0	1.7	24.2
1142	4.5	11.6	2.7		1142	350	2.4	4.8	2.0	24.2
1148	4.9	10.7	2.7		1148	500	1.2	4.8	1.8	24.2
1210	6.8	13	3.9	24.4	1210	500	4.8	7.2	2.2	24.4
1212	6.4	12.3	3.5	24.1	1212	500	7.2	9.6		24.4
1215	2.9	8.9	3.9	23.8	1215	500	3.6	3.6	2.8	24.4
					1225	500	1.5	7.0	3.2	24.3
					1230	500	1.0	1.5	2.2	24.3
					1235		1.0	1.5	1.8	24.3
					1240		1.0	2.0	1.7	24.3
					1245		1.0	2.0	2.0	24.4
					1258		1.5	2.5	2.0	24.4

On 25 October the inhomogeneous distribution of NO concentrations over the Bay was observed. Three traverses across the Bay between Oyster Point and San Leandro Harbor were made over nearly identical paths: the first, west to east 0545 to 0627; the second, a tetraon run, east to west 0756 to 0857; and the third, west to east at 0916 to 0955. The concentration of NO and NO<sub>2</sub> for these traverses was plotted as a function of distance, as shown in Figure 11. The NO<sub>2</sub>, CO, THC, and O<sub>3</sub> concentrations did not vary appreciably during these traverses, except during the interval of the exhaust gas contamination at 5 kilometers from the western shore, as shown in Figure 11(b). However, large variations in

NO concentrations were observed during all traverses. During the first traverse the low concentrations of NO at the center of the Bay are probably the result of limited encroachment of polluted air from the shore during the early morning offshore breezes. The NO concentration plots for the second and third traverses indicate that the air mass containing high NO concentration advected toward the western shore of the Bay.

From 1220 to 1255 on 25 October, we again observed the inhomogeneity of NO concentrations over the Bay. Over a distance of about 5 kilometers, the NO concentration changed, on the basis of 5-minute averages, from 5.2 pphm to nearly 40 pphm and then decreased to 6.7 pphm. During this interval the changes in other pollutants, on a 5-minute average basis, were CO = 5.4 ppm  $\pm$  0.5 ppm, THC = 1.9 ppm C  $\pm$  0.1 ppm C, O<sub>3</sub> = 4.7 pphm  $\pm$  0.7 pphm, CN = 15.1  $\times$  10 cm<sup>-3</sup>  $\pm$  5.0  $\times$  10 cm<sup>-3</sup>, and NO<sub>2</sub> = 6.0 pphm  $\pm$  2.6 pphm (Appendix E, Table E-10). On the basis of meteorological observation from shore stations and the houseboat, this "pocket" of high NO concentrations could not be attributed to the emissions from the power plants located at Potrero Point and Hunters Point.

Particulate data were also collected on 25 October. The APC data are summarized in Figure 12; Table 5 is the chemical analyses of the particulate matter collected on a high-volume filter. In contrast to the APC data for 21 September, the particle size distribution did not change with time during the tetron run on 25 October. However, the meteorological conditions were very different, since hot, dry air from the southeast was blowing across the Bay. On the other hand, the chemical analysis of the collected particulate is similar to that collected on 2 November and 6 November (see Section V.B.4 and Appendix C for complete data).

Table 5

CHEMICAL ANALYSIS OF PARTICULATE MATTER COLLECTED  
ON GLASS FIBER FILTERS, 25 OCTOBER 1972

Time (PST)	Mass Loading ( $\mu\text{g}/\text{m}^3$ )	Chemical Composition ( $\mu\text{g}/\text{m}^3$ )			
		Nitrate	Sulfur	Chloride	Lead
0800-1104	108	9.6	3.7	2.5	2.7
1235-1320					

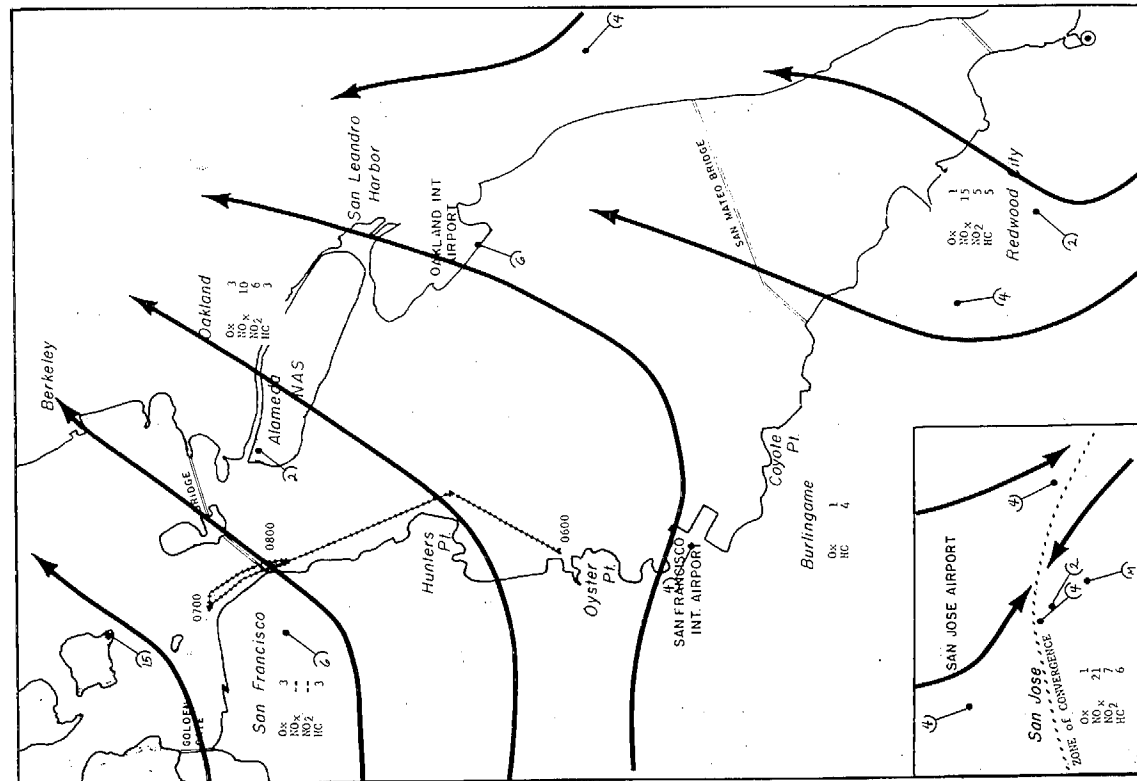
3. 26 October 1972

This date was selected to document the observed inhomogeneities of pollutant concentrations immediately downwind of San Francisco. A tetroon run without evidence of photochemical activity was analyzed to describe the complex dispersion and dilution processes observed over the Bay. In addition an area of high NO concentration was observed that can be at least partially attributed to power generating plants south of San Francisco.

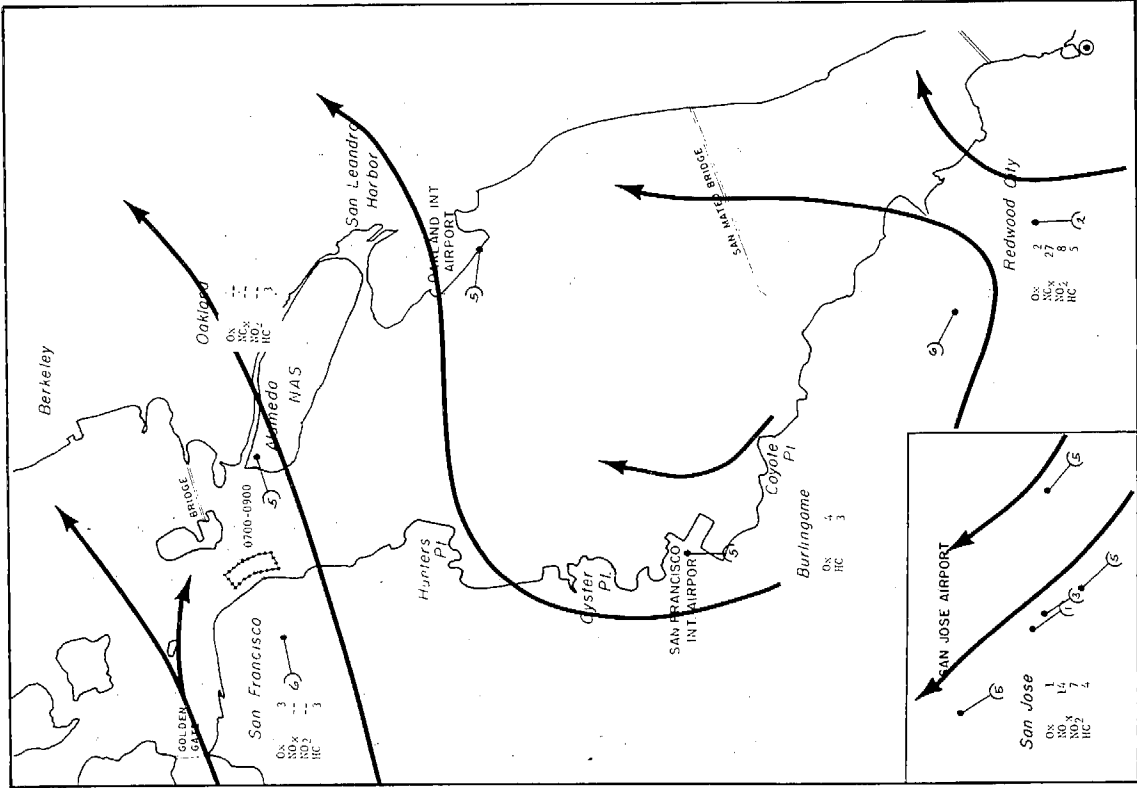
Figures 13 through 15 are maps illustrating wind flow patterns, houseboat sampling paths, tetroon trajectories, rawinsonde observations, and pollutant concentrations.

The winds were west to southwest throughout the sampling day. The stratus layer was overcast to broken throughout the sampling interval. The rawinsonde observations shown in Figure 14 indicate that a surface based shallow inversion (90 meters) was observed at Oakland Airport at 0400.

A tetroon run was made on 26 October from 0907 to 0947. The trajectory of the tetroon and the houseboat path are shown in Figure 13. The tetroon was launched immediately downwind of San Francisco and drifted over Treasure Island. The houseboat temporarily abandoned

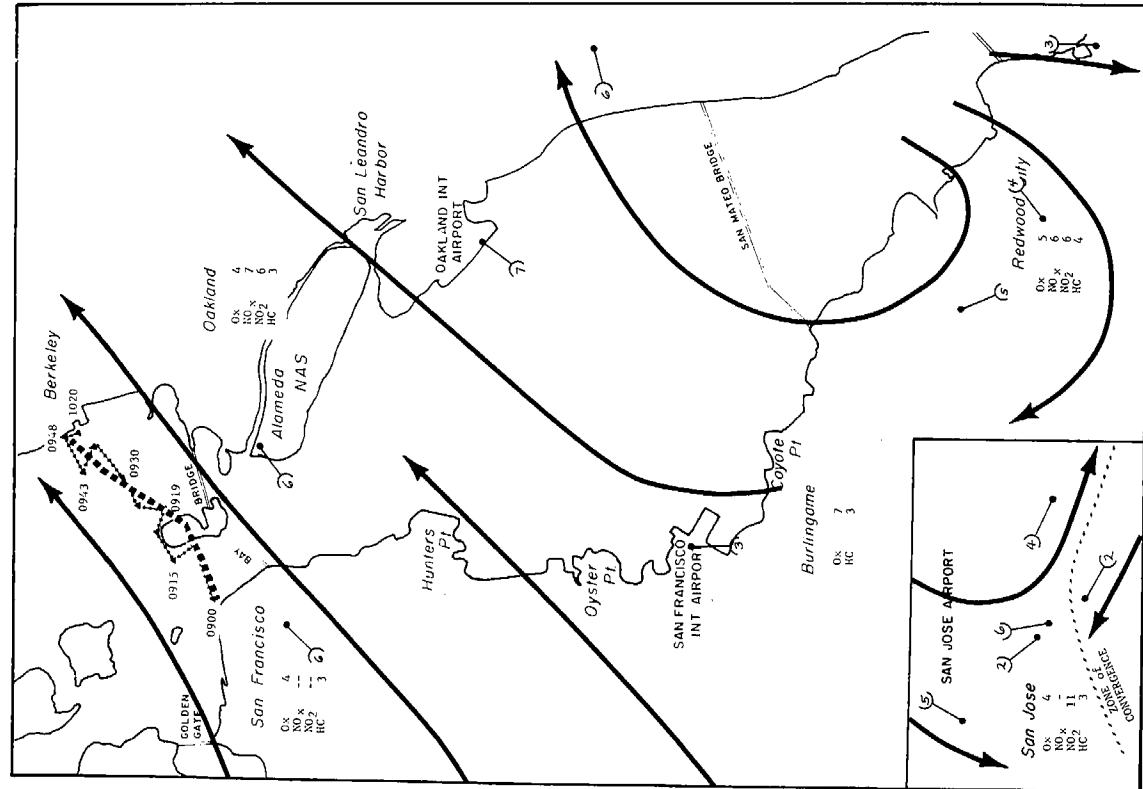


(a) 0700 PST

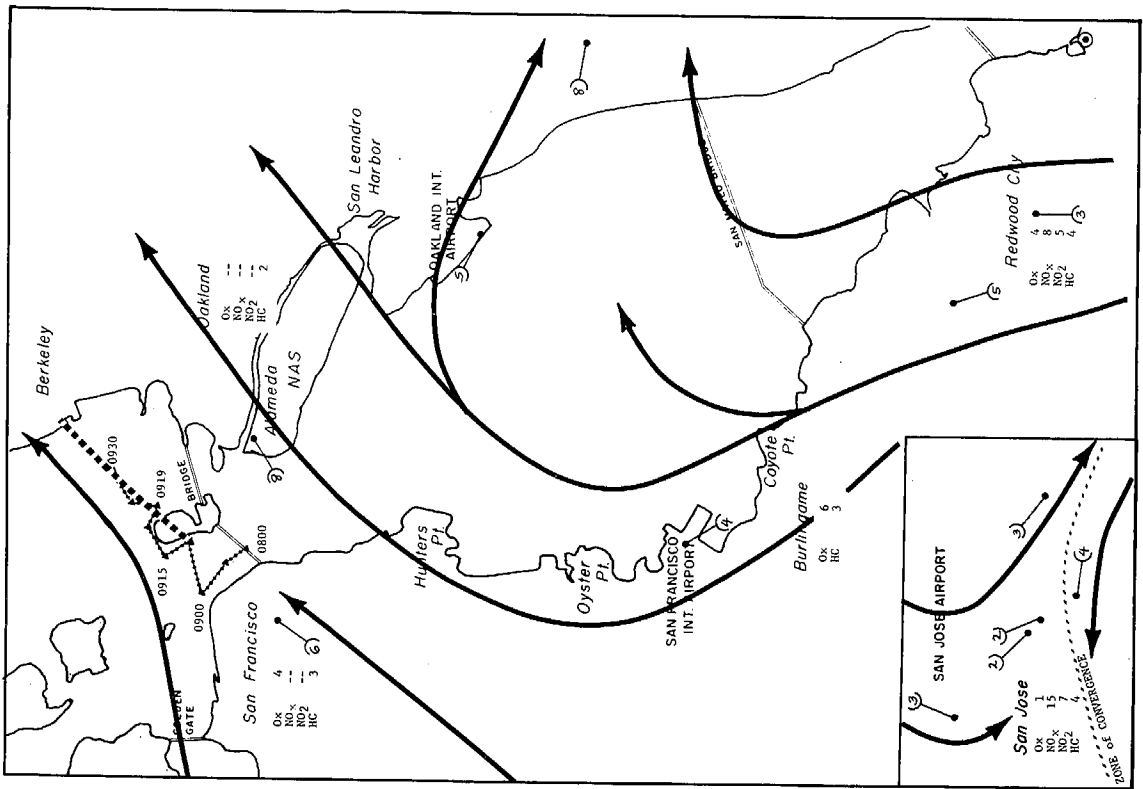


(b) 0800 PST

FIGURE 13 AIR POLLUTION LEVELS, SURFACE WIND FLOW, AND HOUSEBOAT COURSE, 26 OCTOBER 1972



(c) 0900 PST



(d) 1000 PST

FIGURE 13 AIR POLLUTION LEVELS, SURFACE WIND FLOW, AND HOUSEBOAT COURSE, 26 OCTOBER 1972 (Concluded)

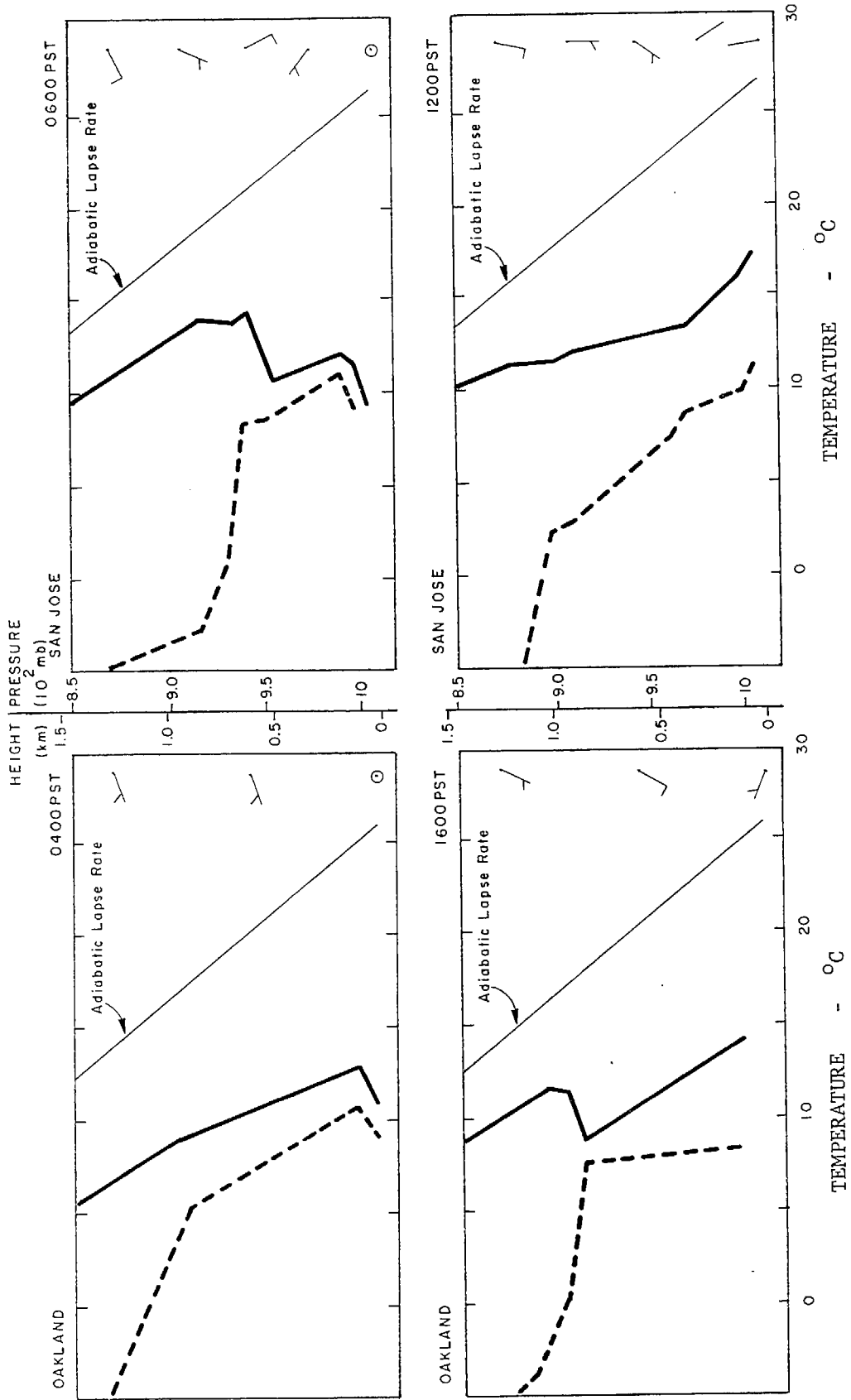


FIGURE 14 RAWINSONDE TEMPERATURE AND DEW POINT OBSERVATIONS, 26 OCTOBER 1972  
 (Temperature ———, Dew Point - - - -)

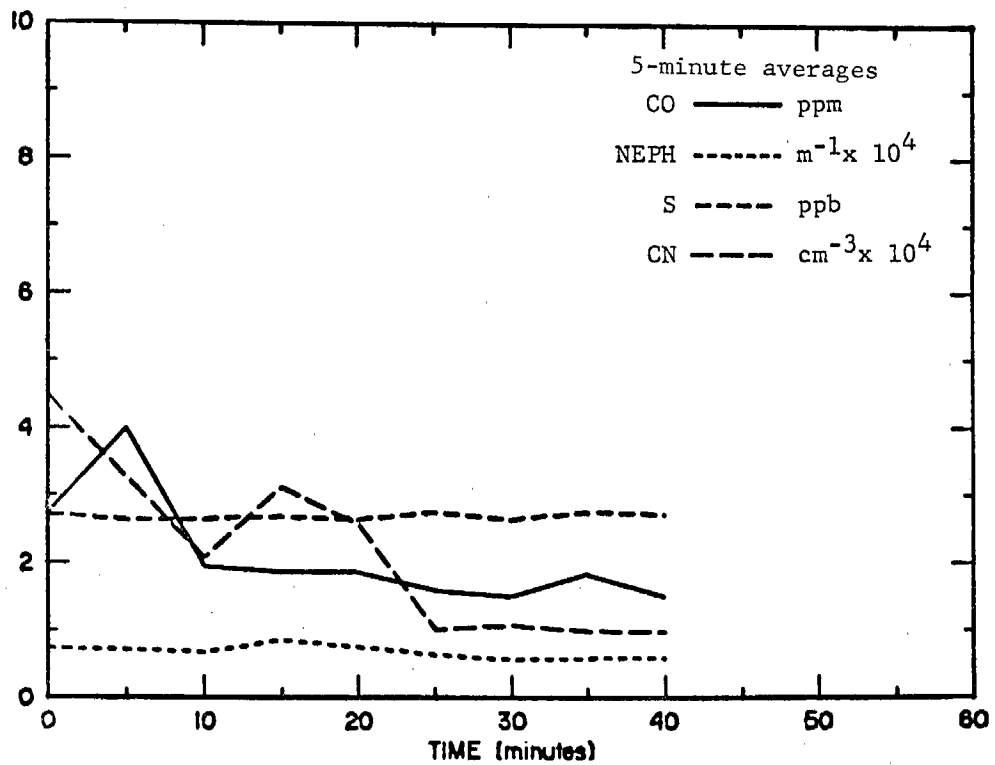
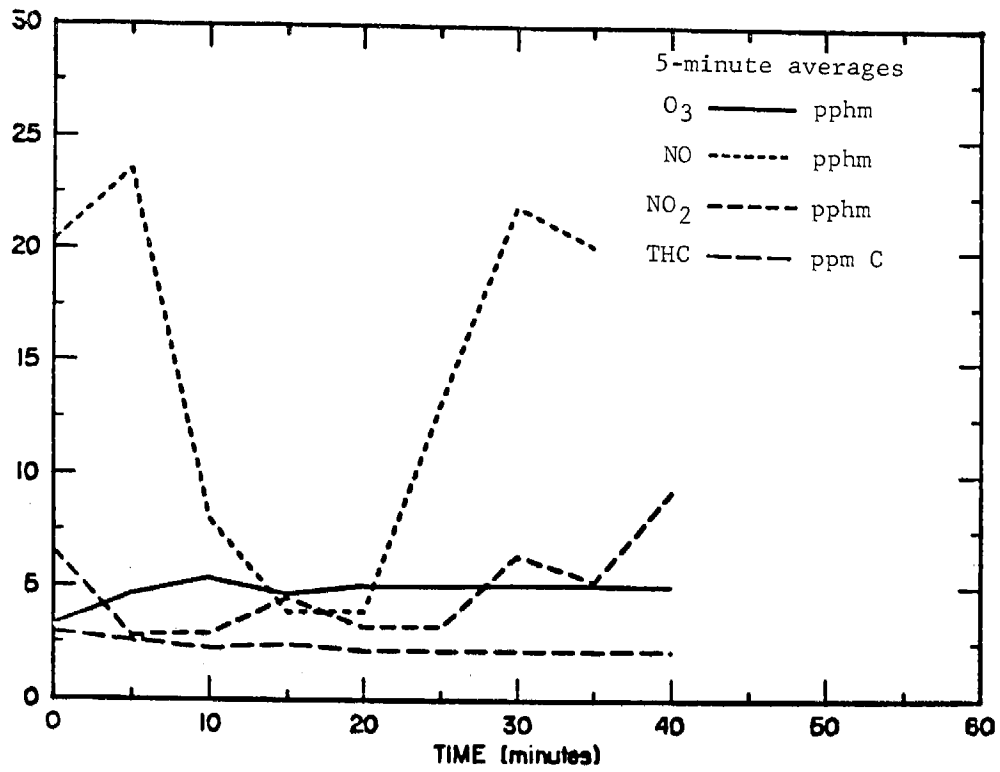


FIGURE 15 POLLUTANT CONCENTRATIONS OBSERVED DURING TETROON RUN, 26 OCTOBER 1972, 0907 to 0947 PST

the tetroon at Treasure Island, resumed tracking beyond Treasure Island at 0919, and followed the tetroon to the Berkeley shore.

The graphs displaying the changes in pollutant concentrations versus time during the tetroon run are shown in Figure 15. Extreme spatial and temporal variability were observed in the concentration of pollutants, particularly NO, within 1 kilometer downwind of San Francisco. Due to the multiplicity of sources in the city, the air mass was not well mixed for appreciable distances downwind of a large urban source.\* The high NO to NO<sub>2</sub> concentrations at the beginning of the tetroon run indicate that auto emissions from San Francisco are the primary source of pollutants. A rapid decrease in the concentration of NO occurred during the initial 15 minutes of the tetroon run. The concentration of other pollutants did not decrease so dramatically during this interval. The marked decrease in NO concentrations relative to other pollutants indicates that dilution occurs by air containing a variable mixture of pollutants after passage over the urban source or that the houseboat is overrunning surface air containing a well-aged pollutant burden. Dilution by clean marine air, on the other hand, would have significantly reduced in similar proportions the concentration of all pollutants. The low pollutant concentrations observed immediately downwind of Treasure Island when tracking was resumed at 0919 remained at low levels until 0931, after which NO and NO<sub>2</sub> concentrations abruptly increased. No corresponding increase in CO, THC, or CN occurred during this later portion of the tetroon run. This pollutant mixture is characteristic of some types of nonautomotive pollution such as power plants. Two

---

\* Estimates of pollutant concentration variability near shore may be found in Table E-12. The variability of pollutant concentration in well-mixed air parcels did not normally exceed  $\pm 10\%$  except on those occasions where NO concentrations were very high. Based on dilution alone (see Figure 15), a rough estimate of the distance required to attain well mixedness is 2 to 4 kilometers downwind of the source. A determination of the well-mixedness as a function of meteorological conditions and source distance could be made by statistical analysis of the data.

power plants are located upwind at Hunters Point and Potrero Point and their plumes could conceivably have reached the houseboat under the meteorological conditions of this day. However, calculations with the model discussed earlier predict increases in NO concentrations of only 1 or 2 pphm, much less than those observed. The 12 to 13 kilometer distance between the houseboat and the power plants would result in plumes being reasonably well mixed and therefore, concentration fluctuations should be small.<sup>11</sup> Other sources, such as San Francisco, Treasure Island, or the Bay Bridge could have contributed to the observed atmospheric burden, but the BAAPCD lists no other major, individual sources of NO in the proper location that are comparable to the two power plants.

Although the sample run on 26 October did not indicate that significant photochemistry was taking place within the air mass, the run was indicative of the complex dilutional processes present over the Bay. In addition, this sample run indicates that the contribution from sources relatively far removed from the trajectory of the tetroon must be considered in interpreting the observed pollutant measurements.

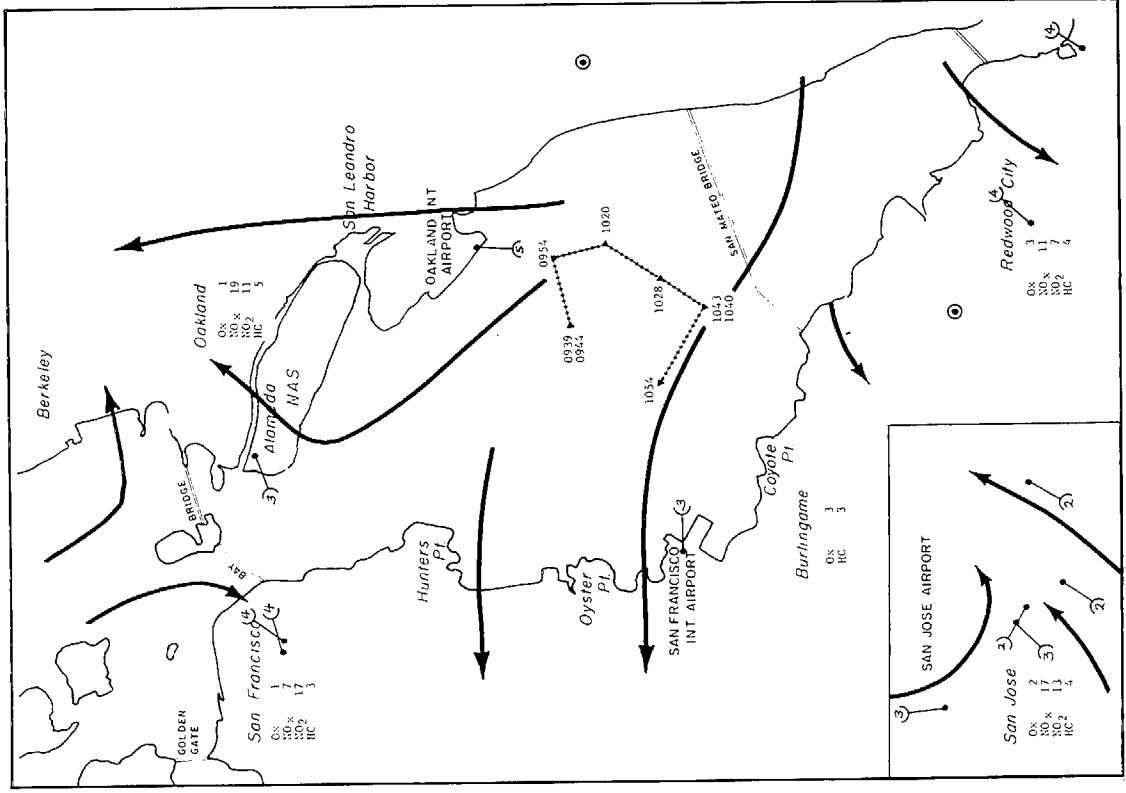
#### 4. 2 November 1972

The meteorological conditions on this day, as on September 21, were almost ideal. The pollutant levels were lower than September 21, but photochemistry definitely occurred during the tetroon run of almost 2 hours. Figures 16 through 19 are maps illustrating wind flow patterns, houseboat sampling paths, tetroon trajectories, rawinsonde observations, and pollutant concentrations. The chemical analyses of Lundgren impactor samples reported by AIHL\* are summarized in Appendix F.

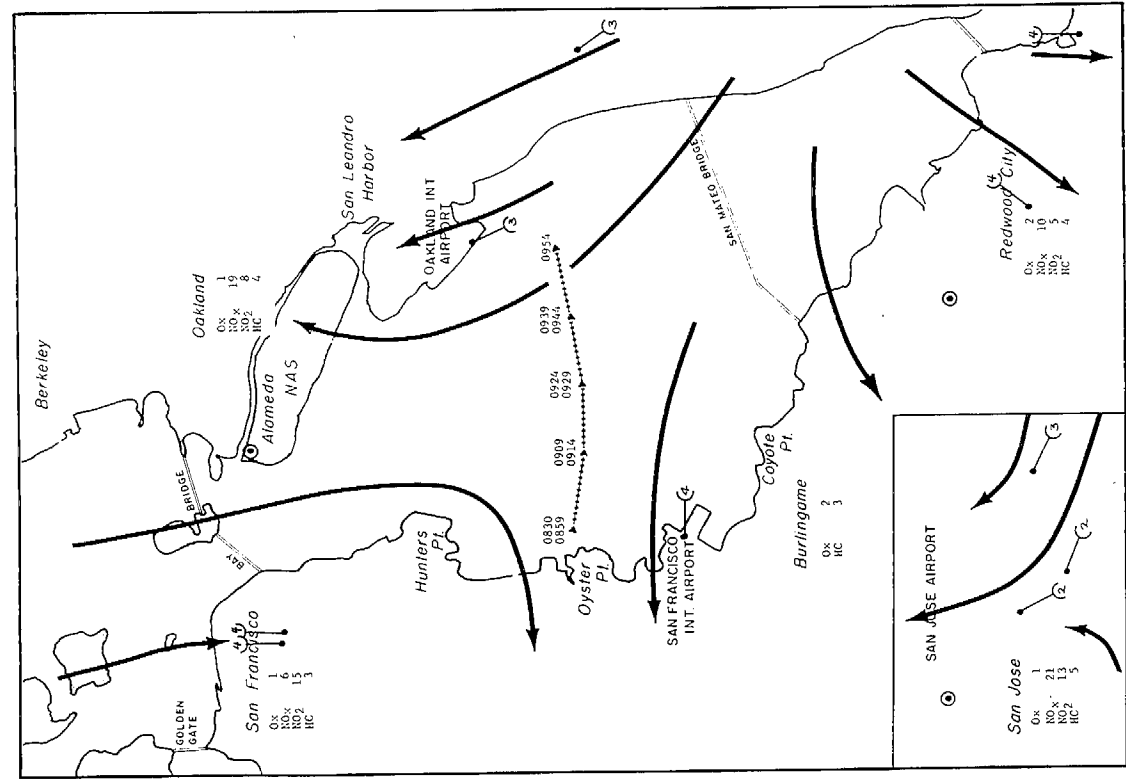
The morning soundings for Oakland and San Jose both show a very shallow surface inversion of about 0.1 kilometer thickness. At San Jose, a second inversion is present between 0.3 and 0.5 kilometers.

---

\*Air and Industrial Hygiene Laboratory, Berkeley, California



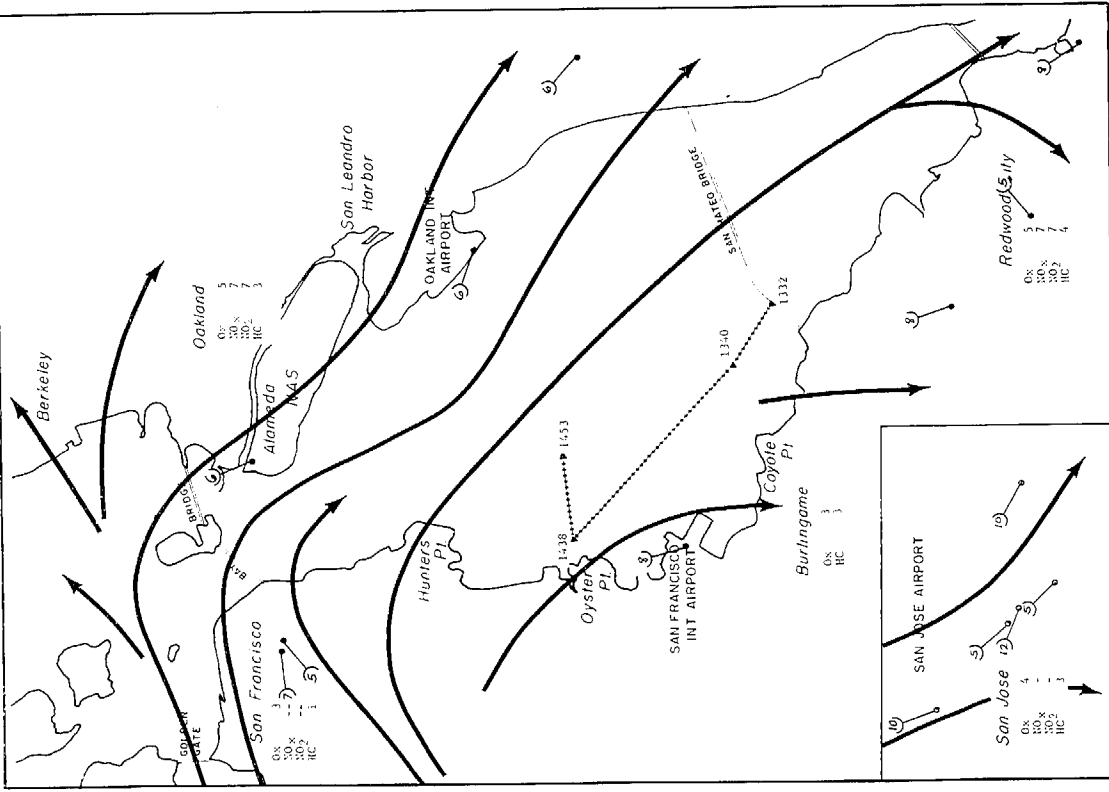
(a) 0900 PST



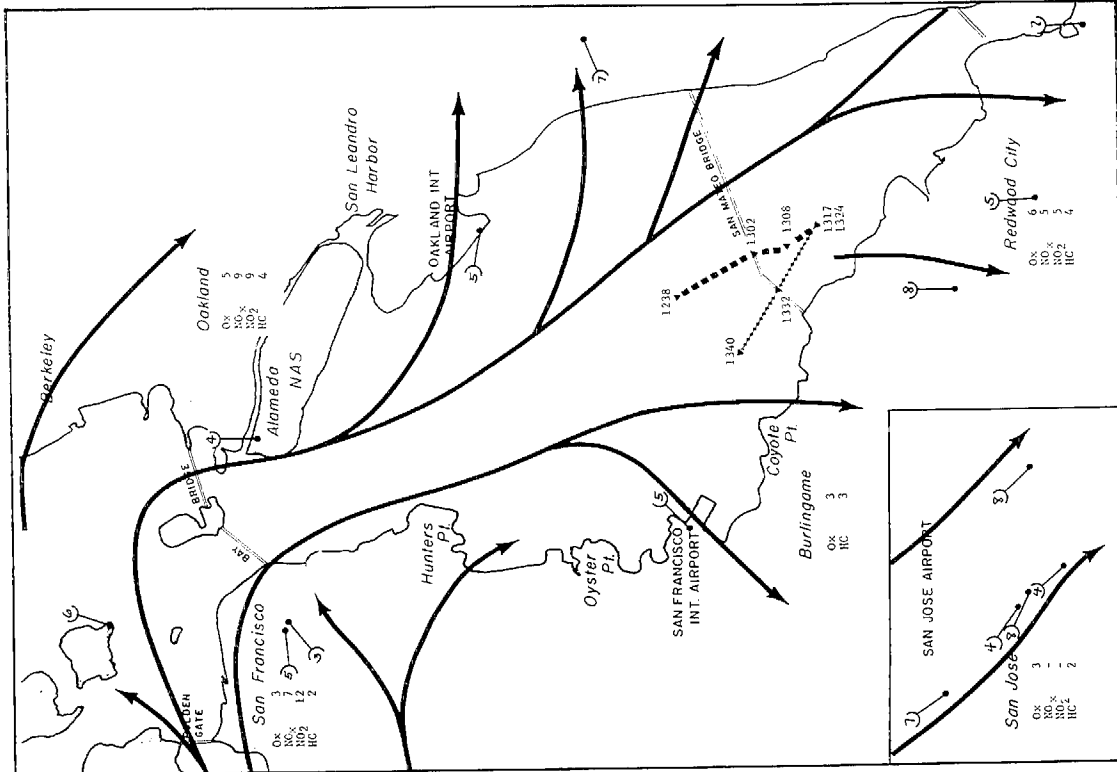
(b) 1000 PST

FIGURE 16 AIR POLLUTION LEVELS, SURFACE WIND FLOW, AND HOUSEBOAT COURSE, 2 NOVEMBER 1972



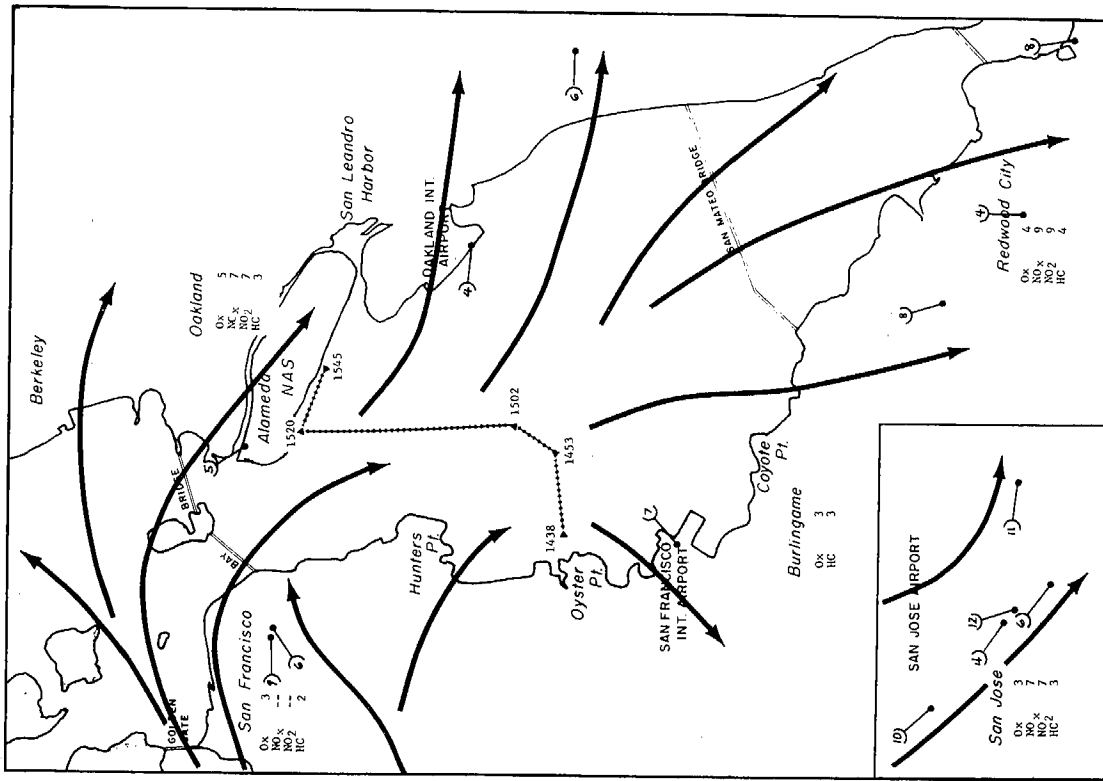


(f) 1400 PST

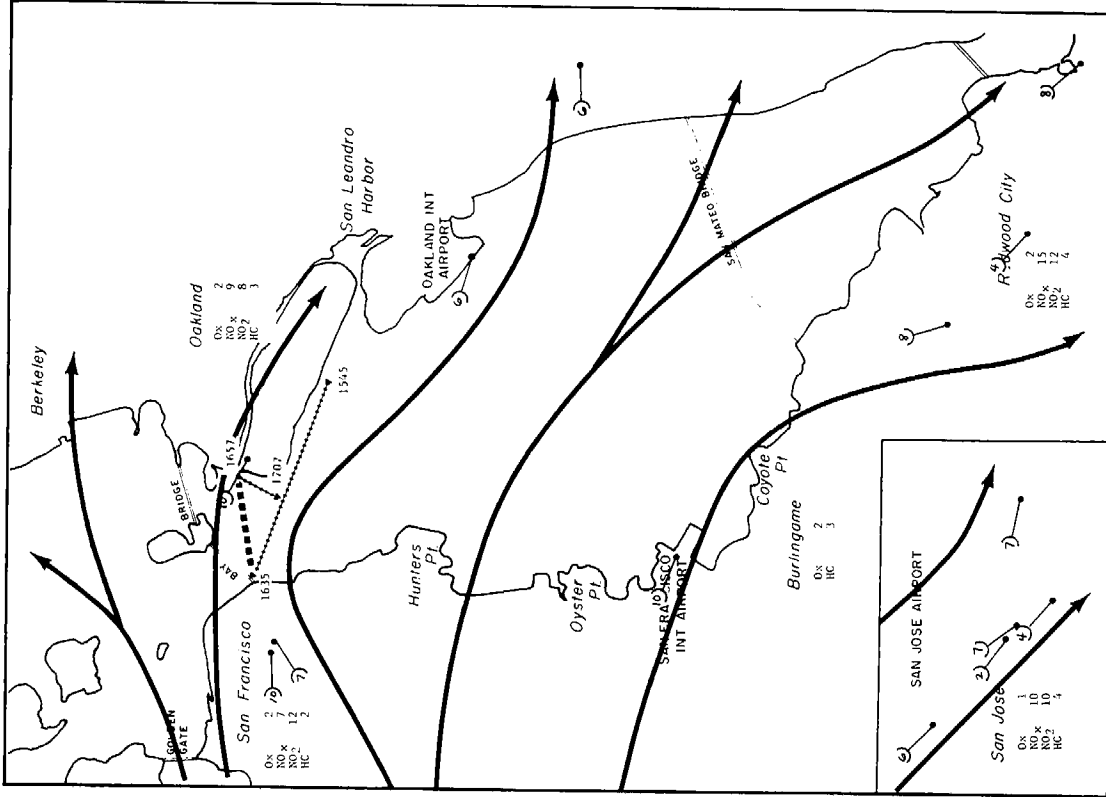


(e) 1300 PST

FIGURE 16 AIR POLLUTION LEVELS, SURFACE WIND FLOW, AND HOUSEBOAT COURSE, 2 NOVEMBER 1972 (Continued)

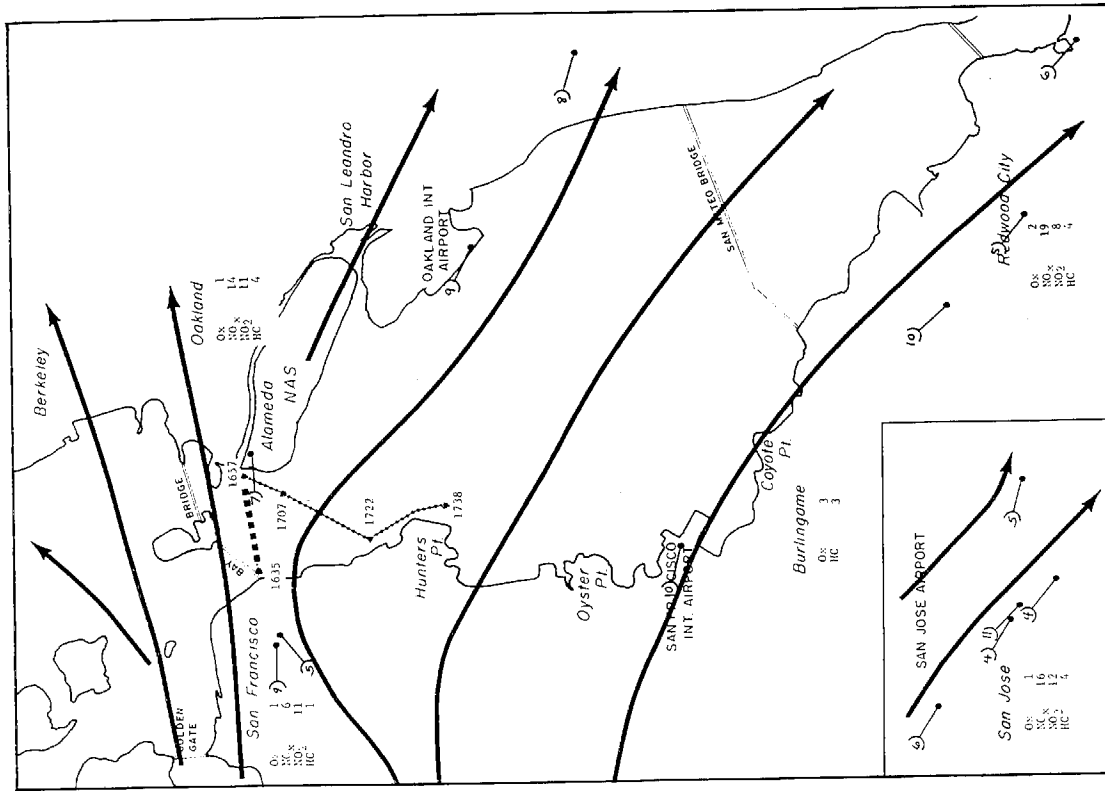


(g) 1500 PST



(h) 1600 PST

FIGURE 16 AIR POLLUTION LEVELS, SURFACE WIND FLOW, AND HOUSEBOAT COURSE, 2 NOVEMBER 1972 (Continued)



(1) 1700 PST

FIGURE 16 AIR POLLUTION LEVELS, SURFACE WIND FLOW, AND HOUSEBOAT COURSE, 2 NOVEMBER 1972 (Concluded)

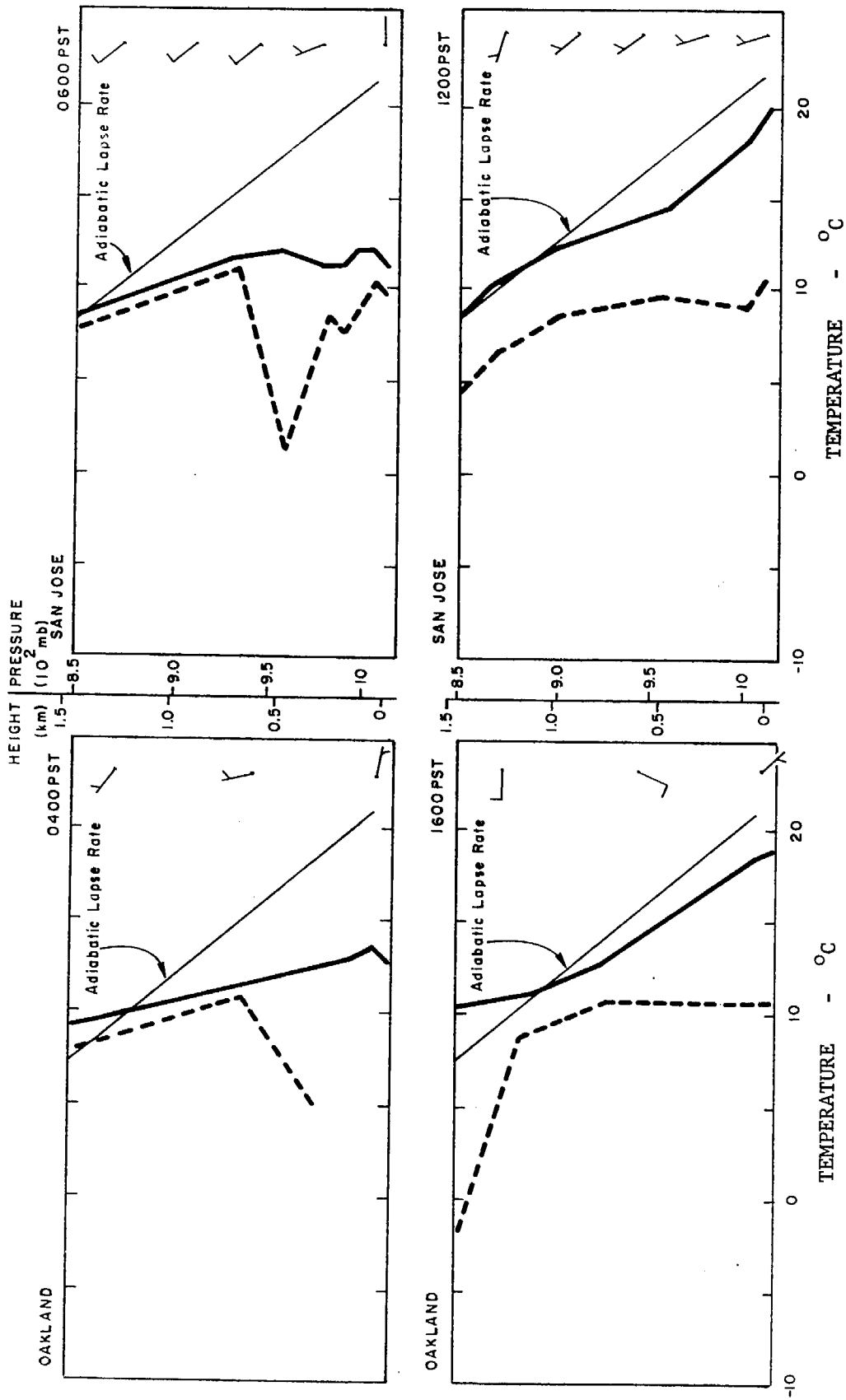


FIGURE 17 RAWINSONDE TEMPERATURE AND DEW POINT OBSERVATIONS, 2 NOVEMBER 1972  
 (Temperature ———, Dew Point - - - - -)

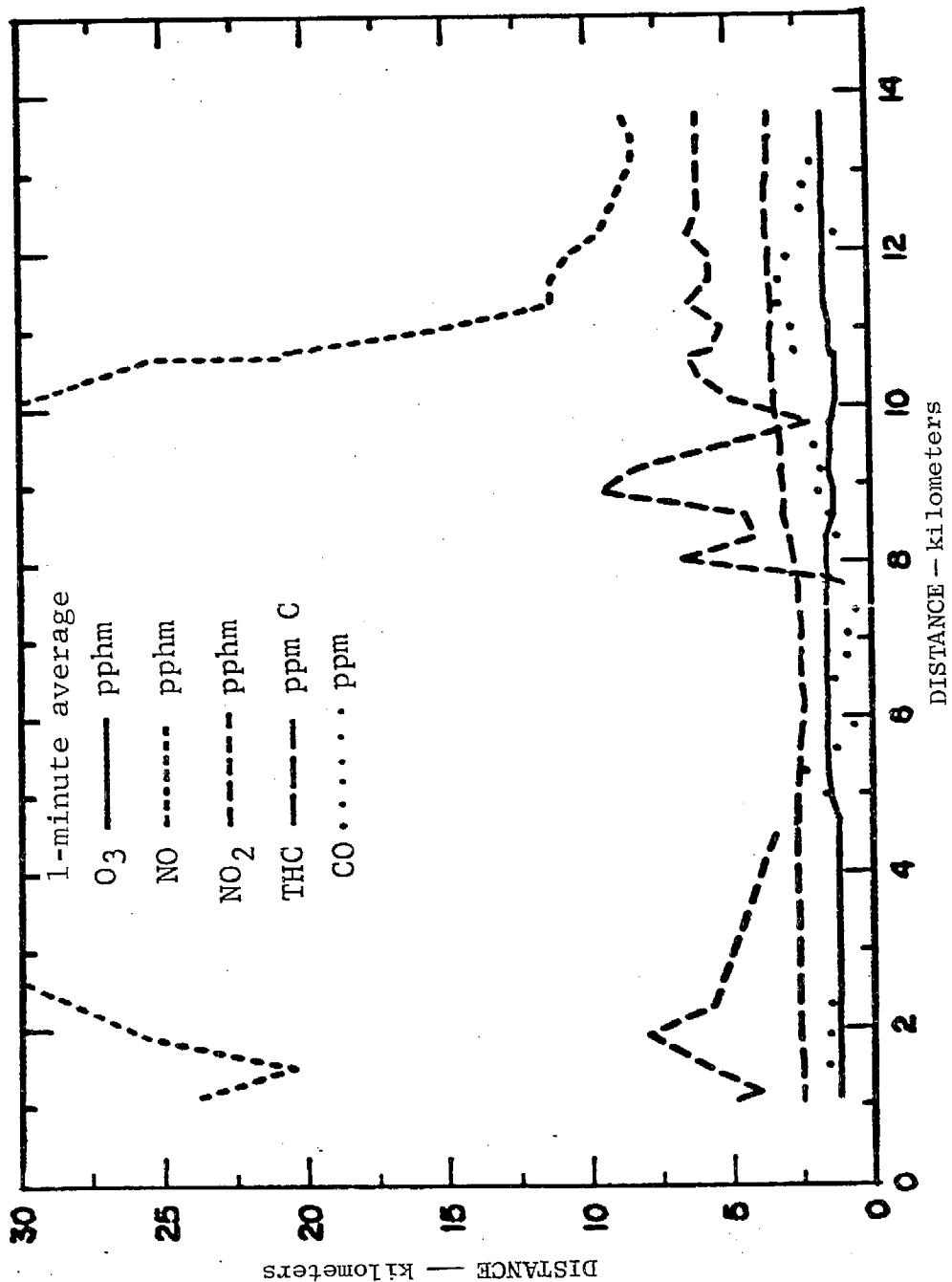


FIGURE 18 POLLUTANT CONCENTRATIONS OBSERVED DURING TRAVERSE OF THE BAY, WEST TO EAST, 2 NOVEMBER 1972, 0843 to 0957 PST

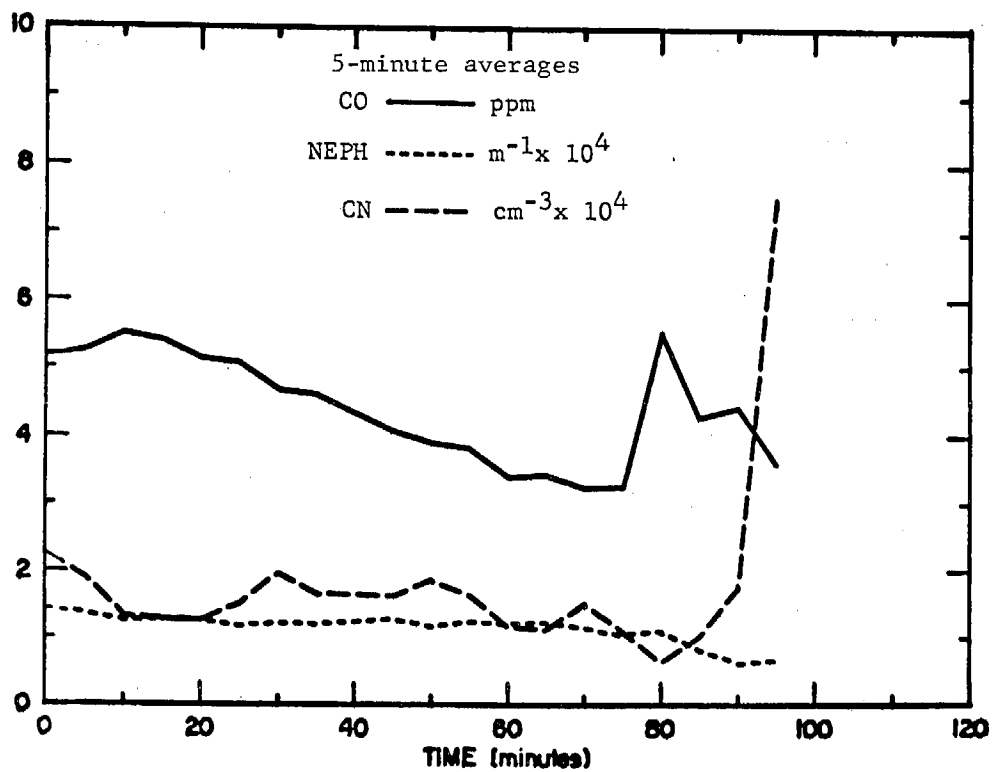
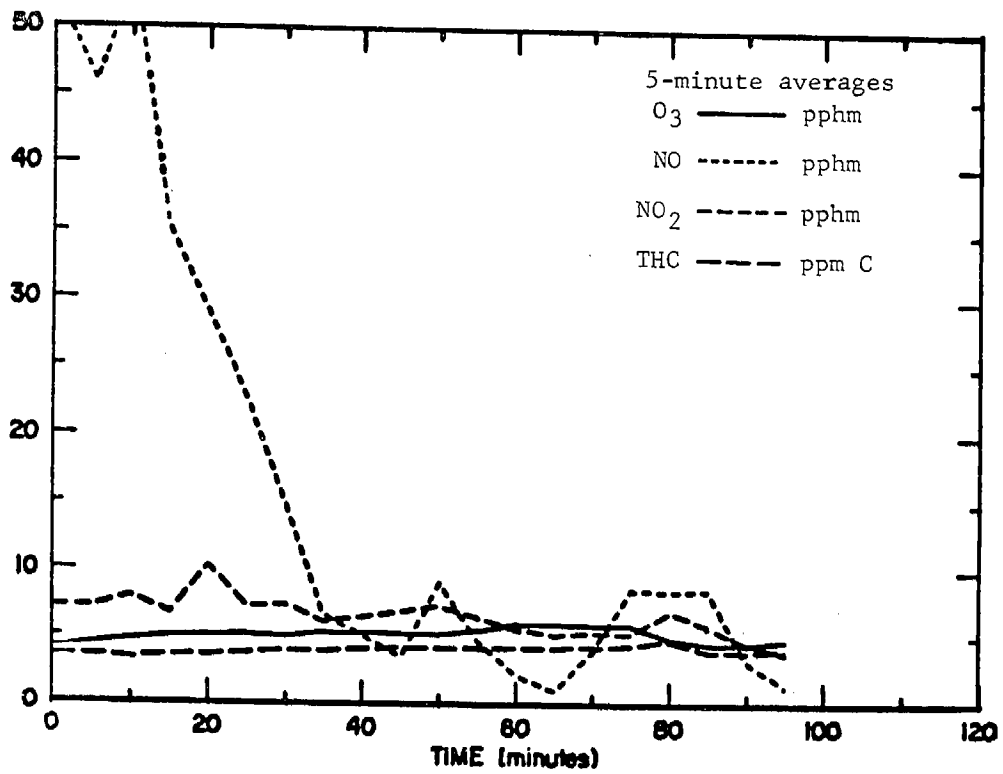


FIGURE 19 POLLUTANT CONCENTRATIONS OBSERVED DURING TETROON RUN, 2 NOVEMBER 1972, 1141 to 1316 PST

By noon, these inversions were completely dissipated by surface heating and mixing. The dry adiabatic lapse rate prevails into the evening Oakland sounding.

A slow traverse was made from Oyster Point to San Leandro Harbor. The houseboat was stopped frequently during the traverse for 5-minute intervals. A 5-minute average of measured pollutant concentrations was obtained during these intervals. Small helium-filled balloons were released to determine wind direction, and wind speeds were measured with an anemometer. The houseboat headed directly into the wind at all times. The NO concentration in the center of the Bay reached 60 pphm; concentrations were observed near the shoreline. The concentration of NO<sub>2</sub>, O<sub>3</sub>, THC, CO, and CN did not increase proportionately in the center of the Bay. The NO to NO<sub>2</sub> ratio was greater than 10, which is characteristic of freshly polluted air. The source of this NO is probably not houseboat exhaust, since increases in CO, CN, and THC concentrations did not occur simultaneously.

The simple Gaussian plume model described previously was used to estimate the contribution of NO from the PG&E power plant plumes. The maximum NO concentration near the houseboat was predicted to be 5 pphm, which is too low to satisfactorily explain the observed concentrations. The meteorological data implied a general northwesterly air flow on the upper half of the Bay. Therefore, the source of the pollution is probably San Francisco and not San Jose.

A tetroon released at 1123 near the center of the Bay rose to about 150 meters altitude, but remained in the vicinity of the release point for about 40 minutes due to stagnation. To avoid contamination from the houseboat exhaust, the houseboat was navigated in circles and figure eights under the tetroon. A tethered helium-filled balloon was

used to determine the resultant wind direction so that a relative forward wind speed could be maintained at all times. The high NO concentrations observed between 1141 and 1211 are ascribed to the houseboat. Spikes in the CN concentrations were observed when the houseboat crossed its own exhaust plume. Similar spikes in NO concentration were not observed simultaneously because the time constant of the NO<sub>x</sub> analyzer is considerably longer than that of the CN counter.

At about 1200, a stronger marine air flow carried the tetroon south over the San Mateo Bridge (1200 to 1316). The houseboat passed under the San Mateo Bridge at 1302. Between 1200 and 1302 the O<sub>3</sub> increased, indicating photochemistry was occurring. As the houseboat passed under the San Mateo Bridge, the expected increases in NO, CO, THC, and CN as well as a decrease in O<sub>3</sub> were observed. Figure 20 is a plot of 1-minute average pollutant concentrations plotted against distances from the San Mateo Bridge. There was an increase of THC, CO, NO, and NO<sub>2</sub> as the houseboat passed under the bridge. The THC, CO, and NO are from automobile emissions. A significant portion of the NO<sub>2</sub> is from the reaction of NO and O<sub>3</sub>. There is a corresponding decrease in O<sub>3</sub> concentration. It is not clear why O<sub>3</sub> decreases 2 pphm while NO<sub>2</sub> increases 6 to 9 pphm, unless a portion of the NO emissions on the bridge are rapidly oxidized by O<sub>2</sub> to NO<sub>2</sub>. Finally, the peak in the NO concentration observed before the bridge cannot be easily explained because CO, THC, and CN did not increase simultaneously, thereby ruling out both bridge and houseboat exhaust.

The chemical analysis of glass fiber filters collected on 2 November is summarized in Table 6. The chemical composition of the particulate is characteristic of aged aerosols. The observation of 5 to 10 percent sulfur was unexpected since there are few SO<sub>2</sub> emissions in the Bay Area; presumably, it comes from sea spray. The chloride to sulfur ratios are low, further supporting the conclusion that the

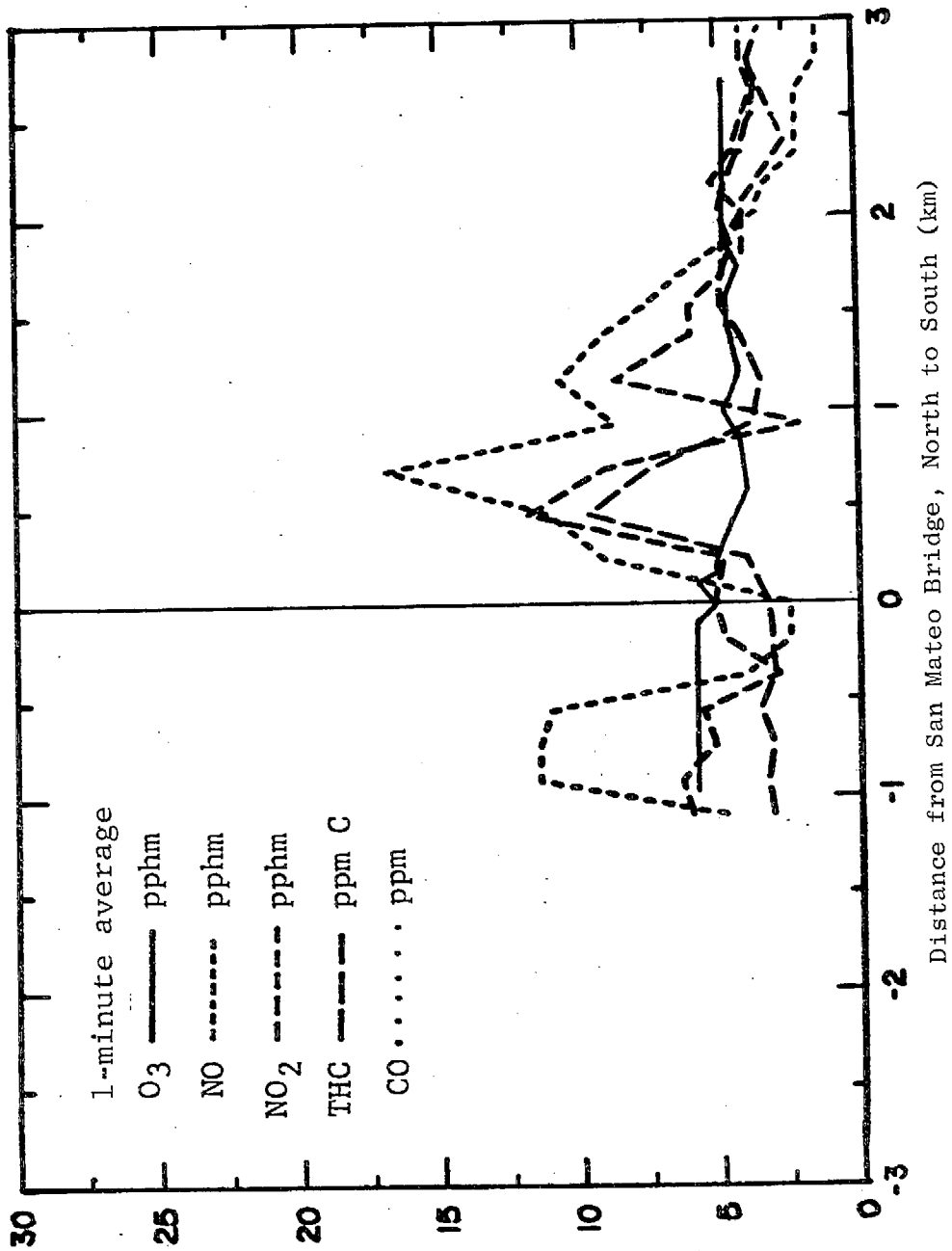


FIGURE 20 POLLUTANT CONCENTRATIONS OBSERVED IN VICINITY OF SAN MATEO BRIDGE DURING TETROON RUN, 2 NOVEMBER 1972, 1253 to 1327 PST

Table 6

CHEMICAL ANALYSES OF PARTICULATE MATTER  
COLLECTED ON GLASS FIBER FILTERS,  
2 NOVEMBER 1972

Time (PST)	Mass Loading ( $\mu\text{g}/\text{m}^3$ )	Chemical Composition ( $\mu\text{g}/\text{m}^3$ )			
		Nitrate	Sulfur	Chloride	Lead
0833 to 1120	108	10.8	6.0	1.0	2.4
1123 to 1317					
1633 to 1745	194	24.7	17.3	3.1	2.6

aerosols were predominately of anthropogenic origin and not sea salt. From 1633 to 1745, aerosol was collected near San Francisco during a tetron run from San Francisco to the Alameda Naval Air Station. The increase in mass loading is probably due to the lack of dilutional effects observed on other days when the particulate samples were collected farther from the sources.

Lundgren impactor samples collected on 2 November 1972 were analyzed and reported by AIHL. The results of their analyses are included in Appendix F. In this report, the chemical composition and size distributions of the 2 November aerosol was compared to aerosol data analyzed and reported on previous studies in the Bay Area. The general conclusion based primarily on the bromine to lead ratios, was that the aerosols are well aged. The collected particulate was not analyzed to determine the organic constituents. Since little or no secondary aerosol formation was observed during this research program, photochemical changes in aerosol composition cannot be determined.

The electronic scattering cross-section analysis spectra for sulfur indicated that the sulfur-containing particulate trapped on the after filter (particles less than about 1 micron) was 70 percent sulfate. The sulfur present in the larger particles was almost 100 percent in

the form of sulfate. We can only speculate about the sources of non-sulfate sulfur. These sources could be anthropogenic or biological, for example, the decomposition of organic materials on the floor of the Bay. More definitive data are clearly required to identify the sources of nonsulfate sulfur particulate material.

The particulate collection data obtained in the research program demonstrate the feasibility of collecting satisfactory samples from a houseboat. However, SRI believes that the following changes in experimental technique are warranted for future programs:

- More frequent hi-vol filters should be collected.
- Total filters should be collected on Gelman GA-1 filters for comparison to the Lundgren data.
- A one-stage Lundgren type of impactor plus an after filter would probably give adequate data at a considerable reduction in analytical costs.
- The samples should be collected over as short a time as possible to improve the resolution of the data.

## VI PRELIMINARY ANALYTICAL RESULTS BASED ON COMBINED DATA FROM SELECTED SAMPLING DAYS

### A. Usefulness of the Data

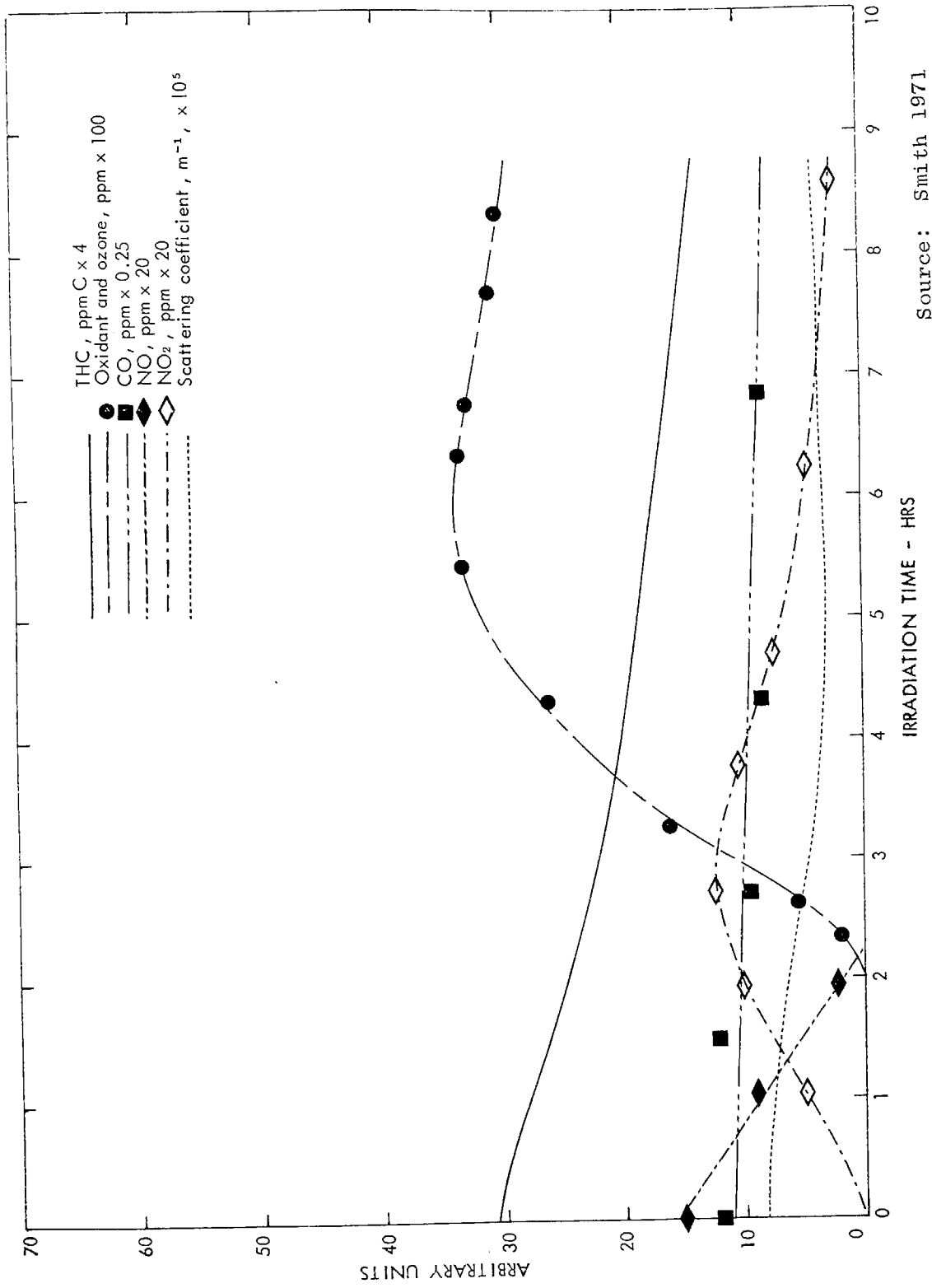
A primary objective of this research program was to collect data that will help provide a basis for defining atmospheric photochemical processes and will provide the background data required to evaluate a simulation model of photochemical smog.\*

To critically assess the degree to which the first of these objectives was accomplished, the analogy of the San Francisco Bay and a large smog chamber was considered. The conclusion is a qualified agreement as to the validity of the analogy. The data must be critically examined to see if photochemical changes occur and, if so, how similar they are to smog chamber experiments. This is admittedly a difficult task because, due to the meteorological conditions of the autumn of 1972, it was not possible to make long tetraon runs and there was little smog.

First, let us consider the changes in pollutant concentrations that occur during a typical chamber experiment. For an example, the data in Figure 21 were obtained during an earlier SRI project.<sup>12</sup> A mixture of 7.5-ppm C automobile exhaust, generated by using a 93-octane gasoline of 55 percent paraffins, 11 percent olefins and 33 percent aromatics, and 0.75 ppm NO was irradiated in the SRI smog chamber. While the concentrations are higher than observed on the Bay, several general characteristics of a static smog chamber reaction are depicted in this example. The first noticeable chemical change is that:

---

\*L. A. Cavanagh, R. C. Robbins, J. H. Smith, SRI Proposal ERU 72-71, "Atmospheric Photochemical Smog Measurements Over San Francisco Bay"



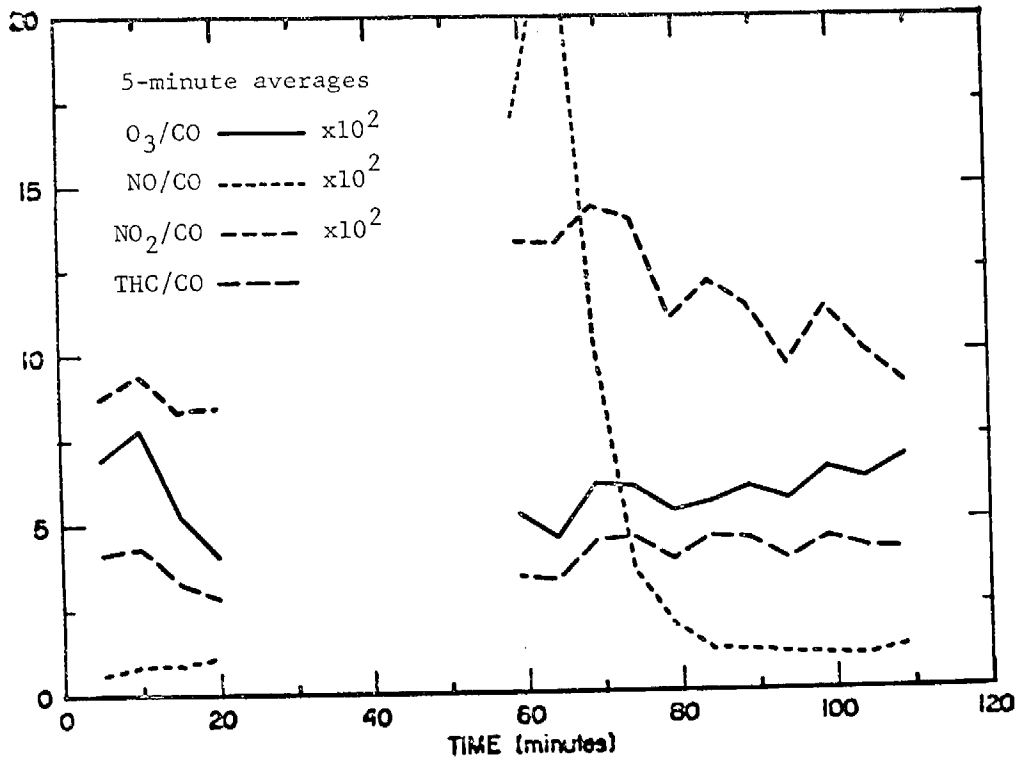
Source: Smith 1971

FIGURE 21 REPRESENTATIVE SMOG CHAMBER RUN IN SRI CHAMBER, AUTOMOBILE EXHAUST (7.5 ppm C) and NO (75 ppbm) 10

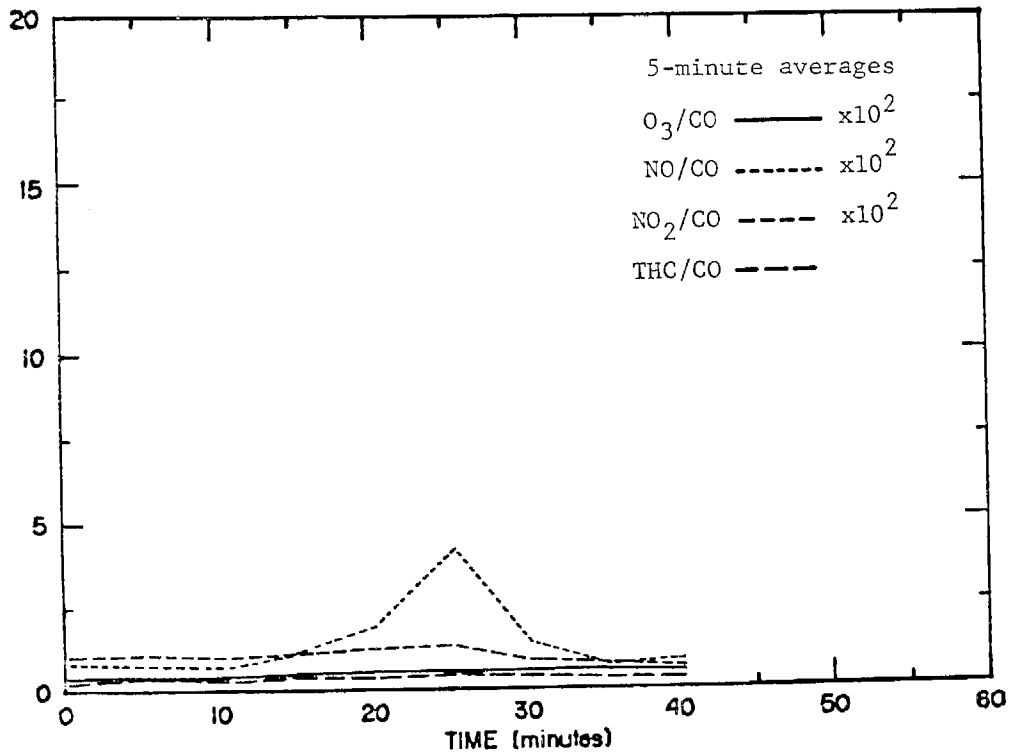
- NO falls to nearly zero
- NO<sub>2</sub> increases proportionately, reaches a maximum value less than or equal to the initial NO concentration, then decreases slowly,
- Oxidant, which is primarily O<sub>3</sub>, builds up only after the NO<sub>2</sub> maximum. A maximum O<sub>3</sub> concentration, followed by a slow decrease, is observed.
- The THC concentrations decrease throughout the run to approximately one half of the initial concentrations. GC analysis showed that only reactive hydrocarbons, such as olefins and substituted aromatics, react within the experimental time frame.
- The apparent decrease in CO is due to dilution of the chamber air as the result of replacement of the air removed by the air quality instrumentation.
- Although this example does not clearly show it, formation of secondary aerosols usually parallels O<sub>3</sub> formation.

Since auto emissions of nitrogen oxide are almost exclusively NO, the value of the NO to NO<sub>2</sub> ratio gives a crude but quick estimation of the age of air mass. High NO to NO<sub>2</sub> ratios, greater than 1.0, are representative of fresh air masses; low NO to NO<sub>2</sub> ratios, less than 1, are found in well-aged air masses. Generally, higher O<sub>3</sub> concentrations are associated with lower NO to NO<sub>2</sub> ratios.

In the atmosphere, dilutional effects can mask photochemical changes. Since CO is essentially inert at these concentrations, we can correct for the dilutional effects by dividing the other pollutant concentration by the CO concentration. Figure 22 is a plot of the ratios of NO, NO<sub>2</sub>, O<sub>3</sub>, and THC to CO for the 5-minute averages during the selected sampling days.

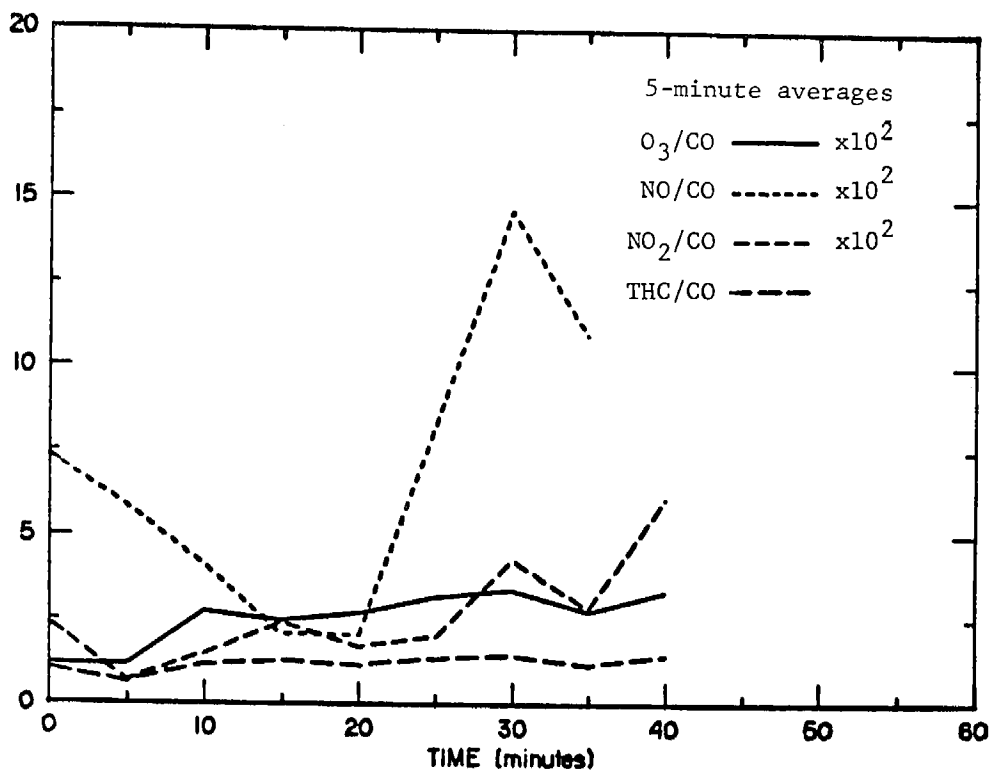


(a) 21 September 1972, 1037 to 1226 PST

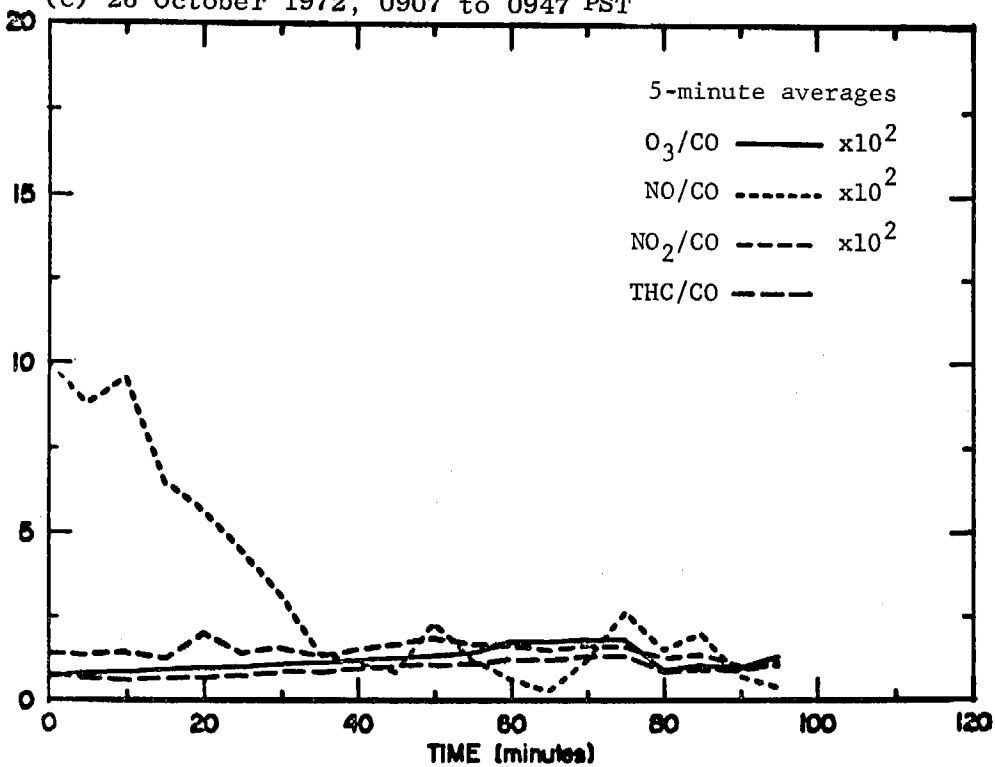


(b) 25 October 1972, 1138 to 1218 PST

FIGURE 22 RATIOS OF POLLUTANTS TO CO CONCENTRATIONS OBSERVED DURING TETROON RUNS (5-minute averages)



(c) 26 October 1972, 0907 to 0947 PST



(d) 2 November 1972, 1141 to 1318 PST

FIGURE 22 RATIOS OF POLLUTANTS TO CO CONCENTRATIONS OBSERVED DURING TETROON RUNS (5-minute averages) (Concluded)

On 21 September, the smog observed from 1034 to 1057 when the houseboat was near San Francisco, is clearly well aged. Significant  $O_3$  concentrations are present and the NO to  $NO_2$  ratio is low ( $\sim 0.2$ ). At this time, freshly polluted air including CO was injected into the air mass (see Figure 4). At 1036, the houseboat passed through a portion of the PG&E stack plume from Potrero Point. Since there is comparatively little CO in the plume, the ratio plot remains valid.

The pollutant ratio plot, Figure 22a, clearly shows the occurrence of classical photochemical smog activity. The  $NO_2$  may be at a maximum from 1036 to 1141 since it decreases steadily after this time. The  $O_3$  also increases, while the THC and NO are nearly constant. The photochemical events occurring on 21 September from 1036 to 1220 correspond to similar events occurring after 3 to 4 hours of irradiation in the smog chamber experiment shown in Figure 21. If the tetroon had not descended at 1220, the  $O_3$  maximum might have been observed.

Judging from the NO to  $NO_2$  ratio, the air masses followed on 21 September, 25 October, and 2 November  $[NO]/[NO_2] \sim 1$  were well aged, while that for 26 October  $[NO]/[NO_2] \sim 3$  was very fresh. Less dramatic photochemical activity was observed during the last three selected tetroon runs. Even though the NO to CO ratio sometimes rose sharply during these runs, the ratios of  $NO_2$  to CO and  $O_3$  to CO apparently were not affected. Since the CO and CN concentrations did

---

\*Fresh pollutants from the city were injected into the tetroon-marked air mass containing aged pollutants as it passed over the eastern shore line. The  $O_3$  in the well-aged air mass oxidizes the NO added by the city to  $NO_2$ . The higher initial  $NO_2$  concentration causes the  $NO_2$  maximum to be observed sooner than would be the case if the NO were added to clean air. Unpublished data previously obtained with the SRI smog chamber have shown that under similar conditions a second  $NO_2$  maximum is rapidly reached after addition of NO to a well-aged irradiated mixture of mesitylene and NO.

not rise at the same time, exhaust contamination was ruled out. However,  $O_3$  concentrations do not decrease and  $NO_2$  concentrations do not increase in the presence of high NO concentrations that would be expected from the reaction  $NO + O_3 \rightarrow NO_2 + O_2$ . There is no obvious explanation for these observations.

The rates of formation or loss of  $NO_2$ ,  $O_3$ , and THC were calculated and corrected for dilutional effects by multiplying the calculated rates by the ratio of the initial to the final CO concentrations (Table 7). The calculated formation rates of  $NO_2$  and  $O_3$  are approximately the same as the rates calculated from the smog chamber data in Figure 21. However, the THC rate of disappearance is an order of magnitude slower in the atmosphere than was observed in the SRI smog chamber.

Table 7  
 POLLUTANT FORMATION OR LOSS RATES  
 (pphm/min)

Date	$NO_2$	$O_3$	THC
21 September	0.17	0.05	0.02
25 October	0.0	0.01	-0.01
26 October	0.18	0.11	0.03
2 November	-0.07	0.02	0.0

In two cases, the THC concentration increases very slowly, contrary to smog chamber observations. The increase may be an artifact of the simple approximation procedure.

A valid comparison of the Bay Area to a large smog chamber can only be made on days when the meteorological conditions are conducive to smog formation. These conditions occur only with a northwesterly air flow down the axis of the Bay at velocities of less than 5 to 8 mph. These same conditions are also the only ones that would permit tetraon flights of 4 to 6 hours. These long reaction

times would permit the development of significant photochemical activity. The only days when these conditions were observed during the fall of 1972 were 21 September and 2 November. The data for these days show definite photochemical activity even though the ambient temperatures were below 70<sup>o</sup>F. Under conditions of extreme stagnation, longer runs would be possible, but the likelihood of houseboat exhaust contamination would also increase significantly.

Formation of secondary (photochemical) particulate matter was not observed during the selected tetron runs, based on the nephelometer readings. However, this study conclusively demonstrated that reliable particle size distribution, mass loading, Lundgren impactor, and high volume sampler data can be collected on a houseboat mobile laboratory.

In view of the lack of significant photochemical activity, these data are of limited usefulness for model validation. The data for 21 September showed the greatest photochemical activity. The failure of the tetron prevented us from collecting 1 to 2 hours of additional data. A longer tetron run would have greatly increased the usefulness of this day's data.

The data collected on 2 November should be useful in two ways. First, data were collected that demonstrated photochemical activity at concentrations approximating the clean air standards established by the Environmental Protection Agency. Second, the data collected between 1253 and 1327 PST (Figure 20) are a unique example of the effect of pollutants from a line source of automobile traffic injected into an air parcel containing well-aged pollutants at near background concentrations.

The remainder of the data were obtained under conditions not conducive to long tetron runs. In shorter tetron runs, significant changes in pollutant concentrations and secondary aerosol composition due to chemical reactions cannot be observed. Therefore, such data will be less useful for model verification.

## B. Mass Balance

In its simplest terms, a mass balance in a photochemical smog reaction will be achieved if the mass of carbon and nitrogen (from HC and  $\text{NO}_x$ , respectively) consumed during the reactions equals the change in the mass of carbon and nitrogen in the products, which are primarily aerosols. To determine the carbon mass balance, the carbon content of the gaseous pollutants and the collected aerosol must be determined. The carbon content of the gaseous pollutants was determined through measurement of total hydrocarbon and through hydrocarbon distribution measurements by gas chromatography. Although the on-board gas chromatograph (see Section "Hydrocarbon Distribution" beginning page B-19, in Appendix B) did not provide adequate resolution of the ambient organics, the laboratory analysis of cryogenically collected samples by gas chromatography provided excellent data. The collected aerosol was analyzed for total C but the organic and inorganic contribution cannot be distinguished. The analysis for carbon is not available from the sticky foil stage of the Lundgren impactor (1B) or from the after filter due to interference from the substrate. The measurement of distribution of organics within the collected aerosol was proposed but not funded by the ARB.

The nitrogen balance requirements were better satisfied by the experimental design of the program than that of carbon balance. However, to obtain a true nitrogen balance, ammonia must be measured in the gaseous phase and ammonium content of the collected particulates must be determined. The measurement of gaseous ammonia or the ammonium content of aerosol is not required as input to photochemical simulation models.

Under conditions where a reasonable amount of photochemical activity is taking place, a carbon mass balance can be approached without differentiating inorganic and organic carbon content of collected particulate. Under the same conditions, a nitrogen mass balance can be approached through measurement of nitrogen oxides and the nitrate content of par-

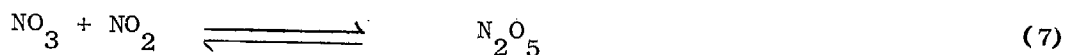
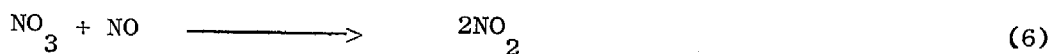
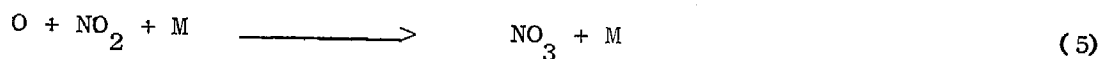
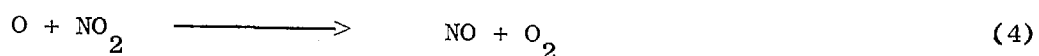
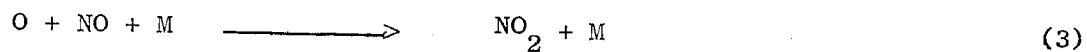
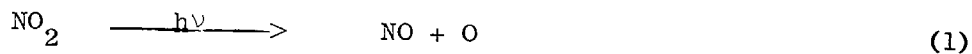
ticulate. However, in the absence of sufficient photochemical activity to produce secondary aerosols and conditions when wind direction and velocity do not permit long tracking times of the tetroon, a meaningful mass balance cannot be obtained. In the Bay Area, intense photochemical activity only occurs under meteorological conditions conducive to long-term tracking of the tetroon.

On 21 September, the sample day that the maximum photochemical activity was observed, no aerosol formation was observed (Figure 5) even when corrections for dilutional effects were applied. However, the concentration of  $\text{NO}_2$  decreased more rapidly than could be attributed to dilutional processes. This implies that secondary aerosol was formed. As previously discussed, the observed aerosol decrease also is greater than can be attributed to dilutional processes. Thus, the consumption of  $\text{NO}_2$ , though implying aerosol formation, cannot be verified by a corresponding formation of aerosol. The aerosol loss mechanisms apparently dominate aerosol formation by HC and  $\text{NO}_x$ . It is possible that with more accurate temperature and relative humidity measurements, combined with complex calculations of water loss from the particles and of aerosol coagulation, a mass balance could be achieved at an intensity of photochemical smog activity comparable to that observed on 21 September 1972. However, measurements made during intervals of significantly more intense photochemical activity would be required to realistically verify that a mass balance is achieved.

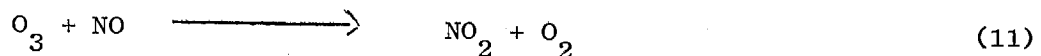
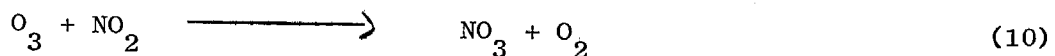
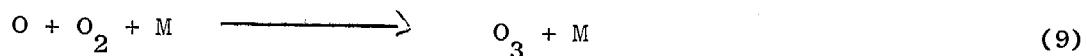
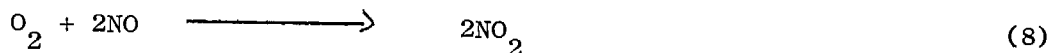
The photochemical activity observed during the other sampling days was significantly less than that of 21 September, and hence the measurement data are not applicable to mass balance determinations.

C. The  $[\text{NO}][\text{O}_3]/[\text{NO}_2]$  Ratio

The important chemical reactions of nitrogen oxides and reaction products in the absence of  $\text{O}_2$  are:



In the presence of  $\text{O}_2$ , these reactions are also important:



The rate constants are such that, in air, reactions (1), (9), and (11) are much faster than any of the others listed above and also faster than the reactions of  $\text{O}_3$  and  $\text{O}$  with HC. The rate of reaction (9) is collision controlled because of the high concentration of  $\text{O}_2$  in the air. Reactions (1) and (7) can be combined to give reaction (12)



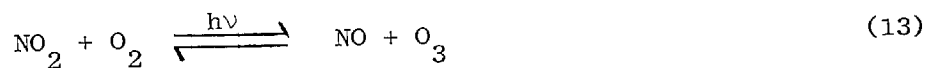
The rate of reaction (12) is controlled by the photodissociation rate of  $\text{NO}_2$ , which in turn depends on the wavelength and intensity of

the incident light. The photodissociation rate of reaction (1) will be the product of the solar intensity  $k_a$  and the quantum yield  $\bar{\phi}$ , which are both a function of wavelength. Integration over the solar spectrum gives

$$k_1 = \int_{\lambda} k_a(\lambda) \times \bar{\phi}(\lambda) d\lambda$$

the photodissociation rate  $k_1$ .

Reactions (11) and (12) can be combined and written as equilibrium (13).



An equilibrium constant K for reaction (13) can be defined by

$$K = \frac{k_1}{k_{11}} = k_a C = \frac{[\text{NO}][\text{O}_3]^*}{[\text{NO}_2]} \quad (14)$$

Since the spectral distribution of sunlight is nearly a constant, <sup>\*\*</sup> it has been suggested by Leighton<sup>13</sup> that the value of K should be directly related to  $k_a$ . The proportionality factor C will be a constant provided the spectral distribution of the sunlight and the temperature are constant. Therefore, it should be possible to calculate the value of  $k_a$  from the measurement of the concentration of NO, NO<sub>2</sub>, and O<sub>3</sub>.

In the presence of hydrocarbons, the rate of NO oxidation and O<sub>3</sub> formation increases. The O<sub>3</sub> and NO<sub>2</sub> concentrations are both higher than would be calculated from equilibrium reaction 13. Therefore, there is no a priori reason to predict that the value of Equation 14 should be equal to the value calculated in the absence of hydrocarbons.

---

\*The square brackets indicate the concentration of the species inside the brackets.

\*\*The amount of particulate matter in the air will have a slight effect on the indirect portion of sunlight, because blue light is scattered more than red light. This effect is small in the Bay Area, due to the low concentrations of particulate observed.

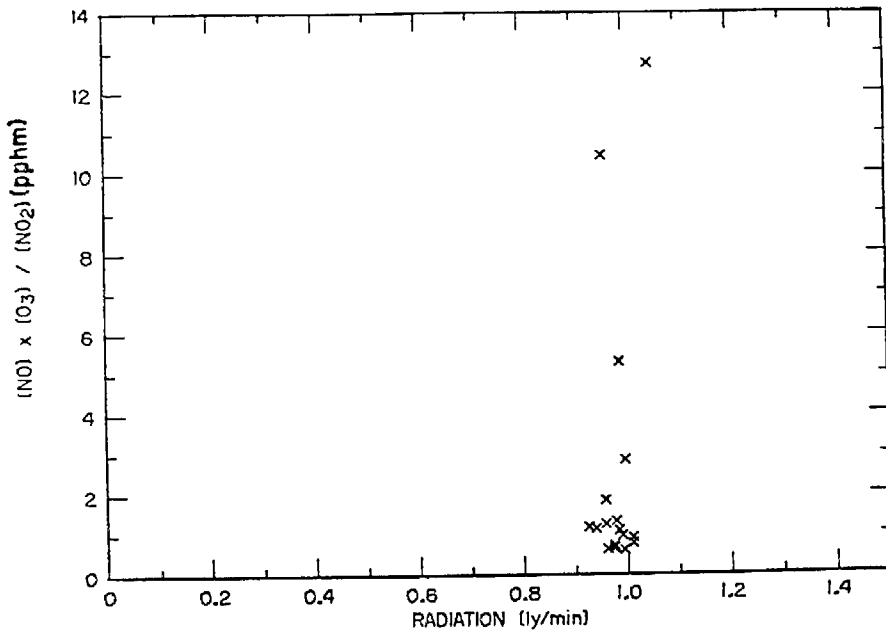
The first analysis of the solar intensity measurements resulted in data where the total solar intensity exceeded that expected for the sampling days.\* Furthermore, the calibration of the instrument using an Eppley pyranometer showed that the output of the instrument was zero at 0.67 Langleys/minute or lower because the sensing element was recessed in the housing. A reexamination of the data showed that the digital voltmeter of the Nova computer system over ranged above 1.0 volt (that is, a 1.5 volt input would be read as 0.5 volt). A computer program was written to correct for these errors. The resulting data for the four selected days are presented in Figure 23. The data for the four days were also combined and are presented in Figure 24.

A preliminary analysis of the houseboat data has been made using the four selected days as examples. The  $O_3$  concentrations were recorded every 30 seconds. Each recorded value is an average; the measured values were updated every minute. Solar intensity was recorded every 30 seconds, but these values must be smoothed by averaging to correct for the roll of the boat. For this preliminary analysis we have used the 5-minute averages of NO,  $NO_2$ , and  $O_3$  to calculate K and have compared these values to the 5-minute average solar intensity measured on the four selected days. A linear least-squares fit was applied to the data. The correlation coefficients of the ratio with solar intensity (Table 8) are low. This result agrees with the conclusions reached earlier in this section.

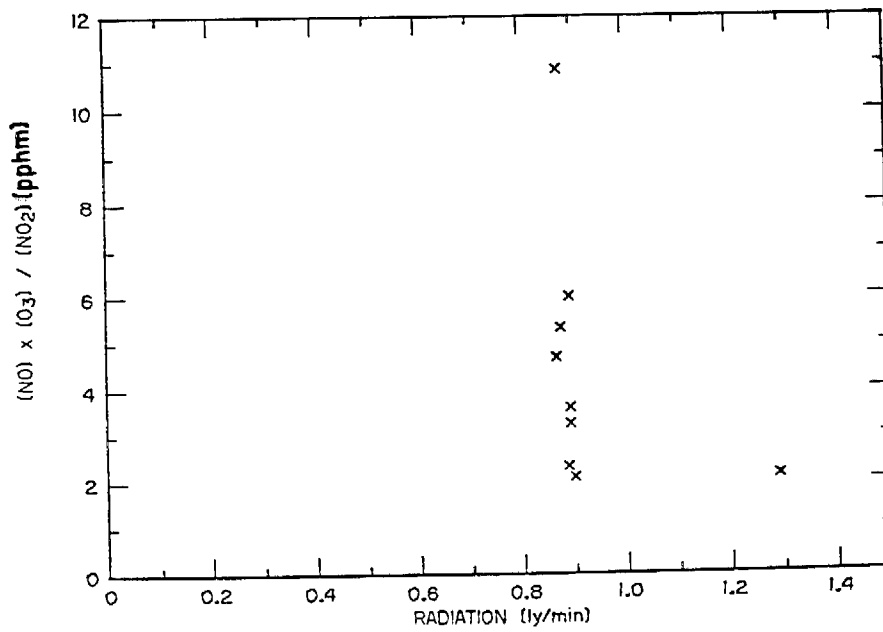
Plots of K versus time for each day suggested that K may correlate well with NO concentration. Plots of K versus NO concentrations were made (Figure 25), and the data for each of the four selected days were combined (Figure 26).

---

\*The expected maximum solar intensities are: 21 September, 1.4 Langleys/minute; 25 October, 1.25 Langleys/minute; 26 October, 1.15 Langleys/minute; 2 November, 0.95 Langleys/minute.

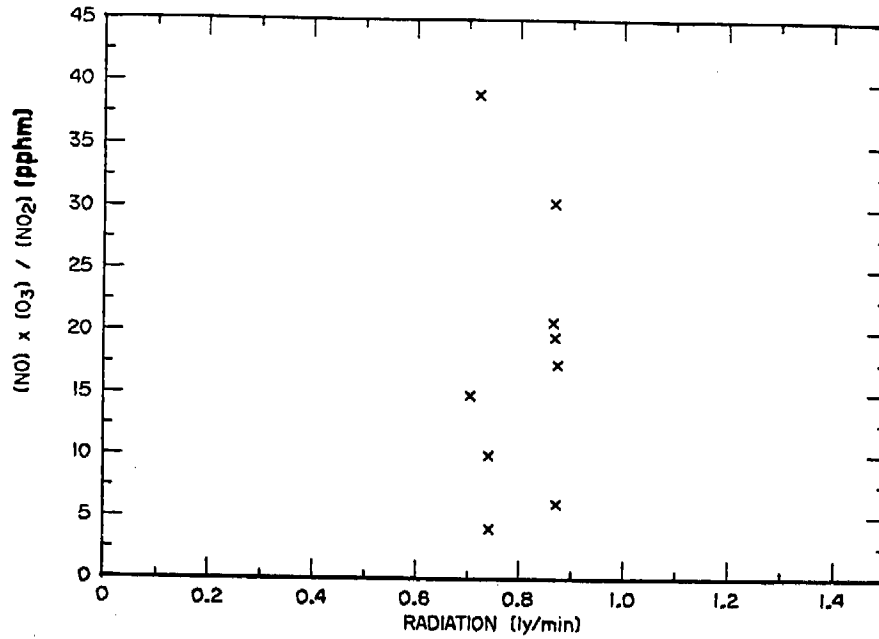


(a) 21 September 1972, 1037 to 1226 PST

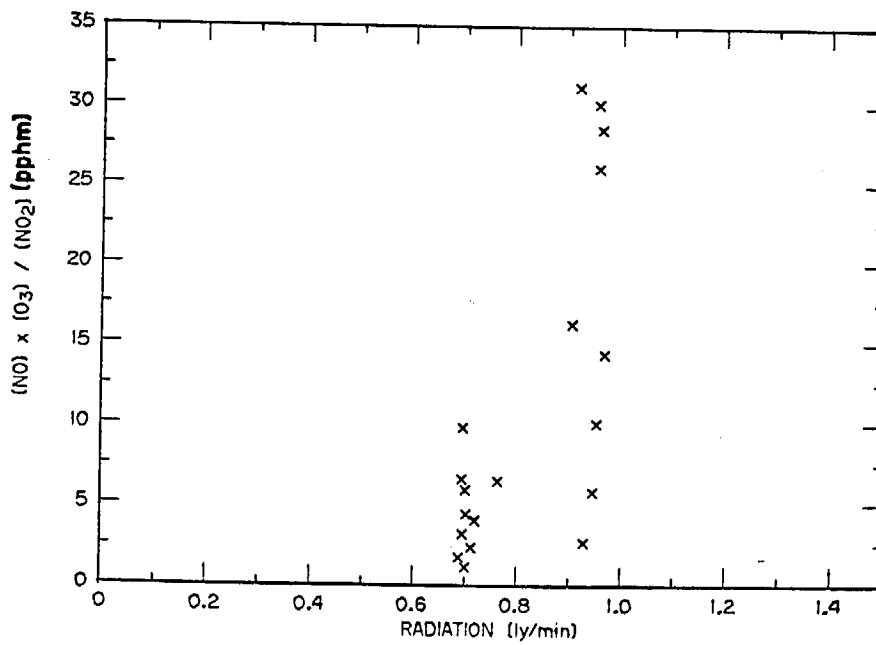


(b) 25 October 1972, 1138 to 1218 PST

FIGURE 23  $\frac{[NO][O_3]}{[NO_2]}$  RATIOS VERSUS SOLAR INTENSITY FOR TETROON RUNS (5-minute averages)



(c) 26 October 1972, 0907 to 0947 PST



(d) 2 November 1972, 1141 to 1316 PST

FIGURE 23 [NO] [O<sub>3</sub>] / [NO<sub>2</sub>] RATIOS VERSUS SOLAR INTENSITY FOR TETROON RUNS (5-minute averages) (Concluded)

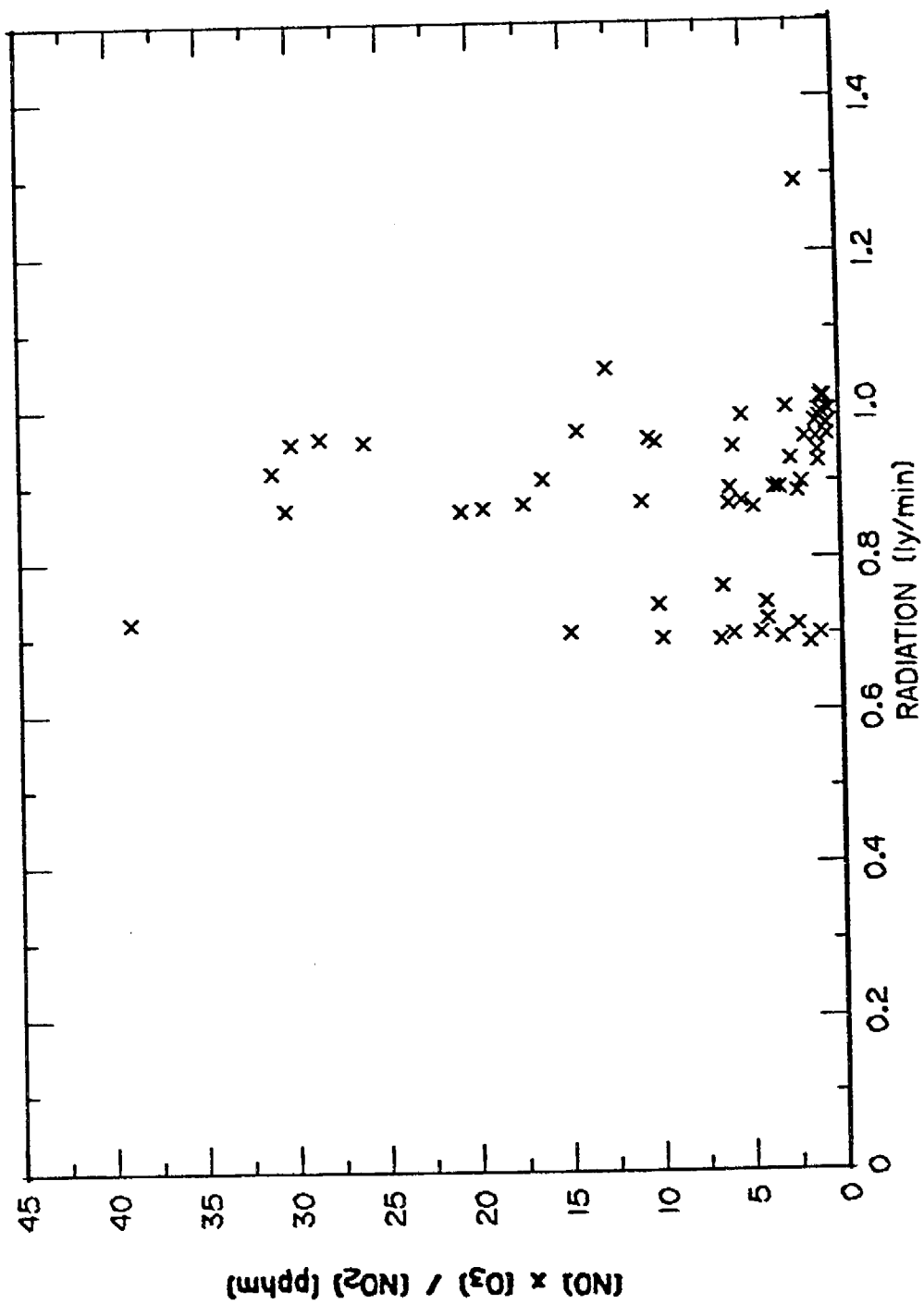
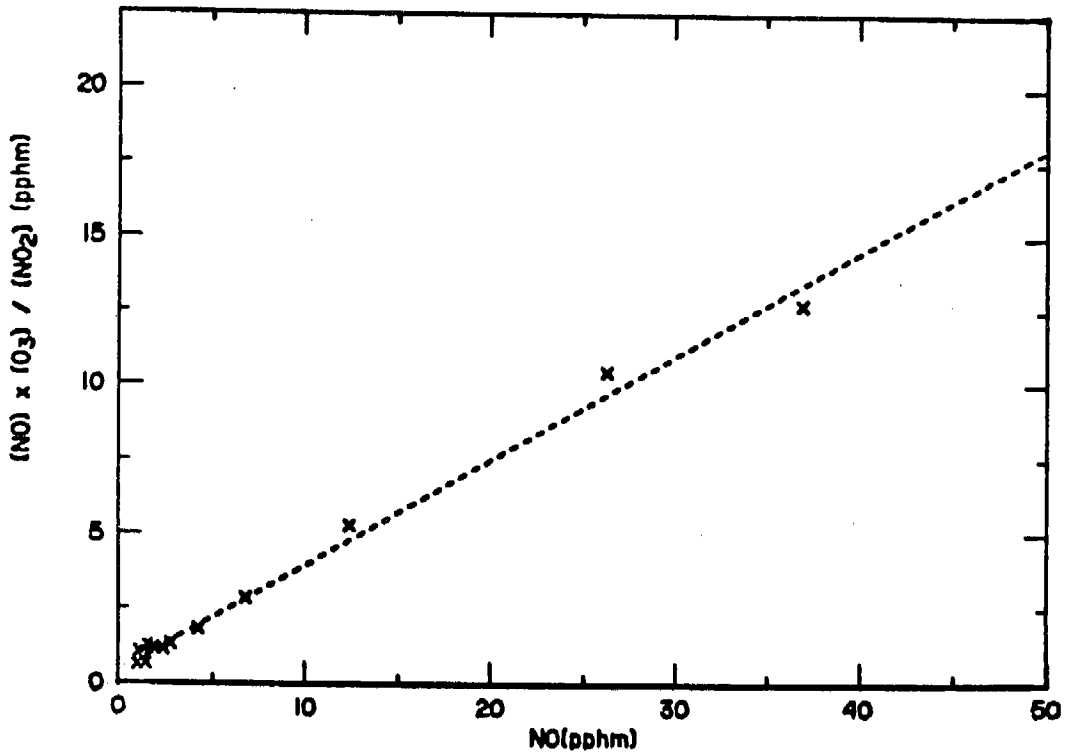
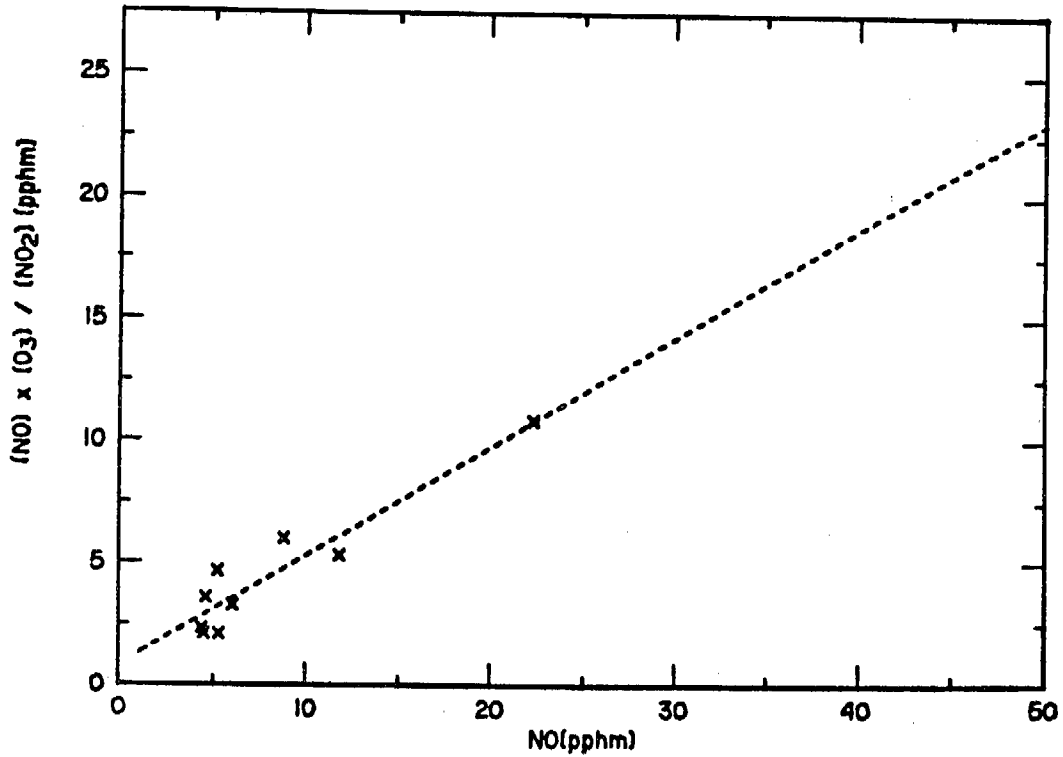


FIGURE 24  $[NO] [O_3] / [NO_2]$  RATIOS VERSUS SOLAR INTENSITY, COMBINED DATA FROM FIGURE 23

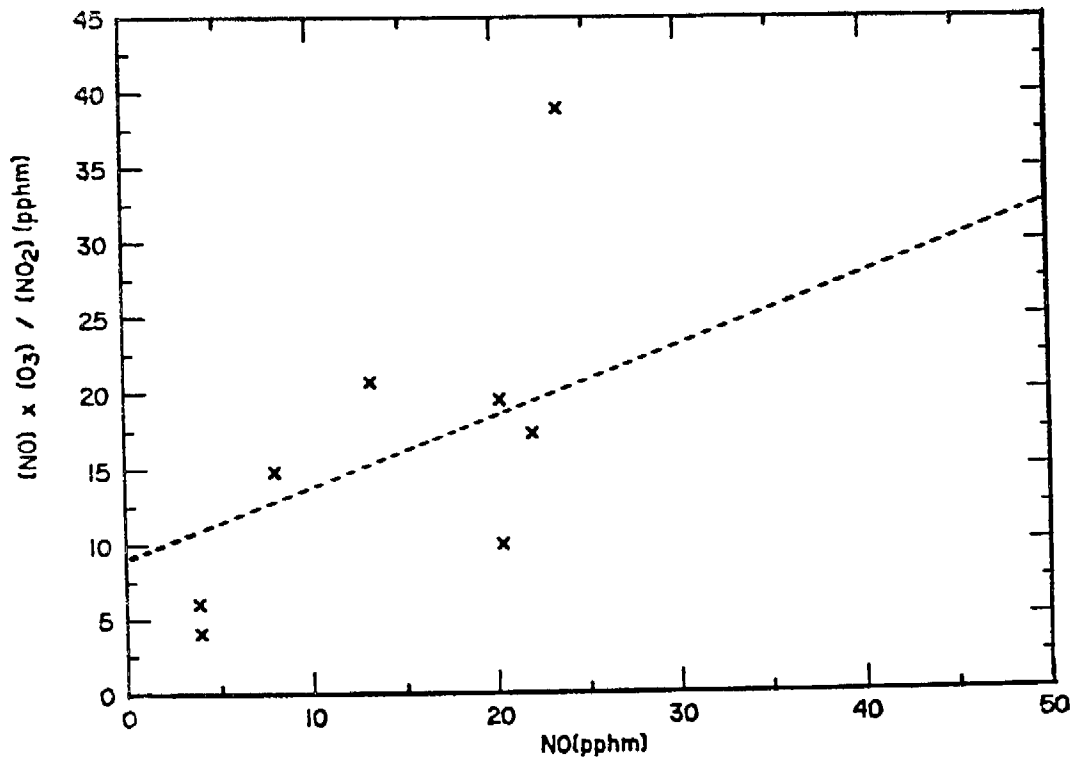


(a) 21 September 1972, 1037 to 1226 PST

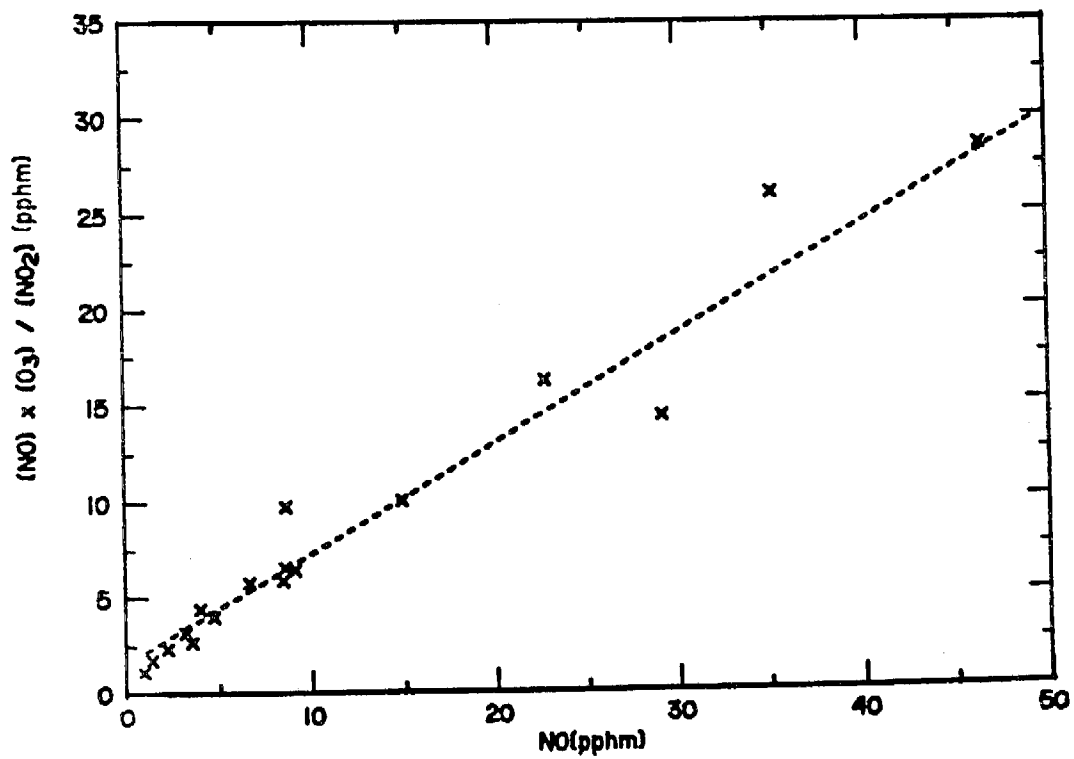


(b) 25 October 1972, 1138 to 1218 PST

FIGURE 25 [NO] [O<sub>3</sub>]/[NO<sub>2</sub>] RATIOS VERSUS NO CONCENTRATION FOR TETROON RUNS (5-minute averages)



(c) 26 October 1972, 0907 to 0947 PST



(d) 2 November 1972, 1141 to 1316 PST

FIGURE 25 [NO] [O<sub>3</sub>]/[NO<sub>2</sub>] RATIOS VERSUS NO CONCENTRATION FOR TETROON RUNS (5-minute averages) (Concluded)

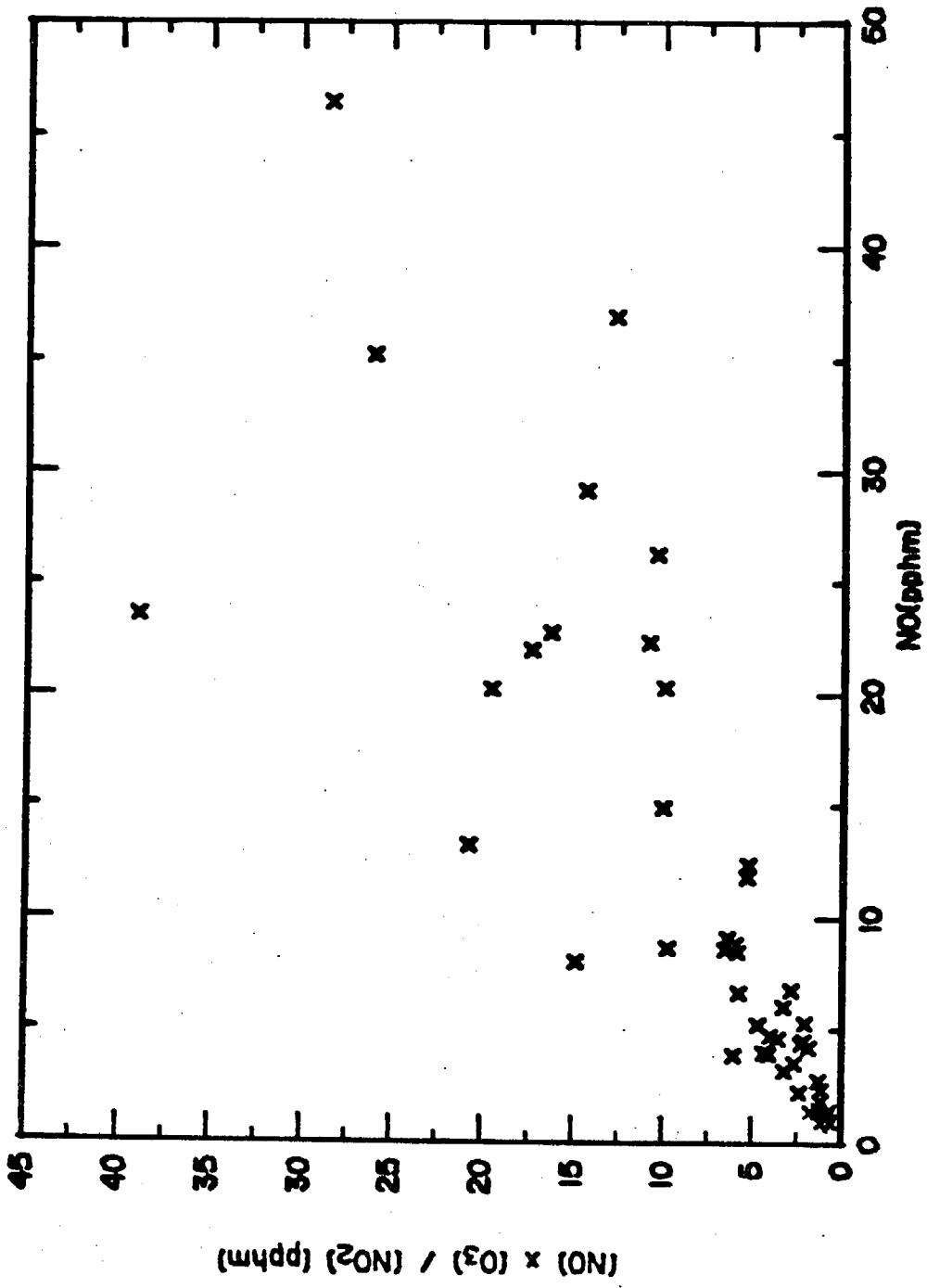


FIGURE 26 [NO] [O<sub>3</sub>]/[NO<sub>2</sub>] RATIOS VERSUS NO CONCENTRATION, COMBINED DATA FROM FIGURE 25

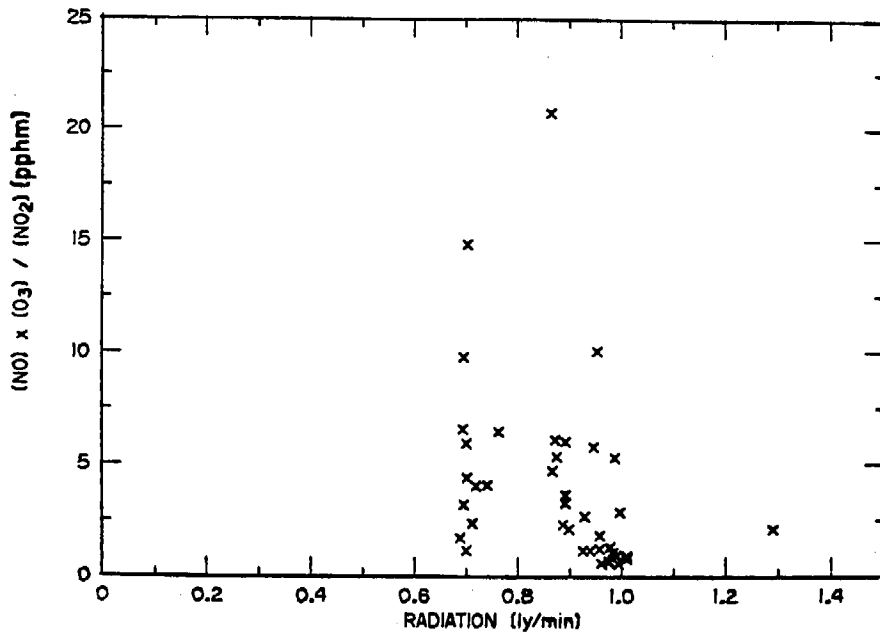
Table 8

## LINEAR LEAST-SQUARES FIT TO VALUES OF K

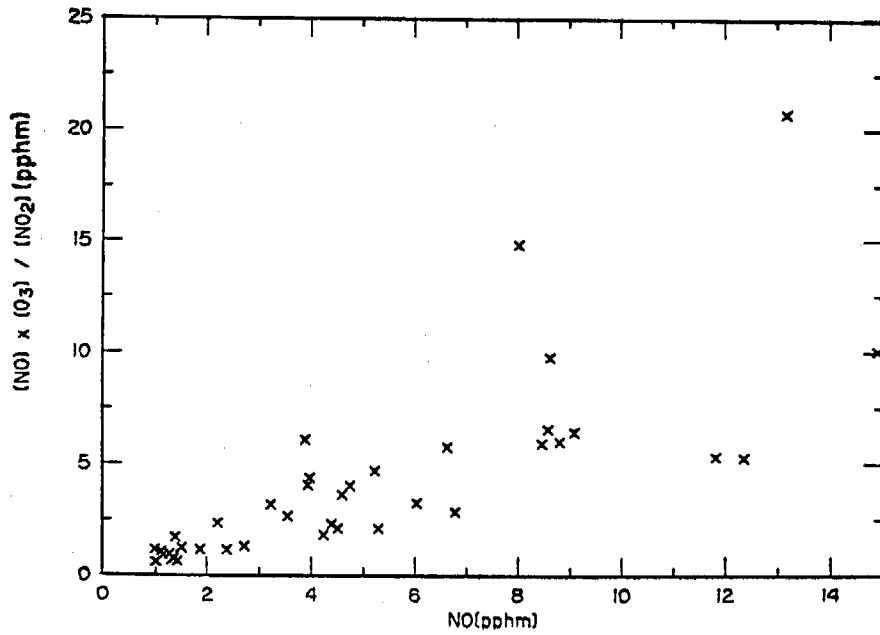
	<u>Slope</u>	<u>Correlation Coefficient</u>	<u>Photochemical Activity</u>
Correlation with Solar Intensity			
21 September	45.5	0.37	High
25 October	- 7.2	-0.35	Low
26 October	4.0	0.027	Very low
2 November	57.4	0.68	Medium
Combined data	- 7.2	-0.09	
Correlation with NO			
21 September	0.35	1.00	High
25 October	0.45	0.94	Low
26 October	0.48	0.67	Very low
2 November	0.63	0.97	Medium
Combined data	0.58	0.87	

The correlation coefficients with NO are high in all cases. One reason for the high correlation with NO is that in cases where exhaust contamination is observed, the NO concentration will be high. Furthermore, the rate of reaction (11) is slow enough that equilibrium (14) will not be reestablished before the exhaust-containing air is sampled. In an attempt to eliminate the effects of exhaust contamination, all data for NO concentrations greater than 15 pphm were excluded, the data for the four days were replotted (Figure 27), and the correlation coefficients recalculated. For K versus radiation, the slope was -10.4 with a correlation of -0.33; for K versus NO concentration, the slope was 0.84 with a correlation of 0.77.

There are possible errors in the radiation measurement due to dirt or sea spray on the pyranometer or to variations caused by boat roll.



(a)  $[\text{NO}] [\text{O}_3] / [\text{NO}_2]$  Ratios Versus Solar Intensity



(b)  $[\text{NO}] [\text{O}_3] / [\text{NO}_2]$  Ratios Versus NO Concentration

FIGURE 27 COMBINED DATA FROM FIGURES 25 AND 26 WITH DATA FOR NO CONCENTRATION GREATER THAN 15 pphm OMITTED (5-minute averages)

These errors do not explain the wide variation that was observed in solar intensity. If the two high values of K are excluded in Figure 22(b), the value of K would be less dependent of the NO concentration. However, the correlation with light intensity is still not good.

A detailed comparison of the ratio calculated with smog chamber and atmospheric measurements from other studies with solar intensity is beyond the scope of this research program. We have evaluated some recent data reported by Demerjian, Kerr, and Calvert for chamber experiments and theoretical calculations of  $K$ .<sup>14</sup> In all cases, they used a value of  $k_a \phi = 0.48 \text{ min}^{-1}$ , which corresponds to a solar zenith angle of 40 degrees. These data are given in Table 9. The average value of K is about 2.1 pphm from their theoretical data. However, experimental values from smog chambers are badly scattered, probably due to the poor accuracy of NO measurements at low concentrations. Since these data are calculated or measured at one level of solar intensity, it is difficult to compare the two types of measurements.

For future work, a more intensive analysis should be made of our data as well as the literature. A small modeling effort should be made to calculate values of  $k_a$  and K for other solar intensities. An ultraviolet sensor and an Eppley pyranometer should be added to the instrument complement. Data from an ultraviolet sensor would provide a better estimate of  $k_a$ .

Table 9

VALUES OF  $[\text{NO}][\text{O}_3]/[\text{NO}_2]$  FROM OTHER WORK<sup>14</sup>

Initial Conditions (pphm)	Irradiation Time (min)	$[\text{NO}][\text{O}_3]/[\text{NO}_2]$ (pphm)	
		Predicted	Experimental
$[\text{NO}] = 7.5; [\text{NO}_2] = 2.5; [\text{HC}] = 0$	60	2.1	--
$[\text{NO}] = 2.5; [\text{NO}_2] = 7.5; [\text{HC}] = 0$	60	2.1	--
$[\text{NO}] = 90; [\text{NO}_2] = 10;$ $[\text{Propylene}] = 210$	25	1.8	0.69
	50	1.9	1.8
	75	2.9	5.1
	100	2.3	6.3
$[\text{NO}] = 7.5; [\text{NO}_2] = 2.5;$ $[\text{t-2-Butene}] = 10$	20	1.8	--
	60	2.0	--

D. Observed Pollutant Inhomogeneity over San Francisco Bay

Apparent "pockets" of air containing high NO concentrations were frequently observed during tetron runs when new air was continuously overrun at the surface. These pockets were characterized by inhomogeneous NO concentrations (based on the variability in the data used to calculate the 5-minute averages), no corresponding increase THC, CO, and CN concentrations, and no corresponding decrease in O<sub>3</sub> concentration (due to reaction 11). Two explanations are possible; first, the NO was from shore sources, and second, it resulted from contamination by house-boat exhaust. The data do not adequately fit either explanation.

During intervals when exhaust gas contamination was known to occur, simultaneous increases in the concentrations of NO, CO, and CN were observed. Of these indicator pollutants, both NO and CN are extremely sensitive indicators of contamination, whereas CO is far less reliable

in identifying intervals of contamination. During maneuvers where the houseboat crossed its own path, increases in CN concentration were always observed but increases in NO concentrations may or may not be observed. Furthermore, the inlet to the sample mast was located 6 meters above and 7 meters forward of the exhaust gas exit ports of the houseboat. Since these "pockets" of air containing high NO concentrations were repeatedly observed when the houseboat was traveling at speeds greater than 20 km/hr, the source of NO cannot be satisfactorily explained by exhaust gas contamination.

Complex calculations of the turbulent mixing occurring in the wake of the houseboat underway at cruising speed have not been made and, realistically, probably could not provide accurate predictions of such mixing. The evaluation of the accuracy of such calculations could only be made by conducting experiments where exhaust gas constituents (NO, CO, and CN) are measured simultaneously from many locations on or near the houseboat superstructure. A definitive experiment of this nature was beyond the scope of this research project.

The PG&E power plants located at Hunters Point and Potrero Point (emissions of 15 tons of NO<sub>x</sub> per day) could contribute to the observed inhomogeneities, but calculations of plume concentrations indicate that in most instances additional significant source contributions would be required to produce the NO concentrations observed. These power plants are the largest stationary source of NO<sub>x</sub>, based on a list of pollutant sources supplied by the BAAPCD, that could significantly contribute to the burden within the area of interest. Other major stationary sources are located to the northeast near upper San Pablo and Suisun Bays. Due to the division of the wind flows, the emission from these other sources would not contribute to the atmospheric burden over the Bay near or to the south of San Francisco. The inhomogeneities of CN observed over the Bay are less significant since the sources of these particles are more

varied (combustion, sea spray, photochemical processes, and the like) and less well understood.

On the other hand, the observation that the  $O_3$  concentrations did not decrease in the presence of the high NO concentrations suggests that the source of NO is the houseboat exhaust. The half-life of reaction 11 is of the order of several seconds at the ambient concentrations. If the NO sources are on the shore, the time available for the NO to react with the  $O_3$  in the air parcel will be several minutes or longer. The observed  $O_3$  concentrations should be very low and certainly lower than those observed in the presence of the high NO concentrations. This anticipated reduction of the  $O_3$  concentration was not observed (with the exception of the data collected on 2 November near San Mateo Bridge, Figure 20). On the other hand, the residence time in the sampling line was 2 seconds which is short enough that only a small fraction of  $O_3$  should react.

The increase in the NO concentrations observed on specific occasions over San Francisco Bay without a corresponding increase in  $O_3$  concentration is compelling evidence suggesting partial exhaust gas contamination. The lack of substantiating increases in the concentration of CO and particularly CN during these intervals remains unexplained if contamination is actually the cause. The location of the sample inlet relative to the source of exhaust gases during traverses in the wind likewise nearly, but not absolutely, precludes exhaust gas contamination. The conflicting results obtained in this project cannot be interpreted with absolute certainty on the basis of known data.



## VII CONCLUSIONS AND RECOMMENDATIONS

### A. Applicability of Methods and Data for Model Verification

The objectives of this research project were twofold: first, determine the feasibility of a mobile laboratory to mark a parcel of air and measure the changes in constituents and concentration during aging; second, obtain measurements defining photochemical activity in tetraon-marked air parcels and present these in a form suitable for verification of photochemical models.

This research program demonstrated that a mobile laboratory can be used to follow an air parcel and to collect air quality data in a Lagrangian mode. Marking an air parcel by a tetraon is a feasible approach to a Lagrangian measurement of pollutant concentrations. Due to surface frictional effects, a wind shear of approximately  $-0.01$  m/sec/m was observed. This meant that the surface laboratory overran air parcels at a rate of about  $0.5$  m/sec. If the air parcel moves at speeds greater than about  $1.5$  m/sec, measurements can be made without contamination by the houseboat exhaust. At speeds of less than about  $1.5$  m/sec, the possibility of contamination is always present.

The appropriate logistics to effectively coordinate the operation of surface and airborne mobile laboratories were developed. The concept of using a houseboat as a mobile laboratory proved to be very effective. The houseboat provides a stable platform well suited for the operation of air quality instruments. The navigational procedures employed provided position fixes with excellent resolution throughout the Bay. The speed of the houseboat was adequate to accommodate tetraon tracking at a variety of wind speeds. The line power available from the onboard

generator had adequate stability for operation of the air quality sensors. The battery-inverter system was an adequate power supply for frequency-sensitive equipment such as the data tape recorder and the computer. The voltage decrease that was observed as the batteries discharged could be corrected by the use of a variable transformer.

The helicopter instrument package was designed to be easily installed and removed from a nondedicated helicopter. The procedures developed to keep the airborne instrument package warmed up and operational prior to installation in the helicopter were satisfactory. Communication between the houseboat and the helicopter was excellent. The equipment used and procedures developed during this research program represent a viable approach to the study of atmospheric photochemistry.

The measurement data obtained during the program, even though the pollutant concentrations were uniformly low, could provide useful data as to the role of photochemistry at low concentrations that approach the air quality standard and the concentration gradients that accompany these levels. In addition to pollutant measurements made during tetron runs, a limited effort was made to map pollutant concentrations over San Francisco Bay and to identify the sources of emission responsible for the observed pollutants. During more normal meteorological conditions, wind flow patterns and wind speeds more conducive to photochemical smog formation would have been established. Under these conditions, the tetron runs could more often have been initiated immediately downwind of an urban source with high concentrations of pollutant precursors to smog. In addition, the direction of tetron travel under these conditions would have permitted longer tetron runs and hence a longer interval for photochemical reactions to occur.

The observed microscale inhomogeneities in the distribution of pollutants over San Francisco Bay, particularly NO, were greater than anticipated. As discussed in the previous section of this report, two explanations are possible -- shore sources and exhaust gas contamination. The data do not adequately substantiate either explanation. Thus, on the basis of the data, the source of high NO concentration cannot be identified with absolute certainty.

The observations of pollutant concentrations immediately downwind of a large urban source also indicated that the pollutant burden was inhomogeneously mixed in the air mass. Wide variations in pollutant concentrations were observed both spatially and temporally downwind of San Francisco. At distances of less than 2 kilometers offshore of San Francisco, the urban source must be considered as a multiplicity of individual sources rather than a diffuse source. Thus, tetron runs with the objective of determining a mass balance should be initiated as a sufficient distance downwind of an urban source to ensure homogeneity through adequate mixing. The determination of a mass balance could also be accomplished by vertical and horizontal concentration mapping and averaging by the mobile laboratories prior to tetron launch. This technique coupled with simulation modeling to predict the pollutant contribution of adjacent air masses, through vertical and horizontal diffusion, could provide the basis for a mass balance determination in the air parcel under observation.

A major problem encountered under certain operational modes was contamination of the gas samples (and, to a lesser extent, the particulate samples) by engine exhaust. In addition to raising the height of the sample inlets, modifications to the engines could be made to reduce the exhaust emissions. Two alternative types of controls could be used: a combination of exhaust gas recirculation and a catalytic converter or modification of the induction system so that very lean operation is possible.

Catalytic converters would require complete overhaul of the engines and replacement of the exhaust systems to remove all traces of lead deposits. It would be necessary to use unleaded gasoline. Prototype induction systems have been shown (at SRI as well as elsewhere) to permit very lean operation (an air to fuel ratio of 18 or higher) at constant speed operation. This operational mode decreases hydrocarbon and NO<sub>x</sub> emissions very effectively (factors of 10 or higher). The major problem is that satisfactory operation during acceleration or deceleration is not possible with current devices known to us. Since the houseboat was normally operated at a constant speed, one could release the throttle and then adjust the air to fuel ratio to minimize the exhaust emissions.

In summary, the acquired data will be useful for photochemical modeling of low pollution conditions. The measurement approach was sound and a wealth of valid measurements were obtained. In addition, a good understanding was acquired of meteorological conditions over the Bay with respect to shore observations. The knowledge gained during this research program will provide an excellent basis for future photochemical studies over San Francisco Bay.

#### B. Recommendations for Future Research

A follow-on program is strongly recommended that would capitalize on the extensive experience SRI has gained in this program. It should begin in June to increase the likelihood that high smog levels could be studied. Although the basic approach used in this program was viable, several changes are recommended:

- Provide a better facility to weigh off tetrooms--A transparent plexiglas housing should be fabricated and located on the deck space forward of the main cabin of the houseboat. This housing would provide a turbulence-free location to accurately weigh off tetrooms during full or partial exposure to sunlight. Also, the transparent walls of the shelter would not blind the lower cabin, which was the case during intervals when the tetroom shelter was erected. Better tetroom weigh-off procedures are required so that the tetrooms will float at lower altitudes.
  
- Locate sample inlet mast at a higher elevation--The sample inlet mast should be extended above the houseboat as high as is practical; it could easily be extended 11 meters or more above the water. The additional height would reduce the possibility of exhaust gas contamination and improve the ratio of sample inlet height to tetroom height. The higher sample mast in conjunction with tetroom flights at lower altitude would also improve the objective of measurement in a discrete air parcel.
  
- Mount a wind vane and anemometer--A permanently mounted recording wind vane and anemometer should be mast-mounted on the houseboat. These wind measurements should be integrated into the data acquisition system and recorded on the data tape. The compass heading at selected intervals could be entered manually into the data acquisition system by teletype. If a navigation compass with an analog output voltage could be obtained or fabricated, the inclusion of these measurements into the data would be very useful. The wind vane and anemometer would primarily serve to log differential wind speed and directions.
  
- Gimbal the solar intensity sensor--The solar intensity sensor should be replaced with an Eppley pyranometer mounted on a gimballed platform to reduce short-term variation due to boat motion. A gimballed ultraviolet sensor should be added to the instrument complement.
  
- Delete the gas chromatograph from the onboard instrumentation--The gas chromatograph did not operate in a satisfactory manner under the normal motions of the boat. Cryogenic samples should be collected at 1/4 to 1/2 hourly intervals and returned to the laboratory for analysis of selected samples.

- Install a catalytic accessory for THC sensor--A switchable catalytic converter should be installed in series with the inlet to the THC sensor to provide methane only and THC measurements. The catalytic converter would be operated at periodic intervals to obtain in-situ methane measurements.
- Delete the Lundgren impactor from the aerosol instrumentation--A two-stage collector for particulate material should be substituted for the Lundgren impactor. The design of the Lundgren does not permit sample foils to be easily installed or removed. The sample analysis is complex, expensive, and does not provide particulate data vital to understanding the photochemical processes.
- Increase the frequency of particulate collection--The high-volume samples collected during this measurement program were large enough that shorter collection times of 1 hour or less should be used. This data would permit a more accurate determination of the mass balance.
- Shock-mount the nondispersive infrared CO analyzer--The NDIR CO analyzer should be shock mounted to improve the signal-to-noise ratio at cruising speeds. At tetron tracking speeds, the performance of the NDIR was adequate without shock mounting.
- Use a different measurement principle for airborne CO measurements--The mercury displacement CO analyzer used in the helicopter was not satisfactory. Concentration gradients or relative measurements could be made, but absolute concentrations were difficult to retrieve from the acquired data. An Andros Isotope Fluorescence CO analyzer is recommended for future airborne instrumentation.
- Improve communication and in situ recording of conversation and radio transmissions--The houseboat should be equipped with an intercom system with voice recording of all communication between the bridge and the main cabin. In addition, communication from the houseboat to the helicopter should be directly to the instrument operator rather than relayed through the pilot.
- Improve instrumentation for wet and dry bulb temperatures--The wet bulb temperature measurement was erratic due to the design of the wick reservoir.

- Reduce houseboat engine emissions--Equip the houseboat engines with an induction system designed to reduce HC and NO<sub>x</sub> emissions through the use of a very lean air to fuel mixture.

These recommendations do not represent basic changes in the approach that was employed during this research program. However, they do represent changes in equipment or operating techniques that, if incorporated, would improve data capture and data interpretation for future studies.

CARB LIBRARY



08564

Appendix A

THE CLIMATOLOGY OF THE SAN FRANCISCO BAY AREA

## Appendix A

### THE CLIMATOLOGY OF THE SAN FRANCISCO BAY AREA

#### 1. Introduction

The pollution climate of an area is the product of all the meteorological factors that affect atmospheric transport and dispersion, including wind, atmospheric stability, and precipitation. The meteorological factors are disrupted and modified by topographical and geographical features so that very important local effects are observed. Figure A-1 shows the topography of the region. It is characterized by a large body of water and an encircling range of hills. The "Bay" (San Pablo and San Francisco Bays) is the world's largest natural harbor, covering approximately 1000 square kilometers. High densities of population and industrial activity have settled on the low lands surrounding the Bay. Modification of the natural surface is very extensive and is likely to continue or accelerate.

#### 2. Topographic and Geographic Factors

The San Francisco Bay area centers about an elongated body of water enclosed by various mountains and hills that comprise the Coast Ranges. The Golden Gate is one sea level entrance to the Bay; the other is at Carquinez Strait, where the Sacramento River empties into the northeast end of the Bay. The effect of the barrier of hills is to restrict air flow, giving rise to certain typical mesoscale circulation patterns that are governed by the gradient wind field, the thermal stability, and the topography. The effectiveness of the topographic barriers in determining airflow barriers is dependent on weather regime, with summer and fall months providing the greater frequencies of topographically controlled

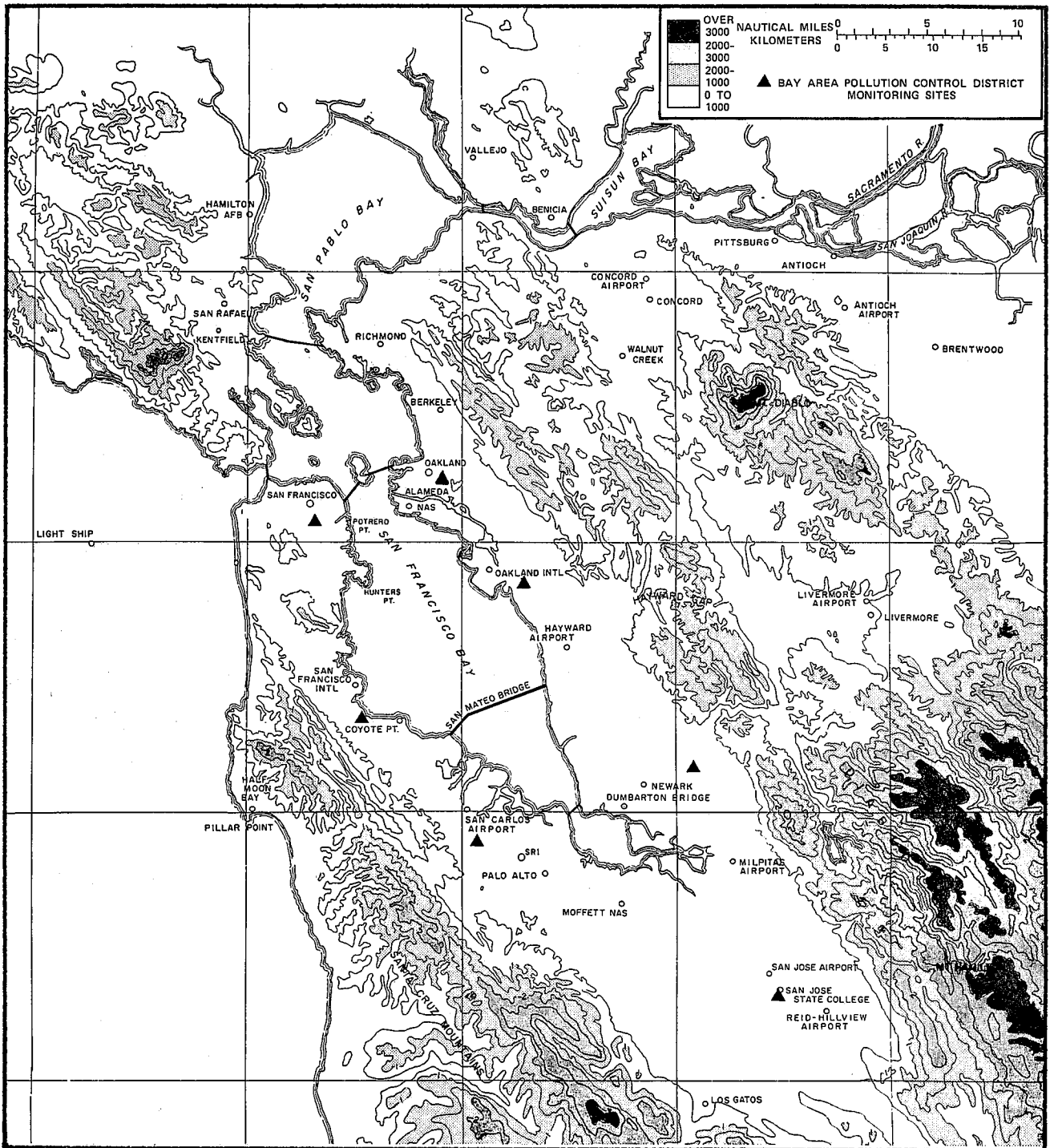


FIGURE A-1 THE SAN FRANCISCO BAY AREA

situations. Typically, during these seasons, there is limited sea-level flow to the east through the narrow Carquinez Strait. There is also some flow into the Livermore area through the Hayward Gap and Niles Canyon. The geography provides a nearly closed system with a uniform base surface.

### 3. Meteorological Factors

#### a. Winds

The semipermanent Pacific high that dominates the summer climate of the Bay area reaches its maximum intensity in August. Characteristic features of the high are the persistent west-northwest flow and the strong subsidence inversions above a cold marine layer with its attendant stratus cloud system. Large-scale temperature gradients are at their maximum because a thermal low pressure area develops over the Central Valley of California. During the fall, the Pacific high moves southeastward, merging occasionally with continental high cells to form large, stagnant, blocking systems. Wind speeds decrease, become northerly or northeasterly, and in turn drastically reduce the onshore movement of the cold marine layer. Shorter days and clear nights contribute to the lessening of the large-scale thermal gradient between the ocean and Central California. This, in turn, brings about a seasonal reduction of the onshore wind patterns that, in the summer, carry cool marine air throughout much of the Bay area.

Within the Bay area, wind flow distortion arises when air is channeled by terrain features and forced to rise above or move around hills. Wind observations in the Bay area often show patterns of confluence and diffluence, caused by physical features in the terrain. Differential heating also plays a large role in determining Bay area wind patterns because the total water surface is not much less than the total land surface. The familiar patterns of land-sea breezes is strongest in the summer, but with decreasing solar radiation over the land area in the fall, the onshore sea breeze flow weakens accordingly. Light and variable wind con-

ditions are prevalent favoring air pollution accumulation. Highest frequency of light and variable surface winds occurs during November, as evidenced by Smalley's findings shown in Table A-1.<sup>8</sup>

Table A-1

PERCENTAGE FREQUENCY OF LIGHT-VARIABLE SURFACE  
WINDS IN THE SAN FRANCISCO BAY AREA  
(1952 to 1955)<sup>8</sup>

Month	Time of Day (PST)				All Hours
	0400 (%)	1000 (%)	1600 (%)	2200 (%)	
Jan	39	32	30	35	34
Feb	41	29	20	43	33
Mar	31	30	4	26	23
Apr	33	19	1	13	16
May	31	14	2	14	15
Jun	17	7	0	6	7
Jul	12	5	0	4	5
Aug	9	15	0	4	7
Sep	38	38	2	22	22
Oct	52	39	5	34	32
Nov	58	44	23	51	44
Dec	35	27	22	31	29
Annual	33	24	9	24	22

Smalley's study includes a summary of prevalent surface wind flow patterns that occurred over a four-year period. Figure A-2 is an October pattern showing a wind flow typical of the transition from summertime westerly flow to a wintertime north-northeasterly flow. A more recent study by Meteorology Research Inc.<sup>5</sup> found airflow patterns

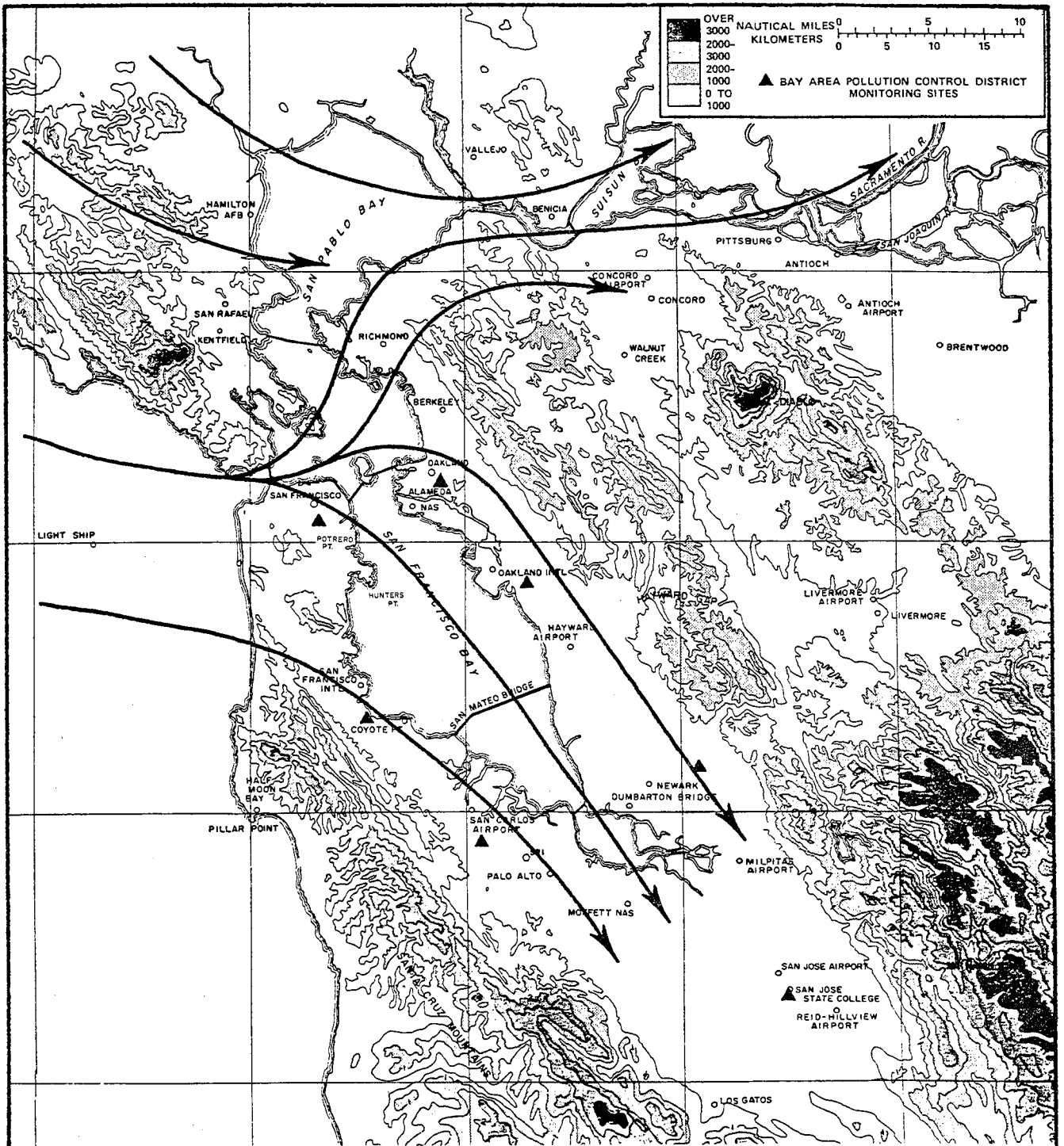


FIGURE A-2 PREVALENT SURFACE WIND FLOW PATTERN FOR OCTOBER

during October afternoons over San Francisco Bay that were essentially the same as those found by Smalley.<sup>9</sup> Incidence of marine air intrusions over mountain tops and passes is restricted by the lowering of the inversion. The implication of such wind patterns for air pollution problems is obvious with pollutants generated in San Francisco and western parts of the area being carried to the east and especially south-east across San Francisco Bay.

b. Temperature

The daytime temperatures in the Bay area are very strongly influenced by the topography. The airflow induced by that topography and the cold coastal waters of the Pacific Ocean (Figure A-3) shows the average maximum temperatures for July.<sup>15</sup> The influence of the Bay is very marked with a cooler tongue of air penetrating over the Bay and southward into San Jose and the Santa Clara Valley. This is partly due to the moderating effect of the Bay waters and partly due to the movement of air cooled by the ocean through the Golden Gate and down the Bay.

Figure A-4 shows the average October maximum temperature field,<sup>16</sup> The same general features are visible as in Figure A-3 for July. However, the gradients are much weaker, indicating less penetration of air from the Pacific. Further evidence of this is indicated by the fact that the average maximum temperatures are higher in San Francisco in October than in July. This is because the influx of cold Pacific air is less frequent in the latter month and lighter wind conditions generally prevail.

c. Inversions

Temperature inversions occur in the Bay area as two general types: summer subsidence inversions and winter radiation inversions. Autumn appears to be a period of transition between the seasonal extremes of a high-subsidence inversion and a low-radiation inversion. Subsidence inversions are often accompanied by stratus clouds, whereas the surface-based radiation inversions are best developed under cloudless skies. Often in the fall, both types of inversions can be found together or merged when

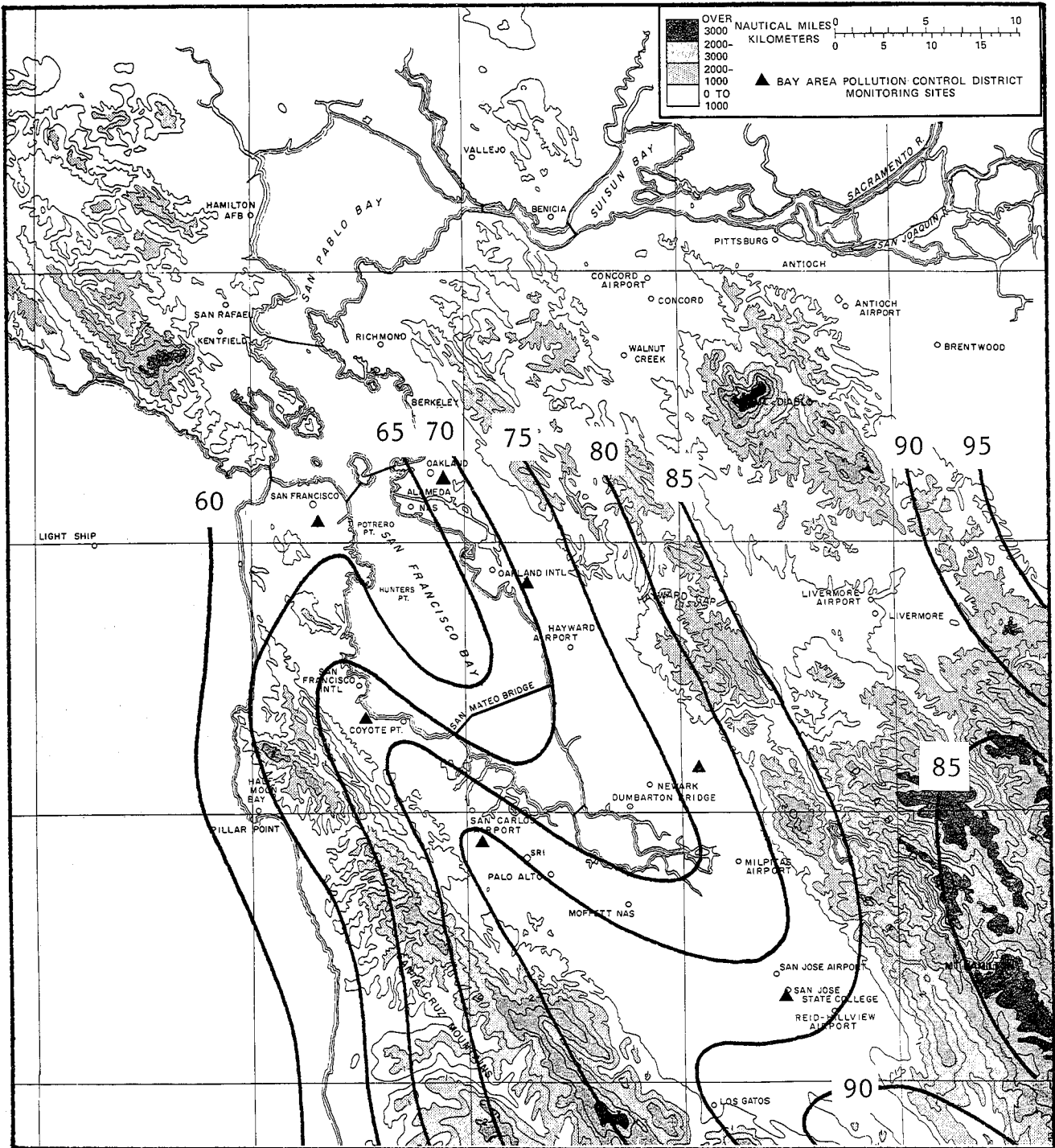


FIGURE A-3 JULY AVERAGE MAXIMUM TEMPERATURES (°F)

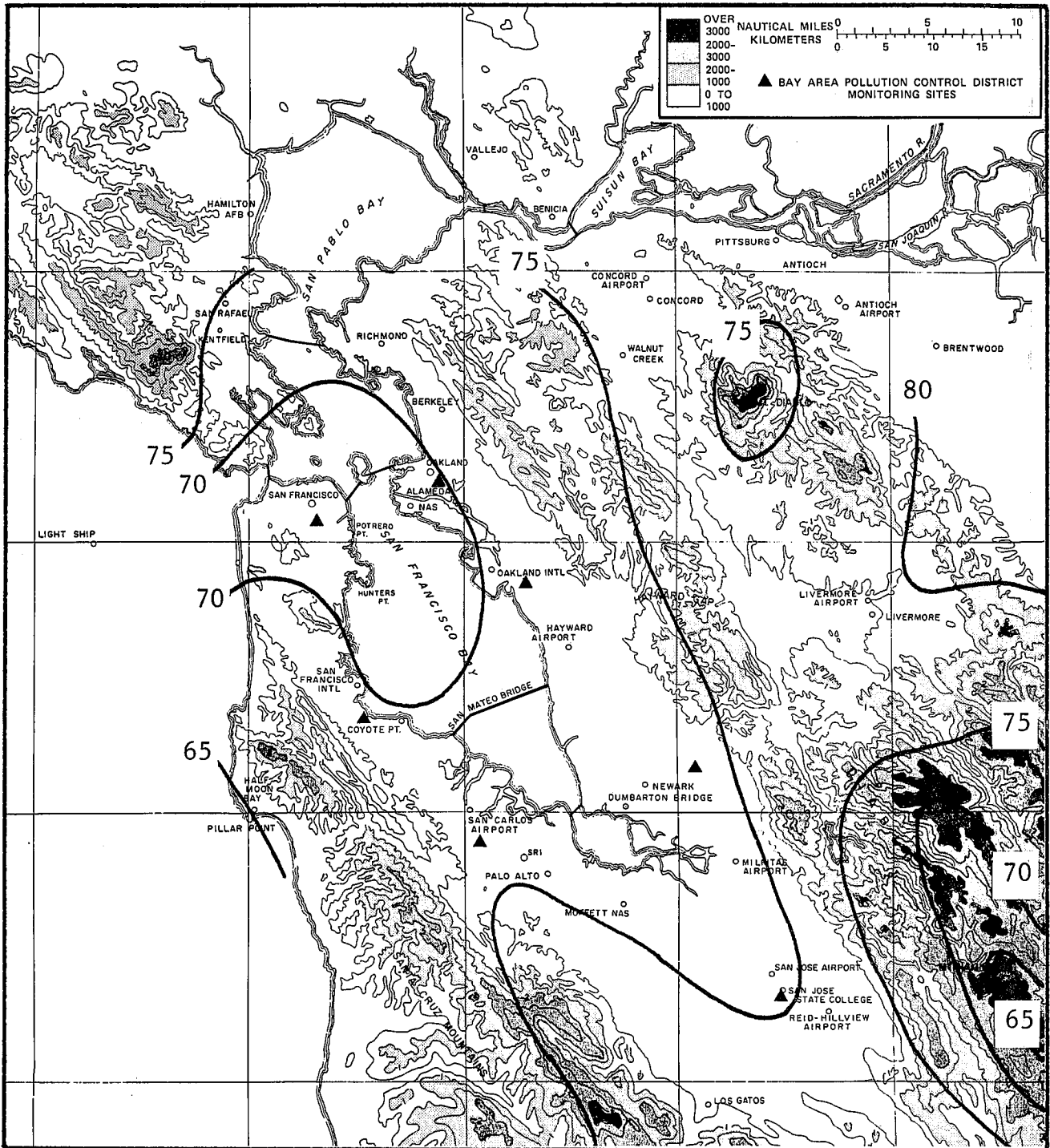


FIGURE A-4 OCTOBER AVERAGE MAXIMUM TEMPERATURE (°F)

conditions favor the simultaneous development of both types. During clear northwesterly and westerly wind conditions, the inversion base averages 200 meters. When north to northeast winds prevail, the average inversion base is less than 60 meters.<sup>17</sup> An SRI study found the most frequently occurring inversion base height during October to be less than 100 meters.<sup>18</sup> The height of the inversion base is slightly lower over the South Bay than over the North Bay. More recent observations by Ahrens and Miller show that the height and the intensity of the subsidence inversion vary over the Bay area, being typically lowest over the Bay and increasing in height toward the surrounding hills.<sup>19</sup>

Average inversion base heights for Oakland in the fall months are listed in Table A-2. A lowering of the average height of the inversion base from September to November shows the transition from a summer subsidence to a winter radiation type. Most radiation inversions have dissipated by 1600 PST, whereas subsidence inversions tend to persist with only slight diurnal changes.

d. Cloud Cover and Precipitation

In the summer, the dominant cloud type in the Bay area is stratus. This cloud forms at the top of the marine layer, just below the inversion. Its occurrence tends to mark the flow of marine air in the region. Figure A-5 shows the percentage of occurrence of stratus during the summer forenoons of 1952.<sup>17</sup> The airflow patterns that have already been discussed are reflected in these frequencies. The high frequencies seem to pass through the Golden Gate and down over the Bay because typical flows of marine air and associated stratus follow this path. As these flows weaken in the fall, there is a corresponding decrease in the frequency of stratus over the Bay. Cloud amounts increase from September through November, but they are not usually of the summer stratus variety. The autumn increase of cloudiness is caused by an increasing frequency of synoptic disturbances, some of which produce precipitation.

Table A-2

FREQUENCY AND AVERAGE INVERSION BASE HEIGHTS BY MONTH FOR OAKLAND

Observation Time	0400 PST		0700 PST		1600 PST		1900 PST	
	% Frequency	AV Ht						
Below 2501 feet	77	731	83	853	67	847	92	742
	76	396	74	506	47	790	79	579
	78	232	90	157	33	1125	85	187
Below 5001 feet	91	1100	97	1196	76	1164	97	912
	86	739	77	672	62	1481	87	905
	87	498	92	206	59	2155	85	187

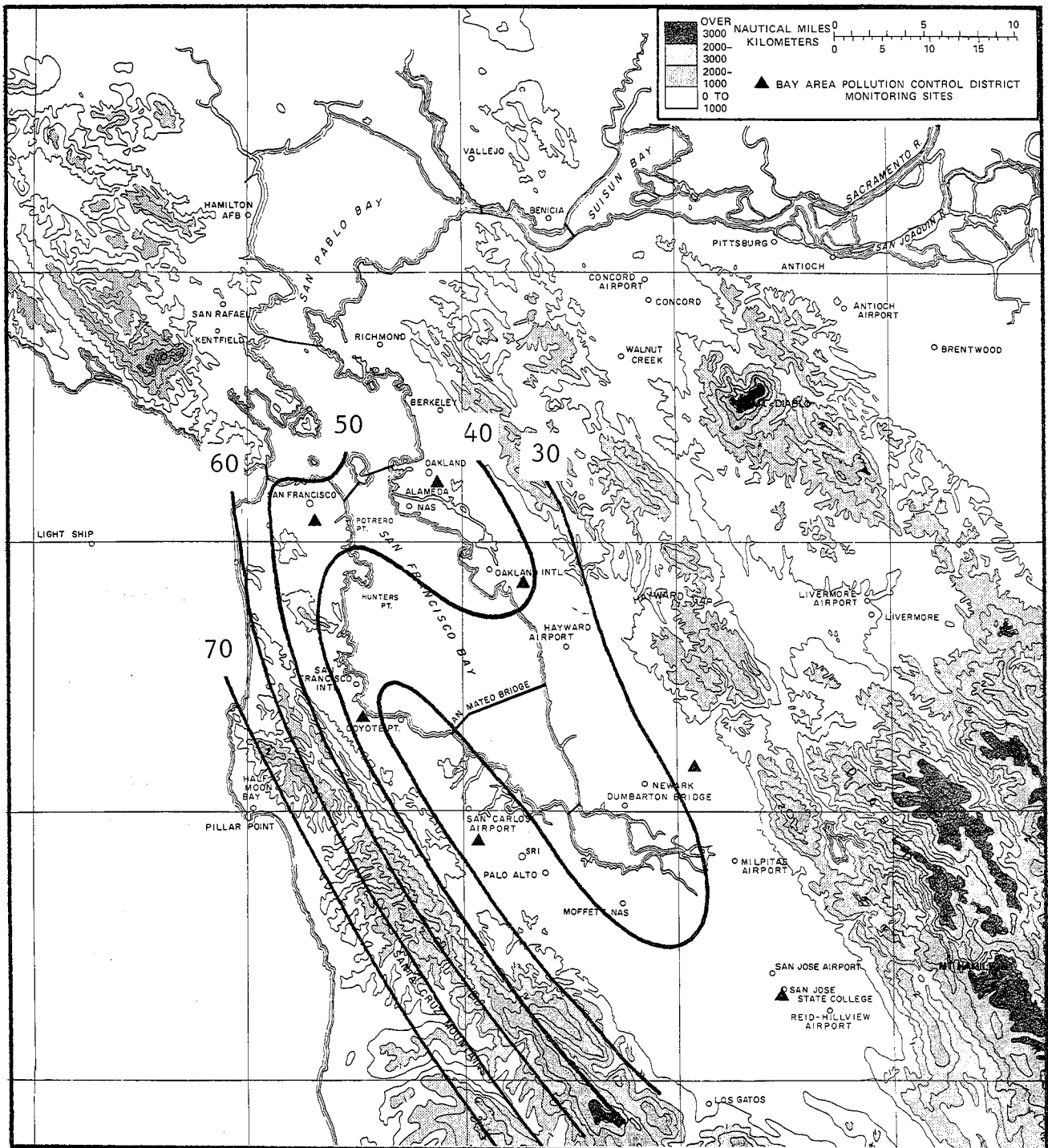


FIGURE A-5 PERCENTAGE OF OBSERVATIONS OF FOG OR STRATUS AT 1030 PST DURING SUMMER, 1952

Precipitation is also greatly affected by local terrain. Mechanical lifting is the principal mechanism, producing heavier amounts at high elevations, particularly along slopes that face the west. The spatial pattern of average annual precipitation is shown in Figure A-6. There is considerable variation from year to year. Precipitation-producing mechanisms are synoptic in scale, with a trend in the autumn toward a gradual increase in precipitation from a summer minimum to a winter maximum.

#### 4. Oxidant Concentrations

##### a. Trends in the Bay Area

The occurrence of high oxidant levels in the Bay area varies considerably from year to year. The BAAPCD has six monitoring stations<sup>\*</sup> with long-term historical oxidant concentration data. Data from these stations are used to determine the oxidant concentration trends throughout the district.<sup>20</sup> The number of days where the high hourly average equalled or exceeded 15 pphm at one or more of the stations was 57 in 1965, 28 in 1966, 44 in 1967, 36 in 1968, 44 in 1969, 31 in 1970, 19 in 1971, and 4 in 1972.

Meteorological factors, along with the emissions of reactive organics and  $\text{NO}_x$ , play important roles in determining observed oxidant concentrations. To assess the effectiveness of control measures, the BAAPCD has objectively selected certain days from the complete data base; these days have comparable meteorological conditions of a kind that tend to occur with high oxidant concentrations. Specifically, days are only chosen for comparison when the afternoon Oakland sounding shows an inversion base below 300 meters and the maximum temperature at the benchmark station exceeds 84°F. The temperature criterion for San Francisco and San Leandro is 74°F, rather than the 84°F used for the other stations.

<sup>\*</sup> Located in San Francisco, San Leandro, San Jose, Redwood City, Walnut Creek, San Rafael, and, more recently, Livermore.

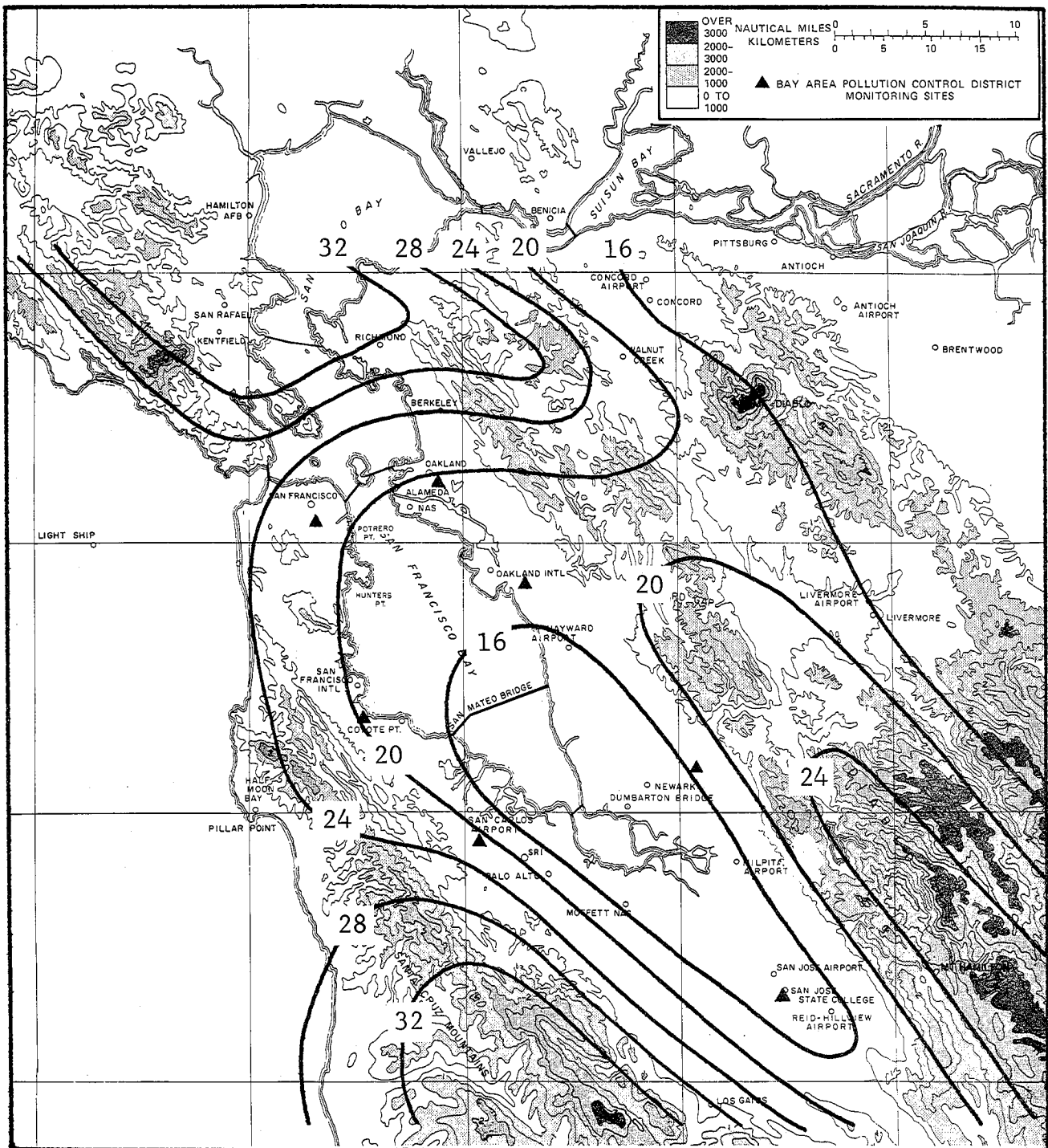


FIGURE A-6 NORMAL ANNUAL TOTAL PRECIPITATION (Inches)

The annual highest hourly average oxidant concentrations for each BAAPCD station are plotted in Figure A-7. As a result of the selection process, the variations due to meteorological changes from year to year have been minimized and the trends exhibited probably reflect the results of control measures on sources of pollutants.

b. Geographical Distribution

The broad climatological patterns of the Bay area that have already been discussed indicate that the most severe oxidant episodes will be encountered in the valleys downwind of the highly urbanized districts. During the April to October smog season, airflows are such that reactive pollutants are carried from their sources in the major city areas into several of the valleys, e.g., Livermore and Santa Clara, where warmer temperatures and light winds are conducive to higher oxidant buildups. Of course, the buildups also occur as the reactants are being transported to these valleys, so that on days of high oxidant concentrations, the hour of peak oxidant concentration generally occurs sequentially from northwest to southeast on both the west and east sides of the Bay. In general, oxidant concentration levels also reflect the airflow pattern, with the more southerly stations reporting higher concentrations on a given day. The monitoring stations on the East Bay perimeter generally report higher concentrations than those on the West Bay perimeter. Sandberg and Thullier's data indicate that the oxidant concentrations at the Bay center often exceed those observed at the perimeter.<sup>20</sup>

5. Concluding Remarks

The preceding discussions have indicated considerable interrelationship among the various meteorological and pollution observations. The principal unifying consideration is the wind field. Large-scale climatological features, particularly the Pacific anticyclone, combine with local topography in the Bay area to produce airflows that are generally predict-

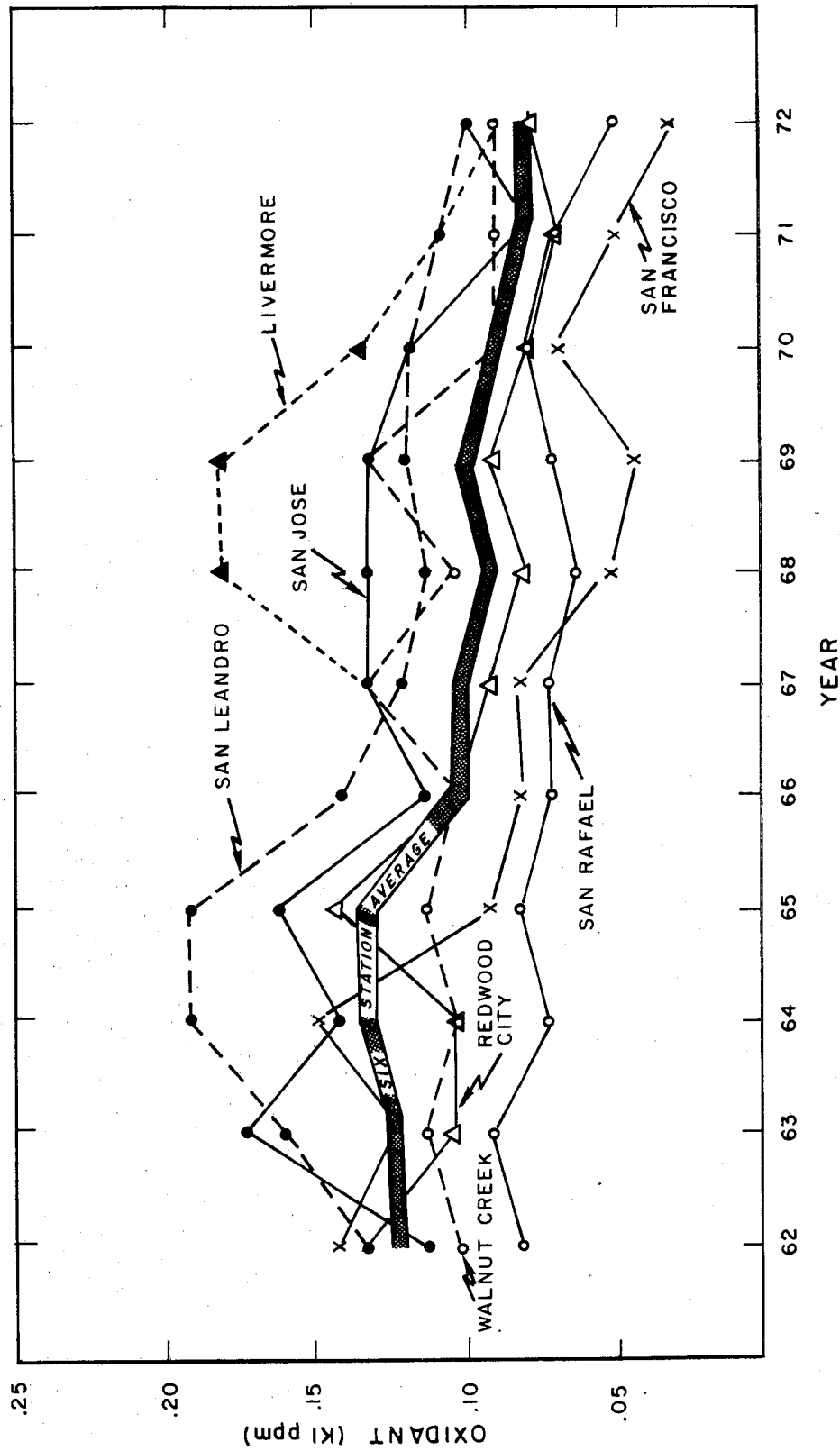


FIGURE A-7 AVERAGE OXIDANT CONCENTRATION ON COMPARABLE WARM DAYS FOR EACH BAAPCD STATION

Source: "A Study of Oxidant Concentration Trends (1962-1972)," BAAPCD Information Bulletin 1-16-73

able, especially during conditions conducive to smog formation. The inversion associated with the anticyclone generally limits surface air-flow into, and out of, the Bay to the low level passes and valleys. Thus, the marine air, with its special characteristics tends to flow over San Francisco, through a few passes and spread southeastward and northward into the southern and northern part of the Bay. As it does so, it carries the cooler temperatures and stratus clouds with it. It also carries a burden of pollutants picked up from the cities over which it passes. It is not surprising that temperatures, cloudiness, and concentrations of secondary pollutants all have climatological gradients that parallel the typical streamlines of the summer and fall seasons.

Appendix B

AIR QUALITY INSTRUMENTATION AND CALIBRATION



## Appendix B

### AIR QUALITY INSTRUMENTATION AND CALIBRATION

#### 1. Introduction

The instrumentation utilized during the San Francisco Bay Study is listed in Table 1, which is repeated here as Table B-1 for the reader's convenience. The details of the gas and particulate sampling inlet systems are diagrammed in Figures B-1 and B-2.

The air quality instrumentation and associated instrumentation was contained in four standard instrument mounting racks.

- Rack 1 contained the nephelometer and aerosol particle counter (APC) electronics. A coupler\* (Coupler 3) was specially modified so that the computer could be used to control the start, stop, and printout of the APC. The condensation nuclei (CN) counter was mounted on top of this rack.
- Rack 2 contained the optics and pumps for the APC. It was located immediately under the particulate sampling system to minimize the number of bends in the sample tubing.
- Rack 3 held the gas sampling instruments, and the amplifiers required for the Bacharach CO analyzer, the wet and dry bulb thermistors, and the pyranometer (total solar intensity).
- Rack 4 held the NOVA computer, the three couplers,\* and the reference voltage supply. The magnetic tape unit was mounted in a smaller rack on top of Rack 4.

---

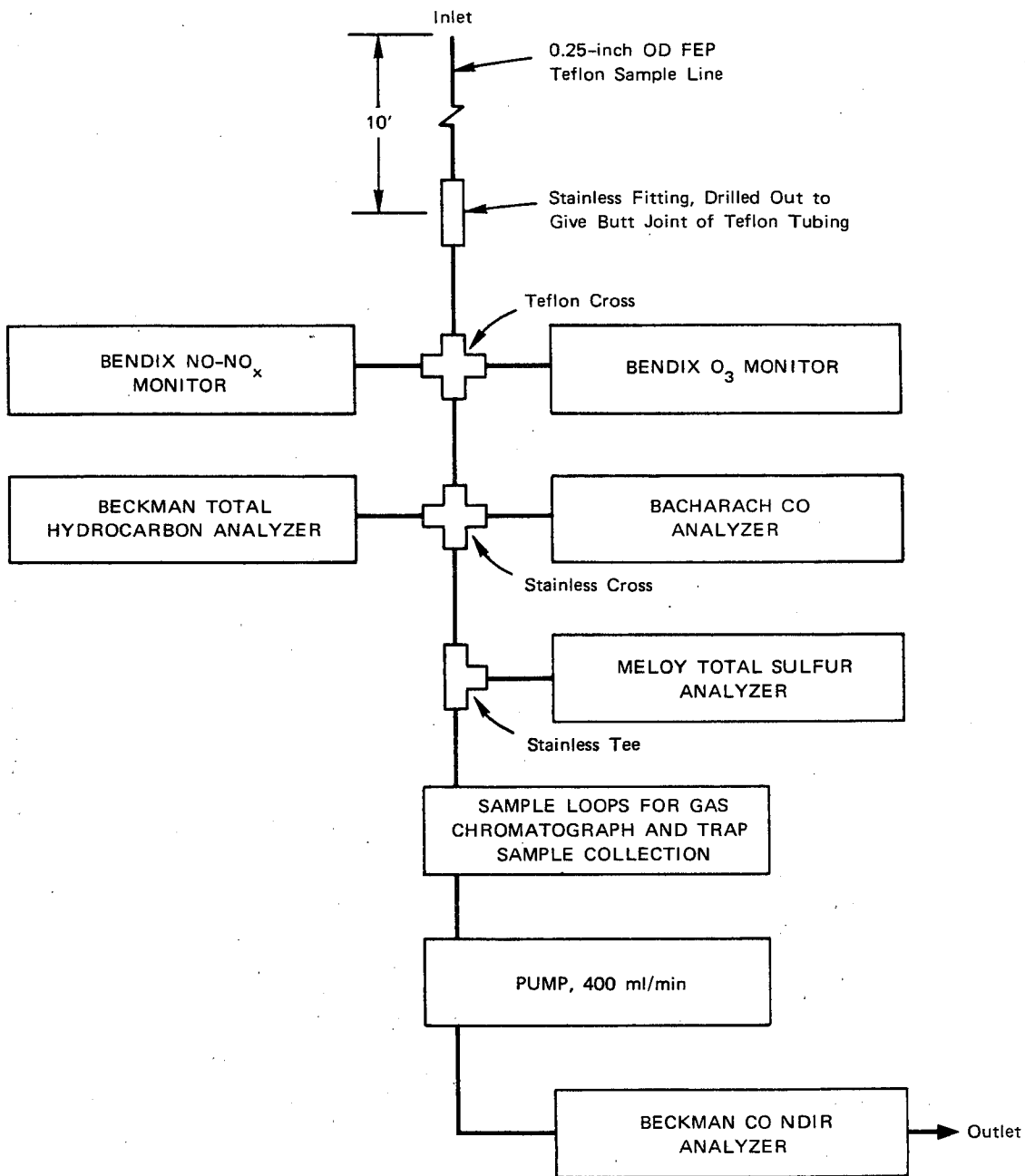
\* The couplers are basically digital voltmeters which, upon command from the computer, convert the analog signals from the instruments into digital form. See Appendix D for further details.

Table B-1

## PROJECT INSTRUMENTATION

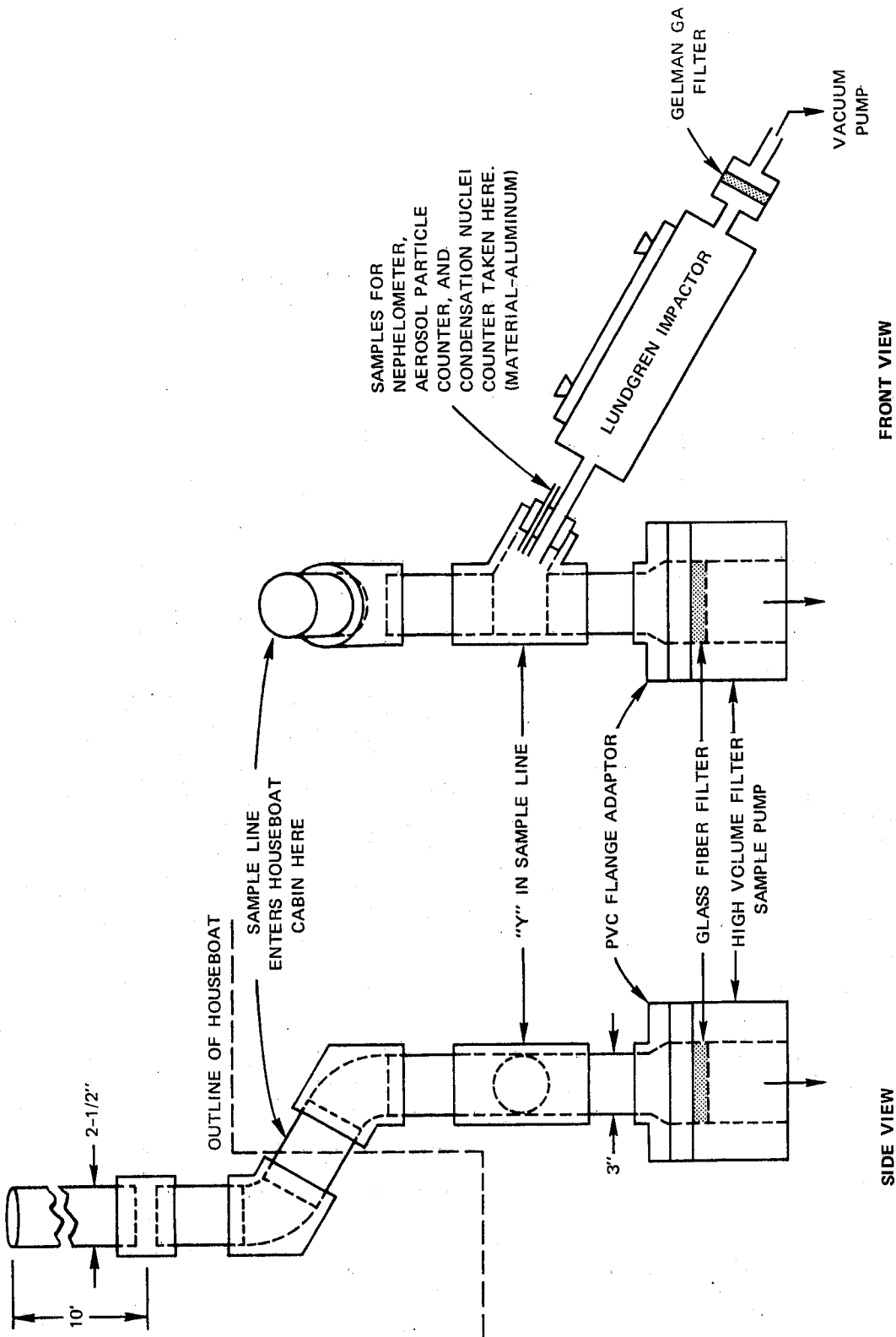
<u>Measurement</u>	<u>Measurement Principle</u>	<u>Supplier and Model</u>
<u>Coordinating Research Council</u>		
Ozone	Chemiluminescent	Bendix Model 8002
NO and NO <sub>x</sub>	Chemiluminescent	Bendix Model 8101 B
Total hydrocarbon	Flame ionization detector	Beckman Model 400 A
Carbon monoxide	Mercury displacement	Bacharach Model US400L
Carbon monoxide	Nondispersive infrared	Beckman Model 315AL
Turbidity	Integrating nephelometer	Meteorological Research Model 1550
Temperature	Thermistor (dry)	
Relative humidity	Thermistor (wet)	
Solar intensity	Thermopile	Honeywell
Hydrocarbon distribution	Gas chromatography	Hewlett Packard Model 5750*
<u>California Air Resources Board</u>		
Total sulfur	Flame photometric	Meloy Model SA120
Condensation nuclei	Continuous reading	Environment/One, Model Rich-100
Particle size distribution	90° Light scattering	SRI
Total particulate	Hi-vol filter	
Particulate distribution	Lundgren impactor	Environmental Research

\*Two columns: C<sub>1</sub> to C<sub>3</sub> on 1/8 in. × 10 ft packed column on phenyl-isocyanate on Porasil C; C<sub>3</sub> to C<sub>10</sub> on 0.02 in. × 300 ft capillary column coated with squalane. Grab samples were collected cryogenically.



SA-2098-1

FIGURE B-1 SCHEMATIC FOR GAS SAMPLE LINES AND INSTRUMENTATION



NOTE: Material for particulate sample lines is polyvinyl chloride (PVC) pipe.

SA-2098-2

FIGURE B-2 PARTICULATE SAMPLE LINE AND INLET SYSTEM

Power for the instruments was supplied from three sources. The 6-kVA generator in the houseboat did not provide sufficient power for all of the instruments and pumps. An auxiliary 4-kVA generator was mounted on the stern of the houseboat. Its power was used to operate the filter pumps and the APC only. The auxiliary generator failed midway during the research project and was replaced. The replacement generator was less well voltage regulated than the original and caused some operational difficulties in the operation of the APC.

The computer and tape deck require 60-cycle power with excellent frequency stability. The frequency stability requirements could not be met with the onboard motor generators. Therefore, we used four 12-V deep-cycle batteries and a 1-kVA inverter to provide line power for the computer and tape deck. Although the inverter provides excellent frequency stability, voltage regulation was poor. The output voltage of the inverter decreased steadily as the batteries were drained. The computer failed if the voltage dropped below 114 V, but was not voltage sensitive above this threshold voltage. Therefore, a Variac was used, as required, to maintain the output voltage above 114 V during a sampling day.

The schematic of the gas sampling system is shown in Figure B-2. All tubing connections are 0.25-inch OD FEP Teflon. Stainless steel fittings were used after the O<sub>3</sub> and NO/NO<sub>x</sub> connections. The total flow through the sample line was about 3 l/min, giving a residence time for the 5 meter sample line of 1.8 seconds.

The particulate sampling line was constructed of 10 cm OD polyvinyl chloride (PVC) plastic pipe and fittings. This material was selected due to its low cost, the availability of suitable fittings, and the ease with which it can be machined and sealed. The sample line passed through a window at the base of the flying bridge. Since a hole could not be cut in the roof, two bends in the sample line were required. The particulate

sample line was divided by a 3-inch PVC Y fitting\* located inside the houseboat cabin. One branch of the Y connected to a PVC flange. This flange was machined to mate to a 4-inch diameter high-volume filter collector. The increase in diameter of the sample line to the filter was gradual to eliminate shoulders where particulate matter would collect. The sample flow through the filter was 10 ft<sup>3</sup>/min (the procedures for washing and analyzing the filters are described on Page B-31).

An aluminum plug was machined with double O-ring seals to fit in the other branch of the Y. Tubes were inserted through holes in the plug to provide sample flow to particulate instrumentation. The size of the tube was determined by the sample flow requirements of the specific instrument. This particulate manifold is designed to provide near iso-kinetic sampling. The sample diameters and flow rates are given in Table B-2.

Table B-2

PARTICULATE INSTRUMENTATION SAMPLING RATES

<u>Instrument</u>	<u>Sampling Rate</u>	<u>I.D. of Sampling Tube (in)</u>	<u>Flow Rate (ft/sec)</u>
4-inch high volume filter	10 ft <sup>3</sup> /min	3.0	3.4
APC	200 ml/min	0.19	0.6
Nephelometer	1 ft <sup>3</sup> /min	0.65	3.8
CN counter	1 l/min	0.19	3.0
Lundgren impactor	3 ft <sup>3</sup> /min	1.38	4.8

\*This fitting was not available in 2-1/2-inch pipe size.

2. Instrumentation Funded by Coordinating Research Council - Houseboat

Ozone

The Bendix Model 8002 ozone analyzer operates by the chemiluminescent reaction of  $O_3$  with ethylene. The reaction is quantitative and there are no known interferences. The accuracy of the internal calibration system was checked using a REM Model 242 ozone generator and the reference method (neutral buffered potassium iodide).<sup>21</sup>

The instrument was zeroed and calibrated according to the procedure given in the Bendix manual. A sample of  $O_3$  generated by the REM ozone generator (0.192 ppm) was passed through the instrument and through a bubbler containing neutral buffered potassium iodide. The volume passed through the bubbler was measured with a wet test meter. In duplicate runs, the instrument read 0.190 and 0.192 ppm, while the bubbler read 0.192 ppm in both cases. We concluded that the internal calibration standard was correct. The test was repeated by Barbara Wright, Air and Industrial Health Laboratories, Berkeley, California (AIHL) using a similar procedure and  $O_3$  concentrations of 0.14 and 0.32 ppm. The analyzer results for zero and span agreed with the results from the manual samples.

NO/NO<sub>x</sub>

The Bendix Model 8101B nitrogen oxide analyzer utilizes the chemiluminescent reaction of  $O_3$  and NO to detect NO. The instrument is specific for NO and there are no known interferences.  $NO_x$  is determined by first passing the sample over a hot gold catalyst. While the exact chemistry is not well understood, the  $NO_2$  is catalytically reduced to NO.  $NH_3$  is not oxidized to NO by the gold catalyst at the temperature required for quantitative reduction of  $NO_2$  to NO and therefore is not detected.

In the operational mode used on the houseboat, the NO signal from the photomultiplier (which detects the chemiluminescence) is integrated for

30 seconds, electronically averaged and transferred to a holding amplifier and stored for 1 minute. The instrument then automatically switches the catalyst in series with the sample stream to determine  $\text{NO}_x$  and integrates the photomultiplier signal for 30 seconds as previously described. The averaged  $\text{NO}_x$  concentration is then transferred simultaneously to a holding amplifier and to a subtractive circuit. In the subtractive circuit, the previously stored NO signal is subtracted from the  $\text{NO}_x$  signal being stored at the  $\text{NO}_x$  holding amplifier. The difference (the  $\text{NO}_2$  concentration) is then transferred to a third holding amplifier where it is stored for 1 minute. The result is that each 30-second average of NO,  $\text{NO}_2$  and  $\text{NO}_x$  is updated at 1-minute intervals.

External zero and calibration is required for this instrument. Two procedures were used. Primary calibrations were carried out at the beginning and end of the experimental phase of this project. Gas from a compressed cylinder of NO in  $\text{N}_2$  was diluted into air to provide NO concentrations in the 0.2 to 1.0 ppm range.  $\text{NO}_2$  was removed by passing the gas through triethanolamine on firebrick.<sup>22</sup> The sample stream was split with sample flow provided to the NO- $\text{NO}_x$  analyzer and through an oxidizer and into Saltzman solution.<sup>21</sup>

Several oxidizers were used and evaluated during the project: an impinger containing acid potassium permanganate, as recommended by Saltzman;<sup>21</sup> potassium dichromate on glass fiber filter paper, which was folded and inserted into a glass tube; and chromium trioxide dissolved in water and adsorbed on to coarse firebrick. The first method was totally unsatisfactory because it did not give repeatable results and the conversion of NO to  $\text{NO}_2$  was only 50 to 75 percent complete. The second method was satisfactory but the oxidizer did not last very long. The third method is most satisfactory. Since the procedure is not readily available, it is described here.

Coarse firebrick (10-12 mesh) is washed with water and decanted. It is then covered with a 17 percent aqueous  $\text{CrO}_3$  solution. The slurry is stirred for about 15 minutes and decanted. The treated firebrick is spread out in a large dish and dried in a hood. The dried firebrick should be dark yellow; if it is too dark, it is too dry. Allow it to stand in the room to pick up more moisture. The dry  $\text{CrO}_3$ /firebrick is packed into a tube which is inserted in the gas stream. Conversion of NO to  $\text{NO}_2$  is quantitative and the tube lasts for months.

A convenient method for zeroing the instrument was also suggested to us by AIHL. A drying tube is packed with glass wool, a layer of TEA/firebrick, a layer of glass wool, a layer of  $\text{CrO}_3$  firebrick, and a glass wool plug. The tube is connected to the zero inlet of the instrument. The instrument zero, which may drift 2 percent/day, can easily be checked.

To determine NO and  $\text{NO}_2$  simultaneously, air is pulled through two impingers in series; the first impinger contains Saltzman solution for direct determination of  $\text{NO}_2$ . The second impinger also contains Saltzman solution for determination of NO as  $\text{NO}_2$ . A tube containing one of the oxidizers precedes the second impinger and converts NO to  $\text{NO}_2$ . Since there is a 12 percent conversion of  $\text{NO}_2$  to NO in Saltzman solution, the NO produced in the first impinger must be corrected in the calculation of the NO concentration determined by the second impinger.

For calibration on board the houseboat, a certified cylinder of 5 ppm NO in air was purchased from Matheson. Our analysis of this cylinder, using the above procedures, showed that the certified analysis was incorrect, but that the NO concentration did not change during the course of the experiment. This cylinder was used to span the instrument on board the houseboat, using the entire sampling inlet system as a sample line.

The instrument calibration was also checked by AIHL midway in the project. Their results suggested that the calibration of the 1.0-ppm full-scale range may be different from that of the 0.5-ppm range (the range

normally used throughout the project). Also, the results of the cylinder analyses repeated during the experimental phase suggested that the instrument calibration changed between November 8 and 20. Since we do not know when the change occurred, we have used the same calibration factors for all data collected, recognizing that the data for November 17 may be as much as 15 percent high.

The calibration data are summarized in Table B-3.

Table B-3

CALIBRATION DATA FOR HOUSEBOAT NO/NO ANALYZER<sub>x</sub>

Date	Saltzman (ppm)		Instrument (ppm)			Remarks
	NO	NO <sub>2</sub>	NO	NO <sub>2</sub>	NO <sub>x</sub>	
Aug 25	--	--	0.71	0.15	0.82	Cylinder on houseboat
Nov 8	--	--	0.72	0.16	0.77	Cylinder on houseboat
Nov 20	0.45	0.00	0.59	-0.02	0.55	Calibration on houseboat by AIHL (Range 1.0 ppm f.s.)
Nov 20	0.24	0.0	0.26	-0.01	0.24	Calibration on houseboat by AIHL (Range 0.5 ppm f.s.)
Nov 20	0.42	0.0	0.53	0.02	0.50	Calibration on houseboat by AIHL (Range 1.0 ppm)
Nov 28	--	--	0.89	0.14	0.98	Cylinder in laboratory, using span values set 25 August
Nov 28	--	--	0.70	0.13	0.84	Cylinder in laboratory, using span values set on 20 November.
Nov 29	0.71	0.13	--	--	--	Average of 3 duplicate sets of analysis of span tank

### Total Hydrocarbons

A Beckman Model 400A total hydrocarbon analyzer was used. The sample was pulled through the instrument by a small mechanical pump. The instrument was zeroed using Matheson Zero Gas Air. The span calibration was performed using a Matheson certified cylinder containing 1.88 ppm (v/v) of n-hexane in N<sub>2</sub>. The calibration of this cylinder was verified by AIHL, who found 1.63 ppm. The span of this instrument was set for 10 ppm C using the 1.88 ppm calibration value. All THC values are reported as ppm C as hexane. No correction for methane was made.

### Carbon Monoxide

In view of the vibration on board the houseboat, we initially decided to use the Bacharach Model US 4001 mercury displacement CO analyzer. The instrument performed well during the first runs and was switched to the helicopter instrument package. The second Bacharach analyzer was used on the houseboat but failed to operate satisfactorily. Both SRI and Bacharach technicians were unable to repair this instrument. To correct these problems a Beckman Model 315AL nondispersive analyzer (NDIR) was installed in early October. The cell was carefully located amidships and with the diaphragm perpendicular to the fore and aft line of the houseboat to minimize vibrational instabilities. Shock mounts would probably have improved the instrument's performance by reducing noise, but no difficulty was experienced in zeroing or spanning the instrument when seas were calm.

A switching valve manifold was used to provide zero or span gas to the CO sensors. Nitrogen was used to zero the instruments daily (less than 1 ppm CO). A tank of about 10 ppm CO in nitrogen was made up at SRI. It was calibrated in the laboratory by comparison with Matheson certified tanks containing 20 and 40 ppm CO using another Beckman 315AL NDIR. The concentration of CO was determined to be 10.5 ppm. The spans were set to 25 ppm full scale and were checked several times during each sampling day. Instrumental drifts as great as about 10 percent can occur within a day if the span is not regularly checked.

#### Atmospheric Turbidity (Integrating Nephelometer)

A Meteorological Research Incorporated integrating nephelometer was used to measure the scattering coefficient of the air. The manufacturer's calibration procedures, using Freon 12 for primary calibration and the internal calibration, were used. The calibration was checked twice during the experimental phase of the project, using the internal standard.

#### Temperature and Relative Humidity

The temperature sensors were Veco 34D1 thermistors which served as one leg of a Wheatstone bridge network. The thermistors were mounted on brass screws which extended about 12 mm into PVC particulate sampling line. The wet bulb thermistor was covered with a wick, which passed through a 6 mm hole in the PVC pipe and into a water reservoir mounted outside the pipe.

A cable connected the thermistors to the bridge inside the houseboat. Any of three ranges could be selected: -18 to 20°C, 0 to 20°C, or 18 to 38°C. Values of the bridge resistors were chosen for optimum linearity. Low-temperature-coefficient trim potentiometers were incorporated for zero and span adjustments. Mercury batteries provided a stable bridge voltage source. The bridge output served as input to a differential amplifier located on the same chassis. The thermistors were calibrated before and after the experimental phase by comparison with an accurate thermometer in an oven. Since the output of the device was linear below the 18°C, it was not necessary to change the range when the temperature went below 18°C. The wet bulb thermistor did not perform satisfactorily; it always read high compared to readings made with a hand-held wet bulb thermometer. Presumably, the water evaporated from the wick faster than it could be carried up to the thermistor from the reservoir. Therefore, our measurements of relative humidity reported on the data tape are not reliable.

#### Solar Intensity

A Honeywell pyranometer, with a quartz dome and mounted in a SRI-built housing, was used to measure solar intensity aboard the houseboat. It was mounted on the port-side upper deck after-rail of the houseboat. A coaxial cable carried the millivolt signal to a temperature stabilized amplifier, where the signal was amplified by a factor of 95.

When the experimental phase of this project had been completed, a comparison calibration was made between the Honeywell pyranometer and an Eppley precision spectral pyranometer, Model PSP. When the solar angle is low, the houseboat pyranometer produced no signal due to the geometry of its housing. The sensor itself is located about 1/2 inch below the rim of the housing. Since the houseboat tetron runs were made in the middle of the day, this effect should not cause problems. At higher light intensities, the output of the houseboat pyranometer output is linear. The calibration equation for the houseboat pyranometer was calculated from the slope and intercept of the calibration plot, the calibration factor of the Eppley pyranometer, and the amplification factor.

#### Gas Chromatography-Mass Spectrometry

A LKB 9000 gas chromatograph-mass spectrometer (GC-MS) was used to evaluate the applicability of the technique to the analysis of atmospheric samples collected cryogenically on the Bay. In preliminary experiments, auto exhaust samples were diluted to concentration levels similar to the concentration levels found over the Bay during the low smog conditions of this autumn. The results were found to be marginal due to the low levels of HC. A computer-tape deck peripheral system was installed during December of 1972 that improved the signal-to-noise ratio for analysis of trace constituents. The cryogenically collected samples were maintained at liquid nitrogen temperature while awaiting

the completion of the peripheral system. When the complete peripheral system was operational, the system was again evaluated with diluted auto exhaust samples.

Two outputs are available from the GS-MS during operation. The output from the total ion current monitor produces a record of total ion current versus time. This record is analogous to a gas chromatogram with detection by conventional techniques. During analysis by GC-MS, the record produced by the total ion current monitor is visually monitored and the mass spectrometer triggered into repetitive scans during the elution of each peak.

The second evaluation of the GS-MS with the computer peripheral on diluted auto exhaust samples showed improved performance but was not considered satisfactory. The sensitivity of the mass spectrometer is adequate for identification of many trace HC constituents of the simulated samples, but the sensitivity of the total ion current monitor is considerably less than can be obtained by a hydrogen flame detector under laboratory conditions.

An air sample that was cryogenically collected on 17 November 1972 was submitted for GC-MS analysis. The water vapor collected in the cryogenic traps was released more slowly than were the HC constituents upon release into the GC column of the GS-MS. Therefore, the total ion current monitor displayed a constant, large background of water over the midportion of the total ion current display. The presence of

relatively large concentrations of water required that the amplification of the total ion current display be reduced to maintain the display on scale. A zero offset (integral to the GC-MS) could not be employed since the concentration of the water was high and changed rapidly. As a result of the water interference, mass spectra were recorded every 6 seconds rather than triggering on the basis of the total ion current monitor display. Water vapor does not interfere with a GC flame ionization detector (FID), since the FID is insensitive to water vapor. In addition, the presence of GC column liquid phase bleed presents a more serious interference to GC-MS than it does to the FID. Thus special precautions must be taken to include a bleed trap for GC-MS column. The same GC column was used for both GC-MS and high resolution GC (Section 2-Hydrocarbon Distribution). Manual examination of the data in the mass spectral patterns at low mass numbers identified rare gases, methyl mercaptan,  $\text{SO}_2$ , and  $\text{C}_4$  saturated compounds. In spectra from mass 200-350, the following compounds were present:

- Ethyl benzene
- At least one xylene
- Styrene
- n-propyl benzene
- At least one methyl ethyl benzene
- At least three trimethyl benzenes
- Dichlorobenzene
- Two unknown - MW 282 and 356

Thus, although the potential useful sensitivity of the GC-MS should be equal to the FID, in actual practice it is considerably less. Since either GC with FID or GC-MS destroys the samples during analysis, FID cannot be combined with MS detection. Under heavy smog conditions with much greater HC concentrations, the GC-MS could have provided invaluable additional information concerning the HC distribution. Since the performance of the GC-MS was marginal, only one sample was analyzed by this technique. The remainder of the cryogenically collected samples were analyzed by GC. The decision to analyze these samples by GC alone was also influenced by the marginal performance of the on-board GC.

#### Hydrocarbon Distribution - Gas Chromatography

The HC composition of the air was determined by gas chromatography in real time on the houseboat and from cryogenically trapped samples. The basic instrument was a Hewlett-Packard Model 5750, with flame ionization detection, modified to permit low temperature operation, direct injection of cryogenically collected samples, and passage of the output of two columns through the same flame detector. It was necessary to use two columns, one for the C<sub>1</sub>-C<sub>3</sub> hydrocarbons and one for the C<sub>3</sub>-C<sub>10</sub> hydrocarbons to provide adequate separation of all materials.

The air sample was pulled through two sample loops, one 21-ml loop for the C<sub>1</sub>-C<sub>3</sub> hydrocarbons and one 200-ml loop for C<sub>4</sub>-C<sub>10</sub>

hydrocarbons, by a pump at about 1 liter per minute. Two 8-port valves permitted switching the air contained in sample loops to cryogenic traps. Each cryogenic trap was a loop of 6 inches by 1/8 inch diameter stainless tubing. The C<sub>1</sub>-C<sub>3</sub> trap was packed with Porapak S; the C<sub>3</sub>-C<sub>10</sub> trap was packed with 20 percent Carbowax 20M on Chromosorb W. The general procedure for each sample was to flush the sample loops several times with air (in practice, sample air was pulled through the GC inlet system continuously), cool the trap with liquid oxygen, and pull out the appropriate 8-port valve to inject the air sample from the loop onto the trap. When three volumes of carrier gas (nitrogen for C<sub>1</sub>-C<sub>3</sub>, helium for C<sub>3</sub>-C<sub>10</sub>) had passed through the trap, the liquid oxygen was removed and the trap was rapidly heated with boiling water to release the sample.

The C<sub>1</sub>-C<sub>3</sub> analysis was performed on a 10 foot by 1/8 inch column packed with phenylisocyanate on Porasil C, supplied by Waters Associates, using a helium carrier gas at 25 ml/min. The column was held at 20-25°C by immersion in water contained in a large dewar. Our initial experiments in the laboratory using samples of known concentration indicated that adequate separation of all C<sub>1</sub>-C<sub>3</sub> compounds could be made. The relative retention times are given in Table B-4.

Table B-4

RELATIVE RETENTION TIMES OF C<sub>1</sub>-C<sub>3</sub>  
 HYDROCARBONS ON PHENYLISOCYANATE ON PORASIL C

Methane	1.00
Ethane	1.92
Ethylene	3.36
Propane	6.23
Acetylene	10.6
Propylene	21.6

It was necessary to backflush the phenylisocyanate column to remove the high molecular weight hydrocarbons, whose retention time was long compared to the C<sub>3</sub> hydrocarbons. Otherwise, these compounds eluted as very broad peaks and had the effect of raising the background noise level. This was accomplished by means of the rotary backflush valve.

The C<sub>3</sub>-C<sub>10</sub> analyses were performed on a 200 foot by 0.02 inch capillary column. A column coated with DC-200 was used for analyses made on board the houseboat. The performance of this column deteriorated during initial GC-mass spectrometer experiments (Section 2-Gas Chromatography) and a column packed with squalane was used for analyses of the cryogenically collected samples by GC-mass spectrometer and by GC.

The flow rate for the capillary column must be about 7 ml/min for optimum resolution. The time required to transfer the 200-ml air

sample to the cryogenic trap at 7 ml/min would be excessively long. Therefore, the rotary trap-column switching valve was used to isolate the trap from the column and detector, yet maintain a flow of helium carrier gas through the capillary column during sample transfer to the cryogenic trap. The 200-ml sample was transferred from the sample loop to the trap at a flow rate of 40 ml/min of helium. To inject the collected sample onto the capillary column, the trap-column switching valve was switched, the liquid oxygen was removed, and the trap was immersed in boiling water.

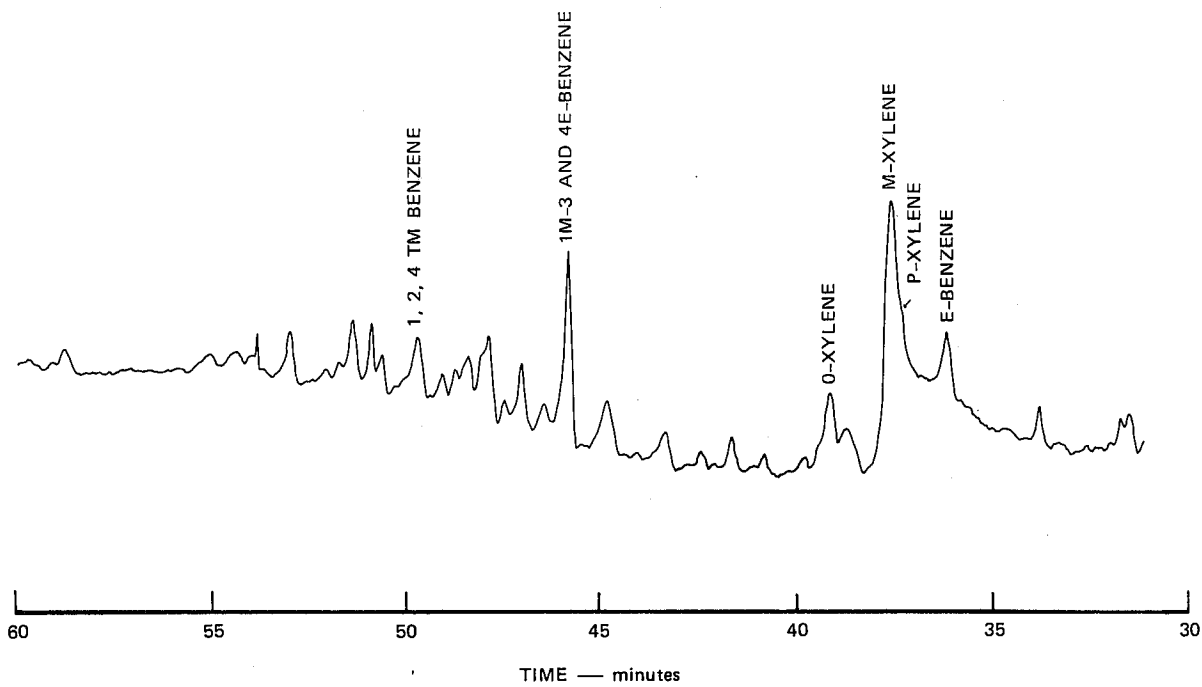
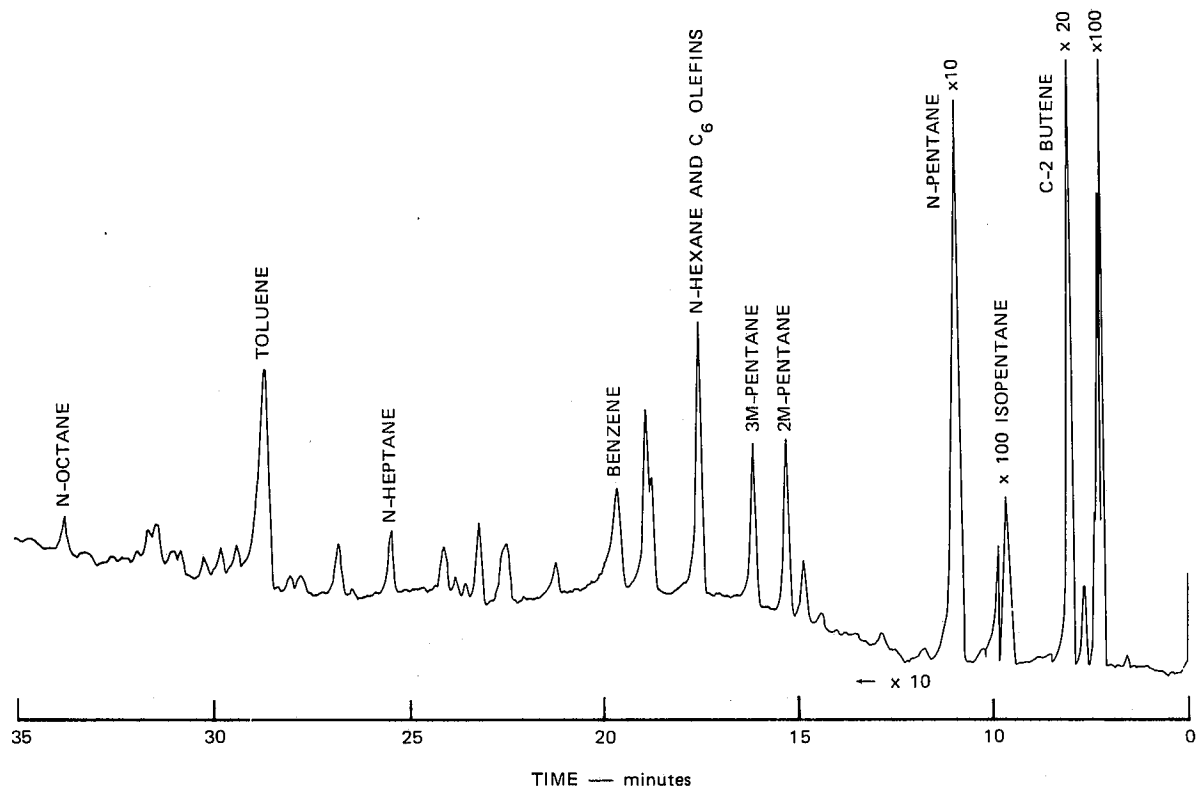
The GC oven was modified on an earlier SRI project to permit low temperature operation.<sup>12</sup> The oven was cooled with liquid CO<sub>2</sub> sprayed into the oven. The oven heater was used to maintain the oven temperature at -20°C during the first 5 minutes of the temperature program. Then the CO<sub>2</sub> was turned off and the oven temperature raised at 4°C/min on the houseboat and 2°C/min for the laboratory experiments using the squalane column. The final temperature, 90°C, was held for an additional 10 minutes. The time required for the complete cycle was about 1 hour on the houseboat.

Although some good data were obtained for C<sub>2</sub> and C<sub>3</sub> hydrocarbons aboard the houseboat, the measurements for methane were completely unsatisfactory. Peaks were observed at the methane elution time, but the calculated methane values based on the appropriate elution peak were meaningless. Although a considerable effort was made to

retrieve the methane concentrations from the chromatograms, we were not successful.

To obtain improved resolution of the HC constituents, atmospheric samples were collected and stored cryogenically for return to the SRI laboratory for analysis. We had originally proposed that these cryogenically collected samples would be submitted for analysis by gas chromatography-mass spectrometry on a LKB 900 GC-MS.

Figure B-3 illustrates a high resolution gas chromatograph of a sample cryogenically collected on October 25, 1972 over San Francisco Bay. This sample contains some 70 constituents, nearly all of which can be identified on the basis of auto exhaust constituents. A computer program developed on a previous study can identify and quantify the 80 constituents of auto exhaust. Table B-5 lists the elution order of auto exhaust constituents that have been separated and identified through high-resolution gas chromatography at SRI.



SA-2092-5

FIGURE B-3 HIGH RESOLUTION GAS CHROMATOGRAM OF HYDROCARBON DISTRIBUTION ON OCT. 25, 1972

Table B-5

## ELUTION ORDER OF AUTO EXHAUST CONSTITUENTS

Column: Squalane 0.02 in. × 300 ft.  
 Temperature: -20 to 90°C at 2°C/min.  
 Initial hold: 6 min. - final hold 10 min.  
 Helium flow rate: 8 ml/min.

	<u>Class*</u>	<u>Carbon No.</u>
1. C-2 hydrocarbons	--	2
2. Propylene and propane	O	3
3. Isobutane	P	4
4. Isobutylene and 1-butene	O	4
5. N-butane	P	4
6. T-2-butene	O	4
7. C-2-butene	O	4
8. 3-M-1-butene	O	5
9. Isopentane	P	5
10. 2-M-1-butene	O	5
11. N-pentane and C&T-1-pentenes	P	5
12. 2-M-2-butene	O	5
13. 2,2-DM-butane	P	6
14. Cyclopentene	O	5
15. 3&4-M-1-pentenes	O	6
16. Cyclopentane and 2,3-DM-1-butene	P	5
17. 2,3-DM-butane + 4M-T-2-pentene	P	6
18. 2-M-pentane	P	6
19. 3-M-pentane	P	6
20. C&T-3-hexenes	O	6
21. N-Hexane and C-6 olefins (4)	P	6
22. 4,4-DM-T-2-pentene and 3-M-T-2-pentene	O	7
23. M-Cyclopentane	P	6
24. 2,4-DM-pentane	P	7
25. Benzene	A	6
26. 1-M-cyclopentene	O	7
27. 2,3-DM-T-1-pentene and C-6 olefins (2)	O	6
28. Cyclohexane and 3,3-DM-pentane	P	6
29. 3-M-2-E-1-butene and 5-M-T-2-hexene	O	6
30. 2-M-hexane and DM-pentanes (2)	P	7
31. 3-M-hexane and 1-C-3-DM-cyclopentane	P	7
32. 1-T-3-DM-cyclopentane	P	7
33. 3-E-pentane and 1-T-2-DM-cyclopentane	P	7
34. 2,2,4-TM-pentane and T-3-heptene	P	8

Table B-5 (Continued)

	<u>Class*</u>	<u>Carbon No.</u>
35. 3-M-C&T-hexenes and 2-M-2-hexene	O	7
36. N-heptane and C-7 olefins	P	7
37. 1-C-2-DM-cyclopentane	P	7
38. M-cyclohexane and 2,2-DM-hexane	P	7
39. 2,5-DM-hexane and E-cyclopentane	P	8
40. 2,4-DM-hexane	P	8
41. 1-T-2-C-4-TM-cyclopentane	P	8
42. Toluene and 3,3-DM-hexane	A	7
43. 2,3,4-TM-pentane	P	8
44. 2,2,3-and 2,3,3-TM-pentane	P	8
45. 2,3-DM-hexane and 2-M-3-E-pentane	P	8
46. 2-M-heptane	P	8
47. 4-M-heptane	P	8
48. 3-M-heptane	P	8
49. 2,2,5-TM-hexane and 1,2,4,-TM-cyclopentane	P	8
50. 1-C-3-DM-cyclohexane	P	8
51. 1-M-T-3-E-cyclopentane	P	8
52. 2,2,4-TM-hexane and 2,3-DM-2-hexene	P	8
53. Cycloheptane and 1-M-1-E-cyclopentane	P	8
54. N-octane	P	8
55. 2,3,5-TM-hexane and 2,2-DM-heptane	P	9
56. 2,4-DM-heptane and 1-M-2-E-cyclopentane	P	8
57. C-9 paraffins (4)	P	9
58. E-cyclohexane and C-9 paraffins	P	9
59. Ethylbenzene	A	8
60. C-9 paraffins (4)	P	9
61. M&P-xylenes and 3,3,4-TM-hexane	A	8
62. 2&4-M-octanes	P	9
63. O-xylene and 2,2,4,5-TM-hexane	A	8
64. TM-heptanes	P	10
65. TM-heptanes	P	10
66. N-nonane	P	9
67. TM-heptanes	P	10
68. TM-heptanes	P	10
69. N-P-benzene and C-10 paraffins	A	9
70. 1-M-3&4-E-benzenes	A	9
71. 1-M-2-E-benzene and 5-M-nonane	A	9
72. 1,3,5-TM-benzene	A	9
73. 2&3-M-nonane	P	10

Table B-5 (Concluded)

	<u>Class</u> *	<u>Carbon No.</u>
74. 1,2,4-TM-benzene and butylbenzenes	A	9
75. N-decane	P	10
76. 1,2,3-TM-benzene and 1-M-1-P-benzene	A	9
77. 1-M-3-N-P-benzene	A	10
78. DE-benzenes	A	10
79. 1,3-DM-E-benzene	A	10
80. DM-E-benzenes	A	10

---

\* O - Olefins

P - Paraffins

A - Aromatics

### 3. Calibration of Instrumentation Supported by the California Air Resources Board

#### Total Sulfur

The Meloy Model SA120 flame photometric sulfur analyzer was operated according to the manufacturer's instructions. The instrument was always operated on the  $10^{-8}$  amp range. The voltage output (V) was recorded by the data acquisition system. It was converted to concentration during the subsequent data analysis using the equation, which was taken from the manufacturer's calibration curve.

$$\log [S] = 0.611 \log V + 1.828$$

The accuracy of this calibration was checked using  $\text{SO}_2$  generated by bubbling air through a solution of  $\text{KHSO}_3$ . The concentration of  $\text{SO}_2$  was simultaneously determined by the West-Gaeke method.<sup>23</sup> At low concentrations (less than 50 ppb), the data reported here were shown to have an accuracy of  $\pm 10$  percent.

#### Condensation Nuclei

A continuously reading Environment/One Model RICH-100 condensation nuclei (CN) counter was used during this program. The instrument was rented from the manufacturer. Their calibration was used. The calibration was also checked against a General Electric Model A-518 hand operated CN counter. The readings were within 10 percent of the Environment/One furnished calibration.

An external load resistor was selected to provide a 0 to 1 volt

full-scale output. Since it was anticipated that several ranges would be used during this study, a separate voltage supply consisting of a mercury battery, a rotary switch, and several resistors was constructed. Seven voltages between 0 and 1 volt were available. The data acquisition system was programed to multiply the CN counter output by the exponential factor indicated by the voltage from the separate voltage supply.

#### Particle Size Distribution (Aerosol Particle Counter)

The aerosol particle counter (APC) was constructed at SRI for use on an earlier smog chamber program. Its optical design has been described before;<sup>24</sup> it is similar to the more familiar Royco counters. The electronics of the APC differ from the Royco counters in that particles in five size ranges are counted simultaneously.

The APC was calibrated using Dow latex spheres. Solutions of the latex spheres were prepared by dilution into distilled water. Several sources of distilled water were available within the Institute; the sample giving the lowest background count was used for all calibration runs. The particles were nebulized and spray dried in a Collison nebulizer (Environmental Research Corporation, Aerosol Generator Model 7300). The manufacturer's calibration data permitted us to choose a dilution of the concentrated latex spheres that would yield 5.6 particles/ml in air.

The nebulized latex spheres were sampled by the APC. The sampling rate was 200 ml/min. The raw data are listed in Table B-6. An

Table B-6

## APC CALIBRATION DATA

Latex Radius ( $\mu\text{m}$ )	Impactor	Counts				
		Channel 1	Channel 2	Channel 3	Channel 4	Channel 5
None*	Yes	207	29	6	3	0
None*	No	132	1	0	0	0
0.109	Yes	184	1	0	0	0
0.357	Yes	1721	997	36	13	4
0.500	Yes	372	1564	491	54	10
0.714	No	760	913	582	1409	772
0.79	No	802	2868	2186	4701	2994
1.011	No	367	766	488	1079	2124

\* Distilled deionized water only.

impaction filter in the nebulizer was used for the smaller particles to remove large droplets of water. The data for the large particles show a significant number of counts in channels 1, 2, and 3 due to these water droplets. Using the data for pure water, we corrected for these spurious counts. The counts for a particular size of latex spheres were assumed to be log normally distributed in the five channels.<sup>25</sup> Using this assumption, the cumulative relative counts were plotted on both log and normal probability paper to determine the channel index mode of the distribution. The plots for a given size particle were nearly linear. Some deviation can be expected due to the limited number of channels. The channel index modes were then plotted against the particle size. The best fit straight line was drawn through the points. Little difference could be distinguished between using a normal or a log normal distribution. This was probably due to the limited number of channels. Assuming that the division between channels was halfway between two adjacent channels, the

size range of particles counted in each channel could be determined. The results are summarized in Table B-7.

Table B-7

APC CALIBRATION DATA

<u>Channel</u>	<u>Size Range</u> <u>(<math>\mu</math> diameter)</u>	<u><math>\Delta r</math> (<math>\mu</math>)</u>
1	< 0.46	(< 0.08)
2	0.46-0.61	0.07
3	0.61-0.76	0.08
4	0.76-0.92	0.08
5	> 0.92	(> 0.1)

Total Particulate

Aerosol samples were collected on 4-inch diameter Gelman glass fiber filters as described earlier in this Appendix. It was necessary to carefully prewash the filters to reduce the background levels of  $\text{NO}_3^-$ ,  $\text{Cl}^-$ , and  $\text{SO}_4^{2-}$ . The following procedure was used. All glassware and equipment were washed successively in  $\text{CHCl}_3$ , acetone, and distilled deionized (DDi) water. A stainless steel screen was boiled in DDi water three times for 40 minutes duration each. The filters were sandwiched in the screen. Each filter was boiled in DDi water three times for 40 minutes duration each. The washed filters were dried in a stream of warm, filtered, dry nitrogen.

This type of filter absorbs considerable amounts of water when exposed to normal laboratory air. Therefore, humidifiers were constructed of pyrex jars with tight fitting lids. A screen inside the jar supported the filters midway in the jars. A saturated solution of  $\text{K}_2\text{CO}_3$ , which has an equilibrium relative humidity of 43 percent, was placed in the bottom of the jar to provide a constant humidity atmosphere. The filter was equilibrated overnight in this atmosphere and quickly weighed on a micro-

balance. After exposure, the same procedure was used to determine the weight of the filter. The weight of collected particulate was calculated by subtraction. Since the flow through the filter was 283 l/min and the exposure time was known, the particle mass loading was readily calculated. The analytical methods are described in the following paragraphs.

Sample Preparation -- One-half of the filter was placed in a small extractor made from a graduated test tube connected to a small water-cooled condenser. The filter was extracted with boiling water and concentrated to 2 ml. Aliquots of this concentrated extract were used in the analysis of nitrate, sulfur (as sulfate), and chloride. The other half of the filter was ashed in a low-temperature asher to remove any organics. The ashed filter was washed twice with 8 M  $\text{HNO}_3$  and twice with water, using enough liquid to cover the filter in each case. The extracts were combined and evaporated to about 1 ml. The concentrated extract was diluted to 10 ml in a volumetric flask.

Nitrate Analyses<sup>26</sup> -- An aliquot of the aqueous extract was reacted with brucine to produce a yellow compound according to the literature procedure. For concentrations between 0.05 to 0.60 mg/liter of nitrate nitrogen, the color development follows Beer's Law. The absorbance of standards and unknown solutions were measured at 410 nm on a Cary Model 14 M spectrophotometer using 1-cm cells. A standard curve was drawn, and the concentrations of unknowns were determined.

Sulfur Analyses<sup>27</sup> -- A 0.5-ml aliquot of the aqueous extract was placed in a platinum boat and evaporated to dryness in a heated nitrogen atmosphere. The sample and platinum boat were heated to 900°C in a hydrogen-helium atmosphere. The sulfate was reduced to  $\text{H}_2\text{S}$  which was swept from the boat into a microcoulo-

metric cell where it was treated with iodine. The change in voltage due to the change in iodine concentration was measured on a recorder. The peak areas of a set of standards in the range of 0.2 to 3.0  $\mu\text{g/ml}$  of sulfur were measured and plotted on a graph. The concentration of sulfur in the unknowns was determined from this standard curve. Concentrations in  $\mu\text{g/ml}$  of sulfur were converted to  $\mu\text{g/ml}$  of sulfate by multiplying by a factor of 3.

Chloride Analyses<sup>28</sup> -- An aliquot of a chloride sample was introduced into a microcoulometric titration cell. The chloride was titrated with  $\text{Ag}^+$  ion. A recorder monitored the voltage drop during titration. The peak heights for a set of standards were used to construct a calibration curve. The cell is suitable for titration of 0.1 to 1000  $\mu\text{g}$  chloride per sample.

Lead Analysis<sup>29</sup> -- An aliquot of the 8 molar nitric acid extract was analyzed on a Perkin-Elmer Model 303 atomic absorption spectrophotometer at 2833  $\text{\AA}$ . Dilute samples (5-20  $\mu\text{g/ml}$  of lead) were analyzed using the 5X scale expansion.

#### Particle Size Distribution (Lundgren Impactor)

A Lundgren impactor was rented from Environmental Research Corporation for this program. The device used was a prototype five-stage impactor constructed for AIHL for use on the California Aerosol Study. A 47-mm Milipore filter holder was used with Gelman GA-1 cellulose acetate after filters. A GAST Model 1022-V103-G272X pump was equipped with a large rotameter on its output, a vacuum gauge, and a bleeder valve on its input to measure and regulate the volume of air pulled through the impactor and after filter at 85  $\ell/\text{min}$ .

The procedures for cutting, washing, and mounting the "foils" on the impactor drums were recommended by AIHL. Mylar and Teflon foils

were supplied by AIHL and cut on their apparatus. Each foil was washed thoroughly in fresh, reagent grade acetone. They were dipped in 0.1N  $\text{HNO}_3$  for approximately 1 minute (the 0.1N  $\text{HNO}_3$  was prepared from DDi water). After a final wash in fresh, reagent grade acetone, the foils were dried under an infrared lamp in a stream of dried, filtered nitrogen. After drying, the foils were stored in acetate boxes, supplied by AIHL, which had previously been washed in DDi water and air dried. Each foil was weighed three times on a microbalance. A plutonium static discharger dissipated the static charge which accumulated on the foils with any motion.

Stages 1A, 2, 3, and 4 were first wrapped with a 2-inch Teflon foil. A 1-inch Mylar foil was wrapped over the Teflon foil. In each experiment the Mylar was placed on the lower half of the drum. Stage 1B was wrapped with a piece of 2-inch sticky polyethylene tape, sticky side out, which was used as supplied by AIHL.

Two batches of Gelman GA-1 filters were used. Filters 100 to 109 were washed and supplied by AIHL. Filters 200 to 203 were washed at SRI using the AIHL-recommended procedure. A stack of 15 filters was placed in a clean ceramic Buchner filter. About 1 liter of DDi water was slowly poured through the filters, using an aspirator to provide suction. The washed filters were dried in a vacuum oven and then under a stream of dry  $\text{N}_2$ . The filters were weighed before and after exposure on the microbalance and stored in individual plastic boxes. The weights of particulate collected are given in Table B-8.

Table B-8

## LJUNGGREN IMPACTOR SAMPLES

Date	Time (hr:min)	Stage	No.	Mylar		Polyethylene Tape	After Filter		Volume Sampled (m <sup>3</sup> )
				( $\mu$ g)	( $\mu$ g)		No.	$\mu$ g	
721019	1141-1220						101	151	2.8
721025	0800-1104 1235-1320						100	294	13.0
721026	1006-1050						102	533	3.3
721031	1352-1407								
721102	0833-1120	1A 1B	9 Z	75			103	970	13.2
	1123-1317	2 3	10 11	67 110	186 199	233	104	1384	9.1
	1633-1745	4	12	130	272		105	441	5.7
721106	1038-1201	1A 1B	13 Y	42	159	449	106	138	15.7
	1210-1405	2 3 4	14 15 16	0 26 0	147 203 88		108	161	4.6
721117		1A 1B	17 X	0	100	45	200	17	1.2
		2 3 4	18 19 20	6 8 0	195 151 0		201	~ 0	2.4

Appendix C

AIR QUALITY AND METEOROLOGICAL DATA  
FOR SELECTED SAMPLING DAYS



**STANFORD RESEARCH INSTITUTE**  
Menlo Park, California 94025 · U.S.A.

*Final Report Appendices*

*August 1973*

## **ATMOSPHERIC PHOTOCHEMICAL SMOG MEASUREMENTS OVER SAN FRANCISCO BAY**

*By:* L. A. CAVANAGH and J. H. SMITH

*Prepared for:*

COORDINATING RESEARCH COUNCIL  
30 ROCKEFELLER PLAZA  
NEW YORK, N.Y. 10020

ENVIRONMENTAL PROTECTION AGENCY  
DIVISION OF METEOROLOGY  
RESEARCH TRIANGLE PARK, NORTH CAROLINA 27711  
CRC APRAC CONTRACT CAPA-12-72 and EPA CONTRACT 68-02-1009

AIR RESOURCES BOARD  
1025 P STREET  
SACRAMENTO, CALIFORNIA 95814  
CONTRACT 2-021

SRI Projects 2092 and 2098

*Approved by:*

R. T. H. COLLIS, *Director*  
*Atmospheric Sciences Laboratory*

R. L. LEADABRAND, *Executive Director*  
*Electronics and Radio Sciences Division*

## Appendix C

### AIR QUALITY AND METEOROLOGICAL DATA FOR SELECTED SAMPLING DAYS

Figure C-1 is a map of the San Francisco Bay area. The insets define the area of the subsequent maps. The maps following Figure C-1 show the hourly meteorological and air quality measurements reported by all available monitoring stations in the Bay area for sampling days that were not selected for detailed analysis. The wind streamlines derived from these observations are shown as broad arrows. The houseboat course and times are also plotted on these maps. The San Jose and Oakland rawinsonde temperature-humidity profiles are included for each day data were available. Figures C-2 to C-9 show these map and vertical profiles, respectively, for selected sampling days. Detailed data are included for the following sample days: 6 October, 7 October, 19 October, and 6 November.

Helicopter flight paths for 19 October, 31 October, and 6 November are shown by Figures C-10, C-11, and C-12, respectively. The airborne measurements for these days are tabulated in Tables C-1, C-2, and C-3, respectively.

The results of chemical analysis of particulate matter collected on 19 October, 24 October, 25 October, 26 October, 31 October, 2 November, 6 November, and 17 November are shown in Table C-4.

The hydrocarbon distribution of cryogenic samples collected on 25 October, 26 October, 31 October, 2 November, and 6 November are tabulated in Table C-5. Table C-5 also shows the hydrocarbon distribution and concentration ranges of typical auto exhaust.

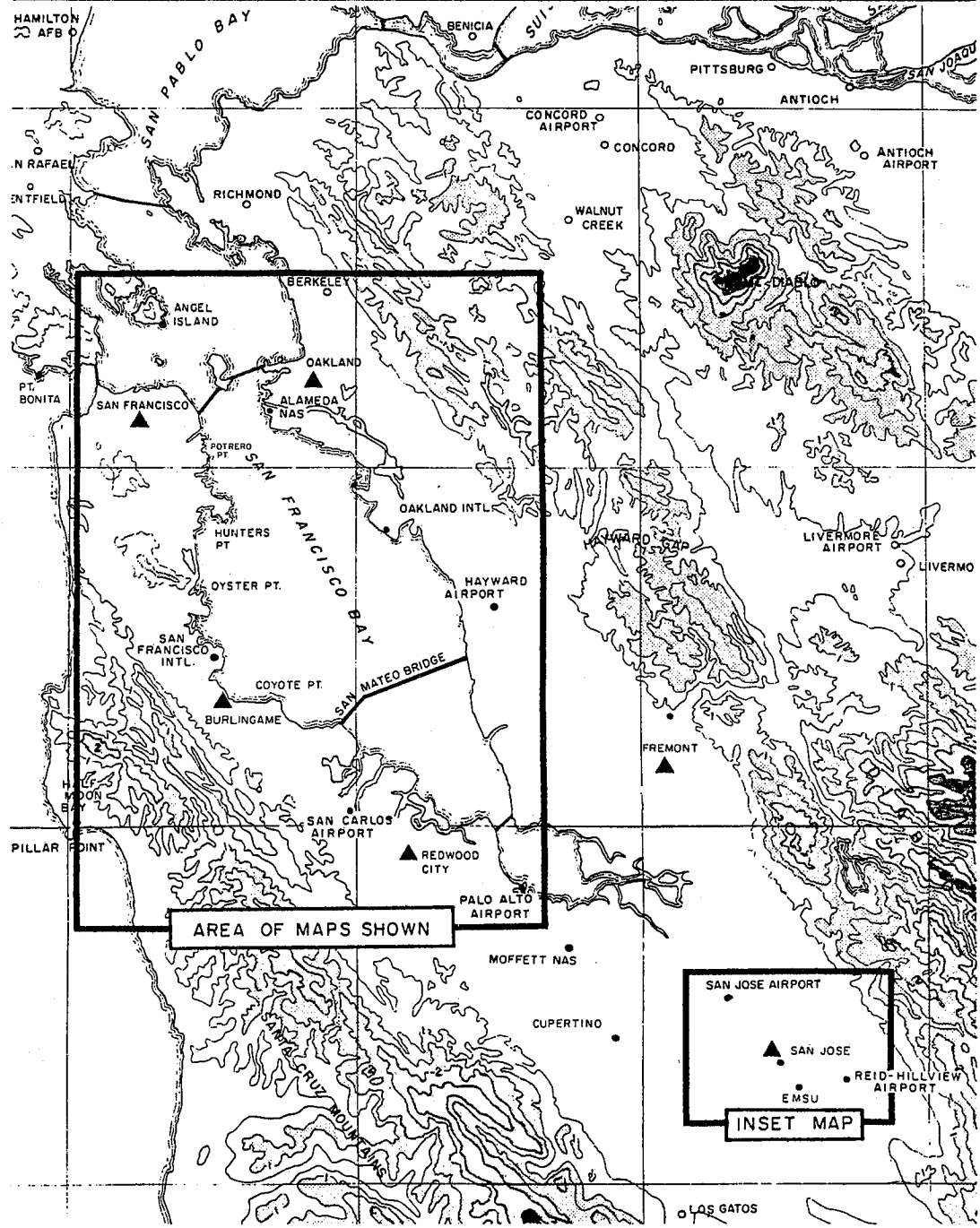
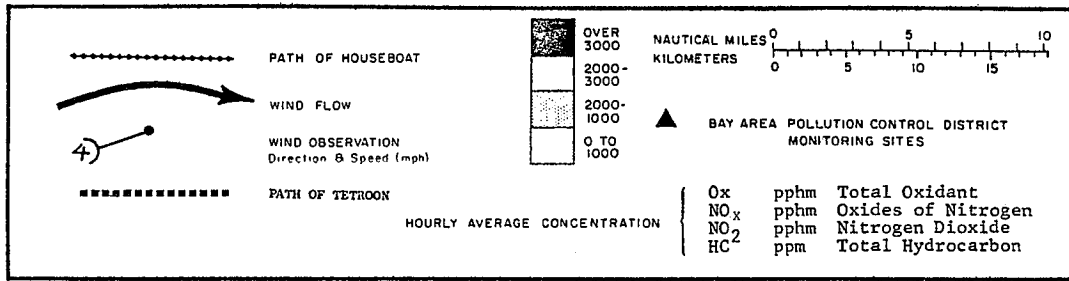
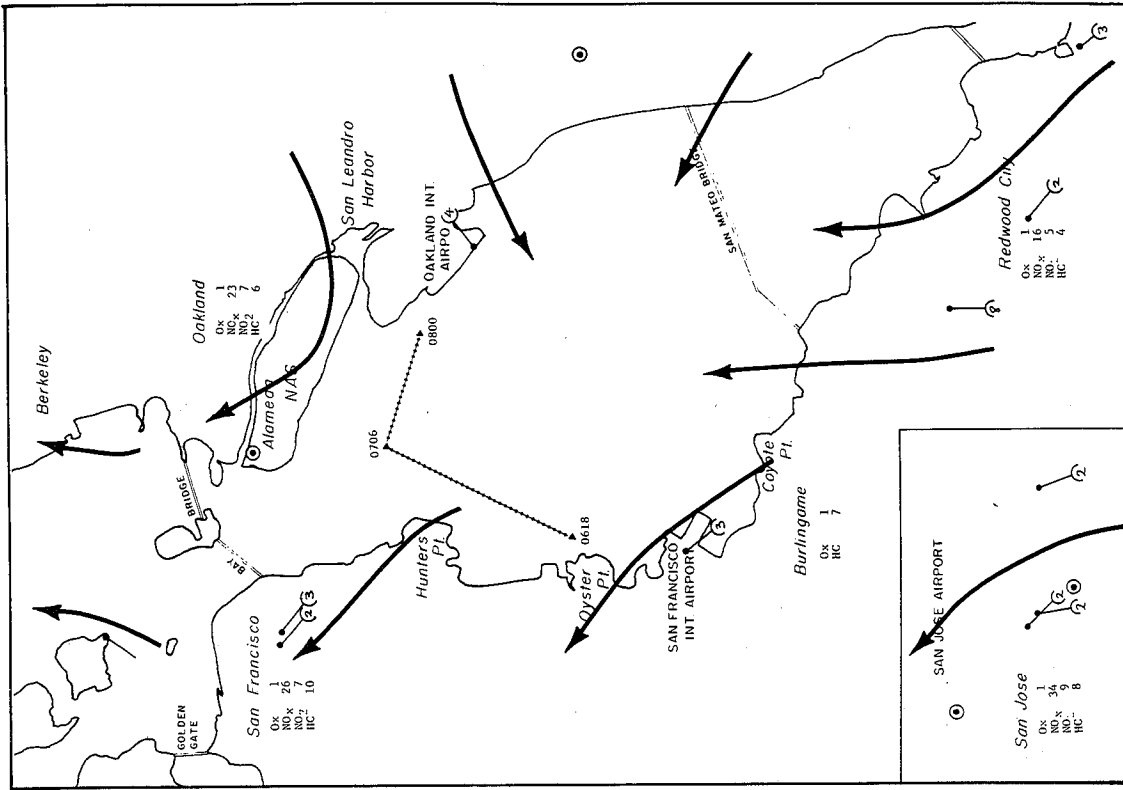
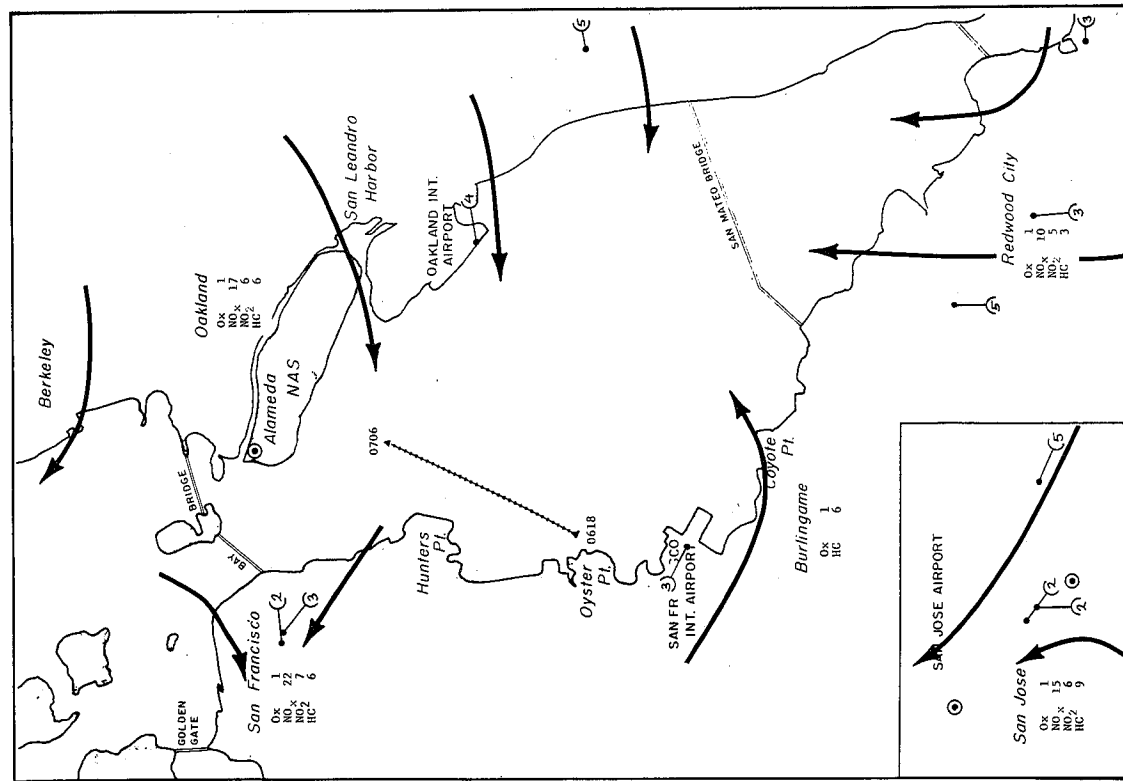


FIGURE C-1 OVERALL AREA OF SAN FRANCISCO BAY SHOWING SAMPLING AREA INSET



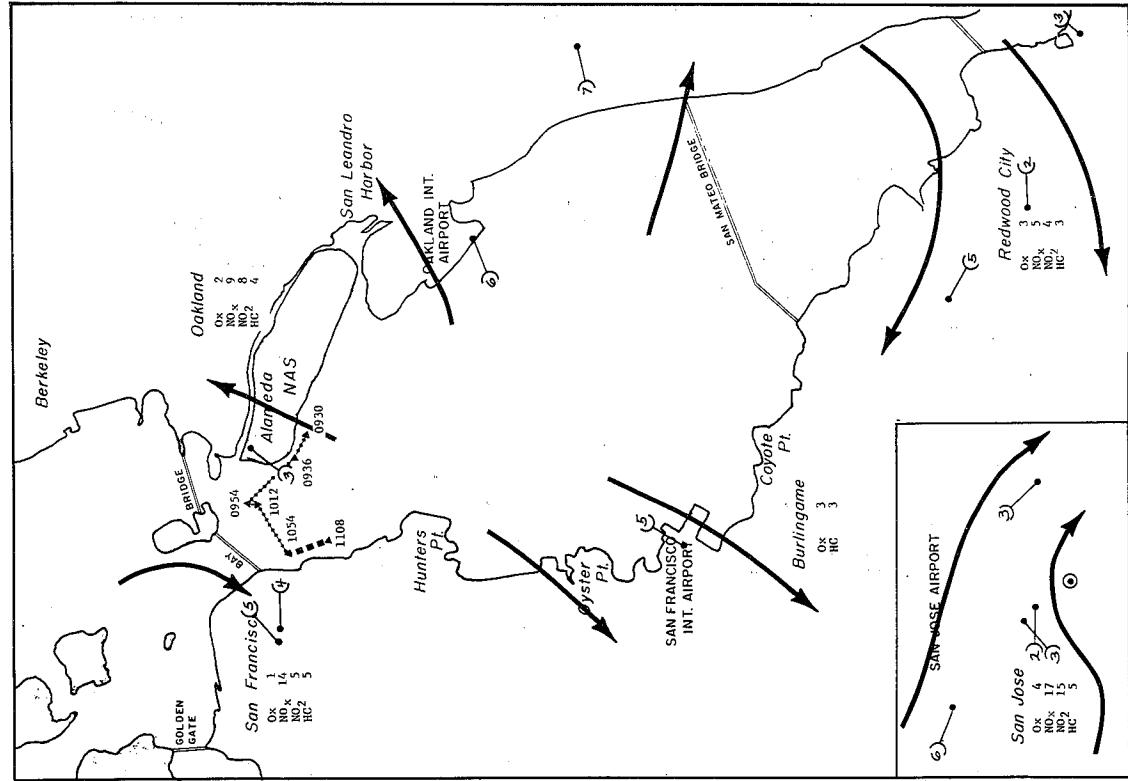
(a) 0600 PST



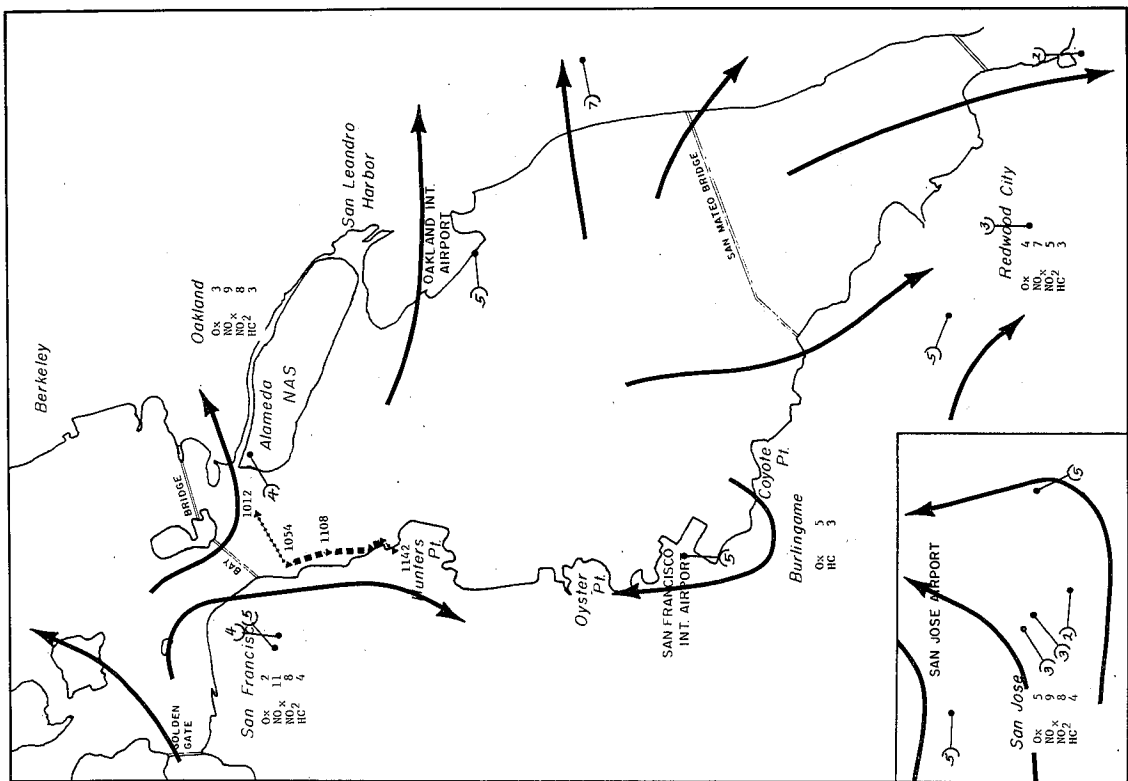
(b) 0700 PST

FIGURE C-2 AIR POLLUTION LEVELS, SURFACE WIND FLOW, AND HOUSEBOAT COURSE, 6 OCTOBER 1972





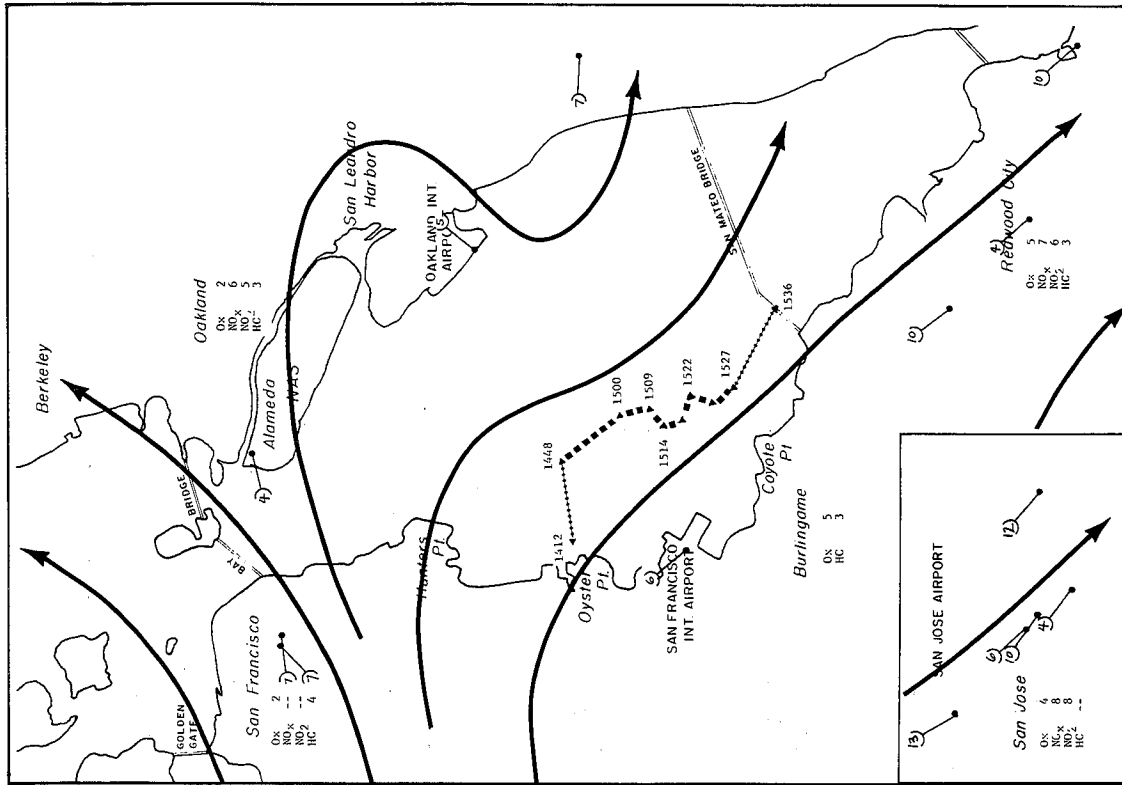
(e) 1000 PST



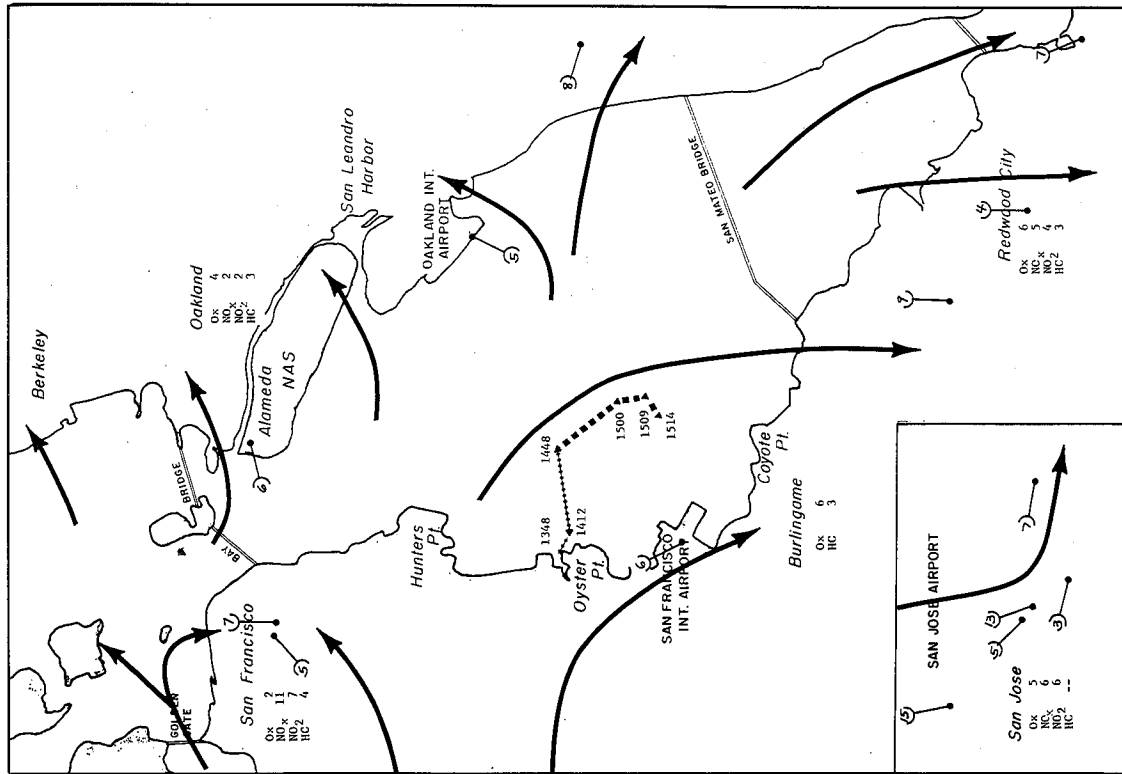
(f) 1100 PST

FIGURE C-2 AIR POLLUTION LEVELS, SURFACE WIND FLOW, AND HOUSEBOAT COURSE, 6 OCTOBER 1972  
(Continued)



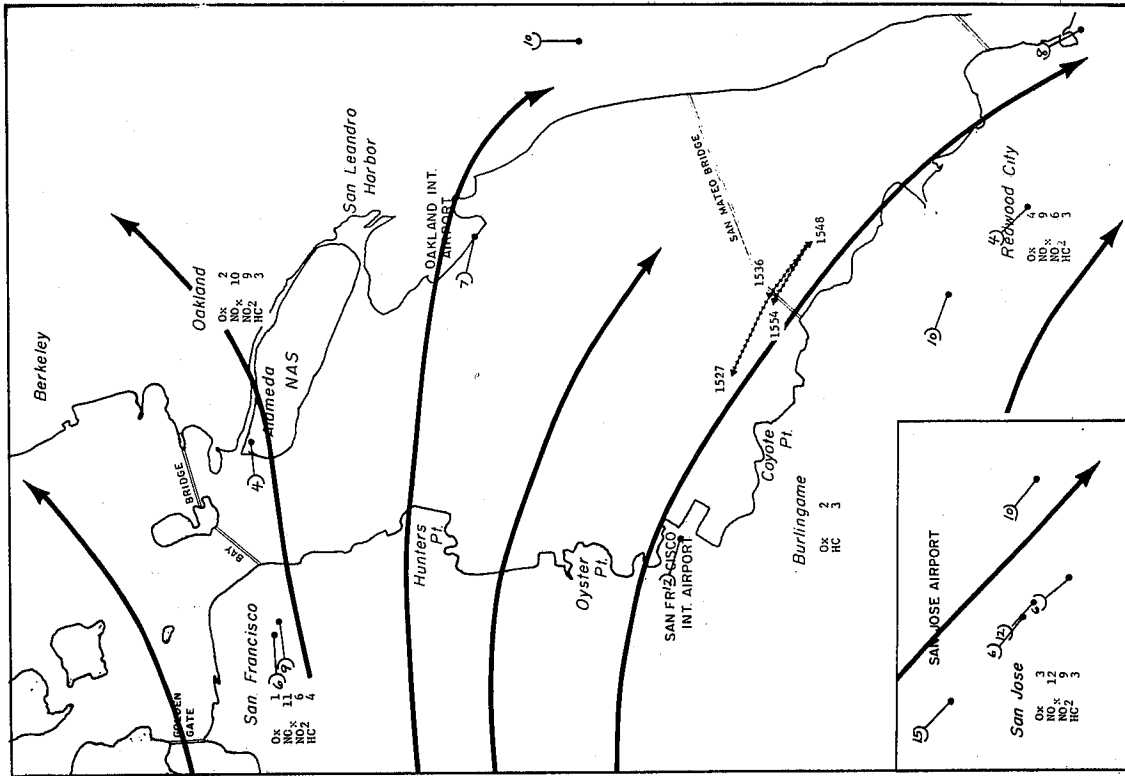


(j) 1500 PST



(i) 1400 PST

FIGURE C-2 AIR POLLUTION LEVELS, SURFACE WIND FLOW, AND HOUSEBOAT COURSE, 6 OCTOBER 1972  
 (Continued)



(K) 1600 PST

FIGURE C-2 AIR POLLUTION LEVELS, SURFACE WIND FLOW, AND HOUSEBOAT COURSE, 6 OCTOBER 1972  
(Concluded)

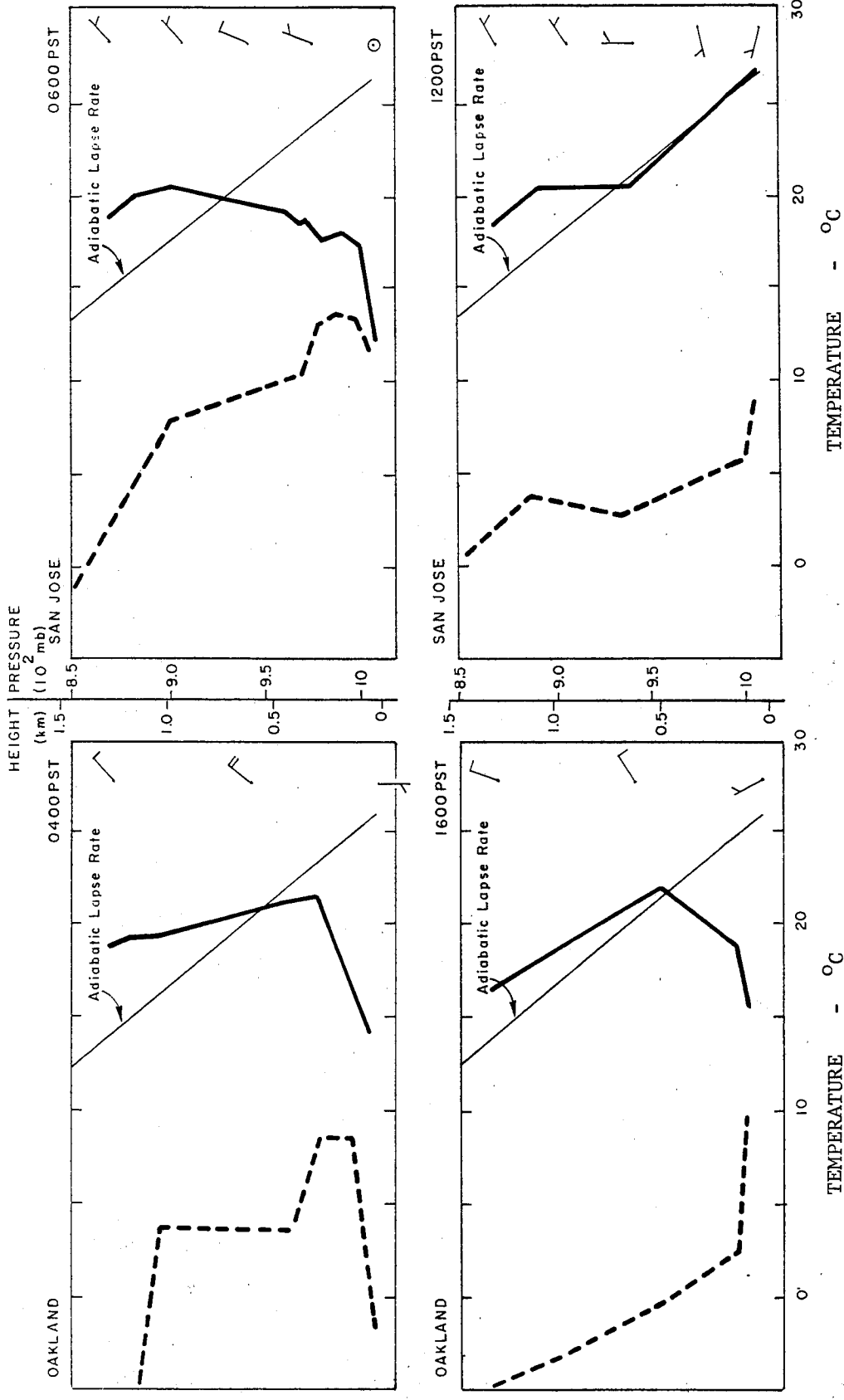
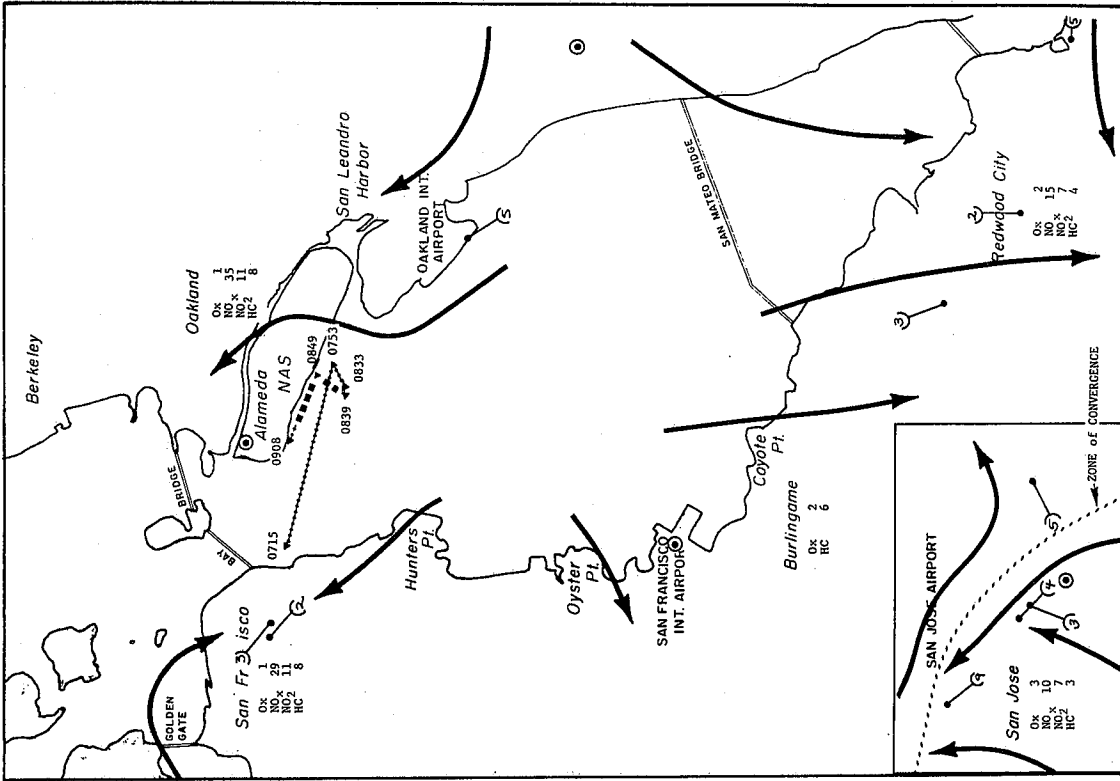
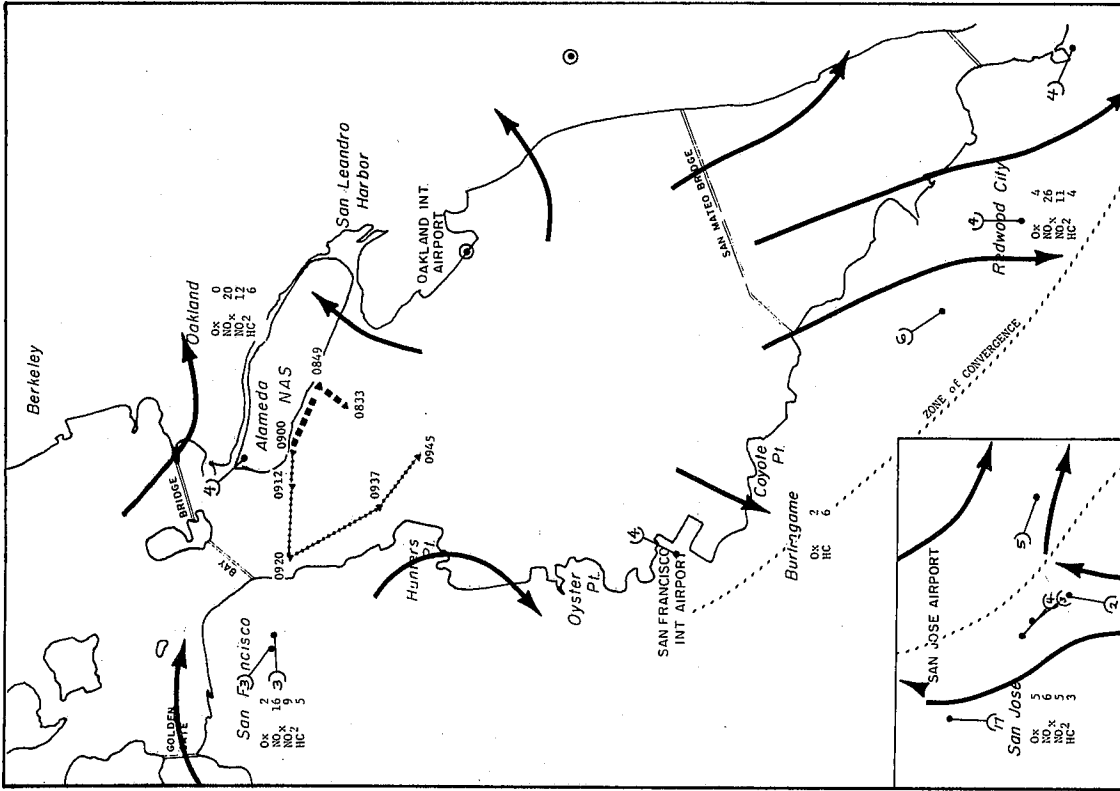


FIGURE C-3 RAWINSONDE TEMPERATURE AND DEW POINT OBSERVATIONS, 6 OCTOBER 1972  
 (Temperature ———, Dew Point - - - - )

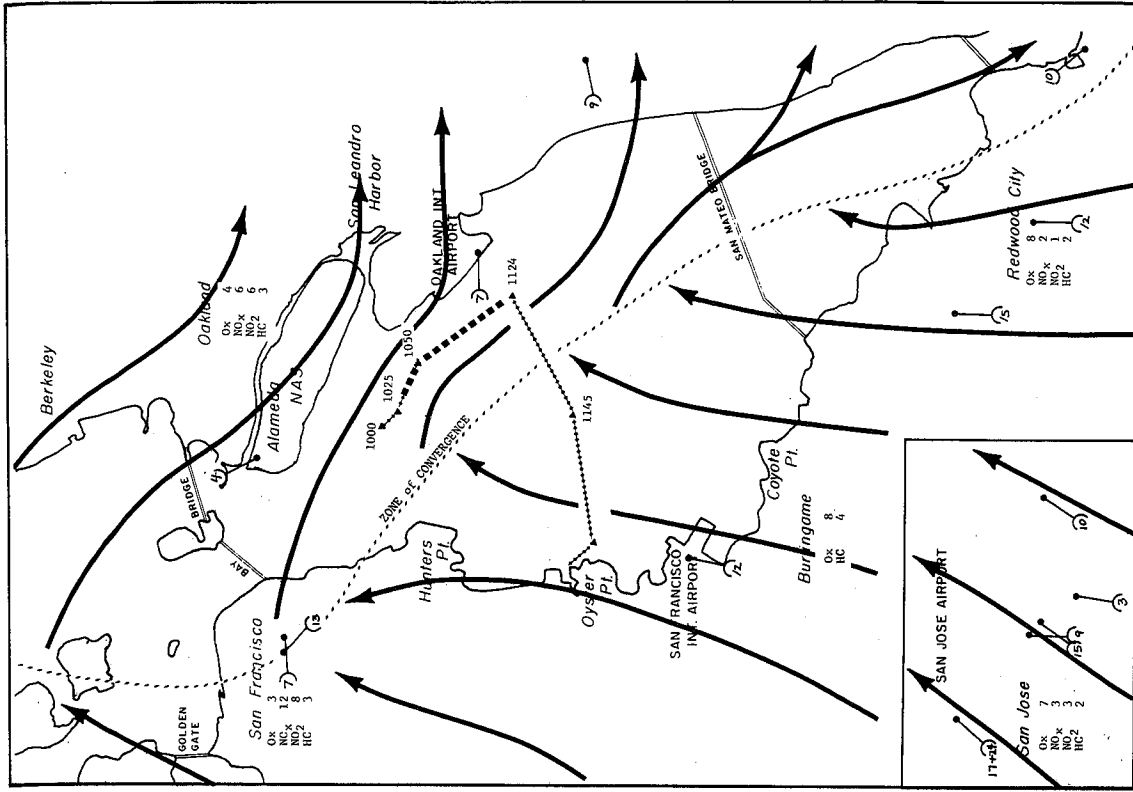


(a) 0800 PST

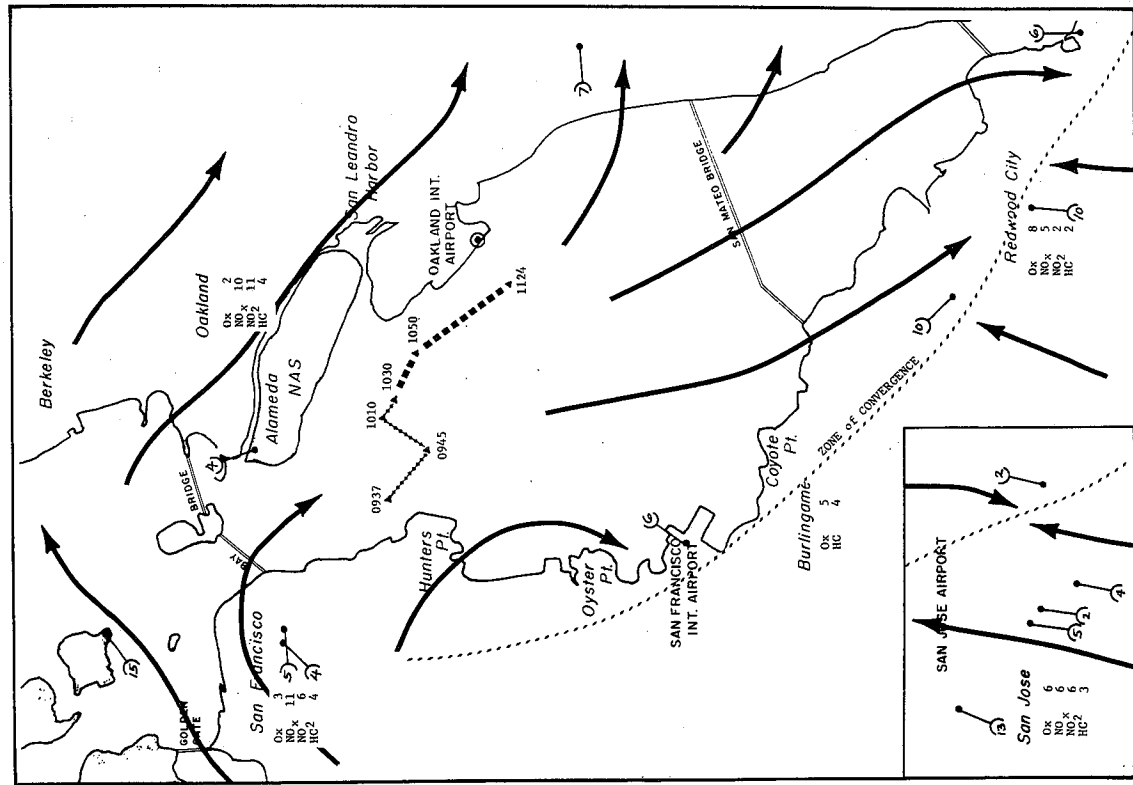


(b) 0900 PST

FIGURE C-4 AIR POLLUTION LEVELS, SURFACE WIND FLOW, AND HOUSEBOAT COURSE, 7 OCTOBER 1972

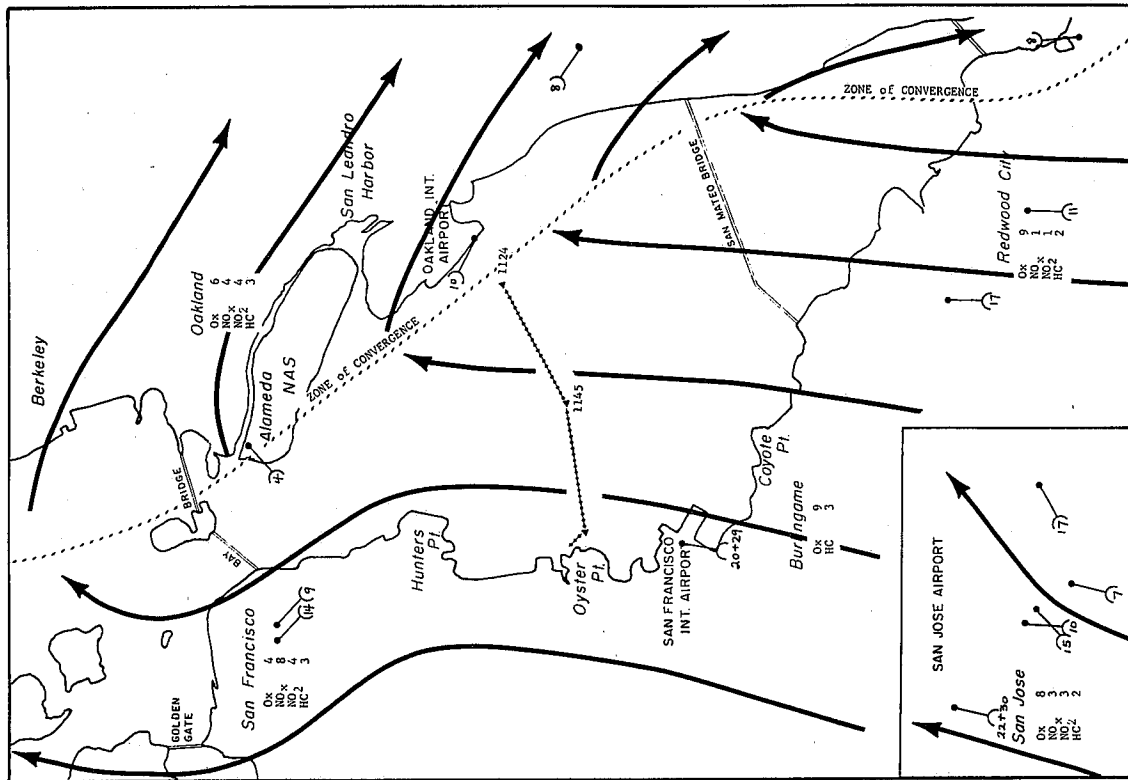


(d) 1100 PST



(c) 1000 PST

FIGURE C-4 AIR POLLUTION LEVELS, SURFACE WIND FLOW, AND HOUSEBOAT COURSE, 7 OCTOBER 1972  
(Continued)



(e) 1200 PST

FIGURE C-4 AIR POLLUTION LEVELS, SURFACE WIND FLOW, AND HOUSEBOAT COURSE, 7 OCTOBER 1972  
(Concluded)

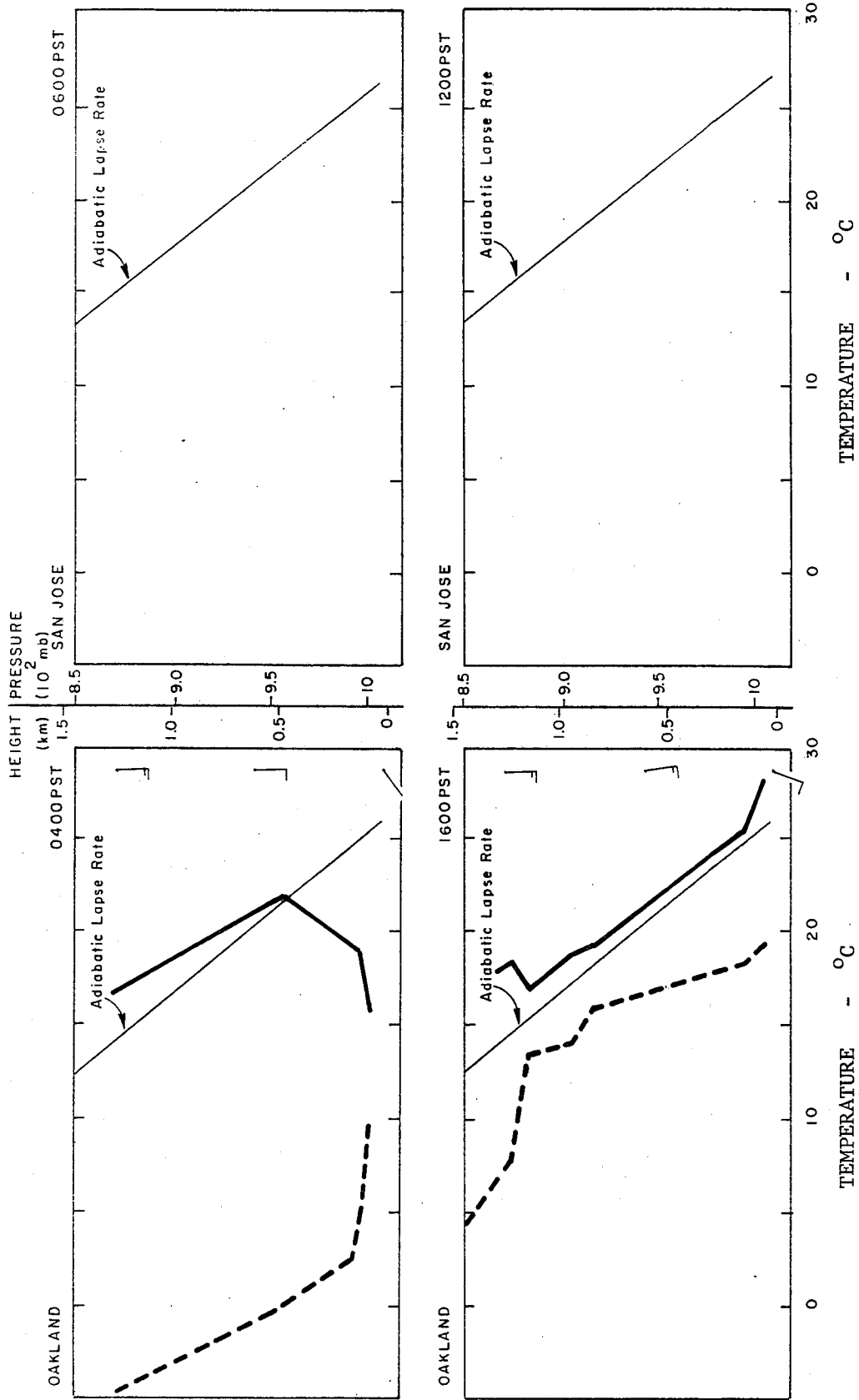
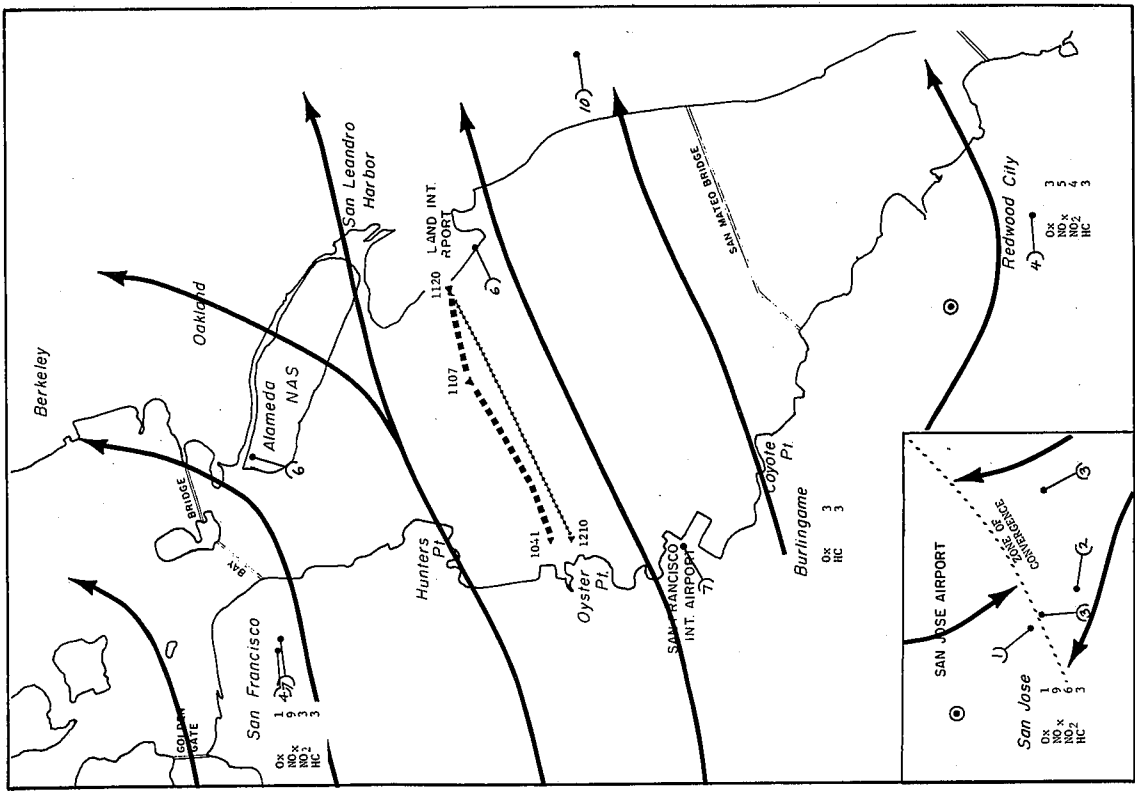
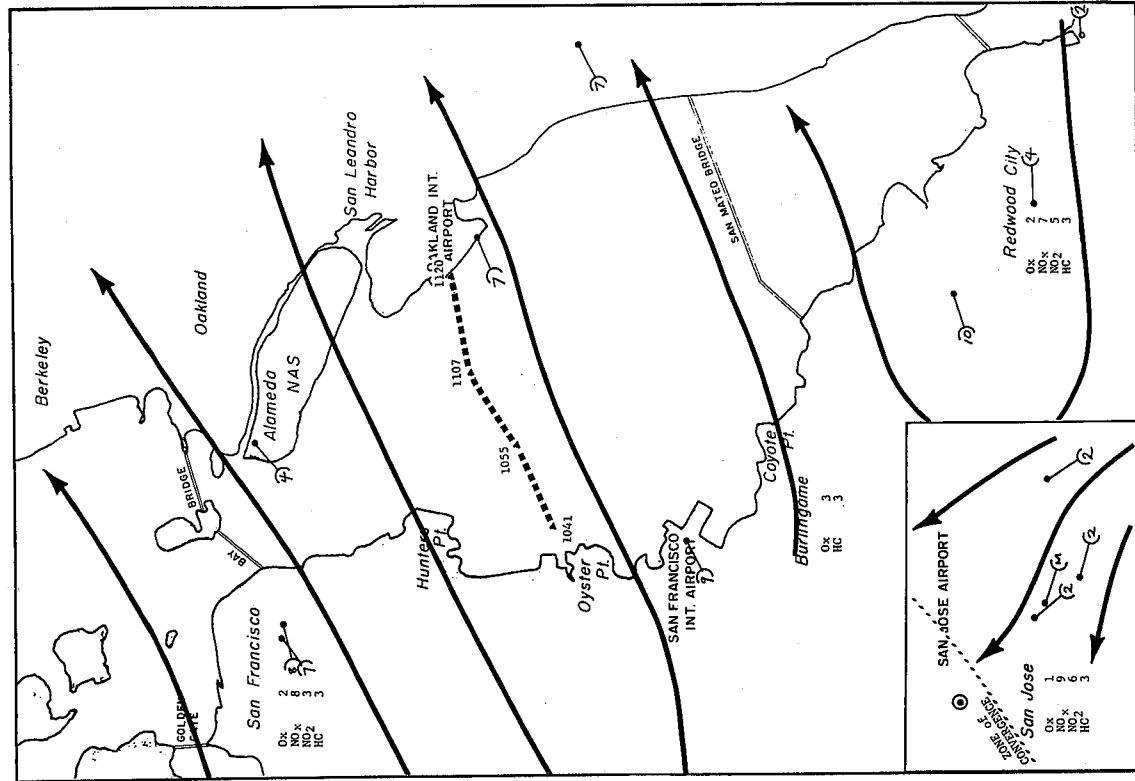


FIGURE C-5 RAWINSONDE TEMPERATURE AND DEW POINT OBSERVATIONS, 7 OCTOBER 1972



(b) 1100 PST



(a) 1000 PST

FIGURE C-6 AIR POLLUTION LEVELS, SURFACE WIND FLOW, AND HOUSEBOAT COURSE, 19 OCTOBER 1972

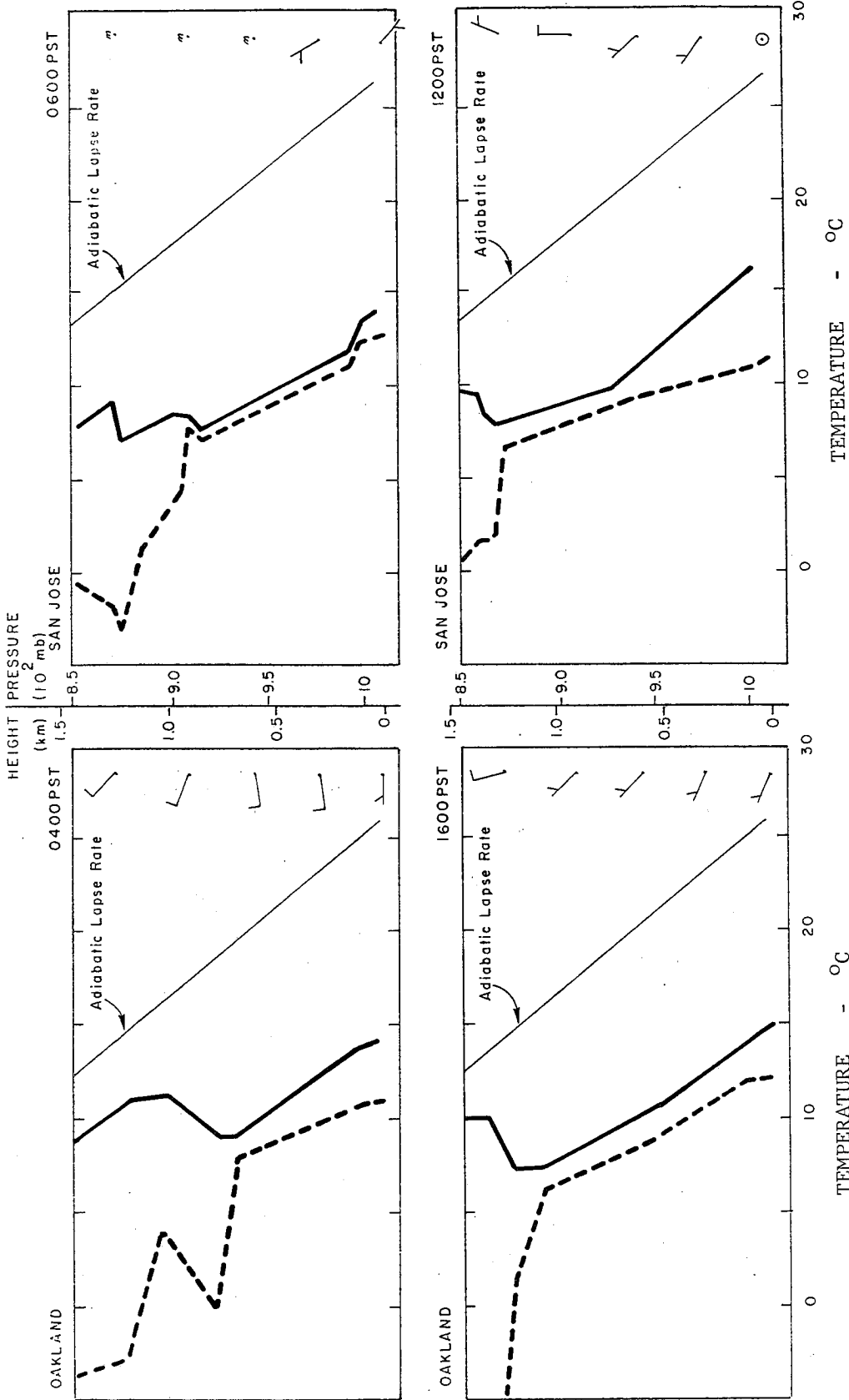
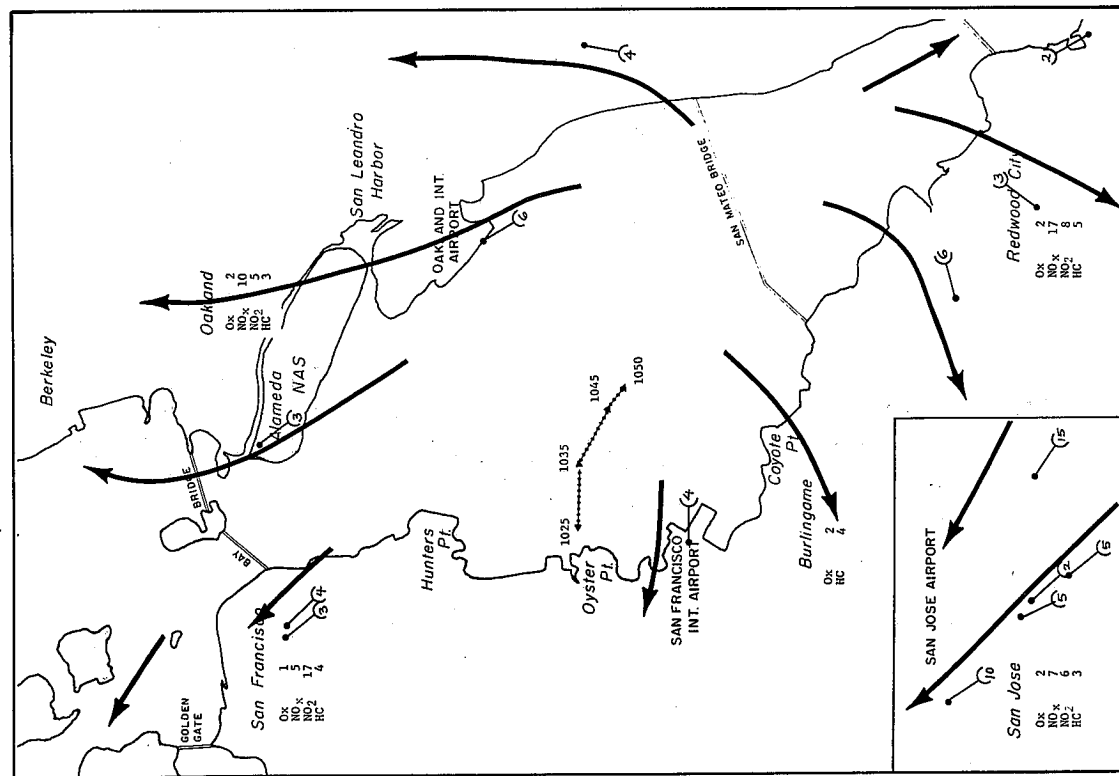
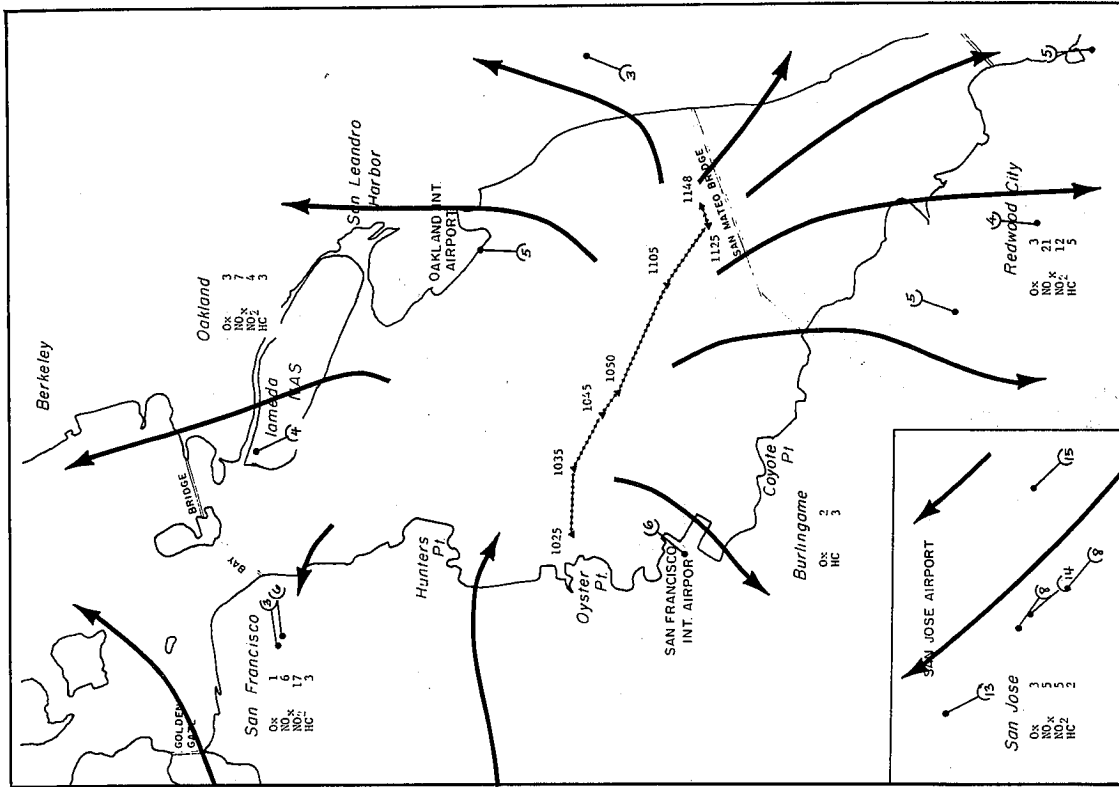


FIGURE C-7 RAWINSONDE TEMPERATURE AND DEW POINT OBSERVATIONS, 19 OCTOBER 1972  
 (Temperature ———, Dew Point - - - -)

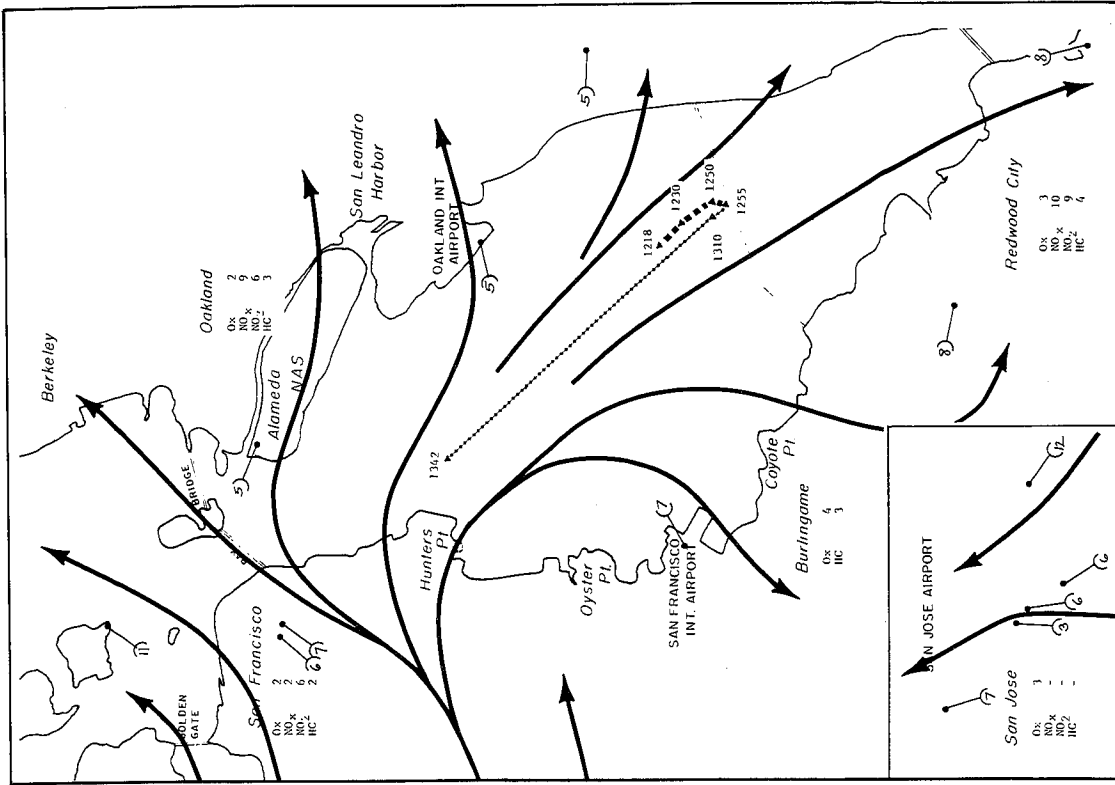


(a) 1000 PST

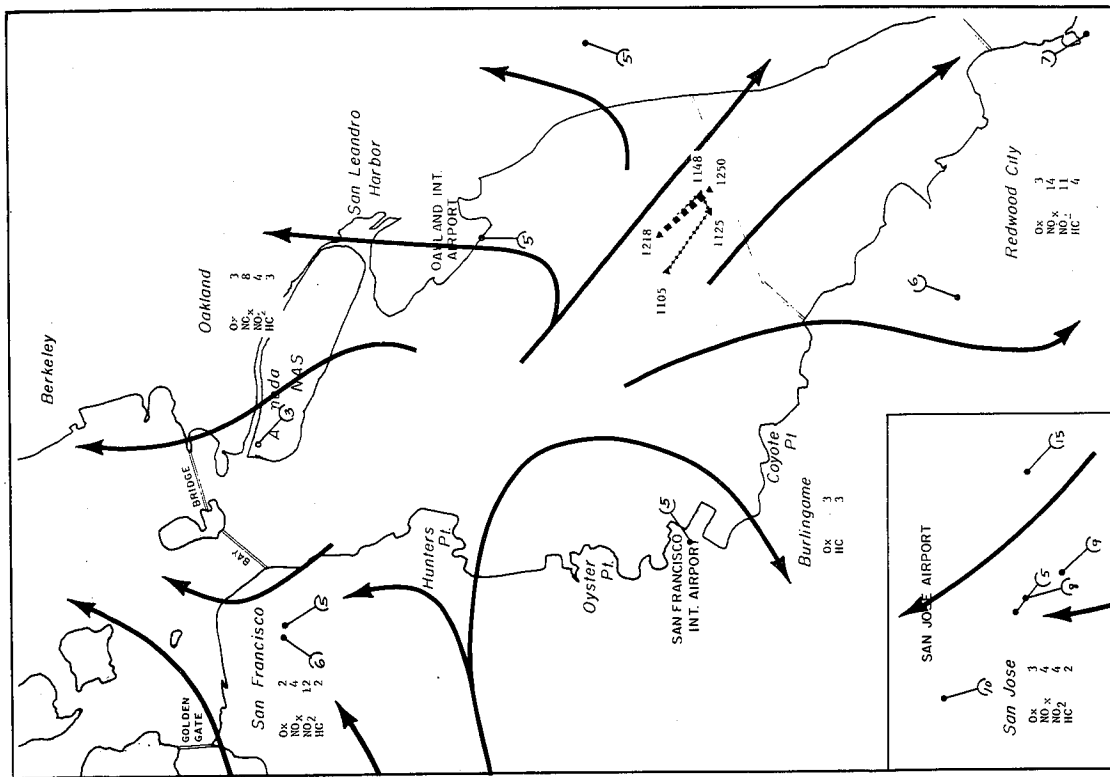


(b) 1100 PST

FIGURE C-8 AIR POLLUTION LEVELS, SURFACE WIND FLOW, AND HOUSEBOAT COURSE, 6 NOVEMBER 1972

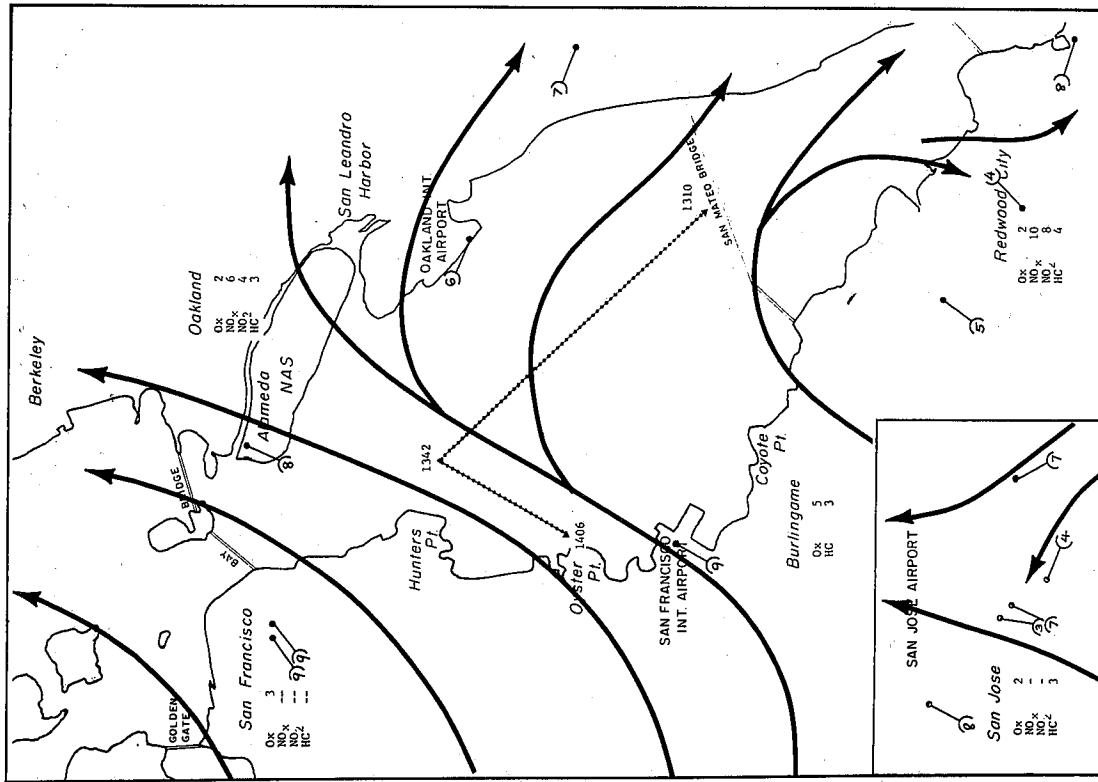


(d) 1300 PST



(c) 1200 PST

FIGURE C-8 AIR POLLUTION LEVELS, SURFACE WIND FLOW, AND HOUSEBOAT COURSE, 6 NOVEMBER 1972  
 (Continued)



(e) 1400 PST

FIGURE C-8 AIR POLLUTION LEVELS, SURFACE WIND FLOW, AND HOUSEBOAT COURSE, 6 NOVEMBER 1972  
(Concluded)

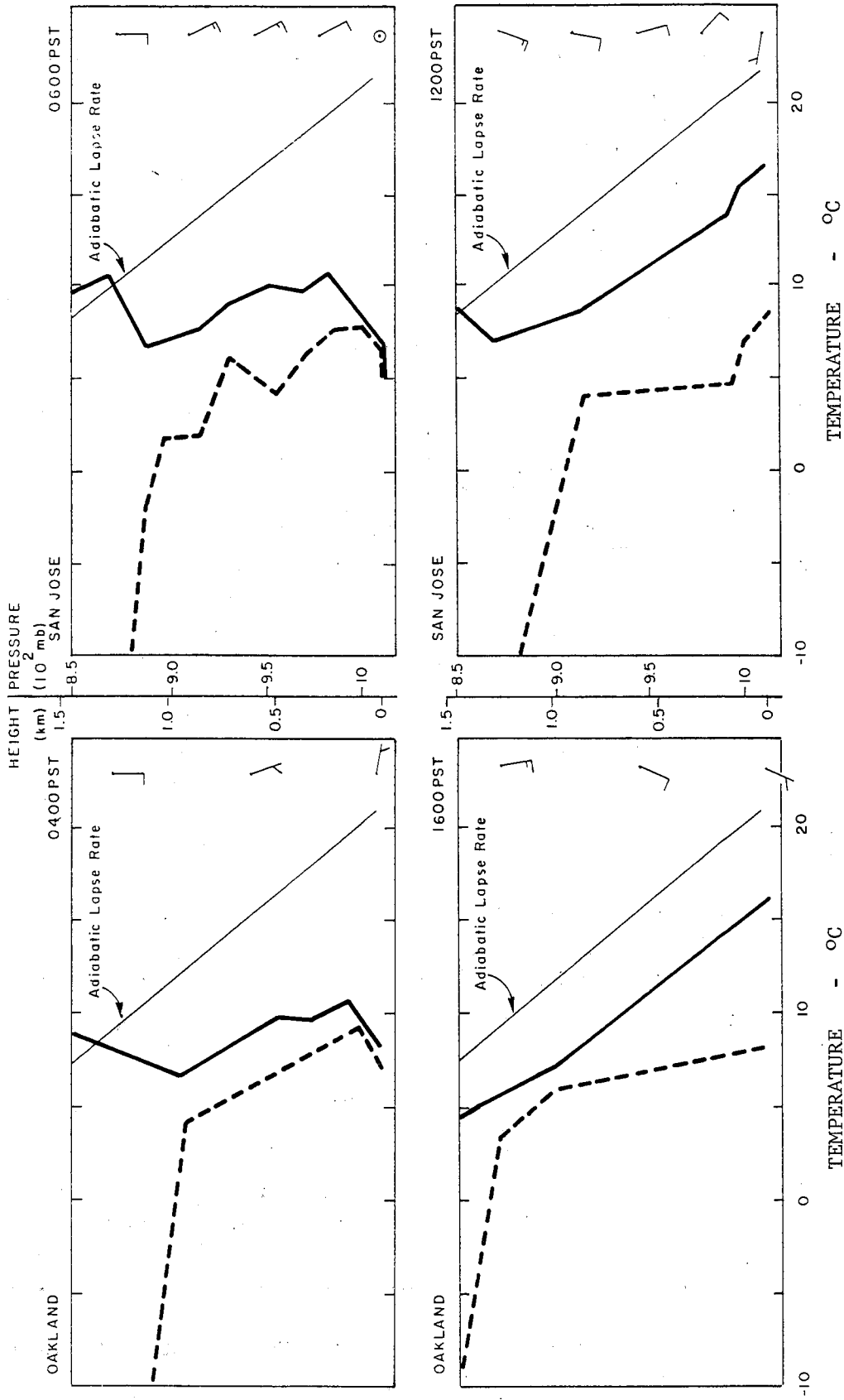


FIGURE C-9 RAWINSONDE TEMPERATURE AND DEW POINT OBSERVATIONS, 6 NOVEMBER 1972  
 (Temperature ———, Dew Point - - - - -)

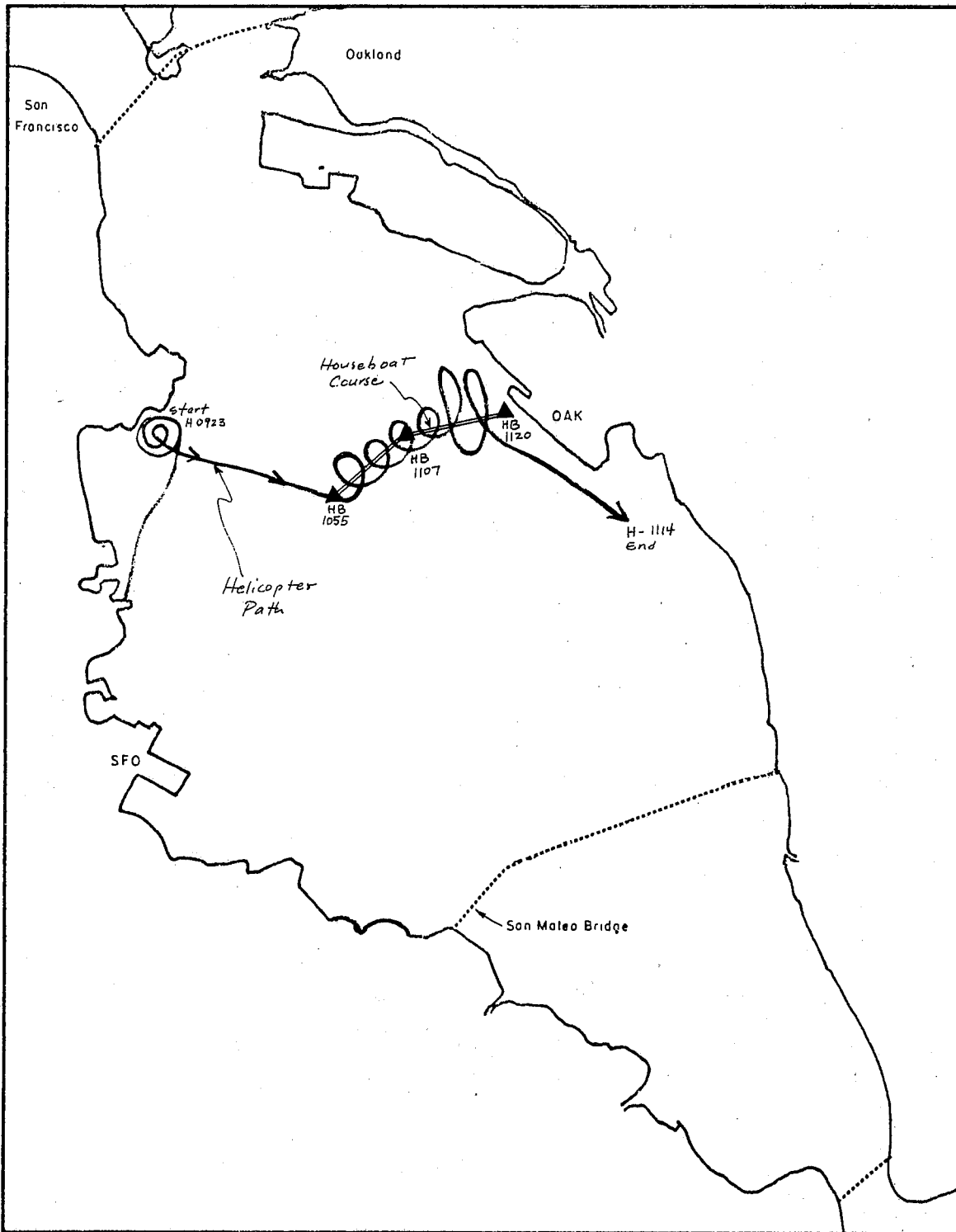


FIGURE C-10 SAMPLING PATHS OF MOBILE LABORATORIES ON 19 OCTOBER 1972  
(HB - houseboat, H - helicopter)

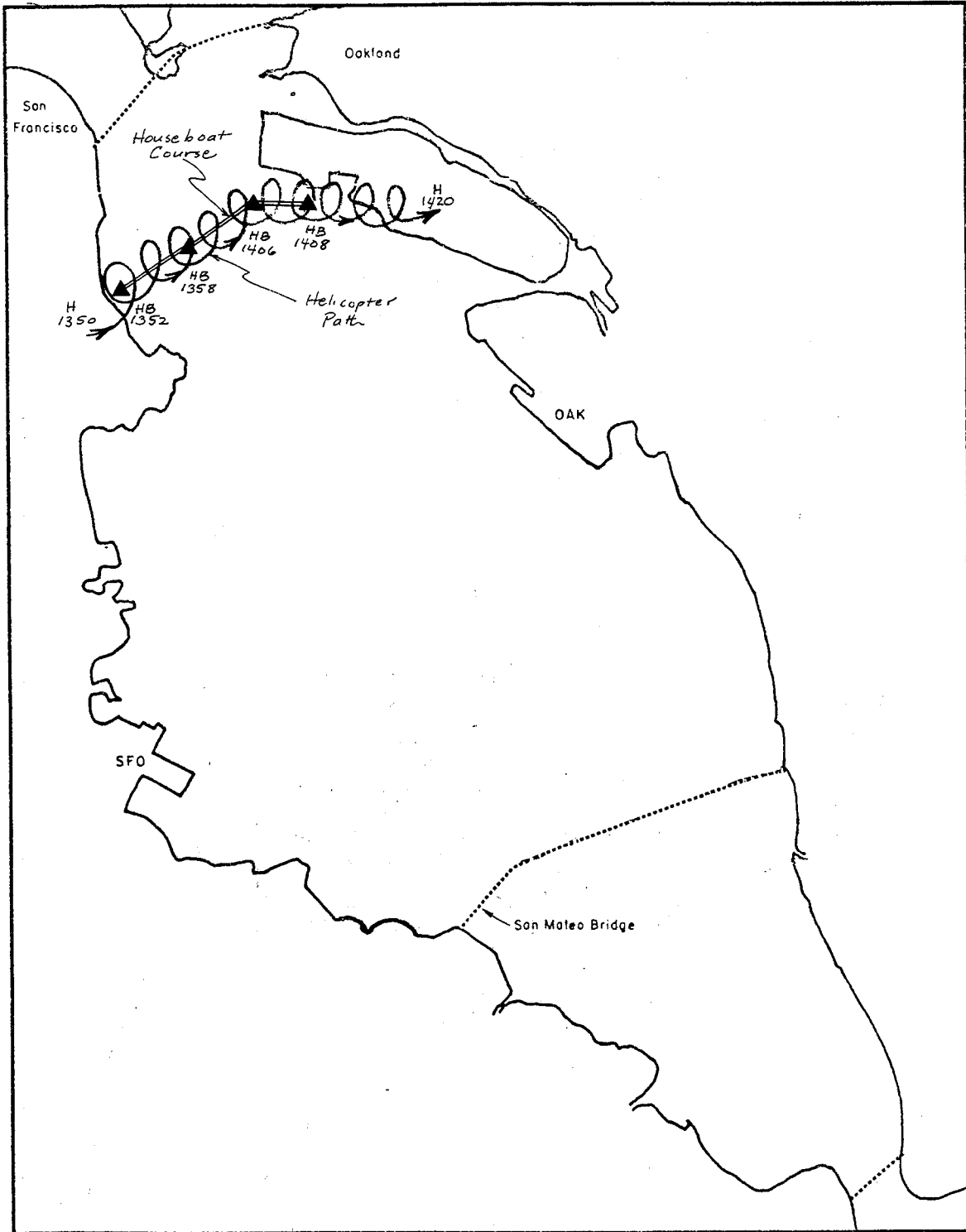


FIGURE C-11 SAMPLING PATHS OF MOBILE LABORATORIES ON 31 OCTOBER 1972  
 (HB - houseboat, H - helicopter)

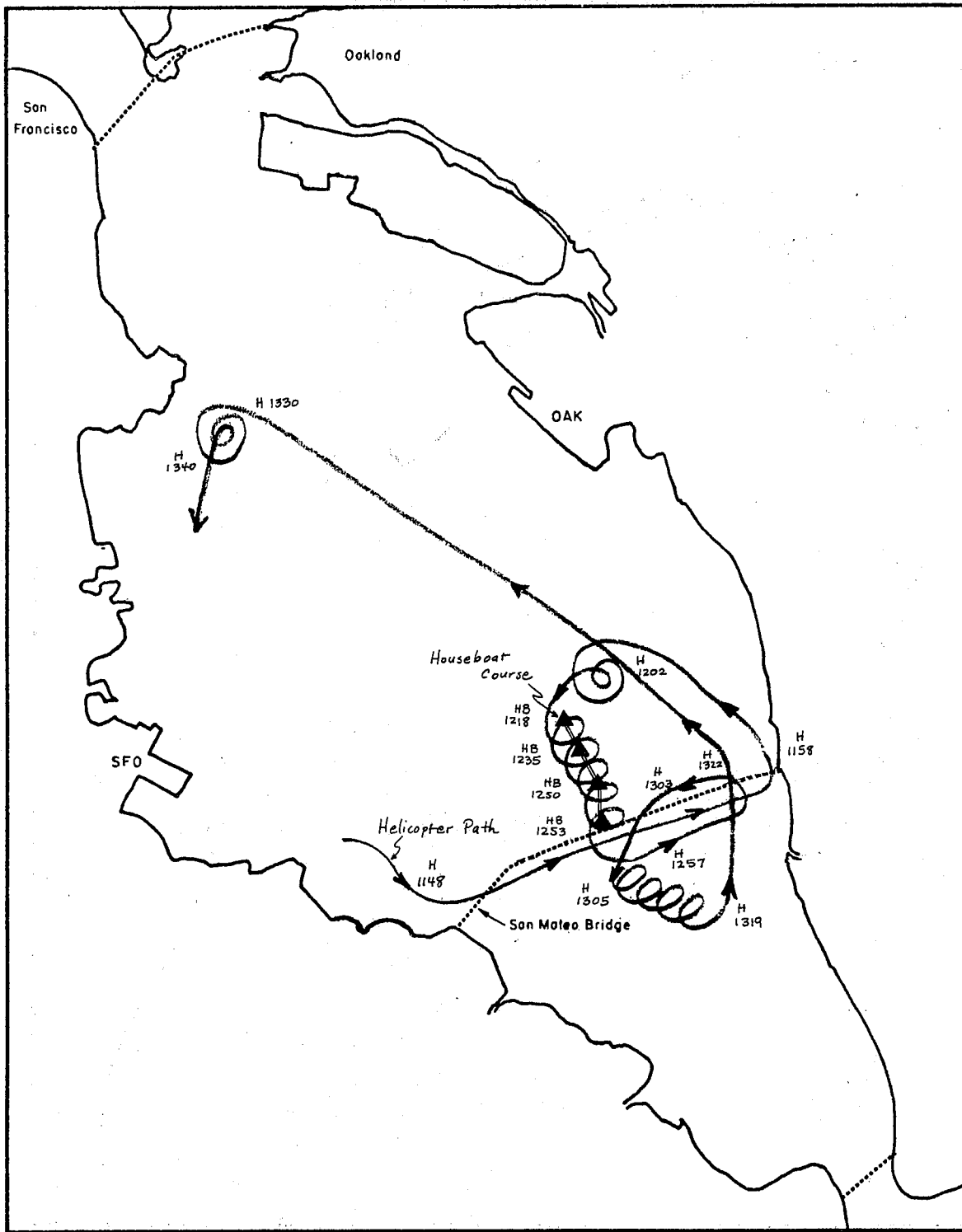


FIGURE C-12 SAMPLING PATHS OF MOBILE LABORATORIES ON 6 NOVEMBER 1972  
 (HB - houseboat, H - helicopter)

Table C-1

HELICOPTER MEASUREMENTS FOR 19 OCTOBER 1972

<u>Time</u> <u>(PST)</u>	<u>Altitude</u> <u>(ft)</u>	<u>CO*</u> <u>(ppm)</u>	<u>Ox</u> <u>(pphm)</u>	<u>Temp</u> <u>(°C)</u>	<u>NO</u> <u>(pphm)</u>	<u>NO<sub>x</sub></u> <u>(pphm)</u>
Vertical concentration gradient measurements off Hunters Point:						
0923	100		12.3	15.7	15	15
0927	200		10.3	15.6	11	15
0930	300		9.2	15.2	15	15
0932	400			14.8	11	15
0934	500			14.5	11	15
0936	600			14.1	11	15
0938	700			13.8	11	15
0939	800		8.1	13.5	11	15
0941	900			13.2	11	15
0943	1000			12.8	11	15
0945	1100		8.0	12.5	11	15

Measurements made while  
following tetraon:

1050	200	┌───┐	2.2	24.4	15	22
1053	580	+1		23.6	11	18
1055	250	└───┘	2.1	23.6	15	15
1058	260	┌───┐		24.8	11	15
1100	550	-1	2.1	23.8	15	
1103	800	└───┘		22.7	15	15
1105	400	±0.5	2.2	23.3	15	15
1108	300	└───┘		24.0	11	15
1110	300	└───┘	2.1	24.3	11	--
1112	200	└───┘	2.1	24.6	--	--

\*The number is the CO concentration change over the indicated time interval.

Table C-2

## HELICOPTER MEASUREMENTS FOR 30 OCTOBER 1972

<u>Time</u> <u>(PST)</u>	<u>Altitude</u> <u>(ft)</u>	<u>Ox</u> <u>(pphm)</u>	<u>Temp</u> <u>(°C)</u>	<u>NO</u> <u>(pphm)</u>	<u>NO<sub>x</sub></u> <u>(pphm)</u>
Measurements made while <u>following tetroon:</u>					
1251		1.8	14.4	6	8
1253	100		15.1		
1255	600	1.7	14.6		14
1257	900		14.2	9	14
1300	900	1.5	14.2	8	12
1303	500		14.5	9	11
1306	150	1.4	15.1	6	10
1309	500	1.6	14.5	6	6
1311	500		14.8	6	12
1315	500	1.7	14.4	9	11
1318	500		14.6	11	16
1320	400		14.6	10	12
1322	600		14.7	10	13
1325	600	0.2	14.7	9	12
1327	600		14.6	8	12
1330	500	3.1	14.6	8	11
1332	500	2.2	15.0	8	11
1340			14.8	8	10

Table C-3

## HELICOPTER MEASUREMENTS FOR 6 NOVEMBER 1972

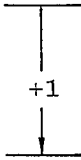
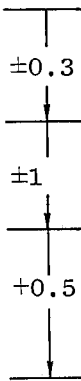
<u>Time</u> <u>(PST)</u>	<u>Altitude</u> <u>(ft)</u>	<u>CO</u> <sup>*</sup> <u>(ppm)</u>	<u>Ox</u> <u>(pphm)</u>	<u>Temp</u> <u>(°C)</u>	<u>NO</u> <u>(pphm)</u>	<u>NO<sub>x</sub></u> <u>(pphm)</u>	
<u>Horizontal concentration gradient measurements:</u>							
1150	450			13.1	23	30	
1155	450			13.0	16	26	
1157				13.0	14	15	
1159				13.6	16	25	
1201				13.5	18	24	
<u>Vertical concentration gradient measurements:</u>							
1202	50			13.6	25	27	
1203	120			13.6	28	29	
1205	270			13.0	28	29	
1206	330			13.0	28	29	
1208	400			12.9	26	24	
1209	530			12.9	14	22	
1210	730			13.0	15	22	
1211	930			12.7	16	22	
1212	1700			12.0	10	21	
<u>Measurements made while following tetroon:</u>							
1220	< 400		1.8	12.9	12	21	
1222	< 400			13.2	14	21	
1224	400		1.4	13.0	16	23	
1226	~ 450			13.4	16	22	
1228	500			1.7	13.1	18	23
1233	500				13.2	14	21
1235	500			1.9	13.2	15	22
1238	500				13.2	14	22
1239	500				13.1	14	22
1240	≈ 425			1.9	13.0	14	23
1242	450				13.1	15	22
1246	200			1.9	13.1	14	20
1248	100				13.6	15	21
1251	350			1.9	13.1	16	21

Table C-3 (Concluded)

<u>Time</u> <u>(PST)</u>	<u>Altitude</u> <u>(ft)</u>	<u>CO*</u> <u>(ppm)</u>	<u>Ox</u> <u>(pphm)</u>	<u>Temp</u> <u>(°C)</u>	<u>NO</u> <u>(pphm)</u>	<u>NO<sup>x</sup></u> <u>(pphm)</u>
-----------------------------	--------------------------------	----------------------------	----------------------------	----------------------------	----------------------------	--

Horizontal concentration gradient measurements:

1255			1.9	13.2	15	20
1300			2.0	13.2	16	21
1303	400			13.2	16	22

Measurements made while  
following tetraon:

1305	400		2.0	13.2	16	22
1308	800			13.0	15	20
1310			2.0	12.9	14	20
1315	400		1.9	12.7	12	18
1320			1.8	13.0	14	18

Vertical concentration gradient  
measurements off Hunters Point:

1340	100		2.2	14.0	6	18
1342	200			14.0	8	20
1344	300			14.0	9	19
1345	410			13.8	8	20
1347	640			13.2	8	20
1349	1580			12.4	8	19
1351	2620		6.4	11.1	8	19

\*The number is the CO concentration change over the indicated time interval.

Table C-4

CHEMICAL ANALYSES OF PARTICULATE MATTER  
COLLECTED ON GLASS FIBER FILTERS

<u>Time (hr:min)</u>	<u>Mass Loading (<math>\mu\text{g}/\text{m}^3</math>)</u>	<u>Chemical Composition (<math>\mu\text{g}/\text{m}^3</math>)</u>			
		<u>Nitrate</u>	<u>Sulfur*</u>	<u>Chloride</u>	<u>Lead</u>
<u>October 19</u>					
11:41-12:20	109	0	7.9	5.2	0.61
<u>October 24</u>					
12:53-13:16	225	0	4.6	31.5	0
<u>October 25</u>					
8:00-11:04 } 12:35-13:20 }	108	9.6	3.7	2.5	2.7
<u>October 26</u>					
10:06-10:50 } October 31 } 13:52-14:07 }	90	0	11.1	6.9	1.1
<u>November 2</u>					
8:33-11:20 } 11:23-13:17 }	108	10.8	6.0	1.0	2.4
16:33-17:45	194	24.7	17.3	3.1	2.6
<u>November 6</u>					
10:38-12:01	173	29.8	9.4	4.5	3.8
12:10-14:05	202	0	7.0	1.0	0.33
<u>November 17</u>					
11:05-11:20 } 13:17-13:47 }	325	0	7.1	9.9	0.56

\* All water-soluble sulfur compounds are included as sulfate.

Table C-5

## GAS CHROMATOGRAPH DATA-CRYOGENIC TRAP SAMPLES

Hydrocarbon Class	25 October, 0845		26 October, 0929		31 October, 1346		2 November, 0925		2 November, 1100		6 November, 1220		Typical Exhaust	
	ppb C	%	ppb C	%	ppb C	%	ppb C	%	ppb C	%	ppb C	%	ppb C	Range (%)
<b>Olefins</b>														
Ethylene	18	1.2	21	1.3	< 0.1	< 0.1	127	4.4	141	10.8	675	26.0		12-13
Acetylene	21	1.4	< 1	0.1	< 0.1	< 0.1	31	1.1	36	2.8	< 1	< 0.1		9-11
C <sub>3</sub> -C <sub>5</sub>	23	1.6	7	0.6	387	12.2	36	1.3	4	0.3	19	0.7		4-6
C <sub>6</sub> -C <sub>7</sub>	13	0.9	46	3.7	< 0.1	< 0.1	61	2.1	17	1.3	106	4.1		1
C <sub>8</sub> -C <sub>10</sub>	2	0.1	< 1	0.1	< 0.1	< 0.1	1	0.1	< 1	< 0.1	< 1	< 0.1		1
Subtotal	77	5.3	76	6.0	498	15.7	256	9.0	199	15.2	801	30.9		25-30
<b>Paraffins</b>														
Ethane	18	1.2	23	1.8	< 1	< 0.1	136	4.8	77	5.9	111	4.3		0-2
Propane	15	1.0	< 1	0.1	< 1	< 0.1	18	0.6	42	3.2	< 1	< 0.1		1-2
C <sub>4</sub> -C <sub>5</sub>	523	35.9	398	31.9	868	27.4	189	6.6	178	13.6	208	8.0		8-12
C <sub>6</sub> -C <sub>7</sub>	274	18.8	200	16.0	728	23.0	250	8.7	58	4.4	359	13.8		6-14
C <sub>8</sub> -C <sub>10</sub>	179	12.3	199	16.0	303	9.6	453	15.8	103	7.9	225	8.7		7-13
Subtotal	1009	69.3	821	65.8	1901	60.0	1046	36.6	458	35.1	904	34.9		30-40
<b>Aromatics</b>														
Benzene	34	2.3	56	4.5	106	3.3	47	1.6	10	0.8	131	5.0		2-3
Toluene	80	5.5	88	7.1	207	6.5	144	5.0	27	2.1	205	7.9		5-6
Ethyl Benzene	20	1.4	24	1.9	39	1.2	169	6.0	17	1.3	53	2.0		1-2
m-,p-Xylene	71	4.9	78	6.2	138	4.4	130	4.6	53	4.1	137	5.3		6-8
o-Xylene	38	2.6	5	0.4	87	2.7	54	1.9	29	2.2	107	4.1		3-7
C <sub>9</sub> -C <sub>10</sub>	127	8.7	100	8.0	194	6.1	1012	35.4	512	39.2	255	9.8		14-18
Subtotal	370	25.4	351	28.2	771	24.3	1557	54.5	648	49.7	888	34.2		30-45
TOTAL	1456		1247		3170		2859		1305		2593			

Appendix D

DESCRIPTION OF EDITED DATA TAPE

## Appendix D

### DESCRIPTION OF EDITED DATA TAPE

The thousands of individual observations made during this project have been consolidated, edited, and recorded at high-density, odd-parity mode on a single reel of seven-channel magnetic tape. In this consolidation, all the primary data were retained. Each record of the summary tape corresponds to a record as originally recorded by the data collection during a 5-minute period.

All the data have been converted to engineering units. The units used for the various parameters are shown in Table D-1. Missing data are marked by the number -99.9. Each record contains 340 words. Table D-2 shows the organization of the records. The first 30 words are devoted to averages and other items that apply to the entire 5-minute period. The next 200 words give the data collected at 15-second intervals. Another 100 words are used for the 30-second data. The last 10 words, and several spaces among the first 30 words are listed as spares. These locations can be used for derived quantities of special interest, without requiring a reorganization of the record. For example, one of the locations that was designated as spare in the original formatting has subsequently been used for relative humidities. Another space has been used to indicate periods of tetron tracking.

Table D-1

## UNITS USED IN DATA SUMMARY

Parameter	Unit
Date	Year-month-day, e.g., 720911 is 11 September 1972
Time	Hours (decimal) Pacific Standard Time
Location	Kilometers - See Figure D-1 for coordinate system
Particle concentration	Number $\text{cm}^{-3}$ per channel
Carbon monoxide concentration	Parts-per-million-by-volume (ppm)
Total hydrocarbon concentration	ppm carbon (ppm C) as hexane
Nitric oxide concentration	parts-per-hundred-million (pphm)
Nitrogen dioxide concentration	pphm
$\text{NO}_x$ concentration	pphm
Ozone condensation	pphm
Total sulfur concentration	pphm
Condensation nuclei	Thousands per $\text{cm}^3$
Scattering coefficient	$\text{m}^{-1} \times 10^4$
Solar radiation	$\text{cal cm}^{-2}\text{min}^{-1}$
Temperature	degrees centigrade
Relative humidity	percent

Table D-2

ENGINEERING UNIT MAGNETIC TAPE RECORD FORMAT

First three lines of data	Date	Record Time (decimal hours PST)		X at Start (km)	Y at Start (km)	X at End (km)	Y at End (km)	Particle Count During Period		
		Start	End					Chan. 1 (No. cm <sup>-3</sup> )	Chan. 2 (No. cm <sup>-3</sup> )	Chan. 3 (No. cm <sup>-3</sup> )
		Particle Count During Period						Av. Condensation Nuclei (cm <sup>-3</sup> × 10 <sup>-3</sup> )	Average CO (ppm) †	Ti Room Run ‡
	Spare	Average NO (pphm)	Average NO <sub>2</sub> (pphm)	Average CO Hydrocarbons (ppm C)	Average O <sub>3</sub> (pphm)	Average Sulfur (pphm)	Av. Scattering Coefficient (m <sup>-1</sup> × 10 <sup>4</sup> )	Av. Reference Voltage (V)	Av. Relative Humidity (percent)	Spare
Typical data	721025.000 087 -99.900	13.183 .060 8.492	13.263 -99.900 4.547	12.522 1.711 13.815	22.307 5.078 30.734	12.847 8.169 25.969	23.324 .938 2.124	.299 8.508 .961	.372 3.216 74.868	.120 -99.900 -99.900
	Time (hours PST)	X (km)	Y (km)	CO (ppm) *	Hydrocarbons (ppm C)	O <sub>3</sub> (pphm)	Sulfur (pphm)	Scattering Coefficient (cm <sup>-1</sup> × 10 <sup>3</sup> )	Condensation Nuclei (cm <sup>-3</sup> × 10 <sup>-3</sup> )	Reference Voltage (V)
	13.183	12.522	22.307	-99.900	1.719	5.078	9.288	.469	9.844	3.563
	13.187	12.539	22.369	-99.900	1.719	5.078	8.105	.469	8.906	3.000
	13.192	12.556	22.413	-99.900	1.719	5.078	8.105	.547	8.672	3.750
	13.196	12.573	22.467	-99.900	1.797	5.078	8.105	.469	8.906	2.813
	13.200	12.590	22.520	-99.900	1.719	5.078	9.288	.469	9.288	3.000
	13.204	12.607	22.573	-99.900	1.719	5.078	8.105	.469	9.141	3.563
	13.208	12.624	22.627	-99.900	1.719	5.078	3.474	.391	7.969	3.188
	13.212	12.641	22.680	-99.900	1.719	5.078	9.288	.469	8.203	2.813
	13.217	12.658	22.733	-99.900	1.719	5.078	9.288	.391	7.969	2.813
	13.221	12.675	22.787	-99.900	1.641	5.078	8.105	.469	7.969	2.813
	13.225	12.692	22.840	-99.900	1.719	5.078	9.288	.391	8.438	2.625
	13.229	12.710	22.893	-99.900	1.719	5.078	8.105	.469	7.969	4.500
	13.233	12.727	22.947	-99.900	1.719	5.078	8.105	.313	8.906	3.563
	13.237	12.744	23.000	-99.900	1.719	5.078	8.105	.469	7.266	3.563
	13.242	12.761	23.053	-99.900	1.797	5.078	8.105	.391	8.438	3.375
	13.246	12.778	23.107	-99.900	1.641	5.078	8.105	.469	7.969	2.625
	13.250	12.795	23.160	-99.900	1.719	5.078	8.105	.469	9.375	3.188
	13.254	12.812	23.213	-99.900	1.719	5.078	8.105	.313	7.969	3.375
	13.258	12.829	23.267	-99.900	1.641	5.078	8.105	.469	9.141	2.625
	13.262	12.846	23.320	-99.900	1.641	5.078	8.105	.391	9.844	3.563
	Time (hours PST)	X (km)	Y (km)	NO (pphm)	NO <sub>2</sub> (pphm)	NO <sub>x</sub> (pphm)	Dry Bulb Temperature (°C)	Wet Bulb	Radiation (cal cm <sup>-2</sup> min)	Reference Voltage (V)
	13.184	12.523	22.310	17.359	10.328	16.430	31.125	26.437	2.119	.961
	13.192	12.557	22.417	17.359	2.906	20.219	31.281	26.594	2.078	.961
	13.200	12.591	22.524	9.938	2.906	20.219	31.437	26.437	1.931	.961
	13.209	12.625	22.630	9.938	4.469	14.914	31.437	26.281	2.161	.961
	13.217	12.659	22.737	6.813	4.469	14.914	31.125	26.125	2.454	.961
	13.225	12.694	22.844	6.813	4.078	11.883	30.656	25.812	2.203	.961
	13.234	12.728	22.950	4.469	4.469	11.883	30.500	25.656	2.119	.961
	13.242	12.762	23.057	4.859	4.078	11.883	30.500	25.500	2.098	.961
	13.250	12.796	23.164	3.688	4.078	9.609	29.875	25.500	2.057	.961
	13.259	12.830	23.270	3.688	3.688	8.473	29.406	25.344	2.015	.961
Spare	-99.900	-99.900	-99.900	-99.900	-99.900	-99.900	-99.900	-99.900	-99.900	-99.900

\* CO as measured by the Bacharach mercury displacement analyzer.  
 † CO as measured by the Beckman NDIR analyzer.  
 ‡ 0.0 = yes, -99.9 = no  
 § Fifteen-second sampling intervals are indicated by A and 30-second sampling intervals are indicated by B.

The locations shown are referred to the coordinate system shown in Figure D-1. The coordinates are determined from landmark azimuth sightings made on the boat periodically whenever there were significant changes of course. The coordinates on the data tape for each individual time were obtained by time-based linear interpolation for all except the times corresponding to azimuth sightings. The locations shown are estimated to be accurate within about 250 m.

The records include average and summary information to facilitate selection of data sets that meet certain criteria. For instance, data could be stratified and averaged according to time of day, location, radiation intensity, or prevailing carbon monoxide concentrations. The summary data can also be used in preliminary data analysis to produce smoothed time histories.

The data for each experimental day are contained in a separate file. Two end-of-files mark the end of the data tape.

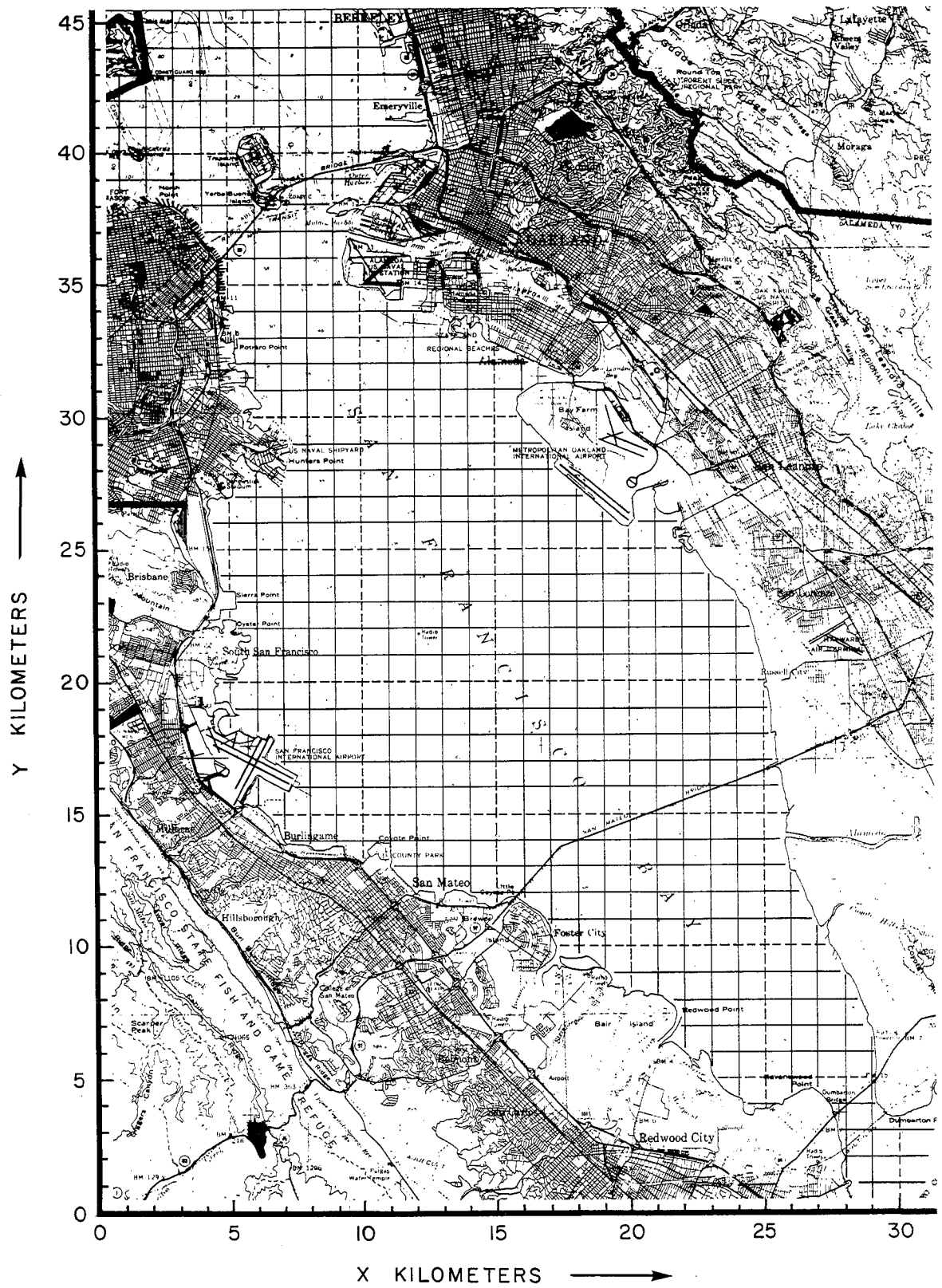


FIGURE D-1 GRID COORDINATE OVERLAY MAP OF THE BAY AREA

Appendix E

CHRONOLOGICAL SUPPORTING DATA FOR  
SELECTED SAMPLE DAYS



## Appendix E

### CHRONOLOGICAL SUPPORTING DATA FOR SELECTED SAMPLE DAYS

The meteorological data, pollutant plots, the particulate data, and the hydrocarbon distribution data for 21 September, 25 October, 26 October, and 2 November were summarized in the Section V of this report. The following discussions are expanded analysis of the data from the four selected days.

#### A. 21 September

The meteorological conditions and pollutant plots for 21 September may be found in Section V.B.

The houseboat was moved from OP to a point halfway between Hunters Point (HP) and Oakland. This position was maintained for 45 minutes while the tetron was weighed off. The data in Table E-1 are selected concentrations observed during this 45-minute interval. Two conclusions can be reached. The low values of the NO to NO<sub>2</sub> ratio indicate that the sampled air was well aged. The increase in O<sub>3</sub> concentration suggests that photochemical reactions were occurring. The houseboat proceeded to a point north of the BB where the tetron was released at 1030. The pollutant concentrations are summarized in Figure 3. The tetron was over San Francisco from 1037 to 1056, so that the data collected during this interval are not truly representative of the same air parcel.

While the NO concentration decreased rapidly after 60 minutes, the concentration of the other pollutants did not. However, there is a steady decrease in the concentration of CO from about 1.3 ppm to 0.8 ppm due to dilution. Since CO is essentially inert under atmospheric conditions, a

Table E-1

HOUSEBOAT DATA FOR 21 SEPTEMBER 1972, 0912 TO 1000 PST  
(5-Minute Averages)

<u>Time</u>	<u>NO</u> (pphm)	<u>NO<sub>2</sub></u> (pphm)	<u>O<sub>3</sub></u> (pphm)	<u>THC</u> (ppm)	<u>Nephelometer</u> (m <sup>-1</sup> × 10 <sup>4</sup> )
0915	5.2	14.6	3.2	6.5	2.7
0930	4.6	14.9	4.5	6.9	2.1
0945*	8.0	16.2	4.3	8.4	2.2
1000	2.7	13.6	6.3	6.4	3.0

\* May have some houseboat exhaust from tetron  
weighoff procedure.

plot of the ratio of pollutant to CO concentrations permits the changes in pollutant concentrations to be assessed without interference or masking by dilutional effects. On the basis of pollutant to CO concentration ratios, the concentration of NO<sub>2</sub> decreases with a corresponding increase in O<sub>3</sub> concentration. The concentration of total hydrocarbons (THC) remains nearly constant. These observations are discussed in more detail in Section VI-A.

The aerosol particle counter data are summarized in Figure 6. Two features of these plots are particularly interesting. First, there is a 20-fold decrease in the aerosol concentrations from 1042 to 1226. A similar decrease was observed in the CN concentration and the nephelometer readings (by a factor of about 2) during the same time interval. Second, the number of particles in the 0.3-micron size range is nearly equal to the number in the 0.2-micron range. There may also be a peak in the size distribution in the 0.4-micron range.

The concentration decrease may be ascribed to a loss of water through evaporation from the individual particles, to coagulation, or to dilutional effects.

The dilutional effects during this period reduce concentrations by about a factor of two or three, as indicated by changes in the concentrations of CN and CO. According to theory,<sup>30</sup> coagulation is a process that changes size distributions only very slowly, and would in any event lead to a replenishment of the particles in the tenth micron size range. Evaporation seems the most likely cause of the reduction in the particles concentrations in the size ranges measured by the particle counter. As shown in Table E-2, the relative humidity at the stations on the perimeter of the Bay (SF and Oakland Airports) was 65 to 75 percent early in the sampling interval and decreased to about 50 to 60 percent at the end. Such changes are likely to be accompanied by evaporation of droplets containing dissolved salts.<sup>30</sup> Therefore, droplets of a few tenths micron diameter would shrink to dry particle sizes below the measurement range of the counter. However, the total numbers of particles would remain about the same and CN concentration would not be affected.

Table E-2

TEMPERATURE AND RELATIVE HUMIDITY  
DATA FOR BAY AREA STATIONS

Time (PST)	San Francisco Federal Building		San Francisco Airport		Oakland Airport	
	Temp (°C)	RH (percent)	Temp (°C)	RH (percent)	Temp (°C)	RH (percent)
1000	23	60	19	68	19	73
1100	22	53	21	61	20	68
1200	25	54	23	53	22	66
1300	22	55	23	49	23	55

B. 25 October

The houseboat made a straight line traverse across the Bay departing from OP at 0545 and arriving at the entrance to San Leandro Harbor (SLH) at 0627. The NO concentration was 29.4 pphm at the western shore of the Bay. A gradual decrease to 0.6 pphm was observed as the houseboat approached a point about 2.5 kilometers to the west of the center of the Bay. Between this point and the SLH entrance, the concentration of NO increased to a maximum of 48.4 pphm. These measurements were made while the houseboat was at cruising speed, and exhaust gas contamination could not have occurred. A summary of the 5-minute average pollutant concentrations is shown in Table E-3.

Table E-3

HOUSEBOAT DATA FOR 25 OCTOBER 1972, 0546 TO 0636 PST  
(5-Minute Averages)

<u>Time</u>	<u>NO</u> <u>(pphm)<sup>a</sup></u>	<u>NO<sub>2</sub></u> <u>(pphm)</u>	<u>O<sub>3</sub></u> <u>(pphm)</u>	<u>CO</u> <u>(ppm)</u>	<u>THC</u> <u>(ppm C)</u>	<u>Nephelometer</u> <u>(m<sup>-1</sup> × 10<sup>4</sup>)</u>
0546	27.8	2.5	1.7	1.688	--	0.9
0556	11.2	1.1	2.3	1.184	3.0	0.4
0606	0.7	1.9	1.4	0.872	3.0	0.5
0616	18.4	3.5	--	1.28	3.3	0.5
0626	37.8	2.7	--	1.2	3.5	0.5
0636	26.7	8.2	--	--	4.2	1.8

Offshore breezes early in the morning probably caused encroachment of polluted air, primarily containing high NO concentrations, near the west and east shores of the Bay. The offshore advection had not advanced sufficiently to modify the very clean air present in the central Bay. While the houseboat remained near the eastern shore of the Bay from 0627 to 0754, easterly winds became established.

A tetroon was released at 0756 and drifted from east to west along essentially the identical path that the houseboat had taken from west to east 2 hours previously. The NO concentration at SLH had declined by nearly 50 percent (to about 19 pphm) from the time of arrival at 0627 until the tetroon was released at 0756. The concentration of NO in this run increased in the central Bay with some inhomogeneity to about 25 pphm; a constant decrease of NO was observed from the central Bay to the western shore. The decrease was somewhat masked by an interval of exhaust gas contamination west of the center of the Bay. The relatively high CO concentrations observed at the western shore earlier had now diminished to below 5 pphm due to advection.

During the 0756 tetroon run on this day, supplemental measurements were made by the helicopter. The helicopter circled the tetroon from 0805 until 0930. The radius of the helicopter circles, based on a constant speed and the time required for completion of a circle, varied from 225 meters to 470 meters with an average radius of about 300 meters. The tetroon was floating at an average altitude of 150 meters. The helicopter circled the tetroon in flight from an altitude of 30 meters to 180 meters. Comparison data of pollutant measurements obtained by the two mobile laboratories are shown in Table E-4.

Table E-4

DATA FOR 25 OCTOBER 1972, 0801 TO 0825 PST  
(1-Minute Averages)

Houseboat					Helicopter					
Time	NO (pphm)	NO <sub>x</sub> (pphm)	O <sub>3</sub> (pphm)	Temp (°C)	Time	Alt (ft)	NO (pphm)	NO <sub>x</sub> (pphm)	O <sub>x</sub> (pphm)	Temp (°C)
0801	19	19.1	0.8	20.2	0807	100	33	40	0.8	24.5
0812	26	2.1	0.8	20.5	0812	100	22	26	0.8	24.0
0814	21.3	25.1	0.8	26.8	0814	190	22	26	0.7	24.0
0815	23.2	25.1	0.8	21.0	0815	250	22	26	0.6	24.0
0818	14.6	19.1	0.8	21.1	0818	290	7	18	0.8	24.0
0820	14.6	17.6	0.8	21.3	0820	380	11	15	0.8	24.0
					0825	600	7	11	0.9	24.0

At 0831 the helicopter moved to a location out of the flight path of the San Francisco and Oakland Airports to obtain a vertical profile of temperature and pollutant concentrations. A spiraling ascent was performed near the San Mateo Bridge beginning at 0831. The data from this vertical profile are summarized in Table E-5.

Table E-5

HELICOPTER DATA FOR 25 OCTOBER 1972, VERTICAL PROFILE

Alt (ft)	Time (PST)	NO (pphm)	NO <sub>x</sub> (pphm)	O <sub>x</sub> (pphm)	Temp (°C)
100	0831	44	58	0.8	24.0
130	0832	29	51		24.0
170	0833	18	36		23.5
220	0834	11	22		23.5
300	0835	18	18	0.5	24.0
400	0837	11	15		23.9
590	0839	11	15		23.9
720	0840	7	7	0.5	24.0
900	0841	7	7		23.0
1900	0844	7	11	0.4	23.0
4800	0849	7	7	0.3	22.0

The temperatures measured during the tetroon run indicate that the atmosphere is relatively stable at the lower altitudes. As anticipated, the pollutant concentrations decreased as the measurement altitude increased.

The helicopter completed the vertical profile and returned to the houseboat to continue tracking the tetroon after the sample run was terminated by the houseboat at 0855. However, the helicopter was unable to locate the tetroon due to the lack of visual contrast between the tetroon and the background of multicolored house roofs. Due to the hilly terrain, the helicopter was unable to fly below the level of the tetroon to improve visual contrast.

The houseboat began a return trip to SLH at 0916, arriving at 0955. During the traverse from 0916 to 0955, the maximum NO concentrations (14 pphm) were observed near the western shore of the Bay. The NO concentration decreased continuously during this traverse until the NO concentrations reached a plateau of about 6 pphm near the eastern shore of the Bay. The concentration of NO<sub>2</sub> appeared stable at 5 pphm throughout this traverse.

The wind flow pattern changed from an east wind to onshore winds with a southerly component at about 1000. The houseboat proceeded south to the San Mateo Bridge in order to use bridge auto traffic as a pollution source. A tetroon was launched at 1135, and the run was terminated by the houseboat laboratory at 1220. The trajectory of the tetroon, as illustrated in Figure 7 (f), was to the west until a period of stagnation occurred at 1156 and lasted until 1208. When the tetroon began moving again, the wind direction had shifted, causing the tetroon to move toward the south as shown in Figures 7 (f) and 7 (g). Although short-term variations in pollutant concentrations were observed, which indicate some inhomogeneity of the air over the sample path, no gross inhomogeneities were observed during this tetroon run.

A summary of 5-minute averages of pollutant concentrations observed by the houseboat during the tetron run is given in Table E-6. The

Table E-6

HOUSEBOAT DATA FOR 25 OCTOBER 1972, 1135 TO 1215 PST  
(5-Minute Averages)

Time	NO (pphm)	NO <sub>2</sub> (pphm)	O <sub>3</sub> (pphm)	CO (ppm)	THC (ppm)	Nephelometer (m <sup>-1</sup> × 10 <sup>4</sup> )	CN (cm <sup>-3</sup> × 10 <sup>-3</sup> )
1135	5.3	5.9	2.3	5.7	2.2	0.6	3.5
1140	4.5	5.8	2.7	5.1	2.1	0.6	5.1
1145	4.4	5.4	2.8	5.4	2.1	0.6	13.7*
1150	6.0	5.7	3.1	5.6	2.1	0.5	21.7*
1155	11.8*	7.3	3.3	5.9	2.1	0.6	19.2*
1200	22.3*	7.5	3.6	5.5	2.1	0.5	12.9*
1205	8.8	5.6	3.8	5.7	2.1	0.6	8.6
1210	4.6	4.9	3.9	5.5	2.0	0.5	6.4
1215	1.95	5.2	3.9	5.8	2.0	0.5	3.4

\* Exhaust gas contamination.

relative pollutant concentrations, particularly the NO to NO<sub>2</sub> ratio indicate the presence of well-aged smog, even though the tetron run was begun downwind of the San Mateo Bridge. The source of pollutants is probably auto exhaust from the East Bay or South Bay. The emissions from automobiles on the San Mateo Bridge were not great enough to significantly alter the pollutant mixture.

During the 1135 tetron run, supplementary pollutant measurements were also obtained with the helicopter to determine horizontal and vertical concentration gradients (the flight path may be found in Figure 9). The measurements obtained by the houseboat and helicopter are summarized in Table E-7 for the first 10 minutes of the tetron run.

Table E-7

DATA FOR 25 OCTOBER 1972, 1137 TO 1148 PST  
(1-Minute Averages)

Houseboat				Helicopter					
Time	NO (pphm)	NO <sub>x</sub> (pphm)	O <sub>3</sub> (pphm)	Time	Alt (ft)	NO (pphm)	NO <sub>x</sub> (pphm)	O <sub>x</sub> (pphm)	Temp (°C)
1137	5.6	11.9	2.3	1137	200	4.8	9.6	1.8	24.2
1140	5.3	11.9	2.3	1140	300	5.0	10.0	1.7	24.2
1142	4.5	11.6	2.7	1142	350	2.4	4.8	2.0	24.2
1148	4.9	10.7	2.7	1148	500	1.2	4.8	1.8	24.2

The helicopter then flew in a zigzag pattern over the San Mateo Bridge at 500 feet altitude until the east shore of the Bay was reached to determine concentration gradients of the source of pollution immediately upwind of the release point of the tetroon. An increase of about 1 pphm was noted in NO concentration following the initial crossing of the San Mateo Bridge followed by a decrease of about 1 pphm. As the eastern shore was reached, the NO and NO<sub>x</sub> concentrations had increased to 3.6 pphm and 6.0 pphm, respectively. During the return travel crossing over and nearly parallel to the San Mateo Bridge, a peak concentration of 7.2 pphm of NO and 9.6 pphm of NO<sub>x</sub> was observed. The helicopter returned to the tetroon at 1212 and began circling the tetroon.

The houseboat and helicopter measurements for the latter part of the tetroon run are summarized in Table E-8. The helicopter continued to track the tetroon until the tetroon went aground at 1248.

The helicopter measurements correlate reasonably well with the concentrations observed on the houseboat. The gradients in pollutant concentration are not marked in either the vertical or horizontal during this afternoon run. The measurement from the helicopter indicates that the pollutant concentrations decreased until near background levels were

Table E-8

DATA FOR 25 OCTOBER 1972, 1210 TO 1258 PST  
(1-Minute Averages)

Houseboat					Helicopter					
Time	NO (pphm)	NO <sub>x</sub> (pphm)	O <sub>3</sub> (pphm)	Temp (°C)	Time	Alt (ft)	NO (pphm)	NO <sub>x</sub> (pphm)	O <sub>x</sub> (pphm)	Temp (°C)
1210	6.8	13	3.9	24.4	1210	500	4.8	7.2	2.2	24.4
1212	6.4	12.3	3.5	24.1	1212	500	7.2	9.6		24.4
1215	2.9	8.9	3.9	23.8	1215	500	3.6	3.6	2.8	24.4
					1225	500	1.5	7.0	3.2	24.3
					1230	500	1.0	1.5	2.2	24.3
					1235		1.0	1.5	1.8	24.3
					1240		1.0	2.0	1.7	24.3
					1245		1.0	2.0	2.0	24.4
					1258		1.5	2.5	2.0	24.4

reached after the houseboat had terminated the run. An increase in NO and NO<sub>x</sub> occurred at the end of the helicopter track with a reduction in tetron altitude. Helicopter measurements for 25 October are shown in Table E-9.

After termination of the tetron run, the houseboat had proceeded northward about 1 kilometer when the NO concentrations abruptly increased from about 5 pphm to concentrations as high as 45 pphm. The 5-minute averages for NO concentrations are summarized in Table E-10. The path of the houseboat is shown in Figure 7 (f). This concentration mapping procedure again indicates the inhomogeneity of pollutant distributions over the Bay.

The relative high concentration of NO observed from 1230 to 1250 over a distance of about 5 kilometers was not accompanied by an increase in CO, THC, or CN. On the basis of meteorological observation from shore stations and the houseboat, this "pocket" of high NO concentrations could not be attributed to the emissions from the power plants located at

Table E-9

## HELICOPTER MEASUREMENTS FOR 25 OCTOBER 1972

<u>Time</u> <u>(PST)</u>	<u>Altitude</u> <u>(ft)</u>	<u>CO*</u> <u>(ppm)</u>	<u>Ox</u> <u>(pphm)</u>	<u>Temp</u> <u>(°C)</u>	<u>NO</u> <u>(pphm)</u>	<u>NO<sub>x</sub></u> <u>(pphm)</u>
Measurements made while <u>following tetroom:</u>						
0808				24.0	33	40
0810				24.1	18	22
0812	100			24.0	22	26
0814	190			24.0	22	26
0818	380			24.1	11	15
0824	600			24.0	7	11

Vertical concentration gradient  
measurements near San Mateo Bridge:

0831	100			24.0	44	58
0832	130			24.0	29	51
0833	170			24.1	18	36
0834	220			24.0	11	22
0835	300			24.0	18	18
0837	400			23.9	11	15
0839	590			23.9	11	15
0840	720			24.0	7	7
0843	1400			24.0	3	7
0845	2420			24.0	7	7
0849	4820			23.8	7	7

Measurements made while  
following tetroom:

1137	200		6.6	24.2	5	10
1140			4.0	24.2	6	12
1142	350			24.2	2	5
1143				24.2	2	2
1148	500			24.2	1	2

Table E-9 (Concluded)

<u>Time</u> <u>(PST)</u>	<u>Altitude</u> <u>(ft)</u>	<u>CO*</u> <u>(ppm)</u>	<u>Ox</u> <u>(pphm)</u>	<u>Temp</u> <u>(°C)</u>	<u>NO</u> <u>(pphm)</u>	<u>NO<sub>x</sub></u> <u>(pphm)</u>
<u>Horizontal concentration gradient measurements:</u>						
1150	500		2.3	24.2	1	2
1155	500		2.3	24.2	2	4
1200	500	↑	3.1	24.2	4	6
1205	500	±0.5	2.1	24.2	5	6
1210	500	↓	2.2	24.3	5	7
1212	500			24.4	7	10
<u>Measurements made while following tetraon:</u>						
1216	500	↑	2.8	24.4	4	4
1224	500	↑	3.2	24.3	2	4
1228	500	±0.5		24.3	2	2
1233	500	↓	1.8	24.3	2	3
1238	500	↓		24.4	2	4
1243		+1	2.0	24.3	4	4
1247		↓		24.4	4	4

\*The number is the CO concentration change over the indicated time interval.

Table E-10

HOUSEBOAT DATA FOR 25 OCTOBER 1972, 1220 TO 1255 PST  
(5-Minute Averages)

<u>Time</u>	NO (pphm)	Position*	
		<u>X</u>	<u>Y</u>
1220	5.2	13.366	14.132
1225	19.4	13.128	16.914
1230	28.8	12.991	15.696
1235	39.3	12.853	16.478
1240	32.4	12.716	17.260
1245	26.5	12.578	18.042
1250	17.6	12.355	18.751
1255	6.7	12.925	19.388

\*The grid coordinate overlay map is found in Appendix D, Figure D-1.

Potrero Point and Hunters Point. The ozone concentrations observed in this area increased to a maximum of 5.3 pphm, an indication of aging within the air mass. A corresponding increase in NO<sub>2</sub> from 4.4 pphm to a maximum of 8.2 pphm confirms the aging of the air mass. The source must be attributed on a meteorological basis to auto traffic on the San Mateo Bridge, a contribution from the East Bay, or both. However, the area of this "pocket" and the concentration of pollutants (particularly NO) within it are much higher than would be anticipated. Pollutant measurements from other days, 21 September and 2 November, indicate that the emissions from the Bay Bridge and the San Mateo Bridge are observed within 1 to 2 kilometers of the line source of the bridges before dissipating to background concentrations.

Aerosol particle counter (APC) data were also collected on 25 October and are summarized in Figure 12; the chemical analyses of the particulate matter collected on a high-volume filter may be found in Table 5 or Table C-4. In contrast to the APC data for 21 September, the particle size

distribution did not change with time during the tetraon run on 25 October. However, the meteorological conditions were very different, since hot, dry air from the southeast was blowing across the Bay. On the other hand, the chemical analysis of the collected particulate is similar to that collected on other days, notably 2 November and 6 November (see Appendix C, Table C-4 for complete data) when substantial amounts of marine air were sampled.

The low molecular weight of hydrocarbon distribution for 25 October for low molecular weight nonmethane hydrocarbons is summarized as follows:

<u>Time</u> <u>(PST)</u>	<u>Ethylene</u> <u>(ppb)</u>	<u>Ethane</u> <u>(ppb)</u>
0849	23	119
1002	26	26
1035	23	21

The C<sub>4</sub> to C<sub>10</sub> hydrocarbon distribution for 25 October at 1029 is summarized in Table E-11; a range of concentrations of typical auto exhaust is included for reference.

The cryogenic sample that was collected at 0845 on 25 October is primarily unreactive hydrocarbons. The ratio of ethylene to ethane is 1.0 in contrast to fresh exhaust where the ratio ranges from 3 to more than 10. The higher molecular weight olefins are present in low concentrations. The C<sub>9</sub>-C<sub>10</sub> aromatic fraction seems to be unusually high and probably contains unresolved higher molecular weight paraffins.

#### C. 26 October

October 26 was selected for analysis not because of extensive photochemical activity, but to illustrate the dispersion of pollutants and the dilutional processes that are observed in complex wind flow patterns. Measurements were made immediately downwind of San Francisco (SF) from 0816 until 0906 along a 3.7-kilometer path parallel to the shore. High

Table E-11

## CRYOGENIC TRAP DATA 25 OCTOBER 1972, 0845 PST

Hydrocarbon Class	Concentration		Typical Exhaust Range (%) <sup>10</sup>
	ppb C	%	
<u>Olefins</u>			
Ethylene	18	1.2	12-13
Acetylene	21	1.4	9-11
C <sub>4</sub> -C <sub>5</sub>	23	1.6	4-6
C <sub>6</sub> -C <sub>7</sub>	13	0.9	1
C <sub>8</sub> -C <sub>10</sub>	2	0.1	1
Subtotal	77	5.3	25-30
<u>Paraffins</u>			
Ethane	18	1.2	0-2
Propane	15	1.0	1-2
C <sub>4</sub> -C <sub>5</sub>	523	35.9	8-12
C <sub>6</sub> -C <sub>7</sub>	274	18.8	6-14
C <sub>8</sub> -C <sub>10</sub>	179	12.3	7-13
Subtotal	1009	69.3	30-40
<u>Aromatics</u>			
Benzene	34	2.3	2-3
Toluene	80	5.5	5-6
Ethyl Benzene	20	1.4	1-2
m-,p-Xylene	71	4.9	6-8
o-Xylene	38	2.6	3-7
C <sub>9</sub> -C <sub>10</sub>	127	8.7	14-18
Subtotal	370	25.4	30-45
TOTAL	1456		

pollutant concentrations were measured while stopped and headed into the wind, and while underway; there was no evidence of exhaust contamination from the houseboat. Extreme spatial and temporal variability was observed in pollutant concentrations, particularly the nitrogen oxide concentrations downwind of San Francisco. The variability of the concentrations of the nitrogen oxides at distances up to 1 kilometer downwind of the urban source reflects the multiplicity of sources in the city and shows that mixing to a relatively homogeneous state has not yet been completed. The observed inhomogeneities indicate that sampling runs to determine mass balance must be initiated at a sufficient distance from the urban source to ensure that a homogeneous air mass is studied, or else that the measurement program should include observations spaced horizontally, vertically, and temporally so that accurate estimates can be made of pollutant fluxes.

Pollutant concentrations, other than  $\text{NO}_x$ , also varied in this area, but their variability was considerably less than the nitrogen oxides. Table E-12 indicates the range of observed concentrations at several locations and along a 1.4 kilometer-segment of the boat's path.

Small helium-filled balloons were used to determine wind direction prior to the tetroon launch. Extrapolation of the paths of the small balloons indicated a sampling track north of Treasure Island (TI) and toward San Pablo Bay. The tetroon was launched at 0906 and passed directly over TI. Figure 13 shows the streamlines during the sampling interval and the path of the mobile laboratory. The average wind velocity was from 230 degrees at 5.3 m/sec along tetroon trajectory between the point of release and TI. Over this interval the concentration of NO dropped very rapidly from 40 to 11.5 pphm.

At 0912 the houseboat began a high-speed run around TI to intercept the tetroon on the eastern side. The tetroon rapidly ascended from 75

Table E-12

HOUSEBOAT DATA FOR 26 OCTOBER 1972, 0656 TO 0704 PST

Time (PST)	Location	Houseboat Operational Mode	Pollutant Concentrations					
			NO (pphm)	NO <sub>2</sub> (pphm)	O <sub>3</sub> (pphm)	CO (ppm)	THC (ppm C)	Nephelometer (m <sup>-1</sup> × 10 <sup>4</sup> )
0656 to 0700	100 meters north of west end of Bay Bridge	Stopped	23-30	2.9- 8.0	0.8-2.7	1.3-2.4	--	--
0716 to 0719	200 meters south of west end of Bay Bridge	Stopped	23-50	2.9-17.0	1.6-4.7	1.3-2.4	2.6-3.4	0.7-0.9
0815 to 0817	Foot of Ferry Building, SF	Stopped	21-34	2.9-11.5	4.7-5.5	0.75-1.7	2.3-2.6	0.8-0.8
0700 to 0704		Underway	23-50	2.9-17.0	1.6-4.7	1.3-2.4	2.6-3.4	0.7-0.4

to 270 meters altitude as it passed over TI and then descended to 200 meters altitude at the point of interception. During the high-speed run around TI, exhaust gas contamination from the houseboat or from the helicopter was not possible, but the measured pollutant concentrations nevertheless varied considerably as shown in Table E-13.

Table E-13

POLLUTANT CONCENTRATIONS DURING HIGH-SPEED RUN  
AROUND TREASURE ISLAND  
(1-Minute Averages)

Time (PST)	NO (pphm)	NO <sub>2</sub> (pphm)	O <sub>3</sub> (pphm)	CO (ppm)	THC (ppm)	Nephelometer (m <sup>-1</sup> × 10 <sup>4</sup> )	CN (cm <sup>-3</sup> × 10 <sup>-3</sup> )
0911	33.4	1.7	5.1	4.17	2.3	0.7	33.4
0912	43.1	3.7	5.5	2.76	2.3	0.5	21.9
0913	15.4	3.7	5.8	1.41	2.1	0.75	15.8
0914	17.7	3.3	5.9	1.73	2.2	0.7	12.3
0915	11.3	2.9	5.9	2.25	2.2	0.7	12.5
0916	9.9	2.5	5.3	2.53	2.3	0.8	18.8
0917	11.5	4.1	4.8	1.45	2.4	0.8	32.8
0918	6.0	2.9	5.1	1.27	2.4	0.8	28.9
0919	1.3	2.7	5.1	1.27	2.3	0.8	28.6

The observed changes in pollutant concentration during this period are probably indicative of the "boundary" between the polluted air from the San Francisco urban source and the clean marine air flowing through the Golden Gate. Of course, this is not a discrete boundary, but is instead marked by irregularities and consequent concentration fluctuations.

The helicopter was in operation during 26 October; however, the nitrogen oxides instrument was damaged by the helicopter vibration. The measured changes in total oxidant and CO concentration as measured along horizontal helicopter flights did not exceed ± 1 pphm for total oxidant or ± 1 ppm for CO. This is comparable to the gradients observed on the houseboat mobile laboratory. Since minimal data were obtained on this flight, the measurements or flight path are not presented here.

A cryogenic sample for HC distribution was obtained and analyzed by high resolution gas chromatography. The concentration of HC by class is shown in Table E-14. The cryogenic sample collected at 0929 on 26 October is primarily unreactive hydrocarbons. The ratio of ethylene to ethane is about 0.9, indicating well-aged pollutants rather than fresh exhaust. The C<sub>9</sub>-C<sub>10</sub> aromatic fraction seems to be high and probably contains unresolved higher molecular weight paraffins.

D. 2 November

The tetroon release from 1123 to 1317 has been selected for additional analysis because it is an example of nearly ideal meteorological conditions. When the houseboat left OP, a slow traverse was made across the Bay to map the pollutants and winds. The houseboat was purposely sailed into the wind during the traverse, and this heading was maintained while 5-minute pollutant averages and meteorological observations were made. The NO concentrations measured during the traverse (Figure 18) were extremely high; values above 0.6 ppm were observed in the middle of the Bay. There is little chance that these measurements could result from houseboat exhaust. The NO<sub>2</sub> and O<sub>3</sub> concentrations at the same point were about 5 and 1.5 pphm and the NO to NO<sub>2</sub> ratio was greater than 10, suggesting that the smog was not well aged. If the pollutants had been generated at San Jose the night (or day) before and was therefore well aged, a lower NO to NO<sub>2</sub> ratio would be expected.

To determine the source of this air mass, the early morning meteorological observations were considered. Surface winds on the east side of the Bay were the typical light drainage type of flow -- that is, east to southeast winds from San Jose to Oakland Airport. South Bay stations observed light to calm conditions from 0000 to 1000. After 1000, the winds were north to northwest and increased until 2100 that evening. The west side showed light easterly onshore winds that persisted through the

Table E-14

## CRYOGENIC TRAP DATA, 26 OCTOBER 1972, 0929 PST

<u>Hydrocarbon</u> <u>Class</u>	<u>Concentration</u>	
	<u>ppb C</u>	<u>%</u>
<u>Olefins</u>		
Ethylene	21	1.3
Acetylene	< 1	0.1
C <sub>3</sub> -C <sub>5</sub>	7	0.6
C <sub>6</sub> -C <sub>7</sub>	23	1.8
C <sub>8</sub> -C <sub>10</sub>	< 1	0.1
Subtotal	53	4.3
<u>Paraffins</u>		
Ethane	23	1.8
Propane	< 1	0.1
C <sub>4</sub> -C <sub>5</sub>	398	31.9
C <sub>6</sub> -C <sub>7</sub>	223	18.0
C <sub>8</sub> -C <sub>10</sub>	199	16.0
Subtotal	844	67.8
<u>Aromatics</u>		
Benzene	56	4.5
Toluene	88	7.1
Ethyl Benzene	24	1.9
m-,p-Xylene	78	6.2
o-Xylene	5	0.4
C <sub>9</sub> -C <sub>10</sub>	100	8.0
Subtotal	351	28.2
TOTAL	1247	

night and morning hours. The winds were calm or light in the Oakland area; northwesterly winds at Alameda and northeasterly winds at Oakland were observed. In San Francisco the winds were also calm or light, with the general northerly direction characteristic of marine air flow. The Oakland rawinsonde for 0400 shows a light north wind at 600 meters and northeast winds above. The San Jose rawinsonde for 0700 showed light variable winds; the 1200 release showed uniformly northerly winds. In summary, there was a general counterclockwise air circulation around the South Bay and a clockwise circulation in the North Bay.

The cloud cover (stratus) observations are the most revealing of the available data. The overcast layer of stratus -- typical in the Bay Area of strong marine air flow -- moved southward through San Francisco during the previous evening and the early morning hours to an area immediately south of a line between San Francisco and Oakland Airports. This is the approximate sample path of the houseboat transect (0830 to 0954). South of this line the Bay was clear throughout the period. These data are evidence of a general northwesterly air flow on the upper half of the Bay. Therefore, the source of the high NO concentrations is most likely San Francisco, and not San Jose.

The possible contribution from the PG&E power plants emissions was calculated using the method described for 21 September. These calculations showed that the maximum concentration of NO attributable to the stacks in the middle of the Bay is about 5 pphm.\* Based on the meteorological data, the source of the pollution observed in the early morning is probably San Francisco, but the very high NO levels cannot be satisfactorily explained.

At 1124 a tetroon was released from a point midway between the Oakland Airport and San Francisco Airport. The surface wind was NNW at 2.2 m/sec. The

---

\*This calculation assumed a mixing height of 150 meters, stability class 2, and a 4-mph northwest wind.

tetroon rose to an estimated altitude of 150 meters but scarcely moved for about 40 minutes. The winds throughout the Bay Area shifted suddenly and the stronger marine air flow carried the tetroon south of the San Mateo Bridge. Selected 5-minute averages are tabulated in Table E-15.

Table E-15

HOUSEBOAT DATA FOR 2 NOVEMBER 1972, 0846 TO 1244 PST  
(5-Minute Averages)

<u>Time</u>	<u>NO</u> (pphm)	<u>NO<sub>2</sub></u> (pphm)	<u>O<sub>3</sub></u> (pphm)	<u>CO</u> (ppm)	<u>THC</u> (ppm)	<u>Nephelometer</u> (m <sup>-1</sup> × 10 <sup>4</sup> )	<u>CN</u> (cm <sup>-3</sup> × 10 <sup>-3</sup> )
0846	4.5	4.2	4.4	1.9	2.8	1.7	13.1
0911	50.8	3.5	1.2	1.5	2.7	1.2	23.5
0926	60.7	5.2	1.5	1.2	3.0	1.3	23.4
0941	20.3	6.0	1.3	2.1	3.4	1.2	29.8
0956	16.5	9.9	1.5	1.1	2.7	0.9	28.9
1006	20.6	6.8	1.6	3.7	2.9	1.1	34.4
1026	14.6	9.1	1.9	4.0	2.7	1.1	34.0
1036	10.4	8.9	2.3	2.3	2.7	1.2	29.4
1109	3.6	7.0	3.5	3.7	3.3	1.3	15.4
1114	2.9	7.1	3.5	3.7	2.8	1.1	11.5
1119	7.0	7.8	3.8	2.9	2.8	1.4	16.2
1124*	9.6	7.9	3.8	5.1	3.3	1.5	29.2
1128	15.1	7.9	3.8	4.5	3.2	1.4	16.4
1154	35.2	6.8	5.0	5.4	3.6	1.3	12.8
1219	4.3	7.8	5.0	5.2	4.5	1.3	18.3
1244	1.0	5.2	5.9	3.4	4.2	1.2	11.3

\*Tetroon release

The wind measurements made on board between 0830 and 1043 were used in an attempt to determine the original of the air mass into which the 1124 tetroon was released. The best estimate is that the houseboat circled around this air mass between 0944 and 1040 but did not pass directly through it. The 5-minute averages in Table E-15 from 0846 to 1036 were obtained while the houseboat was in motion, thereby minimizing the chances of exhaust contamination. The variability of NO, NO<sub>2</sub>, THC, and CO suggests that the pollutant mixture is by no means homogeneous.

The rise of NO concentration immediately following the tetraon release (1124) was accompanied by an increase in CO concentration and sporadic increases in CN concentration. The presence of all three components are strong evidence of contamination due to houseboat exhaust. In an attempt to avoid the exhaust, a helium-filled balloon was tethered at the base of the sample inlet mast. By its position relative to the houseboat's path, the vector sum of the surface wind and the relative wind due to the boat's motion could be estimated by the position of the tethered balloon. The tethered balloon was kept on the side or stern of the boat so that raw exhaust was not pulled into the sampling lines. However, it was not possible to avoid passing through old exhaust because it was necessary to sail in circles or figure eights to stay under the tetraon. Thus, fresh but not raw exhaust was sampled from about 1130 to 1210. Therefore, the NO concentrations observed during the experiment (Figure 14, from 0 to 30 minutes) are not representative of polluted air during that interval.

The data collected immediately prior to the tetraon release (1109 to 1119, Table E-15) are probably representative of the NO concentrations that would have been measured if the houseboat exhaust had not contaminated the air. The data suggest that, based on the low NO to NO<sub>2</sub> ratio, the air mass was well aged.

A limited amount of hydrocarbon distribution data are available for the tetraon release. The C<sub>2</sub> data are summarized in Table E-16; the concentration of propylene was below the detectability limit.

Table E-16

ETHANE, ETHYLENE, AND ACETYLENE CONCENTRATIONS,  
2 NOVEMBER 1972

Time (PST)	Concentration (ppb)			
	$C_2H_6$	$C_2H_4$	$C_2H_2$	$C_3H_8$
0848	22	47	< 1	< 1
0901	38	< 1	< 1	< 1
0946	136	127	31	18
0959	106	117	< 1	< 1
1030	77	141	36	42
1120	187	527	38	37

A leak in the sampling line occurred between 1030, the end of the run, which permitted the HC inlet system to sample some cabin air which was contaminated with ethylene from the  $O_3$  analyzer. It was not discovered and stopped until after the run. The  $C_2-C_3$  hydrocarbon data are not reliable after 1030 on 2 November 1972. Cryogenic samples were also collected at 0925 and 1100 (Table E-17). The 0925 sample is mainly unreactive hydrocarbons. The ratio of ethylene to ethane is 0.84 whereas typical ratios for fresh exhaust range from 3 to more than 10. The percentage of higher olefins is also relatively low. The  $C_9-C_{10}$  aromatic fraction seems to be too high since these compounds are generally more reactive than the  $C_6-C_8$  aromatics. The fraction probably contains some higher paraffins that were not separated by our GC method. The 1100 hydrocarbon sample is also suggestive of partially aged smog. The ethylene to ethane ratio is 1.8. The biggest change is the 5 percent shift from aromatics to olefins plus the lower overall concentration (THC analyzer values averaged 3.0 and 2.4 ppm C, respectively). We conclude that the 1100 sample is fresher and more reactive than the 0925 sample.

The particulate data are discussed in the text of this report.

Table E-17

## CRYOGENIC TRAP DATA, 2 NOVEMBER 1972

Hydrocarbon Class	Concentration			
	0925 PST		1100 PST	
	ppb C	%	ppb C	%
<u>Olefins</u>				
Ethylene	127*	4.44	141†	10.80
Acetylene	31*	1.08	36†	2.75
C <sub>4</sub> -C <sub>5</sub>	36	1.26	3.5	0.31
C <sub>6</sub> -C <sub>7</sub>	61	2.13	17	1.30
C <sub>8</sub> -C <sub>10</sub>	1	0.05	< 1	0.08
Subtotal	265	8.97	199	15.24
<u>Paraffins</u>				
Ethane	136*	4.76	77†	5.90
Propane	18*	0.63	42†	3.22
C <sub>4</sub> -C <sub>5</sub>	189	6.61	178	13.64
C <sub>6</sub> -C <sub>7</sub>	250	8.74	58	4.44
C <sub>8</sub> -C <sub>10</sub>	453	15.84	103	7.89
Subtotal	1046	36.59	458	35.10
<u>Aromatics</u>				
Benzene	47	1.64	10	0.77
Toluene	144	5.04	27	2.07
Ethyl Benzene	170	5.95	17	1.30
m-, p-Xylene	130	4.55	53	4.06
o-Xylene	54	1.89	29	2.22
C <sub>9</sub> -C <sub>10</sub>	1012	35.40	512	39.23
Subtotal	1557	54.46	648	49.66
TOTAL	2859		1305	

\* C<sub>2</sub>-C<sub>3</sub> data from 0946† C<sub>2</sub>-C<sub>3</sub> data from 1030

Appendix F

AIHL REPORT NO. 148 BY THE AIR RESOURCES BOARD



CHEMISTRY OF THE AEROSOL  
FOR THE SRI HOUSEDOAT PROJECT

Final Report

June 1973

AIHL Report No. 148

Prepared by:

S. Wall  
J. J. Wesolowski

Supported by:

Air Resources Board  
Contract 2-442

Air and Industrial Hygiene Laboratory  
California State Department of Public Health  
2151 Berkeley Way, Berkeley, CA 94704  
June 1973

## I. Introduction

This is the final report of the aerosol chemistry work carried out by AIHL in cooperation with the Stanford Research Institute as part of the SRI Houseboat feasibility study. This report details AIHL's role in the experiment, and presents and discusses the aerosol chemical data obtained.

## II. The Role of AIHL in the Sampling Scheme

AIHL provided consultation, technical assistance, gas analyzer calibrations and performed chemical analysis of aerosols collected by SRI as part of the Houseboat Project. Dr. James Hart Smith of SRI consulted with the AIHL gas calibration group concerning calibration of their gas analyzers. AIHL calibrated the houseboat gas instruments on the day of the final SRI run. Dr. Smith and others of the SRI staff consulted with AIHL to learn the procedures for preparing and loading the Lundgren Impactor foils provided by AIHL. All filters and foils were washed and handled by SRI personnel subsequent to their return to AIHL for chemical analysis. Drs. Wesolowski and Appel participated in a houseboat run as observers and consultants.

## III. Sampling Configuration on the Houseboat

The aerosol was collected by a probe separate from the gas probe. The flow characteristics were similar to probes used in the 1972 Aerosol Characterization Study (ACHEXI). The aerosol collection probe had a Reynolds number of 8,900 at 13 CFM and consisted of PVC tubing two and one-half inches in diameter. The Lundgren Impactor was mounted at a 45° angle to the inlet probe. This rather large angle was

necessary because of physical constraints on the boat. The impactor consisted of five stages and an after filter. Four stages, 1A, 2, 3 and 4, had impaction surfaces of two-inch strips of Teflon over which one-inch Mylar strips were placed. The stage 1B foil was sticky polyethylene. The after filter was Gelman GA-1 cellulose acetate. The theoretical cut-off points for the stages (cf. AIHL Report No. 137<sup>1</sup>) were as follows:

<u>Lundgren Stage</u>	<u>Effective 50% Cut-Off Diameters in Microns</u>
1-A	8
1-B	8
2	4
3	1.5
4	0.5
AF	< 0.5

#### IV. Aerosol Chemical Analysis Scheme

AIHL provided SRI with five sets of Lundgren foils, and ten after filters for the houseboat experiment. Various problems, including mechanical failures of the impactor and unusual weather, restricted the number of useful runs to those of November 2, November 6 and November 17, 1972. No chemical analysis was performed on the November 17 samples because the sampling was conducted for only one hour. Thus, the area over which the aerosol was collected was too small to be easily handled with the present analytical schemes. The most emphasis is placed on the November 2 run since this is the only day where more than one two-hour size cut was available for analysis.

V. Validation of Chemical Data Reported to SRI by AIHL

In order to determine the validity of the elemental data, inter-method comparisons were carried out on after filters and foils collected during this study.

- a. After Filters: Neutron Activation Analysis (NAA) and X-ray Excited X-ray Fluorescence<sup>2</sup> Analysis (XRFA).

Bromine concentrations were compared on a series of eight randomly selected after filters from the houseboat experiment. There is reasonable agreement between NAA and XRFA (cf. Figure 1A). A regression line was fitted to the points. The slope of this dashed line, shown in Figure 1A, is 0.91 which is not significantly different from 1, i.e., equal concentrations. The largest discrepancy, HB1100 AF, is 15%.

- b. Foils: Alpha X-ray Emission Analysis ( $\alpha$ -XREA)<sup>3</sup> vs X-XRFA

Four elements were compared; bromine, zinc, calcium and iron. Three impactor runs were used for the comparison. For each run, one 2-hour sample was selected from each stage with a Mylar impaction surface. Thus, the comparison was based on 12 foils. For bromine and zinc, lower limits of detection were reported for many samples. For those cases where the results could be compared, the concentrations reported by the two methods agreed within experimental errors. The results for Ca and Fe are shown graphically in Figures 1B and 1C. For these elements the degree of agreement is not acceptable.  $\alpha$ -XREA has in

the past had difficulty with calcium and iron, reporting values higher than those obtained by NAA and XRFA.<sup>4</sup> However, revisions in the  $\alpha$ -XREA prior to analysis of the houseboat samples have greatly improved the agreement between  $\alpha$ -XREA and other methods. Thus, we would have anticipated better agreement.

## VI. Concentrations

Twenty-three chemical species were detected (see Table 1). For consistency in data evaluation XRFA concentrations are reported here. The sulfur, nitrogen and carbon analyses reported were performed by ESCA.<sup>5</sup> Since total filters were not available to AIHL, the total concentrations of chemical species had to be calculated by summing the species concentration for each of the Lundgren stages plus the after filter for each 2-hour sampling segment (see Table 2). Because of small loadings, many lower limits were reported for foil determinations. In calculating the total concentration for a species, lower limits were included in the summations as  $1/2$  the limit of detection  $\pm 100\%$ . The values listed in Table 2 are from three Lundgren runs: 0833 to 1120 and 1123 to 1317 on November 2, 1210 to 1405 on November 6. ESCA sulfur analysis was routinely reported as  $S^+$  (oxidized) and  $S^-$  (reduced) to reduce the time required to interpret typically complex spectra. However, a more detailed study indicated  $SO_4^{-2}$  to be more than 70% of the  $S^+$  listed in Table 2.<sup>11</sup> Analysis for nitrogen and carbon are excluded from this table since ESCA determinations for these species on the after filters is impractical due to the high background of the sampling substrate.

The concentrations for V, Cr, Mn, Fe, Cu, Zn, Se, Br, and Hg can be compared with a nine station study of San Francisco Bay Area aerosols conducted in July 1970.<sup>6</sup> Agreement between the houseboat data and the average for the nine stations of the 1970 study was within a factor of two except for Fe and Cu. Values for Fe listed in Table 2 were at least a factor of six lower and for Cu a factor of three lower than those reported for the 1970 San Francisco Bay Area study. These differences could be the result of a serious impactor bounce-off problem to be discussed in Section VII.

For the houseboat study correlation coefficients were calculated for pairs of the 20 species for the three houseboat sampling periods. The concentrations for each species were ranked and non-parametric correlation coefficients calculated.<sup>7</sup>

Because of the small number of sampling periods, conclusions concerning species pairs with correlation coefficients with absolute value  $< 1$  are not drawn. From Table 3 correlated species fall into three groups as follows:

1. K, Ti, Cr, Mn, Ni
2. Fe, Ca, Zn, Cu
3. Pb, Br

Similar groupings of trace elements have been noted in previous aerosol studies. The cluster analysis used to interpret the data collected in the 1970 San Francisco Bay Area study determined Mn, Cr, and Fe to be

grouped with Al, Se, Ba, La and Sm with high intercorrelations among the group members. Since in the 1970 study these elements exhibited the same diurnal pattern as wind speed and were present in the relative abundances calculated for crustal rock, it was inferred that they were in the particles generated from the soil by the wind. The 1972 Aerosol Characterization Study (ACHEX) Phase 1 report<sup>8</sup> noted similarities in the diurnal pattern of Cr, Mn and Fe concentrations for samples collected at the San Jose BAAPCD station on days when the site was downwind of the San Francisco Bay. Less often, similar diurnal patterns were also reported for Ti, K, Mn, Cr, and Fe.

These elements, with the exception of Fe, are included in Group 1 listed above. The possibility that these elements are found in wind-blown soil particles is reinforced by the lack of positive correlation between elements of Group 1 and the combustion products Br and Pb (Group 3). It is interesting that the houseboat data indicated Fe correlated with other members of Group 2 such as Zn, when both the 1970 San Francisco Bay and 1972 ACHEX studies conclude Fe to be associated with the soil derived elements of Group 1. However, a similarity in the diurnal patterns for Fe and Zn was observed at the ACHEX Harbor Freeway site on particles less than 0.6 microns.<sup>8</sup> This could indicate that the apparent correlation of Fe and Zn seen for houseboat data was due to large wall losses because of the failure of the large soil derived particles, containing the majority of Fe, to stick on the Lundgren stages.

Correlations of Br and Pb (Group 3) concentrations in ambient particles has been well documented.<sup>8,9</sup> Consistencies in diurnal patterns for

these elements were noted for every ACHEX sampling site. Br/Pb ratios have been suggested as a means of distinguishing between aged and fresh automobile combustion aerosol.<sup>8</sup> Br/Pb ratios near 0.39 have been considered fresh aerosol while lower values represent progressively more aged particles based on the removal of bromine from the lead halides found in automobile exhaust. Br/Pb ratios less than .25 and wind patterns for houseboat sampling periods on the afternoon of the second and sixth of February indicate aging aerosol carried by northwesterly winds from the San Francisco vicinity to the south bay.

#### VII. Particle Size Distributions

Particle size distributions for Fe, Ca, Zn, Pb, Br, C, S<sup>+</sup> are shown in Figures 2A through 2F. Distributions for other chemical species were not included because the concentrations were below the limits of detection on most of the Lundgren impactor stages. With the exception of S<sup>+</sup> and C, the species concentrations plotted at "XA+ST" is the sum of the concentrations determined on stages 1A and 1B. The sticky polyethylene substrate used on stage 1B was not analyzed for C or S<sup>+</sup>, thus, the concentrations plotted for C and S<sup>+</sup> at "XA+ST" does not include the contribution from stage 1B. From Figures 2A, 2C and 2E, Pb, Br, C, and S<sup>+</sup> were detected primarily on sub-micron particles for the three sampling periods. This is characteristic of combustion derived aerosol and was observed for Pb and Br in both the 1970 San Francisco Bay Area study and the 1972 ACHEX. The Pb and Br particle distributions are similar (Figures 2A, 2C, 2E). This was also observed in the San Francisco study.

Detailed analysis of the ESCA spectra for S indicates  $S^+$  to be primarily (~ 70%) sulfate on the after filter and almost entirely sulfate on the impactor stages. When  $S^-$  was present in levels above the limit of detection, it was reported to consist of equal amounts of elemental sulfur and sulfide.

Fe and Ca are most often described as soil derived elements to be found on larger particles corresponding to the first stages of the Lundgren impactor. This is considered generally true for San Francisco Bay aerosols.<sup>10</sup> Zn distributions, however, display both large and sub-micron particle concentration maxima.<sup>10</sup> Houseboat distributions (Figures 2B, 2D and 2F) show serious deviations from these findings. No concentration maxima on large particles was observed for Zn, Fe, or Ca. Because of the good correspondence of Br and Pb distributions with previous studies, it is doubtful that analytical errors can be a cause for the discrepancies. It is probable that the bounce-off problem for large particles discussed in AIHL Report No. 138 is of importance here. This problem is inherent in the use of dry impaction surfaces such as those employed for the houseboat sampling and indeed would cause the distributions to be skewed toward the small particle sizes.

#### VIII. Conclusions

The validation study results indicate that quality chemistry was possible on the particulate samples collected on the SRI Houseboat. Although there were only a small number of houseboat samples available to AIHL, agreement with previous S. F. Bay aerosol studies was obtained

for total concentrations for most chemical species measured and for many of the size distributions. The lack of heavy smog days reduced the number of chemical species which could be discussed. Nevertheless, the fact that the concentrations of many species could be obtained and some interpretation given, although very tentative, demonstrates the feasibility of obtaining significant data on the chemical composition of aerosol collected over two-hour intervals using the SRI Houseboat approach. Of course, the lack of secondary aerosol days during the last "smog" season precludes any comments about the feasibility of obtaining information about secondary aerosol formation using this approach.

Suggested changes which could improve the probability of collecting significant data during future houseboat sampling episodes include:

1. The use of sticky surface foils on all stages of the Lundgren impactor in order to substantially reduce the bounce-off of particles.
2. Total filters as well as after filters and impactor foils should be provided for elemental chemical analysis in order to obtain information on wall losses and also to obtain total particulate concentration data of higher accuracy than obtained by summing the stages and after filters.
3. Of course the main improvement is beyond our control, namely an increase in the number of days having significant secondary aerosol.

## References

1. AIHL Report No. 137, B. R. Appel, J. J. Wesolowski, Calibration and Sampling Media Selection Studies with the Lundgren Impactor, Feb. 1973.
2. The NAA was carried out at Lawrence Livermore Laboratory by R. Ragaini and R. Kaifer, and the X-XRFA at Lawrence Berkeley Laboratory by R. Giauque.
3.  $\alpha$ -XREA was performed at the Crocker Nuclear Lab., University of California, Davis by T. Cahill.
4. AIHL Report No. 134, J. J. Wesolowski, S. Wall, and S. Twiss, Interlaboratory Comparisons of Chemical Determinations from Aerosols Collected on Cellulose Filters, Feb. 1973.
5. Electron spectroscopy chemical analysis performed at Lawrence Berkeley Laboratory by T. Novakov.
6. "Trace Element Concentrations in Aerosols from the San Francisco Bay Area", W. John, R. Kaifer, K. Rahn, and J. J. Wesolowski, Atmospheric Environment, Vol. 7, p 107-118 (1973).
7. Spearman's rank order correlation.
8. Characterization of Aerosols in California Interim Report for Phase 1, G. Hidy et al.

9. "Lead and Bromine Particle Size Distributions in the S. F. Bay Area,"  
C. Martens, J. J. Wesolowski, R. Kaifer, W. John. UCRL 74349.
  
10. Particle Size Distributions of S. F. Bay Area Ambient Air Trace  
Elements (Private communication with J. J. Wesolowski and R. Ragaini).
  
11. Detailed Study of ESCA Spectra (Private communication with A. Harker,  
Lawrence Berkeley Laboratory).

Table 1

CONCENTRATIONS OF CHEMICAL SPECIES FOR HOUSEBOAT SAMPLING  
 SAMPLES LISTED WERE FOULS AND FILTERS USED AS COLLECTION MEDIA IN THE HOUSEBOAT LUNDGREN IMPACTOR  
 (Values in  $\mu\text{g}/\text{m}^3$ )

SPECIES	DATE AND TIME 11-2-72 (0833-1120)						DATE AND TIME 11-2-72 (1123-1317)						DATE AND TIME 11-6-72 (1210-1405)					
	HB1001EA	HB1002E2	HB1003E3	HB1004E4	HB1005AF	HB1001EA	HB1002E2	HB1003E3	HB1004E4	HB1005AF	HB1004A F	HB1005EA	HB1007E3	HB1006E2	HB1007X3	HB1008E4	HB1008AF	
	HB1001XA	HB1001ST	HB1002X2	HB1003X3	HB1004X4	HB1001XA	HB1001ST	HB1002X2	HB1003X3	HB1004X4	HB1004, F	HB1005XA	HB1012ST	HB1006X2	HB1007X3	HB1008X4	HB1008AF	
C	< .20	-	.25 (.12)	1.5 (.70)	-	< .20	-	< .20 (.01)	.60 (.30)	-	< .20	< .40	< .20 (.10)	< .20 (.10)	< .20 (.10)	.20 (.10)	-	
S+	< .20	-	< .20	.20 (.10)	-	< .20	-	< .20	.20 (.10)	5 (1.1)	< .20	-	< .20	< .20	< .20	< .20	1.7 (.50)	
S-	< .20	-	< .20	< .20	-	< .20	-	< .20	< .20	< .11	< .40	-	< .20	< .40	< .40	< .40	< .20	
N+	< .40	-	< .40	.45 (.20)	-	< .40	-	< .40	< .40	-	< .40	-	< .40	< .40	< .40	< .40	-	
N-	< .40	-	< .40	.75 (.35)	-	< .40	-	< .40	< .40	-	< .40	-	< .40	< .40	< .40	< .40	-	
K	< .087	< .146	< .087	< .087	HB103AF	HB1001XA	HB1011ST	HB1002X2	HB1003X3	HB1004X4	HB1004, F	HB1005XA	HB1012ST	HB1006X2	HB1007X3	HB1008X4	HB1008AF	
Ca	< .038	< .076	.119 (.015)	.075 (.014)	.050 (.021)	< .039	< .079	.042 (.014)	.056 (.014)	.020 (.013)	.07 (.02)	.025	< .047	.015 (.008)	.083 (.010)	.024 (.008)	.105	
Ti	< .017	< .026	< .017	< .017	.013 (.008)	< .017	< .027	< .018	< .017	< .017	.02 (.01)	.011	.009 (.006)	< .010	< .011	< .011	.044	
V	< .013	< .020	< .012	< .012	< .019	< .013	< .021	< .013	< .012	< .012	< .01	.008	< .013	< .008	< .008	< .008	.034	
Cr	< .010	< .014	< .009	< .010	< .015	< .010	< .015	< .010	< .009	< .010	< .01	.006	< .009	< .006	< .006	< .006	.027	
Mn	< .008	< .011	< .008	< .008	< .012	< .008	< .012	< .008	< .008	< .008	.01 (.01)	.005	< .007	< .005	< .005	< .005	.020	
Fe	< .006	< .010	.100 (.010)	.095 (.010)	.065 (.004)	< .007	.031 (.004)	.012 (.003)	.031 (.003)	.043 (.004)	.11 (.01)	.015 (.002)	.002 (.002)	< .004	.026 (.003)	.012 (.002)	.041 (.007)	
Ni	.003 (.002)	< .006	< .004	.003 (.002)	.005 (.002)	.007 (.002)	< .006	.003 (.002)	.004 (.002)	< .004	.01 (.01)	.003	< .004	< .003	.005 (.001)	.003 (.002)	.006 (.003)	
Cu	.003 (.002)	< .006	.003 (.002)	.005 (.002)	< .009	.004 (.002)	< .006	.005 (.002)	.004 (.002)	< .005	< .01	.004	< .004	< .003	.003 (.002)	.002 (.001)	.014	
Zn	< .006	.013 (.008)	.013 (.002)	.053 (.005)	.020 (.002)	< .006	< .024	< .006	.003 (.002)	.039 (.004)	.01 (.01)	.004	.033 (.005)	< .004	.003 (.002)	.008 (.002)	.013 (.003)	
Ca	< .003	< .005	< .003	< .004	.007 (.003)	< .003	< .005	< .003	< .003	< .003	< .01	.002	< .003	< .002	< .002	< .002	.010	
As	< .003	< .005	< .006	< .010	< .021	< .003	< .005	< .003	< .004	< .007	< .01	.002	< .003	< .002	< .003	< .004	.025	
Se	< .003	< .006	< .003	< .004	.006 (.003)	< .004	< .006	< .004	< .003	< .004	< .01	.002	< .004	< .002	< .002	< .002	.009	
Br	< .004	.005 (.003)	.010 (.003)	.050 (.005)	.244 (.010)	< .004	< .007	< .004	.005 (.002)	.021 (.002)	.01 (.01)	.003	.003 (.002)	< .003	.006 (.001)	.008 (.001)	.250 (.010)	
Rb	< .006	< .012	< .006	< .007	< .010	< .006	< .012	< .006	< .006	< .006	.01 (.01)	.004	.004 (.003)	< .004	< .004	< .004	.017	
Sr	< .003	< .015	< .008	< .008	< .011	< .008	< .015	< .008	< .008	< .008	.01 (.01)	.005	< .009	< .005	< .005	< .005	.019 (.007)	
Hg	< .005	< .009	< .006	< .006	< .010	< .006	< .009	< .006	< .006	< .006	.01 (.01)	.004	< .006	< .004	< .004	< .004	.016	
Pb	< .006	< .009	.084 (.008)	.239 (.024)	1.05 (.040)	< .007	< .010	.006 (.002)	.029 (.003)	.099 (.010)	1.1 (.1)	.004	< .006	< .004	.025 (.003)	.048 (.005)	1.250 (.050)	
37 <sub>TS</sub>	-	-	.357	.209	.232	-	-	-	.172	.212	.37	-	-	.250	.167	.198		

Key:

&lt; Species concentration below the limit of detection.

- No data available.

( ) Error limits enclosed.

TABLE 2

TOTAL CONCENTRATION BASED ON  
SUMS OF IMPACTOR STAGES AND AFTER FILTER \*  
(Values in  $\mu\text{g}/\text{m}^3$ )

Date (Time PST)	11-2-72 (0833-1120)	11-2-72 (1123-1317)	11-6-72 (1210-1405)
S+	1.90 ± .36	1.05 ± .25	2.10 ± .54
S-	.50 ± .22	.48 ± .21	.50 ± .22
K	.46 ± .12	.50 ± .12	.37 ± .09
Ca	.345 ± .054	.25 ± .057	.21 ± .055
Ti	.060 ± .023	.070 ± .025	.053 ± .025
V	.039 ± .014	.048 ± .021	.039 ± .020
Cr	.034 ± .014	.038 ± .016	.030 ± .016
Mn	.028 ± .012	.032 ± .012	.024 ± .012
Fe	.272 ± .016	.234 ± .011	.105 ± .008
Ni	.021 ± .005	.052 ± .006	.018 ± .004
Cu	.021 ± .006	.020 ± .009	.016 ± .007
Zn	.105 ± .011	.101 ± .014	.061 ± .007
Ga	.016 ± .004	.013 ± .006	.011 ± .006
As	.024 ± .012	.024 ± .014	.020 ± .013
Se	.012 ± .005	.022 ± .006	.010 ± .005
Br	.033 ± .012	.024 ± .010	.020 ± .010
Rb	.024 ± .010	.027 ± .010	.021 ± .009
Sr	.030 ± .013	.036 ± .012	.033 ± .010
Hg	.021 ± .009	.023 ± .010	.019 ± .009
Pb	1.38 ± .050	1.24 ± .050	1.34 ± .050

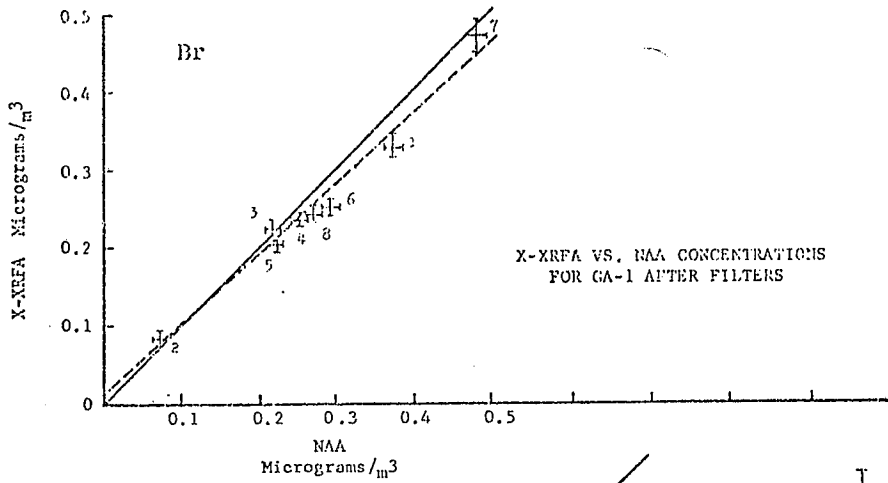
\*

In calculating the total concentration the determinations below the limit of detection were included in the summations as 1/2 the limit of detection ± 100%.

The sums of the errors were calculated as the square root of the sum of the squares of each error.

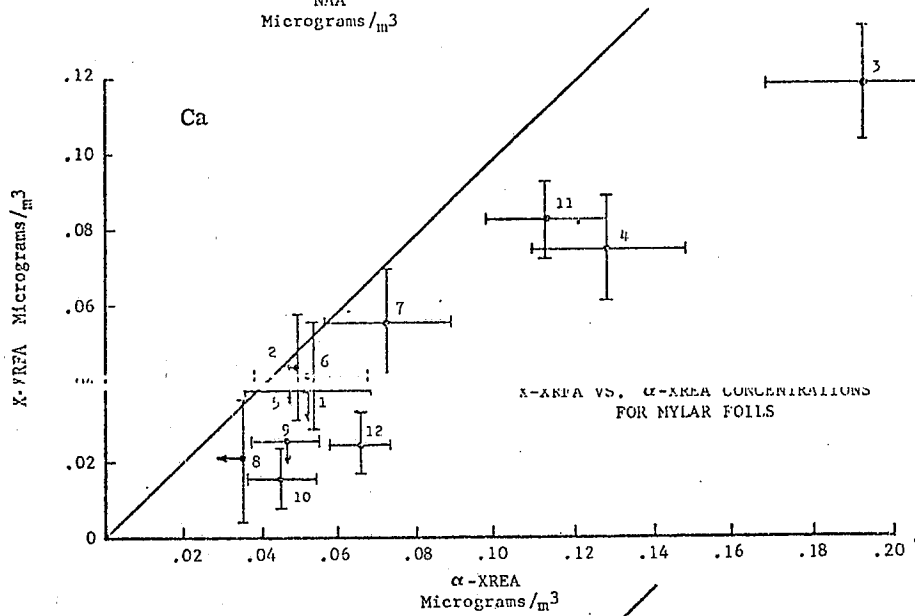


Figure 1A



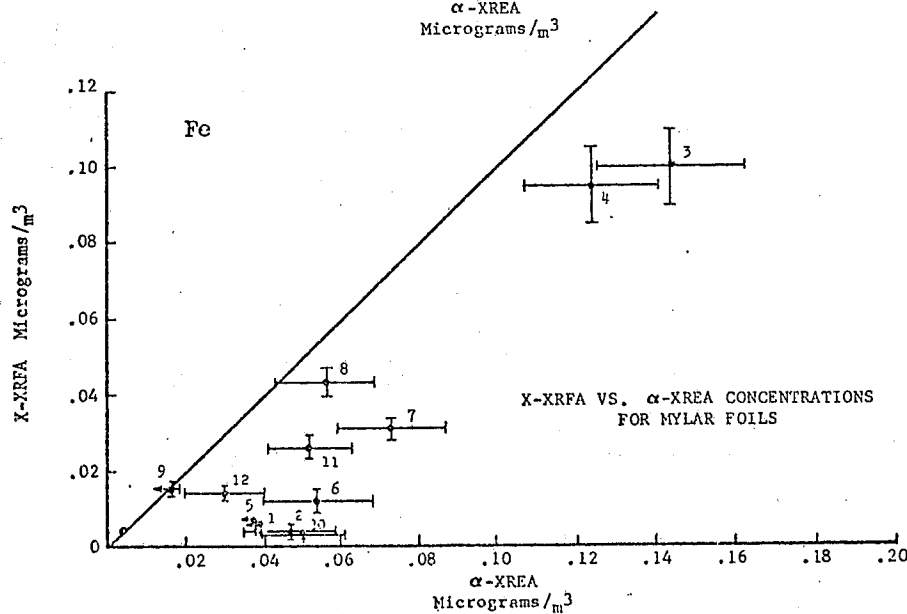
1. HB1100AF
2. HB1101AF
3. HB1107AF
4. HB1103AF
5. HB1104AF
6. HB1105AF
7. HB1106AF
8. HB1108AF

Figure 1B



- 0910-1100
1. HB1001XA
  2. HB1002X2
  3. HB1003X3
  4. HB1004X4
- 1117-1317
5. HB1001XA
  6. HB1002X2
  7. HB1003X3
  8. HB1004X4
- 1210-1405
9. HB1005XA
  10. HB1006X2
  11. HB1007X3
  12. HB1008X4

Figure 1C



- 0910-1100
1. HB1001XA
  2. HB1002X2
  3. HB1003X3
  4. HB1004X4
- 1117-1317
5. HB1001XA
  6. HB1002X2
  7. HB1003X3
  8. HB1004X4
- 1210-1405
9. HB1005XA
  10. HB1006X2
  11. HB1007X3
  12. HB1008X4

({ indicates concentration below the limit of detection)

PARTICLE SIZE DISTRIBUTIONS FOR HOUSEBOAT SAMPLING

(↓ indicates concentration below the limit of detection)

November 2, 1972  
0833-1120 Hrs. PST

November 2, 1972  
1123-1317 hrs. PST

November 6, 1972  
1210-1405 hrs. PST

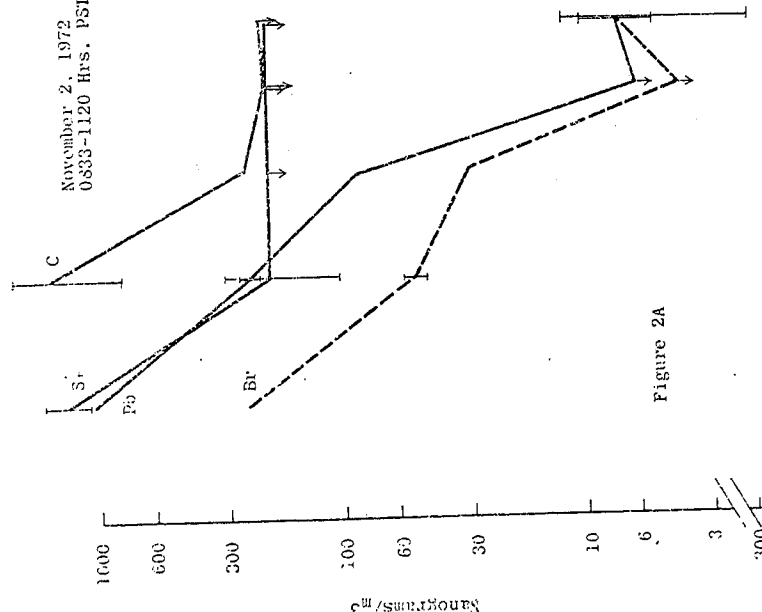


Figure 2A

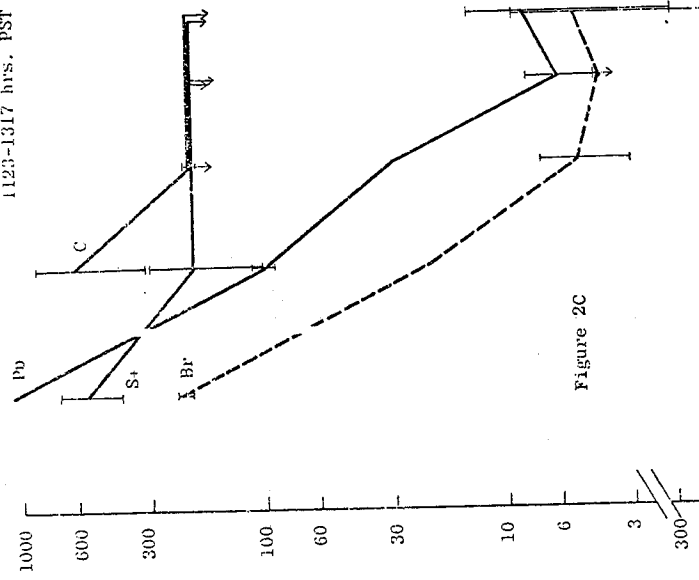


Figure 2C

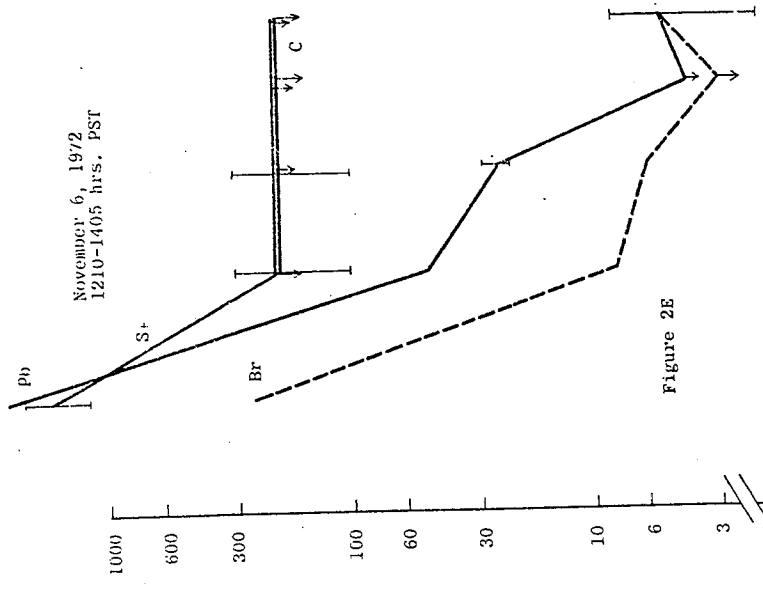


Figure 2E

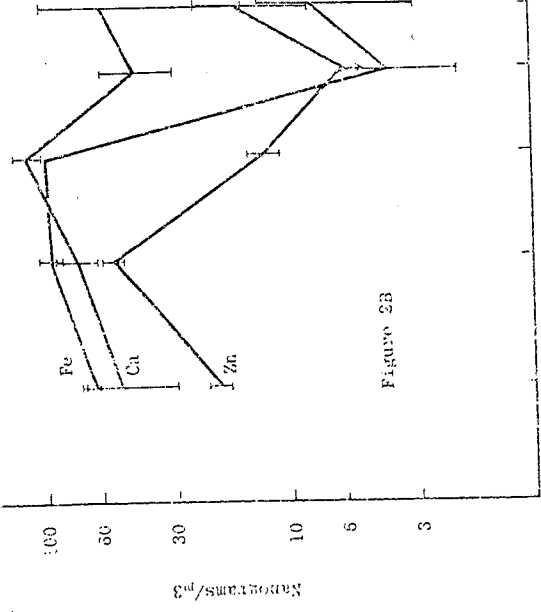


Figure 2B

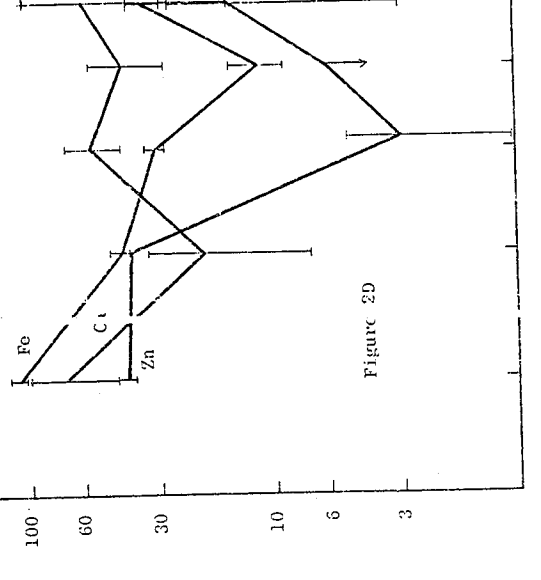


Figure 2D

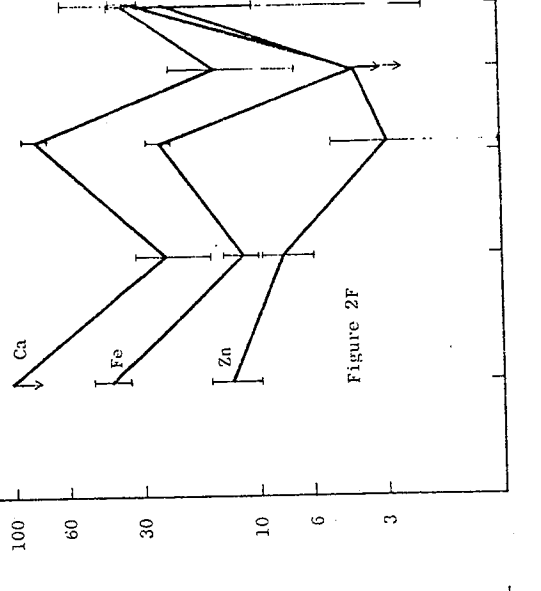


Figure 2F

Lundgren Stage AF X1 X2 X3 X4 X5 XA-ST  
Lundgren Stage AF X1 X2 X3 X4 XA-ST  
Lundgren Stage AF X1 X2 X3 X4 XA-ST

## REFERENCES

1. A. Q. Eschenroeder, J. R. Martinez, and R. A. Nordsieck, "Evaluation of a Diffusion Model for Photochemical Simulation" Final Report, Environmental Protection Agency Contract No. 68-02-0336, General Research Corporation, Santa Barbara, California (1972).
2. J. H. Seinfeld, P. M. Roth, and S. D. Reynolds, "Simulation of Urban Air Pollution", Manuscript to be published in Advances in Chemistry.
3. L. R. Wayne, M. Danchick, M. Weisburd, A. Kokin, and A. Stein, "Modeling Photochemical Smog on a Computer for Decision Making," J. Air Poll. Contr. Assoc., Vol. 21, pp. 334-340 (1971).
4. M. C. McCracken, T. V. Crawford, K. R. Peterson, and J. B. Knox, "Development of a Multibox Air Pollution Model and Initial Verification for the San Francisco Bay Area" Report No. UCRL 73348, Lawrence Radiation Laboratories, Livermore, California (1971).
5. Bay Area Air Pollution Control District, "Contaminant and Weather Summary" (September 1972).
6. Bay Area Air Pollution Control District, "Contaminant and Weather Summary" (October 1972).
7. Bay Area Air Pollution Control District, "Contaminant and Weather Summary" (November 1972).
8. C. L. Smalley, "A Survey of Air Flow Patterns in the San Francisco Bay Area," Mimeographed paper published by U.S. Weather Bureau, S.F. International Airport (1957).
9. D. L. Blumenthal, and T. B. Smith, "Aerosol Characterization Program, Preliminary Airborne Sampling Program", Monthly Report No. 4, Contract No. ARB-358, North American Rockwell Science Center, Thousand Oaks, California (1972).
10. Bay Area Air Pollution Control District, "Air Pollution and the San Francisco Bay Area," (1972).
11. D. H. Slade, "Meteorology and Atomic Energy", U.S. Atomic Energy Commission, Oak Ridge, Tennessee (1968).

12. J. H. Smith, "Motor Fuel Composition and Photochemical Smog," a report to American Petroleum Institute, SRI Project 8558, Stanford Research Institute, Menlo Park, California (October 1971).
13. P. A. Leighton, Photochemistry of Air Pollution, pp 152-157, Academic Press, New York (1961).
14. K. L. Demergian, J. A. Kerr, and J. G. Calvert, "The Mechanism of Photochemical Smog Formation," The Chemistry Department, The Ohio State University, Columbus, Ohio (1972).

---

15. W. A. Williams, and R. E. DeMandel, "Land-Sea Boundary Effects on Small-Scale Circulation," Progress Report No. 2, National Science Foundation Grant GP-4248, San Jose State College, San Jose, California (1966).
16. U.S. Weather Bureau, "Climatography of the United States No. 86-4, Decennial Census of United States Climate, Climatic Summary of the United States--Supplement for 1951 through 1960, California," Washington, D.C. (1966).
17. C. P. Patton, "Climatology of Summer Fogs in the San Francisco Bay Area," University of California Publications in Geography, University of California Press, Berkeley, Vol. 10, pp. 113-200 (1959).
18. G. B. Bell, "The Use of Meteorological Data in Large Scale Air Pollution Surveys," Bureau of Air Sanitation, State of California, Berkeley, SRI Project 2238, Stanford Research Institute, Menlo Park, California (1958).
19. D. Ahrens, and A. Miller, "Variations of the Temperature Inversion over the San Francisco Bay Area," Department of Meteorology, San Jose State College (February 1969).
20. J. S. Sandberg, and R. H. Thullier, "Oxidant Levels Over San Francisco Bay and Adjacent Land Stations," J. Air Pollution Control Association, Vol. 20, pp. 599-602 (1970).
21. U.S. Department of Health, Education, and Welfare, Publication No. 999-AP-38.
22. D. A. Levaggi, Environ. Sci. and Tech., Vol. 6, pp. 250-252 (1972).
23. Annual Book of ASTM Standards No. 23, "Proposed Method of Test for Sulfur Dioxide Content of the Atmosphere (West-Gaeke Modification of the Kozlyaeva Method)," pp. 964-970 (1970).

24. C. T. O'Konski and G. J. Doyle, Anal. Chem., Vol. 27, pp. 694-701 (1955).
25. R. D. Cadle, Particle Size, p. 33 (Reinhold Publishing Corp., New York, 1965).
26. L. Kahn and F. T. Brezenski, "Determination of Nitrate in Estuarine Waters," Environ. Sci. and Tech., Vol. 1, pp. 488-491 (1967).
27. F. Ludwig, et. al., "Size Determination of Atmospheric Sulfate and Organic Particulates," SRI Interim Report Project PAU-4748, Stanford Research Institute, Menlo Park, California pp. 30-34 (December 1964).
28. D. M. Coulson and L. A. Cavanagh, "Automatic Chloride Analyzer," Anal. Chem., Vol. 32, pp. 1245-1247 (1960).
29. D. M. Coulson and D. L. Haynes, "Survey of Manual Methods of Measurements of Lead, Cadmium, Mercury, Selenium, Asbestos, and Beryllium," Final Report for Phase 1, SRI Project SCU-1374, Stanford Research Institute, Menlo Park, California, Section C of Appendix I (December 1972).
30. C. E. Junge, Chapter 2, Air Chemistry and Radioactivity, (Academic Press, New York, 1963).
31. D. B. Turner, "A Diffusion Model for a Urban Area," J. Appl. Meteorol., Vol. 3, pp. 83-91 (1964).